Development of a liposome-based complement assay platform for functional complement activity determination

Dissertation zur Erlangung des Doktorgrades der Naturwissenschaften (Dr. rer. nat.)

an der Fakultät für Chemie und Pharmazie

der Universität Regensburg

Deutschland

vorgelegt von

Clemens Spitzenberg

aus Regensburg

im Jahr 2025

Die vorliegende Dissertation entstand in der Zeit von Januar 2021 bis Dezember 2024 am Institut für Analytische Chemie, Chemo- und Biosensorik der Universität Regensburg.

Die Arbeit wurde angeleitet von Prof. Dr. Antje J. Baeumner.

Promotionsgesuch eingereicht am: 17. Juni 2025
Kolloquiumstermin: 20. August 2025

Prüfungsausschuss

Vorsitzender:	Prof. Dr. Joachim Wegener
Erstgutachterin:	Prof. Dr. Antje J. Baeumner
Zweitgutachterin:	Prof. Dr. Diana Pauly
Drittprüferin:	Prof. Dr. Miriam Breunig

Acknowledgements

First of all, I would like to thank **Prof. Dr. Antje J. Baeumner** for giving me the opportunity to work on this very interesting and challenging but rewarding topic. Special thanks for her trust in me and my abilities and for her continuous support by providing inexhaustible motivation, positive energy, very productive and constructive discussions and an always open door. Many thanks for these very instructive and exciting years.

I would also like to thank **Prof. Dr. Diana Pauly**, who was always available to provide help and advice, particularly with regard to any questions about the complement system. Many informative discussions together have made this work possible. Additionally, I would like to thank her for agreeing to be my second reviewer.

Many thanks also to **Prof. Dr. Miriam Breunig** for her willingness to be my third reviewer, and to **Prof. Dr. Joachim Wegener** for taking on the role of the chairman in my doctoral examination.

I would like to thank all collaborators who have supported me in my work. Especially I would like to thank **Dr. Richard Pouw** for his warm welcome during my stays in Amsterdam and for his support and collaboration, which provided me with valuable expertise and materials. I would also like to thank the entire **SciFiMed project team**, which contributed to the success of the work through scientific discussions, especially during our annual project meetings.

Thanks to **Dr. Christoph Bruckschlegel** and **Dr. Pierre Bauduin** for their support especially with regard to all aspects related to the SAXS measurements. Many thanks also to **Sebastian Boesl-Bichlmeier** and **Prof. Dr. Patrick Nuernberger** for their help in the field of spectroscopy.

I am thankful to **Vanessa Tomanek** for the very pleasant time as colleague in the laboratory, for her practical help with countless ICP-OES measurements, and for her support with graphics, which would certainly not look as professional without her.

Furthermore, I would like to thank **all my colleagues** from the working group for the open and productive atmosphere, which made my time at the university very enjoyable. I would especially like to thank all members of the liposome team for the scientific exchange of ideas in our regular meetings. Special thanks to **Michaela Aichinger**, who actively supported me in experiments and gave me moral support. Thank you to **Ferdinand Holzhausen** for all the good advice in inspiring research discussions, the good times on various project trips, as well as for a helping hand whenever needed.

I would also like to thank **Simon Streif** and **John Galligan** for the time we spent together throughout our studies up to our respective PhD studies. Thank you for your support in all matters, whether inside or outside the lab, and for ensuring a fun and good time.

I would also like to thank my family for their support and everlasting love. Many thanks to **my parents** for their financial support during my studies, which has made all of this possible. Thanks to **my siblings** for always believing in me and having an open ear whenever I needed it.

Finally, I would like to thank **my girlfriend** for her incredible emotional support, for all the time we spent together as a balance to work and for her presence whenever I needed it.

Table of Contents

Declaration of Collaborations

The majority of the theoretical and experimental work presented in this thesis was conducted solely by the author. However, parts of the results were obtained through collaboration with other researchers. In accordance with §8 Abs. 1 Satz 2 Punkt 7 of the “Ordnung zum Erwerb des akademischen Grades eines Doktors der Naturwissenschaften (Dr. rer. Nat.) an der Universität Regensburg vom 18. Juni 2009”, the following paragraphs specify the work carried out by the author and the contributions by third parties.

Chapter 2: The Complement System and Liposomes: Challenges and Opportunities in Functional Complement Analysis

The literature search and writing of the chapter was solely done by the author.

Chapter 3: Encapsulants Affect Liposome Surface Interactions with Biological Systems

This chapter has been published as an original research article in the journal *Small*. Conceptualization of this research article was performed by Antje J. Baeumner and the author and supported by Ferdinand Holzhausen. The methodology was developed by Antje J. Baeumner, Christoph Bruckschlegel, Ferdinand Holzhausen and the author and supported by Pierre Bauduin and Patrick Nuernberger. Christoph Bruckschlegel, Ferdinand Holzhausen and the author contributed equally to the experimental investigations. Christoph Bruckschlegel performed and evaluated the SAXS measurements supported by Coralie Pasquier. Samples for the SAXS measurements were prepared by the author. Ferdinand Holzhausen and the author prepared the samples for spectroscopic investigations performed by Sebastian Boesl-Bichlmeier (Figure 3-1 and 3-4). The author performed and evaluated the liposome-based complement assays and preliminary studies on the fluorophores. Ferdinand Holzhausen, Anna Gebhardt, Michaela Aichinger, Ernst Eberhardt, Sandra Friedrich, Anna-Maria Lauerer and Silvia Haage assisted with the liposome preparation. Funding acquisition was led by Antje J. Baeumner and supported by Pierre Bauduin. Antje J. Baeumner supervised in a leading role and was supported by Pierre Bauduin and Patrick Nuernberger. Antje J. Baeumner contributed by project administration. The author wrote the first draft of the manuscript. Antje J. Baeumner, Christoph Bruckschlegel, Ferdinand Holzhausen, Sebastian Boesl-Bichlmeier, Patrick Nuernberger and Pierre Bauduin revised the manuscript. Antje J. Baeumner is corresponding author.

Chapter 4: Liposomes enable the functional assessment of each complement pathway

This chapter will be further used as manuscript that is intended to be submitted as an original research article in *ACSnano*. Conceptualization of this research article was performed by Antje

J. Baeumner, Diana Pauly and the author. The methodology was developed by Antje J. Baeumner, Diana Pauly and the author and supported by Felix Poppelaars and Richard Pouw. Most of the experimental work was done by the author. Michaela Aichinger contributed with experimental work within the scope of her master's thesis (including in parts inhibitor studies and liposome mannan modification optimizations, the bystander complement lysis assay, the LPS-Liposome content titration and supporting in the donor sera screenings), which is marked with an asterisk [*] in the respective figure caption. Her master's thesis is entitled "Development and Optimization of Liposomes for the Detection of Three Complement Pathways" and was submitted in September 2024 to the Faculty of Chemistry and Pharmacy at the University of Regensburg. This data was reformatted to fit this thesis. Mieke C. Brouwer contributed with performing the ELISA measurements. Anna Gebhart, Christian Griesche, Ernst Eberhardt, Ferdinand Holzhausen, Katharina Weiß, Kilian Höcherl and Michaela Aichinger assisted with liposome synthesis. Richard B. Pouw supported by providing the inhibitors and donor sera. Ernst Eberhardt assisted in experimental investigations of high 4-APM-Liposomes under the supervision of the author. Funding was acquired by Antje J. Baeumner, Diana Pauly and Felix Poppelaars. Antje J. Baeumner and Diana Pauly contributed by project administration. Antje J. Baeumner supervised the project. The author wrote the first draft of the manuscript. Antje J. Baeumner, Diana Pauly, Felix Poppelaars, Ferdinand Holzhausen, Richard Pouw and Michaela Aichinger revised the manuscript. Antje J. Baeumner is corresponding author.

Collaborations of this chapter resulted in a patent application by Antje J. Baeumner, Diana Pauly, Felix Poppelaars and the author (EU: WO2024099816A1, international: PCT/EP2023/080264).

Chapter 5: Feasibility Study for the Applicability of Human Plasma and Animal Sera in the Liposome-Based Complement Assay

Most of the experimental work was solely done by the author. This chapter originated from a collaboration with Diana Pauly. Anna Gebhardt, Kilian Hoecherl, Cornelia Rogoll and Simon Streif assisted in liposome preparation. Antje J. Baeumner contributed with strategic discussions. The chapter was written by the author.

Chapter 6: Conclusion and Future Perspectives

The literature search and writing of the chapter was solely done by the author.

List of Abbreviations and Symbols

In the following, all used abbreviations and symbols are explained, except commonly known abbreviations.

Abbreviation	Meaning
4-APM	4-aminophenyl mannopyranoside
AH50	represents the serum dilution required to cause 50 % lysis of rabbit or guinea pig red blood cells under Mg^{2+}/EGTA conditions
aHUS	atypical hemolytic uremic syndrome
AMD	age-related macular degeneration
ANCA	anti-neutrophil cytoplasmic antibody
BEA	bromoethylamine
Biot-Liposome	liposomes with biotin modifictaion
C1-INH	C1-Esterase-Inhibitor
C3G	C3 glomerulopathy
C3GN	C3 glomerulonephritis
C3NeF	C3 nephritic factors
CH50	represents the serum dilution required to cause 50 % lysis of sensitized sheep red blood cells
CRP	C-reactive protein
DDD	dense deposit disease
DLS	dynamic light scattering
DMPE-PEG2000	1,2-dimyristoyl-sn-glycero-3-phosphoethanolamine-N-[methoxy(polyethylene glycol)-2000]
DMPE-PEG2000-biotin	1,2-distearoyl-sn-glycero-3-phosphoethanolamine-N-[biotinyl(polyethylene glycol)-2000]
DNP	dinitrophenyl
DPPC	1,2-dipalmitoyl-sn-glycero-3-phosphocholine
DPPE-biotin	1,2-dipalmitoyl-sn-glycero-3-phosphoethanolamine-N-(biotinyl)
DPPG	1,2-dipalmitoyl-sn-glycero-3-phospho-(1′-rac-glycerol) (sodium salt)
EDC	1-Ethyl-3-(3-dimethylaminopropyl) carbodiimide hydrochloride
EDTA	tetrasodium ethylenediaminetetraacetic acid
EGTA	ethylene glycol-bis(2-aminoethyl ether)-N,N,N′,N′-tetraacetic acid
ELISA	enzyme-linked immunosorbent assay

ELS	electrophoretic light scattering
EQA	external quality assurance program
ESID	European Society for Immunodeficiencies
FB	complement factor B
FD	complement factor D
FH	factor H
G6P	glucose-6-phosphate dehydrogenase
ghostisomes	liposomes without encapsulated dye
GPI-AP	glycosylphosphatidylinositol-anchored protein
GUV	giant unilamellar vesicle
HEPES	N-2-hydroxyethylpiperazine-N'-2-ethanesulfonic acid
HSS	liposome storage buffer, HEPES saline sucrose buffer
iaCB	inactivation buffer
ICP-OES	optical emission spectroscopy with inductively coupled plasma
IR-783	2-[2-[2-Chloro-3-[2-[1,3-dihydro-3,3-dimethyl-1-(4-sulfobutyl)-2H-indol-2-ylidene]ethylidene]-1-cyclohexen-1-yl]ethenyl]-3,3-dimethyl-1-(4-sulfobutyl)-3H-indolium
LCB	liposome complement buffer
LPS	lipopolysaccharide
LPS-Liposomes	lipopolysaccharide modified liposomes
LUV	large unilamellar vesicle
MAC	membrane attack complex
Man-Liposomes	mannan functionalized liposomes
MASP	mannose-binding lectin associated serine protease
MBL	mannose binding lectin
MLV	multilamellar vesicle
MTP	microtiter plate
MVV	multivesicular vesicle
MWCO	molecular weight cut-off
NAD^+	nicotinamide adenine dinucleotide
NADH	reduced nicotinamide adenine dinucleotide
N-glutaryl-DPPE	1,2-dipalmitoyl-sn-glycero-3-phosphoethanolamine-N-(glutaryl) (sodium salt)
OG	N-octyl-β-d-glucopyranoside
OLV	oligolamellar vesicle
P	properdin
PBMC	peripheral blood mononuclear cell

PDI	polydispersity index
PEG	polyethylene glycol
PHS	pooled human serum
PNH	paroxysmal nocturnal hemoglobinuria
PTSA	1,3,6,8-pyrenetetrasulfonic acid
RID	radial immunodiffusion
RT	room temperature
SAXS	small-angle X-ray scattering
sC5b-9	soluble terminal complement complex
SEC	size exclusion chromatography
SLE	systemic lupus erythematosus
sNHS	N-Hydroxysulfosuccinimide
SRB	sulforhodamine B
SUV	small unilamellar vesicle
tL	total lipid concentration
λ_{Em}	emission wavelength
λ_{Ex}	extinction wavelength

Summary

In the following, the development of a liposome-based complement assay platform was investigated with the aim to improve upon traditional hemolysis assays used in complement diagnostics and research. The complement system is a fundamental part of innate immunity and plays a critical role in pathogen defense, inflammation, and immune regulation. While traditional assays generally have enabled the study of complement activation, they fall short in providing pathway-specific and functional lysis-based insights for all three activation pathways. The research in this thesis aimed to provide an assay which is capable of pathway specific readouts for all three complement pathways and an easier-to-perform, more reproducible and standardizable alternative to the established hemolysis assay and enzyme-linked immunosorbent assay (ELISA).

Inspired by the idea of a multiplexed assay for all pathways, encapsulation of three fluorophores and their influence on the lipid bilayer and the biological reactivity, i.e. on the complement system, were investigated. Once the feasibility of their simultaneous detection had been confirmed, the fluorophores IR-783, sulforhodamine B (SRB), and 1,3,6,8-pyrenetetrasulfonic acid (PTSA) were encapsulated. Spectroscopic and small-angle X-ray scattering (SAXS) analyses, together with subsequent liposome-based complement assay measurements revealed distinct behaviors for each dye. IR-783 exhibited strong interactions with the lipid bilayer. SAXS data showed that IR-783 significantly altered the bilayer's electron density, suggesting the integration of IR-783 into the lipid bilayer. This interaction prevented liposome formation in low cholesterol formulations and required extensive purification for high cholesterol formulations. This indicates its profound impact on the membrane structure. For SRB, SAXS analysis indicated fluorophore adsorption onto the bilayer without significantly altering its internal structure. In contrast to both other dyes, PTSA showed minimal interaction with the lipid bilayer. SAXS and dialysis experiments confirmed that PTSA remained confined to the aqueous solutions and could be removed completely from the liposome exterior. Subsequent analysis of the liposomes in the complement assay revealed altered complement activation patterns when IR-783 and PTSA were entrapped in comparison to the established SRB encapsulating liposomes. In both cases, decreased complement-induced lysis was obtained for the liposomes investigated (including low and high cholesterol content and antibody or lipopolysaccharide (LPS) modification) compared to the respective SRB encapsulating equivalents. These findings emphasize the importance of considering encapsulant effects in the design of liposomes which are applied in biological systems. The altered complement activation for each fluorophore furthermore restricted the subsequent development of a multiplexed liposome-based pathway specific complement assay.

Building on this understanding, the aim of developing a platform for complement pathway specific analysis was still pursuit. Mannan functionalized liposomes (Man-Liposomes) which specifically activated the lectin pathway were achieved through careful optimization of mannan amination chemistry and coupling conditions. These liposomes were shown to trigger complement-mediated lysis via mannose-binding lectin (MBL). A panel of inhibitors targeting the complement proteins C1q, C1s, MBL, MASP-2, Factor B, and C5 was used to confirm their specificity. Subsequent analysis demonstrated long-term stability of the Man-Liposomes. Additionally, validation on a cohort of 97 healthy human serum samples showed strong correlation with ELISA-based C3b deposition assays (Pearson's r = 0.77). The platform was then further extended to also assess the classical and alternative pathways specifically. For the classical pathway, two liposome designs were evaluated: antibody modified liposomes and liposomes with high cholesterol content (hiChol-Liposomes). Liposomes functionalized with biotin and subsequently bound anti-biotin antibodies reliably triggered specific classical pathway activation, which was confirmed by inhibitor studies. HiChol-Liposomes were investigated as a simpler alternative to antibody modification. For those, specific classical pathway activation was also confirmed. However, hiChol-Liposome lysis revealed no correlation to the ELISA-based C3b deposition assay, suggesting that cholesterol mediated activation may involve additional factors compared to the antibody triggered control assay. For the alternative pathway, liposomes were modified with LPS and specificity was confirmed under Mg^{2+}/EGTA conditions, which were used to suppress classical and lectin pathway activity. However, a significant number of serum samples failed to induce LPS-Liposome lysis despite showing activation in the ELISA. This highlights the need for further optimization of liposome surface chemistry or for LPS trigger substitutes for reliable alternative pathway readouts in the future.

Fundamental studies investigating the potential applicability of plasma as an alternative to human serum in the future demonstrated the assay's versatility. EDTA- and citrate-treated serum, once replenished with calcium and magnesium ions, restored complement activity. ETDA-treated serum was determined to be better suited for this assay with 90 % recovery of untreated serum as reference compared to citrate serum with 71 % recovery. The application of citrate serum was limited in this assay due to liposome destabilization, assumed to be caused by too high ion concentrations which were required due to its weaker chelation efficiency. The assay was further tested with animal sera, revealing species-specific differences in complement reactivity. While murine serum exhibited no liposome lysis, porcine and rat sera induced complement-mediated lysis depending on the liposomes used. Contrary to human serum, porcine serum lysed low-cholesterol liposomes more effectively than high-cholesterol ones. Further experiments with pegylated liposomes of varying cholesterol content revealed a dose-dependent response, peaking at 20 %mol. cholesterol. Reactivity across all

investigated rat strains was similar with moderate lysis of low cholesterol liposomes and slightly higher lysis levels of high cholesterol formulations. LPS-modified liposomes exhibited further enhanced lysis while pegylated liposomes remained stable unless modified with antibodies. In summary, while further refinement in liposome surface chemistry optimization and correlation studies will be essential to fully realize this assays potential, this liposome-based assay platform offers a powerful and versatile approach for functional pathway specific complement analysis in diagnostics, therapeutic monitoring, and fundamental research.

Zusammenfassung

Im Folgenden wurde die Entwicklung einer liposomen-basierten Komplement-Assay Plattform mit dem Ziel untersucht, traditionelle Hämolyse-Assays, die in der Komplementdiagnostik und -forschung verwendet werden, zu verbessern. Das Komplementsystem spielt als elementarer Teil der angeborenen Immunität eine entscheidende Rolle bei der Abwehr von Krankheitserregern, bei Entzündungen und bei der Immunregulation. Im Allgemeinen haben herkömmliche Assays zwar die Untersuchung der Komplementaktivität ermöglicht, bieten jedoch nicht für alle drei Aktivierungswege eine pfadspezifische und funktionelle, auf Lyse basierende Analysemöglichkeit. Die Forschung dieser Arbeit zielte darauf ab diese Lücke durch eine funktionelle liposomenlyse-basierte Alternative zu den etablierten Hämolyse- und ELISA-Assays zu schließen, die einfacher durchzuführend, besser reproduzierbar und standardisierbar ist. Ziel war es alle drei Komplementaktivierungswege spezifisch auszulesen zu können.

Inspiriert von der Idee eines Multiplex-Assays für alle Komplementwege wurde zu Beginn die Verkapselung von drei Fluorophoren und deren Einfluss auf die Lipidmembran und auf die biologische Reaktivität anhand des Komplementsystems untersucht. Nachdem die Möglichkeit des simultanen Nachweises der drei Fluorophore bestätigt war, wurden die Farbstoffe IR-783, Sulforhodamin B (SRB) und 1,3,6,8-Pyrentetrasulfonsäure (PTSA) in Liposomen eingekapselt. Spektroskopische und Kleinwinkel-Röntgenstreuungsanalysen (SAXS) sowie anschließende liposomen-basierte Komplement-Assay-Messungen ergaben für jeden Farbstoff unterschiedliche Verhaltensweisen. IR-783 wies starke Wechselwirkungen mit der Lipiddoppelschicht auf. SAXS-Daten zeigten, dass IR-783 die Elektronendichte der Doppelschicht erheblich beeinflusste, was auf eine Integration des Farbstoffs in die Lipidmembran schließen lässt. Diese Wechselwirkung verhinderte die Liposomenbildung bei Formulierungen mit niedrigem Cholesteringehalt und erforderte eine umfassende Abtrennung des überschüssigen Farbstoffs bei Formulierungen mit hohem Cholesteringehalt. Dies weist ebenfalls auf seine tiefgreifende Interaktion mit der Membranstruktur hin. Im Falle von SRB zeigten SAXS-Analysen, dass der Fluorophor an der Lipiddoppelschicht adsorbiert, ohne deren innere Struktur wesentlich zu verändern. PTSA zeigte eine minimale Wechselwirkung mit der Lipidmembran. SAXS- und Dialyseexperimente bestätigten, dass PTSA auf die wässrigen Lösungen beschränkt blieb und vollständig von der Liposomenoberfläche entfernt werden konnte. Im Vergleich zu den etablierten Liposomen, die SRB verkapselten, zeigten Liposome, die IR-783 und PTSA einschlossen, veränderte Komplementaktivierungsmuster. In beiden Fällen wurde für die untersuchten Liposomen (mit niedrigem und hohem Cholesteringehalt, Antikörper- oder Lipopolysaccharid (LPS)-modifiziert) im Vergleich zu den

entsprechenden SRB-verkapselnden Äquivalenten eine geringere komplementinduzierte Lyse erzielt. Diese Ergebnisse zeigen welche Auswirkungen Moleküle bei der Verkapselung in Liposomen auf deren Eigenschaften haben können und unterstreichen die Notwendigkeit der Analyse solcher Effekte bei der Entwicklung von liposomen-basierten Anwendungen im Diagnostikbereich. Die abweichenden Reaktivitäten bei Verwendung der unterschiedlichen Fluorophore schränkten außerdem eine anschließende Entwicklung eines Multiplex-Komplement-Assays ein.

Aufbauend auf diesem Verständnis wurde das Ziel, eine Plattform zur spezifischen Analyse der drei Komplementwege zu entwickeln, trotzdem weiterverfolgt. Mannan-funktionalisierte Liposomen (Man-Liposomen) zur selektiven Aktivierung des Lektinwegs wurden durch sorgfältige Optimierung der Mannan-Aminierung und der Kopplungsbedingungen erreicht. Es konnte gezeigt werden, dass diese Liposomen die Lyse durch das Komplement System über das mannose-bindende Lektin (MBL) auslösen. Die Spezifität wurde mit Inhibitoren bestätigt, die die Funktion der Komplementproteine C1q, C1s, MBL, MASP-2, Faktor B und C5 einschränken. Die Man-Liposome erwiesen sich als langzeitstabil und wurden an einer Kohorte von 97 gesunden humanen Serumproben validiert. Dabei konnte eine starke Korrelation mit einem C3b-ELISA gezeigt werden (Pearson's r = 0.77). Anschließend wurde der Assay für die spezifische Analyse des klassischen und des alternativen Wegs angepasst. Für den klassischen Weg wurden zwei Liposomendesigns untersucht: Antikörper-modifizierte Liposomen und Liposomen mit hohem Cholesteringehalt (hiChol-Liposomen). Mit Biotin funktionalisierte Liposomen, an die anschließend anti-Biotin Antikörper gebunden wurden, lösten zuverlässig die spezifische Aktivierung des klassischen Wegs aus. Dies konnte durch Inhibitorstudien bestätigt werden. HiChol-Liposomen wurden als einfachere Alternative zur Antikörpermodifikation untersucht. Mittels Inhibitorstudien konnte auch für diese die spezifische Aktivierung des klassischen Komplementwegs bestätigt werden. Allerdings zeigten hiChol-Liposomen keine Korrelation mit dem C3b-ELISA, was darauf hindeutet, dass bei der durch Cholesterin ausgelösten Aktivierung zusätzliche Faktoren im Vergleich zum Antikörper getriggerten Kontrolltest eine Rolle spielen könnten. Für den alternativen Weg wurden die Liposomen mit LPS modifiziert, und die Spezifität wurde unter Mg^{2+}/EGTA Bedingungen bestätigt. Mg^{2+}/EGTA wurde verwendet um die Aktivität des klassischen und des Lektinwegs zu unterdrücken. Jedoch konnte eine signifikante Anzahl der Serumproben keine Lyse der LPS-Liposomen induzieren, obwohl sie im ELISA eine ausreichende Aktivität zeigten. Dies unterstreicht, dass für eine zuverlässige Messung des alternativen Weges eine weitere Optimierung der Liposomen-Oberflächenchemie oder die Verwendung von Komplementtriggeralternativen, anstelle von LPS notwendig ist.

Grundlegende Studien, in denen die zukünftige Anwendbarkeit von Plasma als Alternative zu Humanserum untersucht wurde, zeigten die Vielseitigkeit des Assays. EDTA- und citrat-behandeltes Serum stellte nach Wiederherstellung ausreichend hoher Kalzium- und Magnesiumionenkonzentrationen die Komplementaktivität wieder her. ETDA-behandeltes Serum erwies sich als besser geeignet, da 90 % der Aktivität einer unbehandelten Serumkontrolle wieder hergestellt werden konnte im Vergleich zu 71 % bei Citrat-behandeltem Serum. Höhere Aktivitäten konnten im Falle von Citrat-Serum nicht wiederhergestellt werden, da die Liposomen destabilisiert wurden, vermutlich durch zu hohe Ionenkonzentrationen, die aufgrund der geringeren Effizient der Komplexierung von Citrat erforderlich waren. Dies schränkt die Anwendung von Citrat-Serum bzw. Citrat-Plasma in diesem liposomen-basierten Assay ein. Zuletzt wurde der Assay mit Tierseren getestet. Dabei zeigten sich artspezifische Unterschiede in der Komplementreaktivität. Während Mäuseserum keine Liposomenlyse zeigte, führten Schweine- und Rattenseren in Abhängigkeit von den verwendeten Liposomen zu einer komplement-induzierten Lyse. Im Gegensatz zu Humanserum, lysierte Schweineserum Liposomen mit niedrigem Cholesteringehalt effektiver als solche mit hohem Cholesteringehalt. Weitere Experimente mit pegylierten Liposomen mit unterschiedlichem Cholesteringehalt zeigten eine dosisabhängige Reaktion, die bei 20 %mol. Cholesterin ihren Höhepunkt erreichte. Bei allen untersuchten Seren unterschiedlicher Rattenstämme wurde eine ähnliche Reaktion ermittelt. Liposomen mit niedrigem Cholesteringehalt lösten eine mäßige Lyse und Liposomen mit hohem Cholesteringehalt lösten eine etwas stärkere Lyse aus. LPS-modifizierte Liposomen verstärkten die Lyse weiter, während pegylierte Liposomen stabil blieben, sofern sie nicht mit Antikörpern modifiziert wurden. Zusammenfassend bietet diese auf Liposomen basierende Assay-Plattform einen leistungsstarken und vielseitigen Ansatz für die funktionelle Komplementanalyse in der Diagnostik, Therapieüberwachung und Grundlagenforschung, trotzdem bedarf es noch weiterer Optimierung der Liposomenoberflächenchemie und Korrelationsstudien, um das volle Potenzial dieses Assays auszuschöpfen.

1 Motivation and Structure of the Thesis

The first descriptions of the complement system already date back to over one hundred years ago.[1] Since then, the complement system has been uncovered as a crucial part of the human immune system, which connects innate and adaptive immune responses.[1,2] Assays measuring the lysis of red blood cells from animals facilitated the readout of complement activity in the 1960s.[3] Since its discovery, research on the complement system has revealed a complex enzymatic cascade involving three major activation pathways with over 50 participating proteins.[2] These proteins gain growing interest as therapeutic targets in diagnostics since complement dysregulation is increasingly unveiled to play an important role in several diseases.[4] A reliable and specific determination of functionality and activity of the complement activation pathways is therefore crucial in both research and diagnostics. However, the methods for lysis-based functional activity determination of the complement system have not changed much since the delicate hemolysis assays were established. Studies on the functionality of complement proteins, the development of complement therapeutics and the screening of functional complement activity in patients, as examples, would all benefit from an assay enabling mechanistic and functional studies which take the entire cascade into account. Therefore, this thesis focuses on the development of an easy-to-perform, reproducible and standardizable functional liposome lysis-based assay which is capable to determine all three complement pathways specifically.

To provide a theoretical foundation for the development of a new complement assay, fundamentals of the complement system and liposomes are introduced in **Chapter 2**. This is initiated by outlining the biological role of the complement cascade in immune defense with focus on the activation mechanisms of the three complement pathways, which all result in the formation of pores through the membrane attack complex (MAC). This functional pore assembly is the basis for most of the research performed in this thesis. The clinical importance of complement analysis, particularly in diagnosing immune-related and inflammatory diseases are discussed, emphasizing the need for suitable analysis techniques. This is followed by reviewing state-of-the-art diagnostic methods, from ELISAs and hemolytic assays to more complex genetic analyses. Limitations of current complement activity determination methods are critically highlighted, especially the lack of lytic functional assays for the lectin pathway. Subsequently, the potential advantages of liposome-based approaches as substitutes for erythrocytes in complement assays are discussed. In addition, insights into the complement field as raising market, critical parameters in complement analysis and the demand for more standardization in complement analysis provide critical information for the development concept of a liposome-based complement assay in the subsequent chapters.

Our research group developed liposomes which are complement stable and can be subsequently modified with complement triggers.[5] Critical parameters to obtain stable liposomes which do not get lysed in presence of the complement system are the cholesterol content in lipid formulations, as well as the used encapsulant concentration.[5] The general concept was developed using the fluorophore sulforhodamine B (SRB) as encapsulant, which allows an analytical signal upon release after pore formation of the MAC in the lipid bilayer, but was also transferred to encapsulated chemiluminescent probes or electroactive substances.[5]

Building on this basis, flexibility in encapsulant and lipid composition together with the need for specific analysis of each complement pathway originated in the idea to develop a multiplexed liposome-based assay. Fundamental studies, investigating the influence of the encapsulant on the lipid bilayer structure and complement response were performed and are described in **chapter 3**. Due to most experience with SRB as encapsulant in our research group, also in other applications,[6,7] and the simplicity of the readout, two additional, simultaneously detectable fluorophores, i.e. IR-783, and 1,3,6,8-pyrenetetrasulfonic acid (PTSA) were encapsulated in liposomes. Initial investigations focused on proving the simultaneous detectability of the three fluorophores. Subsequent analysis via small angle X-ray scattering and dialysis experiments of empty liposomes incubated with the dyes revealed significant differences in their influence on the bilayer structure. The relevance of these differences on the reactivity of the complement system were studied with the liposome-based complement assay. Even though the results of these studies limited the development of a multiplexed complement assay, since also the complement response between the liposomes encapsulating the varying fluorophores were not interchangeable, complement specific readouts were still investigated in parallel.

Chapter 4 describes the development of liposomes with the goal of a platform which is capable of assessing the functional activity of all three complement pathways specifically via liposome lysis. As mentioned in the introduction, an essential part missing in current complement activity analysis is a lysis-based readout of the lectin pathway. However, this was not yet achieved since no erythrocytes have been described to trigger the lectin pathway specifically. Furthermore, liposomes can not as easily be modified with known lectin pathway complement triggers as it has been described for antibodies in classical pathway specific readouts.[8] Therefore, functionalization of mannan with amino-groups was investigated and is described in this chapter allowing the covalent immobilization of these molecules onto the liposome surface. Through a series of thorough optimizations and inhibitor-based validations, specific lectin pathway liposomes were achieved. The assay's reliability was investigated through correlation with a commonly applied C3b-ELISA in a cohort of 97 healthy human sera. Repeated investigations in the complement assay and liposome characteristics showed the

stability of the prepared liposomes. Adaptations for the classical pathway included studies on antibodies and high cholesterol contents as complement triggers. The alternative pathway was investigated with lipopolysaccharides as complement trigger in combination with Mg^{2+}/EGTA containing buffers to inhibit classical and lectin pathway activation.[9] For both pathways inhibitor studies were conducted to proof pathway specificity. Cohort studies were performed to investigate their reliability through correlation studies to the C3b-ELISA. The chapter concludes by highlighting the platform's potential for high-throughput diagnostics, mechanistic studies, and therapeutic monitoring, but lastly also discusses the current limitations observed for the classical and alternative pathway.

In **chapter 5** fundamental proof-of-principle studies of anticoagulant (EDTA and citrate) containing serum are described, to evaluate the potential applicability of plasma samples in the liposome-based complement assay. The here investigated anticoagulants normally limit the applicability of plasma for complement activity studies since they complex the relevant Ca^{2+} and Mg^{2+} ions. However here, restored complement function after reconstitution of these bivalent ions was investigated. Plasma as alternative to serum would be desirable since complement is a heat labile system and requires careful sample handling to avoid preliminary complement consumption before analysis.[10] However, this is minimized in plasma when complement is inactivated through ion complexation until use. Apart from plasma also investigations on animal sera, i.e. murine, porcine and rat serum, in the liposome-base complement assay are described in **chapter 5.** This is relevant since animal models are often applied in studies exploring the mechanisms of the complement system,[11,12] but the obtained results may not be interchangeable between species. By evaluating different liposome formulations, including variations in cholesterol content, PEGylation, and surface modifications with LPS or antibodies, the general applicability of these sera in the liposome assay but also the obtained interspecies differences were investigated. While animal sera were found to be generally applicable to this assay, the study highlights the need for caution when extrapolating animal data to human systems due to interspecies differences in reactivities.

Chapter 6 concludes the outcomes and accomplishments achieved during the development of the liposome-based complement assay in this study. The main advantages as well as the limitations of the developed assay are highlighted. Finally, perspectives for future investigative approaches are given that could be employed to address remaining issues.

1.1 References

(1) Carroll, M. V.; Sim, R. B. Complement in health and disease. *Adv Drug Delivery Rev* **2011**, *63*, 965–975. DOI: 10.1016/j.addr.2011.06.005.

(2) Merle, N. S.; Church, S. E.; Fremeaux-Bacchi, V.; Roumenina, L. T. Complement System Part I - Molecular Mechanisms of Activation and Regulation. *Front Immunol* **2015**, *6*, 262. DOI: 10.3389/fimmu.2015.00262.

(3) Bangham, A. D.; Standish, M. M.; Watkins, J. C. Diffusion of univalent ions across the lamellae of swollen phospholipids. *J Mol Biol* **1965**, *13*, 238–252. DOI: 10.1016/s0022-2836(65)80093-6.

(4) West, E. E.; Woodruff, T.; Fremeaux-Bacchi, V.; Kemper, C. Complement in human disease: approved and up-and-coming therapeutics. *Lancet* **2024**, *403*, 392–405. DOI: 10.1016/S0140-6736(23)01524-6.

(5) Hoecherl, K.; Streif, S.; Spitzenberg, C.; Rink, S.; Behrent, A.; Holzhausen, F.; Griesche, C.; Rogoll, C.; Foedlmeier, M.; Gebhard, A.; Kulikowski, K.; Schaefer, N.; Pauly, D.; Baeumner, A. J. A homogeneous immunoassay technology based on liposomes and the complement system enables one-step, no-wash, rapid diagnostics directly in serum. *Anal Bioanal Chem* **2025**, *417*, 3257–3273. DOI: 10.1007/s00216-025-05882-4.

(6) Streif, S.; Neckermann, P.; Spitzenberg, C.; Weiss, K.; Hoecherl, K.; Kulikowski, K.; Hahner, S.; Noelting, C.; Einhauser, S.; Peterhoff, D.; Asam, C.; Wagner, R.; Baeumner, A. J. Liposome-based high-throughput and point-of-care assays toward the quick, simple, and sensitive detection of neutralizing antibodies against SARS-CoV-2 in patient sera. *Anal Bioanal Chem* **2023**, *415*, 1421–1435. DOI: 10.1007/s00216-023-04548-3.

(7) Hofmann, C.; Kaiser, B.; Maerkl, S.; Duerkop, A.; Baeumner, A. J. Cationic liposomes for generic signal amplification strategies in bioassays. *Anal Bioanal Chem* **2020**, *412*, 3383–3393. DOI: 10.1007/s00216-020-02612-w.

(8) Yamamoto, S.; Kubotsu, K.; Kida, M.; Kondo, K.; Matsuura, S.; Uchiyama, S.; Yonekawa, O.; Kanno, T. Automated homogeneous liposome-based assay system for total complement activity. *Clin Chem* **1995**, *41*, 586–590. DOI: 10.1093/clinchem/41.4.586.

(9) Platts-Mills, T. A. E.; Ishizaka, K. Activation of the Alternate Pathway of Human Complement by Rabbit Cells. *The Journal of Immunology* **1974**, *113*, 348–358. DOI: 10.4049/jimmunol.113.1.348.

(10) Brandwijk, R. J. M. G. E.; Michels, M. A. H. M.; van Rossum, M.; Nooijer, A. H. de; Nilsson, P. H.; Bruin, W. C. C. de; Toonen, E. J. M. Pitfalls in complement analysis: A systematic literature review of assessing complement activation. *Front Immunol* **2022**, *13*, 1007102. DOI: 10.3389/fimmu.2022.1007102.

(11) Frank, M. M. Animal models for complement deficiencies. *J Clin.Immunol* **1995**, *15*, 113S-121S. DOI: 10.1007/BF01540901.

(12) Gibson, B. G.; Cox, T. E.; Marchbank, K. J. Contribution of animal models to the mechanistic understanding of Alternative Pathway and Amplification Loop (AP/AL)-driven Complement-mediated Diseases. *Immunol Rev* **2023**, *313*, 194–216. DOI: 10.1111/imr.13141.

2 The Complement System and Liposomes: Challenges and Opportunities in Functional Complement Analysis

2.1 Introduction

The complement system is a crucial effector pathway of the human immune system going through a cascade-dependent activation and resulting in a pore-forming complex and pathogen lysis.[1] Dysregulation of the complement system affects millions of people to suffer from inflammation-driven diseases causing complement consumption, damage and destruction of surfaces on which the complement system has been activated including infections and autoimmune diseases.[2] Diagnosis of such diseases can be time consuming and difficult due to the current state of the art in complement analysis with a lack of fast, easy-to-perform and standardized assays. Central laboratories perform specialized protein-based enzyme-linked immunosorbent assays (ELISA) to quantify complement proteins, and hemolytic assays based on animal erythrocytes to assess complement functionality.[3,4] For a subset of those, a liposome-based assay had been established in the 1990s.[5] The hemolysis assay could in theory provide the highest content value, however, the animal-derived erythrocytes come with high setup variability from lab-to-lab, difficulties in reproducibility and are prone to age-related effects making standardization very challenging. Furthermore, no erythrocytes from any species have been identified that specifically trigger the lectin pathway, i.e. one of the three main complement pathways. Hence, its functional specific readout is left to protein quantification via ELISAs. The subsequent chapter will introduce the complement field and liposomes, with the objective of highlighting the significance of complement analysis and elucidating the current status of liposome-based functional complement assays and their benefits.

2.2 The complement system

The complement system first described as a complementary mechanism supporting the role of antibodies as the first line of defense against pathogens has been revealed by subsequent research as a much more versatile system and an important part of the innate immune system.[6,7] Complement proteins have been identified throughout the course of evolution, spanning a period of over 600 million years.[8] This finding indicates that they represent one of the most ancient innate immune systems, whose evolution has commenced prior to that of mammals.[8]

Complement comprises more than 50 components circulating in blood, expressed on cell surfaces, or located intracellularly.[1,9] The complement system is essential for recognizing and eliminating invading pathogens, linking innate and adaptive immune responses, immune surveillance, homeostasis and removing immune complexes, cellular debris and apoptotic cells.[1,10] In fact, it has been demonstrated to be active not only in blood, but also in tissues.[9]

The activation of the complement system follows mostly a similar and straightforward enzymatic cascade that includes particle recognition and opsonization, self-amplification of the cascade, generation of effector molecules (for example the membrane-attack-complex (MAC)) (**Figure 2-1**) and induction of other immune responses.[1,6] Initiation of the complement cascade can be described in a simplified manner in three distinct pathways, the classical, lectin and alternative pathway, each resulting in the terminal pathway.[1,6,7]

The classical pathway has a critical role for pathogen detection via its pattern recognition protein C1q.[11,12] C1q binds a variety of different recognition elements including immune complexes containing antibodies like IgG and IgM,[13,14] surface-bound pentraxins like C-reactive protein (CRP)[15,16] or pathogen-associated molecular patterns including lipopolysaccharide (LPS)[17] and bacterial porins[18]. Besides pathogens, C1q can recognize apoptotic cells via intracellular molecules that are exposed on the outer cell surface upon apoptosis like phosphatidylserine[19,20] or double-stranded DNA[21]. Overall, activators or recognition elements, must be clustered on the surface forming a distinctive pattern.[13] Single activators typically result in reduced complement activation.[1,13] C1q binding ultimately leads to C4 and C2 cleavage via the proenzyme $C1r_2C1s_2$.[22–24] The resulting fragments C4b and the large C2 cleavage product C2b form the C3 convertase complex C4b2b (**Figure 2-1**) for the classical and lectin pathway.[10] C2b is also called C2a in literature as the nomenclature is not consistent for C2 cleavage products.[25] Important is that the larger cleavage product forms the C3 convertase. This C3 convertase is able to cleave the complement protein C3 to bioactive fragments C3a and C3b.[6,10]

Similar to the classical pathway, the lectin pathway comprises pattern recognition proteins, specifically mannose-binding lectins (MBL), ficolins and collectins.[26] All of them primarily recognize carbohydrates.[26] The binding event of the recognition element activates MBL-associated serine proteases (MASP) or ficolin associated MASPs which cleave C4 and C2.[27] This results again in the classical and lectin pathway C3 convertase formation C4b2b.

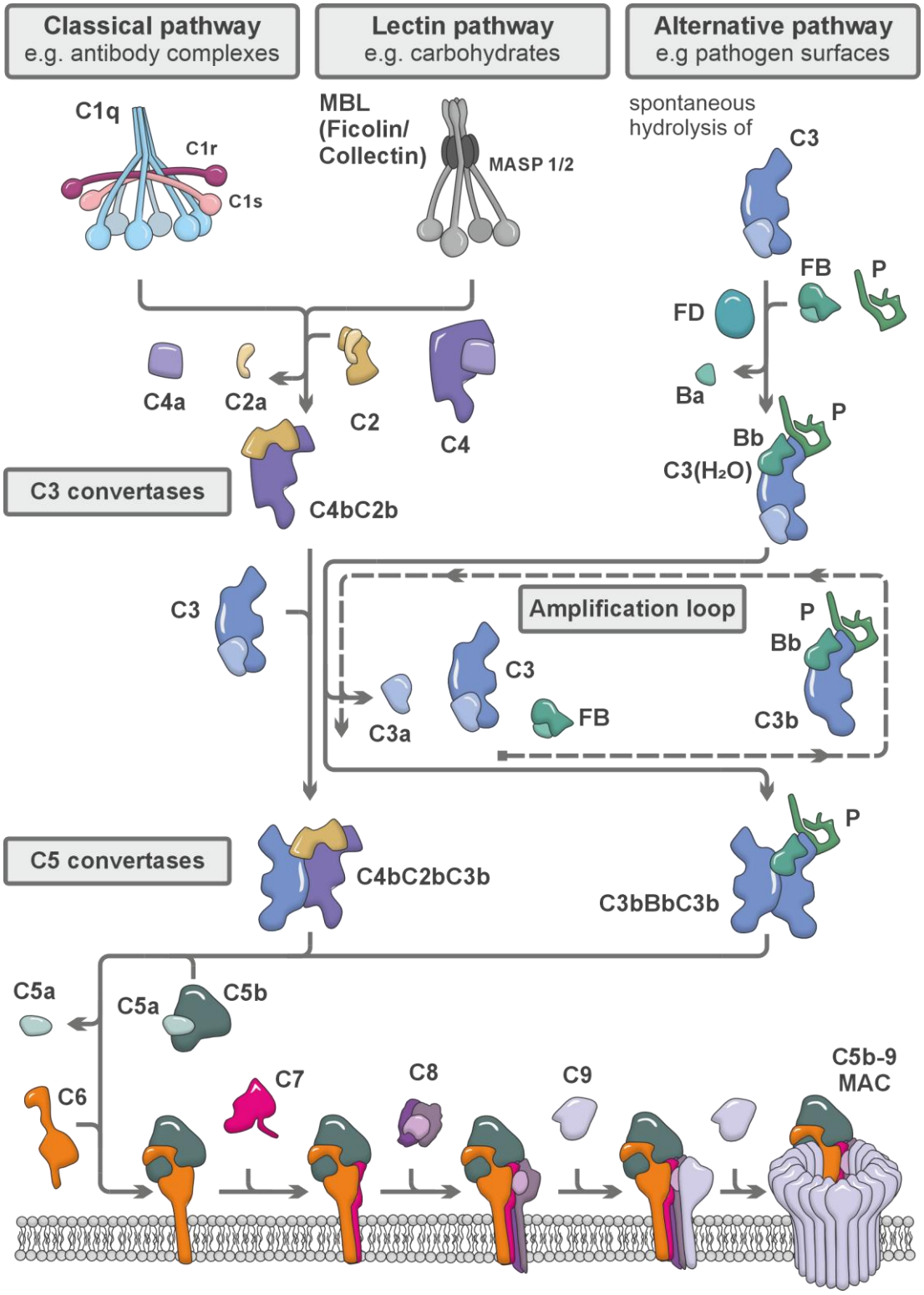

Figure 2-1: Schematic overview of the complement cascade. Simplified, the complement system consists of three distinct activation pathways: the classical, lectin and alternative pathway. The classical and lectin pathway activate via surface bound pattern recognition molecules C1q or MBL, ficolin or collectin. Subsequent cleavage of C2 and C4 by the C1 complex $C1qr_2s_2$ or MASPs cause C3 convertase C4bC2b formation. The alternative pathway relies on spontaneous surface deposition and hydrolysis of C3 and forms the C3 convertases C3bBb or $C3(H_2O)Bb$. C3 bound Factor B (FB) is cleaved by Factor D (FD). Properdin (P) stabilizes C3bBb or $C3(H_2O)Bb$. These C3 convertases cleave the central molecule C3. C3b can further opsonize target membranes, amplifying C3 convertases C3bBb formation. Additionally, C3b can bind to the former C3 convertase which then results in formation of the C5 convertases: C4bC2bC3b or C3bBbC3b. C5 convertases split C5 into the fragments C5a and C5b. C5b can start the assembly of the membrane attack complex (MAC). In a sequential manner C5b, C6, C7, C8 and up C9 molecules gather and bind together to form a MAC.

The alternative pathway lacks a pattern recognition protein, a characteristic that differentiates it from the classical or lectin pathway. It is described that the alternative pathway maintains a low-level complement activity enabling continuous pathogen detection through a process known as “tick-over mechanism”.[1] This process is based on the spontaneous hydrolysis of complement protein C3, resulting in a fluid phase C3(H_2O).[1] However, it is under debate, whether the subsequently formed fluid phase C3 convertase C3(H_2O)Bb is really capable of cleaving C3 into C3a and C3b in physiological relevant quantities, thereby determining its ability to effectively initiate the complement cascade.[28–30] However, interaction of C3 with surfaces such as gas bubbles, material surfaces like polystyrene, glass or polypropylene, LPS or lipid surfaces[29,31] can result in “C3b-like” activity of surface-bound C3(H_2O), causing alternative pathway activation via the surface-bound C3 convertase C3(H_2O)Bb (**Figure 2-1**) and subsequent C3 cleavage.[1,29] Following C3b binding to non-protected surfaces lacking regulator receptors, initiates covalently fixed alternative pathway C3 convertases (C3bBb), which also cleave C3 into C3a and C3b.[1,32] This self-amplifying process is referred to as amplification loop, which in turn causes more opsonization of the pathogen with C3b or C3bBb, respectively.[1] In general, the alternative pathway is not merely an alternative to the classical or lectin pathway but rather can be responsible for the major response of the terminal complement activity with its amplification loop also amplifying C3b opsonization initiated through the other two pathways.[1,32,33]

In all pathways, the resulting C3 convertases of the classical, lectin and alternative pathway C4b2b and C3bBb are also fundamental components of the C5 convertases.[34,35] For biologically active C5 convertases an additional C3b molecule is required for effective C5 cleavage.[34,35] C5 cleavage and therefore activation of the terminal complement pathway results in the formation of the MAC.[1] This complex forms approximately 10 nm wide pores in the target membrane and consists of the protein complex C5b-C6-C7-C8β-C8αγ-C9 (**Figure 2-1**).[36,37]

An additional protection provided by the complement system stems from the anaphylatoxins C3a and C5a, crucial signaling effectors, produced during complement activation which modulate subsequent biological responses.[1,38] Both engage their regulatory effects by binding to their specific transmembrane G-protein-coupled receptors C3aR and C5aR expressed on cell membranes.[39] While traditionally, both anaphylatoxins were described as pro-inflammatory, more recently the role of C3a was described as more complex, revealing a more delicate balance between anti- and pro-inflammatory mode of action, depending on the cell type of the immune system.[38,40] On the one hand C3a can have anti-inflammatory effects on LPS-primed, nonadherent peripheral blood mononuclear cells (PBMCs), pathogens or neutrophils, while on the other hand C3a can cause pro-inflammatory reactions on LPS-

primed, adherent PBMCs, eosinophils, mast cells, macrophages/monocytes and T cell responses.[40] C5a shows potent pro-inflammatory influence by inducing chemoattracting effects on neutrophils, monocytes/macrophages or mast cells at the inflammation cite.[38,41]

Overall, the complement system comprises a complex cascade, of which the significance in diseases is becoming increasingly unveiled. Only recently, complement dysregulation was shown to be a prevalent aspect of long COVID affecting approximately 5 % of all individuals recovering from acute SARS-CoV-2 infection.[42,43] This revelation of the complement system's influence in a viral disease responsible for a pandemic, thereby affecting the global population, can be regarded as parameter indicative for increasing importance of and interest in complement analysis in the diagnostic field worldwide.

2.3 Indications for complement analysis

Complement system defects are generally described to be caused by either hereditary (primary) or acquired (secondary) complement deficiencies[2,44] and can occur throughout the whole complement cascade.[45] Primary complement deficiencies are in most cases a consequence of autosomal recessive traits, which cause deficient levels of the respective functional complement protein.[46] The prevalence of primary complement deficiencies is low, with approximately 0.03 % of the general population affected,[2] excluding homozygous MBL deficiency, which is estimated to occur in about 5 % of the population.[47] An investigation of patient cases from French medical departments over the period from 1988 to 2018 revealed that the majority of patients exhibited defects in the terminal pathway (56 %), followed by the classic pathway (27 %), and, finally, the alternative pathway (17 %).[48] However, clinically more relevant are secondary complement deficiencies which are typically the result of complement consumption due to overactivation through inflammation, decreased protein synthesis, increased catabolism or due to autoantibodies against complement proteins.[44,45,49]

In general, recurrent bacterial infections, autoimmune manifestations, angioedema without urticaria and certain diseases associated with dysregulation of the complement system particularly involving the kidneys and eyes, such as atypical hemolytic uremic syndrome (aHUS), C3 glomerulopathy (C3G), age-related macular degeneration (AMD), as well as paroxysmal nocturnal hemoglobinuria (PNH) characterized by erythrocyte lysis, have been described (**Table 2-1**) as indications for complement dysregulation and require complement analysis.[2,45,50] All benefit from complement analysis for precise diagnosis or treatment monitoring.[45,51] Individuals with primary, inherited complement deficiencies are particularly vulnerable to recurrent bacterial infections largely presenting in childhood, given the important role of the complement system in host defense against pathogens.[44,48,52] Based on data of the European Society for Immunodeficiencies (ESID) registry approximately 65 % of patients with

complement deficiencies are susceptible to such infections, which are predominantly caused by encapsulated bacteria.[53] While patients with hereditary deficiencies of C3, alternative pathway regulators factor H and factor I or components of the classical pathway especially C1, C2 or C4 are generally vulnerable to bacterial infections such as *Streptococcus pneumoniae, Neisseria meningitidis* or *Hemophilus influenza,*[45,53–55] deficiencies of terminal complement pathway (C5-9) or alternative pathway components like properdin and factor D are more strongly associated with meningococcal infections.[45,46,53,56,57] Apart from encapsulated bacteria, also susceptibility towards viral, fungal or protozoan infections are under debate for deficiencies in the lectin pathway especially in immunosuppressive states, for example during the neonatal period, or during immunosuppressive treatments.[55,58,59]

In addition to infections, complement analysis is also indicated in the context of autoimmune diseases (**Table 2-1**). Frequently associated autoimmune diseases to the complement system comprise systemic lupus erythematosus (SLE), rheumatoid arthritis, autoantibody anti-neutrophil cytoplasmic antibody (ANCA)-associated vasculitis and other autoimmune disorders.[60,61] In many cases of SLE, the presence of autoantibodies, particularly those directed against the classical pathway protein C1q have been observed.[62] Consequently, complement consumption occurs due to a lack of functional C1q (acquired or inherited) and therefore ongoing immune complex formation as a result of the inability to effectively eliminate immune complexes and apoptotic materials.[63] It was shown, that the association between SLE and complement deficiency increases from deficiencies in the complement protein C2 (10 %) to C1r/s (50-57 %) to C4 (75 %) to C1q (90-93 %).[64]

Whilst hereditary or acquired angioedema are not complement-mediated diseases, instead they are classified as bradykinin-mediated or histaminergic diseases, the symptoms have traditionally been investigated using complement analysis.[65] The presence of angioedema without urticaria often manifests as subcutaneous and mucosal swellings affecting the face, upper airways, extremities, genitals or intestinal tract.[45] Several subtypes have been described partially connected to deficiencies or malfunction of the complement regulator C1-INH.[65] C1-INH not only serves as classical and lectin pathway regulator, but also regulates components in the contact system like factor XIIa[66] and kallikrein[67], in the coagulation system like factor XIa[68] and in the fibrinolytic system, such as thrombin[69]. Excessive bradykinin generation leading to angioedema can be caused by impaired inhibition of these enzymes.[70] Hence, analysis of the complement system protein levels and function, i.e. of C1-INH have been described as useful tools for diagnosis.[65]

In the case of aHUS, C3G and AMD, the key factor is the dysregulation of the alternative pathway, mostly inducing overactivation and consumption of the complement cascade.[71,72] aHUS is often caused due to genetic mutations in complement regulatory proteins,

predominantly factor H (FH) or the presence of anti-FH autoantibodies.[73] In the majority of cases, aHUS-related mutations have been shown to impair the complement regulation on host cells by for example comprising the binding of FH to endothelial cells.[74] This results in a subsequent absence of host cell protection, leading to microvascular thrombi, hemolytic anemia, thrombocytopenia, and kidney damage.[75] C3G is also driven by overactivation of the alternative complement pathway, leading to C3 deposition in the kidney's glomeruli.[76] C3G comprises two major subgroups, the dense deposit disease (DDD) and C3 glomerulonephritis (C3GN), which have overlapping clinical and pathological manifestations.[77] The deposition of C3 can result from genetic mutations, but mainly by acquired factors affecting complement regulation, such as autoantibodies.[78] The disease manifests as kidney dysfunction and has a poor prognosis without targeted therapies.[76] AMD is widely regarded as a leading cause of blindness in elderly individuals.[79] It is a multifactorial disease that is influenced by genetic predisposition, environmental factors, such as smoking, physical activity and diet, and the age of the patient.[72] Dysregulation of the complement system, particularly the alternative pathway regulator FH, plays a significant role in AMD.[80,81] Genetic studies have identified risk variants in complement-related genes, such as from FH and C3, which contribute to complement activation and inflammation in the retina.[82] This dysregulation can lead to chronic inflammation, increased susceptibility to oxidative stress, and extracellular matrix instability, all of which are risk factors for AMD.[83] Complement activation products, such as C3b and the MAC, accumulate in retinal tissues, potentially increasing damage to retinal pigment epithelial cells and Bruch's membrane.[83] In its advanced stages AMD leads to vision loss due to retinal degeneration or neovascularization.[72]

PNH is a very rare, hematopoietic stem cell disorder caused by somatic mutations in the PIG-A gene, leading to deficient glycosylphosphatidylinositol-anchored proteins (GPI-APs) responsible for anchoring other proteins to the surface of erythrocytes.[51,84–86] The absence of the GPI-anchored complement regulatory proteins CD55 and CD59 results in complement-mediated intravascular hemolysis, thrombosis, and bone marrow failure.[85] The clinical manifestations include anemia, hemoglobinuria, fatigue, abdominal pain, and thrombotic events.[85] Diagnosis is confirmed through flow cytometry to detect the absence of GPI-anchored proteins in granulocytes, monocytes and erythrocytes.[86] Treatment options include supportive care (e.g., supplementation, transfusions and anticoagulation) in addition to targeted complement inhibition for example via eculizumab, a monoclonal antibody that inhibits complement activation to prevent hemolysis.[86]

The multitude, severity and increasing awareness of these indications and diseases demonstrate a clear need for reliable, standardized and easy-to-perform complement assays to be able to assist in accurate analysis, diagnosis and treatments.

Table 2-1: Complement-related diseases and their causes.

Disease	Complement-related cause
Recurrent bacterial infections *Streptococcus pneumoniae, Neisseria meningitidis* or *Hemophilus influenza*	Complement deficiencies throughout the complement cascade impair host defense[45,46,53–57]
Viral, fungal, protozoan infections	Under debate if linked to lectin pathway deficiencies, especially in immunosuppressed states (e.g., neonates, immunosuppressive therapy)[55,58,59]
Autoimmune manifestations Systemic lupus erythematosus (SLE)	Inherited or acquired (autoantibodies) deficiencies (especially of / against C1q, C1r/s, C2, C4) leading to impaired clearance of immune complexes and apoptotic cells[62–64]
Rheumatoid arthritis	Complement activation often triggered by deposited autoantibodies, e.g rheumatoid factor, hence immune complexes, dying cells or exposed cartilage proteins in arthritic joints; mediating local inflammation through anaphylatoxins C3a and C5a[87,88]
ANCA-associated vasculitis	Mechanism not yet fully revealed; complement activation of the alternative pathway, feedback amplification loop between ANCA, neutrophils and complement activation, anaphylatoxin C5a plays a key role[89–91]
Angioedema without urticaria	Not complement but bradykinin-mediated; often due to C1-INH deficiency or dysfunction affecting regulation of contact, coagulation, and fibrinolytic systems[65–70]
Atypical hemolytic uremic syndrome (aHUS)	Often dysregulation of the alternative pathway; genetic mutations in factor H or anti-FH autoantibodies impairing host cell protection[73–75]
C3 glomerulopathy (C3G)	Dysregulation of the alternative pathway; C3 deposition in kidneys due to genetic mutations or acquired dysregulation, e.g. via autoantibodies[76–78]
Age-related macular degeneration (AMD)	Dysregulation of the alternative pathway; genetic risk variants, such as from FH and C3, can lead to chronic inflammation and retinal damage[80–83]
Paroxysmal nocturnal hemoglobinuria (PNH)	Somatic mutation in PIG-A gene; absence of GPI-anchored proteins (CD55, CD59), hence complement regulation causing complement-mediated hemolysis[51,84–86]

2.4 State-of-the-art in complement analysis

Investigations of complement system activity have traditionally been accomplished with hemolytic assays, allowing the analysis of the membrane attack complex (MAC) formation, the terminal step of the complement cascade. This provides insight into the functionality of the cascade reaction in its entirety, since complement activation is dependent on the integrity of each of the contributing components.[52] As such, they are instrumental in the investigation of

suspected complement dysregulation. Hemolytic assays are based on animal erythrocytes and protocols are often based on the method described by Mayer in 1961.[92] For the classical pathway, this protocol involves antibody-sensitized sheep erythrocytes and a full serum titration in Ca^{2+} and Mg^{2+} containing buffers for the determination of the CH50 value (**Figure 2-2**), the reciprocal serum dilution needed to achieve 50 % lysis of a fixed number of erythrocytes.[93] Similarly, the alternative pathway can be investigated with the AH50 value mostly analyzed using rabbit erythrocytes without antibody-modification in the presence of EGTA containing buffers supplemented with Mg^{2+} to remove biologically available Ca^{2+} ions (**Figure 2-2**).[93] This effectively blocks the activation of the classical and lectin pathway, enabling alternative pathway specific readouts.[94] Over the years also simplified variations have been developed reducing the serum titration to one single serum dilution enabling higher throughput analyses in diagnostic screenings.[95] Furthermore, hemolysis assays performed in agarose gels were developed to qualitatively screen for complement deficiencies.[96] The advantage of this approach is the direct visual readout but it lacks precise lysis quantification. Liposome-based approaches substituting animal erythrocytes with marker encapsulating liposomes were investigated occasionally[97,98] offering advantages especially in long-term stability and reproducibility. For the classical pathway, an automated, high-throughput liposome-based assay encapsulating an enzyme for signal amplification is established commercially, and is now widely implemented in clinical diagnostic settings (**Figure 2-3**).[5] However, it is important to note that currently no lysis-based assay analyzing the lectin pathway cascade functionality is available, neither through erythrocytes nor liposomes.

Overall, diagnostics of patients with suspected complement-associated diseases are often initiated by such hemolytic or liposome-based lysis assays assessing the total complement activity via titration of its serum.[99] This provides an overview on the general functionality of the complement system and its pathways to initiate subsequent, more refined analysis where needed.

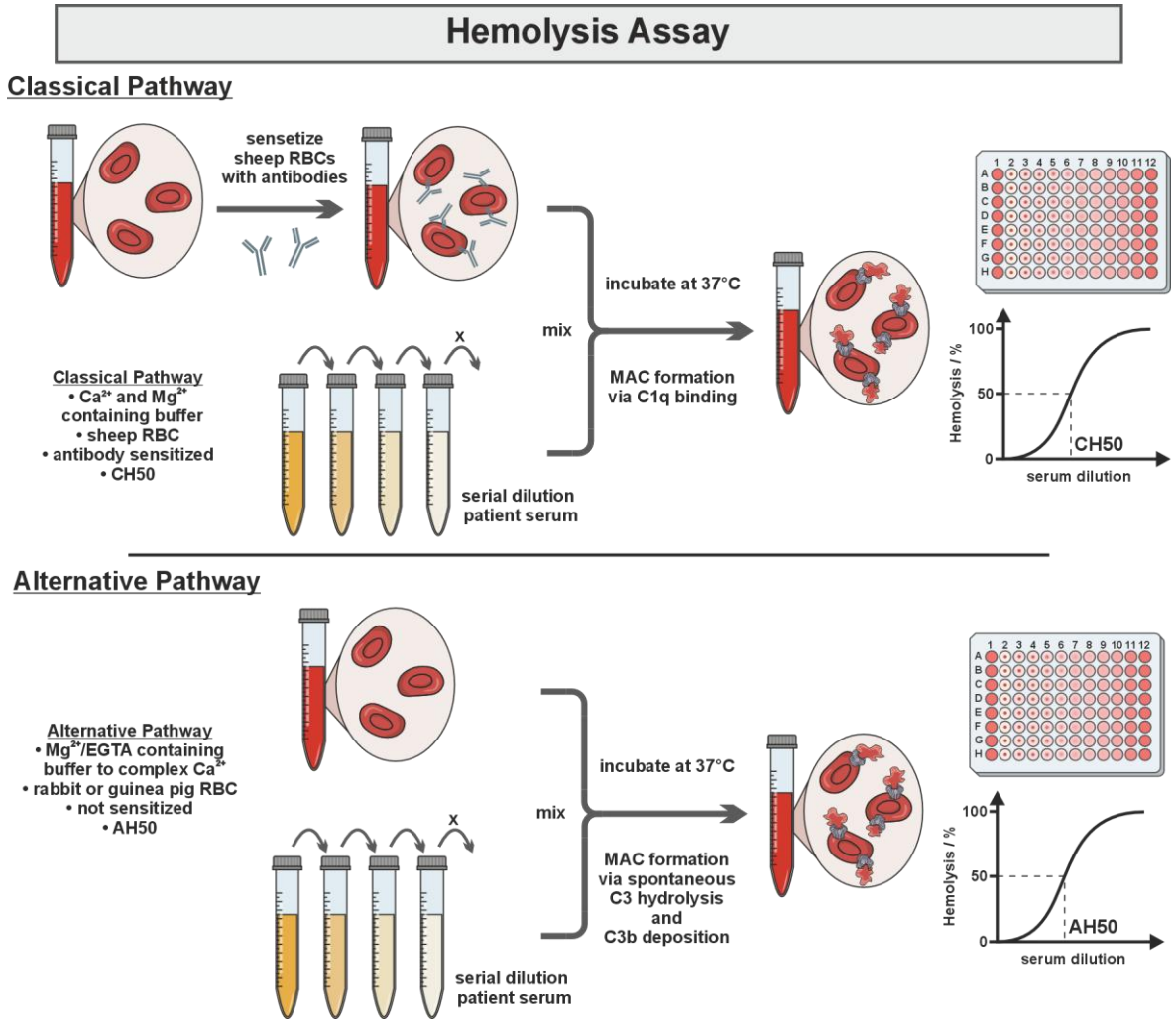

Figure 2-2: Lysis-based hemolytic assays for functional activity determination of the classical and alternative pathway. Hemolytic assays for the classical and alternative pathway differ in the applied animal red blood cells (RBCs) and buffers. Readout of the classical pathway requires sheep RBCs sensitized with antibodies and buffers with Mg^{2+} and Ca^{2+}. Readout of the alternative pathway requires rabbit or guinea pig RBCs lacking factor H protection, hence allowing alternative pathway mediated lysis and buffers with Mg^{2+}/EGTA to complex Ca^{2+} to inhibit both other pathways. Serial dilutions of patient sera incubated with the RBCs cause complement activation resulting in MAC formation and hemolysis. Absorbance readout allows the CH50 or AH50 determination. Both values represent the serum dilution required to cause 50 % lysis of the respective red blood cells. No hemolytic assay for the lectin pathway has been described.

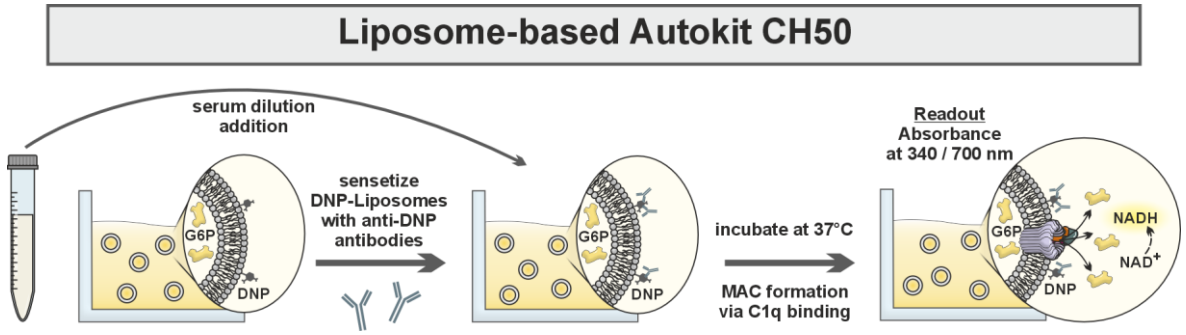

Figure 2-3: Liposome lysis-based complement assay for functional activity determination of the classical pathway. Liposomes encapsulating glucose-6-phosphate dehydrogenase (G6P) and functionalized with dinitrophenyl (DNP) are used as substitutes for animal red blood cells. Liposomes sensitized with anti-DNP antibodies as complement trigger cause classical pathway specific complement activation of the serum. Subsequent MAC formation causes G6P leakage depending on the respective complement activity. Released G6P reduces nicotinamide adenine dinucleotide (NAD^+) in the surrounding buffer to NADH, detected via absorbance measurements at 340 or 700 nm. No liposome-based assay for specific alternative and lectin pathway determination is commercially available.

Supplementary to functional assays based on erythrocyte or liposome lysis, functional enzyme-linked immunosorbent assays (ELISA) enable the detection of activation fragments throughout the complement cascade. These activation products include split fragments such as C3a, C3b, C4a, C4d, C5a, and Bb as well as inhibitor complexes like C1rs-C1 inhibitor or macromolecular complexes like the convertases or the soluble terminal complement complex (sC5b-9).[4] Specific monoclonal antibodies that recognize epitopes exposed only upon activation-induced conformational changes in complement proteins allows for the direct capture of activation fragments without interference from non-activated components.[100–105] The most prominent example is a semiquantitative, commercially available ELISA enabling the specific readout of the three main activation pathways (the classical, alternative, and lectin pathways) followed by the terminal pathway until sC5b-9 formation in their entirety and has come into wide use in routine diagnostic since commercialization (**Figure 2-4**).[106] In contrast to the currently available lysis-based approaches, this assay allows the functional readout of the lectin pathway, more precisely the activation via the mannose-binding-lectin pathway. In addition to this commercially available assay another ELISA enabling the readout of the lectin pathway via the ficolin 3-activation route has been described in literature, but not commercialized.[107]

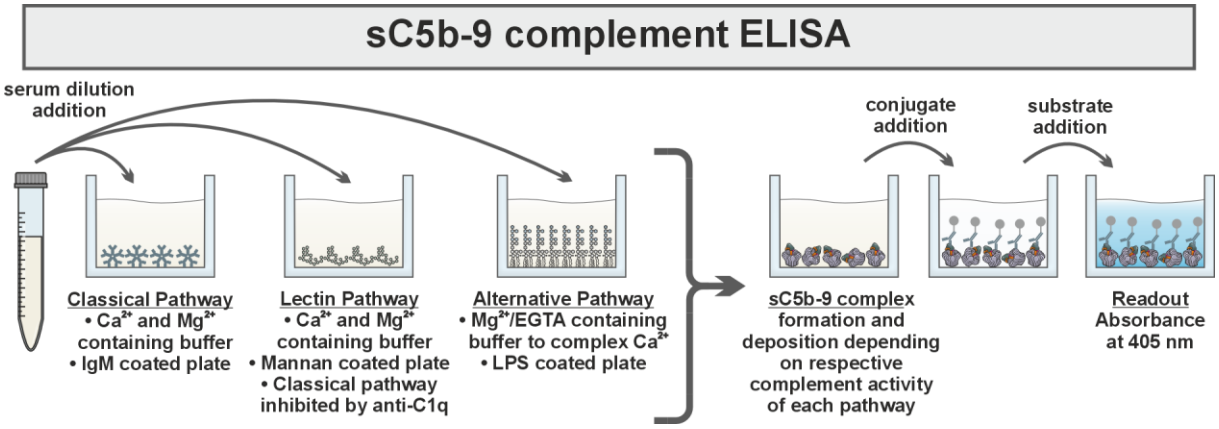

Figure 2-4: ELISA-based complement assays for all three complement pathways via soluble membrane attack complex determination (sC5b-9). Classical pathway readout is based on IgM plate coating, lectin pathway readout is based on mannan plate coating and alternative pathway readout is based on lipopolysaccharide (LPS) coated plates. Readout of the classical and lectin pathway requires buffers with Mg^{2+} and Ca^{2+}. Readout of the alternative pathway requires buffers with Mg^{2+}/EGTA to complex Ca^{2+} to inhibit both other pathways. The lectin pathway readout is performed including anti-C1q antibodies during incubation with serum to inhibit classical pathway activation. Assay follows standard ELISA procedures with coated plates, incubation with serum dilution(s), conjugate and substrate addition including washing steps in between each incubation step. An alkaline phosphatase-labelled detection antibody against C9 is often used in commercial assay kits. Absorbance measurements at 405 nm enable the evaluation of the respective complement activation.

The analysis of complement activity by an initial screening with general functional assays, investigating the complement cascade in its entirety can be refined by followed immunochemical assays focusing on the quantification of individual initial complement components, regardless of their functional activity. Applied immunochemical methods comprise various techniques, including immunoprecipitation assays like radial

immunodiffusion (RID) or nephelometry, ELISAs, and Western blots measuring concentrations of specific proteins.[52,108] In immunoprecipitation assays RID measures the concentration of the proteins by forming immune complexes in a gel[109] and nephelometry determines the concentration in homogeneous solution by detecting the light scattered by these immune complexes.[110] In routine diagnostics, the most frequently measured components are C3 and C4 in order to assess suspected immunodeficiencies.[52] In instances where a deficiency is also confirmed through immunochemical methods, further refined functional analysis of the individual complement proteins may not be necessary. Conversely, in cases where no deficiency is detected, additional assays focusing on the functionality and activity of the individual components may be required.

Apart from these methods focused on the complement proteins themselves, autoimmune diseases need the analysis of potential autoantibodies targeting the individual's own complement proteins and thereby altering complement activation and regulation. Most relevant are the analysis of antibodies directed against C1q, C1-INH, the C3 convertase and FH.[4] Detection of antibodies against C1q, C1-INH and FH are mostly based on commercial or in-house ELISAs quantifying the antibodies bound to the respective target immobilized in a micro titer plate.[4,111–113] Autoantibodies directed against the C3 convertase (C3 nephritic factors, C3NeF) stabilize the convertase and therefore cause increased complement consumption of the downstream cascade. Their analysis either comprises mere quantification or preferably includes verification of their actual ability to influence the C3 convertase stability in a functional assay, which provides the more relevant information for subsequent treatment.[114] Whereas quantification of C3NeF is mostly based on ELISAs, functional assays are currently all hemolysis-based using animal erythrocytes.[114]

Genetic analyses are acquired to confirm inherent complement deficiencies or investigate complement component mutations or polymorphisms in certain diseases. Inherent complement deficiencies are very rare since they are often based on rare homozygous mutations.[2,115] Since genetic analyses are more expensive and time consuming compared to other methods, they are not performed for screening purposes.[116] Furthermore, it is often already sufficient to identify missing or malfunctioning complement components with the aforementioned methods.[116] Nevertheless, they can be advantageous in verifying hereditary mutations and identifying carriers of such mutations among relatives or help to distinguish clinically similar diseases [116]. Genetic analyses generally include amplification of the respective exons and sequencing of the amplified DNA strands to detect mutations.[116]

Despite its frequent application in general proteomics, mass spectrometry is not a routinely utilized technique in complement analysis. Nonetheless, "complementomics" have recently

been described as a suitable method to quantify complement proteins in a multiplexed approach for determining complement deficiencies.[117]

It can be concluded that initial and general complement diagnostics are primarily based on either erythrocyte or ELISA based. While the main disadvantages of the erythrocyte assay are high setup variability from lab-to-lab and difficulties in their reproducibility as well as the lack of the lectin pathway readout, ELISA-based functional complement assays can not provide a direct proof for complement lysis only quantifying the soluble MAC formation. The sole liposome-based assay that is presently available is an appropriate advancement in this field, insofar as it provides an artificial, analytical chemistry-driven solution, which is a designable and standardizable vesicle substituting erythrocytes. It very powerfully demonstrates its capability for the classical pathway and may offer a solution for all three individual pathways in the future.

2.5 Liposome introduction

Liposomes are a highly versatile class of structures that have been described as self-assembled lipid bilayer structures containing an inner aqueous cavity (**Figure 2-5**).[118,119] These structures have attracted significant attention in a number of fields, including drug delivery, biosensing and bioanalysis.[120–122] These artificial vesicles, primarily constituted of phospholipids, mimic biological membranes and can serve as effective carriers of hydrophilic compounds within the aqueous cavity and hydrophobic compounds within the lipid bilayer, depending on their application.[121,123,124] Their unique properties, such as biocompatibility, biodegradability and especially their versatility in membrane characteristics, encapsulation and surface modifications, make them ideal candidates for various medical and bioanalytical applications.[120–122] Encapsulation of compounds in clinical settings range from anticancer drugs[121], antibiotics[125] and genetic materials[126]. In bioanalytical or biosensing applications, the substantial internal volume of the cavity together with the large outer surface area renders them an ideal tool for signal amplification in various biosensing modalities.[120,122] A single binding event between target and liposome subsequently results in the signal amplification through multiple entrapped signaling molecules. Molecules encapsulated inside the liposomes range from fluorescent dyes[127], electroactive species[128] or enzymes[129,130].

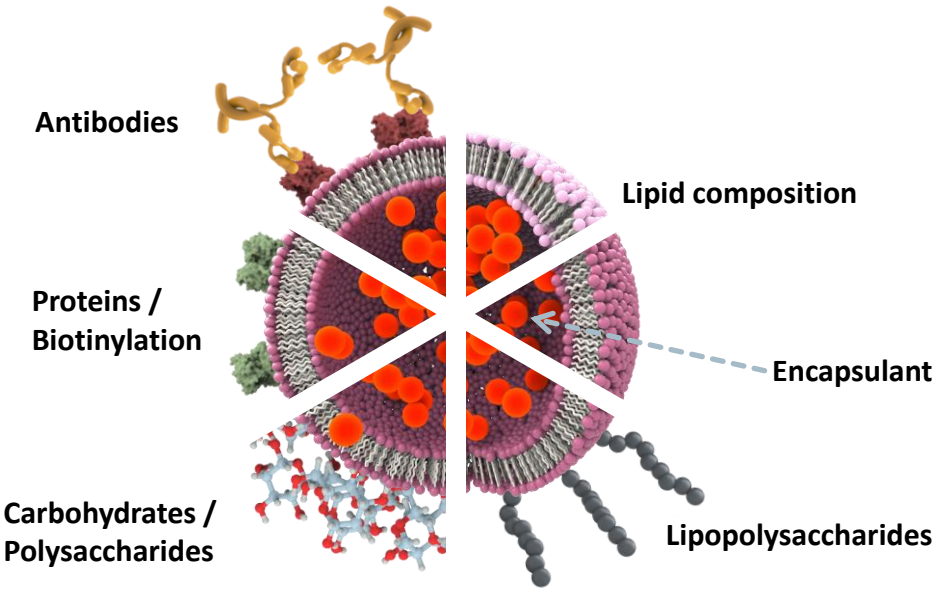

Figure 2-5: Schematic overview of the liposome structure and parameters enabling flexibility in liposome characteristics. Lipid composition allows flexibility in liposome characteristics with respect to surface charge, functionality (such as amine or carboxylic groups), biocompatibility and stability. Encapsulants enable variability in application such as optical, electrochemical or drug delivery approaches. Flexibility in surface modifications allows for adaptability to the respective requirements of the application and can range from carbohydrates, proteins to antibodies.

The discovery of liposomes dates back to 1965 when Bangham et al.[131] first demonstrated the spontaneous formation of closed bilayer vesicles composed of phospholipids in aqueous solutions. This groundbreaking finding laid the foundation for extensive research focused on the optimization of liposome formulations to enhance their biocompatibility, drug efficacy and safety in medical applications,[124,132–135] as well as sensitivity, versatility and long-term stability in bioanalytical applications.[120,136–140] Since their initial discovery several synthesis methods have been described including conventional methods such as thin film hydration, reverse phase evaporation and alcohol injection or more recent approaches mainly developed with the focus of higher encapsulation efficiency and large-scale production such as methods based on microfluidics, supercritical fluids or freeze drying.[141,142] Depending on the synthesis method and the lipid composition the resulting liposomes can be classified into categories based on their size and lamellarity. Liposomes which only have one bilayer separating the inner and outer aqueous phase can be classified into small unilamellar vesicles (SUVs, 20-100 nm), large unilamellar vesicles (LUVs, 0.1-1 µm) and giant unilamellar vesicles (GUVs, >1 µm) (**Figure 2-6**).[119] Liposomes with multiple bilayers can be categorized in oligolamellar vesicles (OLVs, 100-500 nm, 2-5 bilayers), multilamellar vesicles (MLVs, >0.5 mm, >5 bilayers) with concentric bilayers, and multivesicular vesicles (MVVs, >1 µm) in case a single bilayer encapsulates several separate bilayer vesicles (**Figure 2-6**).[143]

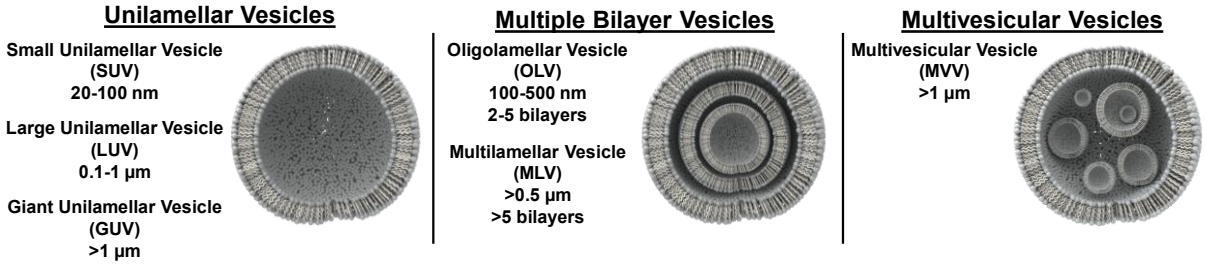

Figure 2-6:Classification of liposomes according to lamellarity and size.

Apart from the size, liposomes can be altered in their membrane characteristics, such as membrane fluidity, functionality and surface charge. For example, the incorporation of cholesterol highly influences the membrane fluidity and lipid distribution (**Figure 2-5**).[144,145] Moreover, the use of special lipids and surface modifications allow for controlled encapsulant release. Such liposomes can for example respond to specific environmental triggers, such as pH changes or heat, or can be targeted towards desired sites of action due to surface modifications with specific recognition elements, such as antibodies or peptides.[146]

Liposome characterization after successful synthesis often comprises methods to analyze the size and morphology of the liposomes, analysis of the surface charge, encapsulation efficiency, liposome concentration and liposome stability.[147]

Size and morphology are mostly analyzed via dynamic light scattering (DLS) and electron microscopy, for example scanning electron microscopy or cryo-transmission electron microscopy.[147] DLS measures the size and size distribution of particles by analyzing the fluctuations in scattered light caused by Brownian motion. The hydrodynamic diameter is calculated based on the diffusion coefficient, providing information on particle uniformity and aggregation.[148] Electron microscopy methods have established as precise method to determine the lamellarity of the liposomes.[149] The surface charge is mainly assessed through zeta potential measurements, which are a measure of the electrical potential at the interface between a particles surface and the surrounding liquid medium.[150] This is an important parameter determining the stability of such liposome dispersions and can also be significant for their reactivity towards biological systems.[151–153] Analysis of the encapsulation efficiency is highly dependent on the entrapped molecule and can range from UV-VIS, fluorescent, enzymatic, high-performance liquid chromatography or electrochemical analyses.[147] In most cases, the liposome or lipid concentration is determined through techniques quantifying the phosphate concentration of the phospholipids for example via Bartlett assays or inductively coupled plasma.[147,154] In addition also nanoparticle tracking analysis can directly count the liposome particles in solution allowing for the analysis of particle number concentrations.[155]

The primary application of liposomes within the medical field remains drug delivery.[156] However, they are also employed in vaccines[157] and gene therapy[126]. The bioanalytical

applications of liposomes consist of a variety of uses, including immunoassays[154,158], microfluidic devices[159,160], lateral flow assays[161,162] and the use as biomimics[163,164]. In the context of complement-related research, the general reactivity of the complement system towards liposomes has been studied with increased focus on enhancing circulation time of liposomes in the blood stream[165–167] as well as with focus on liposomes as substitute for erythrocyte-based assays.[5] Studying the reactivity of the complement system towards liposomes in medical applications is of relevance since liposomal drugs are frequently exposed to the bloodstream, leading to protein deposition and subsequent clearance and the complement system being one of the relevant factors contributing to this clearance.[168] Consequently, general studies included investigations of liposome and lipid interactions with complement proteins.[165] While frustratingly contrary results are described in literature, the general trends of complement promoting factors are charged liposomes (positively charged vesicles may rather activate the alternative pathway, while negatively charged liposomes may rather activate the classical pathway), liposome size (smaller liposomes are more complement stable compared to larger ones) and cholesterol content, with increasing content leading to complement activation.[165] To circumvent complement activation the incorporation of polyethylene glycol (PEG) on the liposome surface has been shown to reduce opsonization and prolong circulation time, i.e. making these liposomes less susceptible to clearance.[169,170] However, unfortunately the subsequent widespread use of PEGylation in pharmaceuticals, food and cosmetic products has now resulted in abundant presence of anti-PEG antibodies in many patients which cause accelerated clearance of PEGylated particles[171], significantly induced due to increased activation of the complement system by such surface bound anti-PEG antibodies.[166] Hence, investigations on stealth, serum and complement stable liposomes remains an important research question which necessitates a long-term solution.

The readout of complement system activation with liposome-based assays has been described occasionally including liposomes encapsulating glucose[172], fluorophores[97,173] or enzymes[5]. The development of liposomes that encapsulate enzymes has reached a point where the aforementioned commercial assay has been created, enabling the readout of the classical pathway.[5] Nonetheless, structured investigation on a liposome platform, capable of analyzing more than just one pathway specifically, is completely lacking and involves an interdisciplinary understanding of liposomes, surface chemistries and the complement system.

2.6 The complement field as raising market

The scientifically long neglected complement system has not only gained significant interest in fundamental studies of its complex action cascade, many components and potential medical relevance. Instead, also tightly related to unveiling the participation of the complement system

in diseases is the increasing interest and increasing number of participating labs in the external quality assurance program (EQA) established in 2010 and organized and evaluated now by INSTAND.[174] This program started with the comparison of the activity of the three complement pathways, C3, C4, C1q and C1-INH protein levels and activity among 12 participating laboratories.[175] Until the year 2022 the number of participating laboratories increased to 347 investigating up to 20 parameters of the complement system including overall pathway functionality, protein levels and function as well as activation products and autoantibodies.[176] This clearly indicates a raising market which demands the development of companion diagnostics assisting in diagnosis and treatment monitoring. This trend is further evidenced by the enhanced accessibility of commercial complement assay kits over recent years. ELISA kits for research use investigating pathway functionality, complement protein and activation product levels of over 20 components or complement hemolysis assays are available from companies such as HycultBiotech Inc.[177], Creative Biolabs Inc.[178], HaemoScan BV[179] and Invitrogen/Thermo Fisher Scientific Inc.[180]. Svar Life Science AB offers the Wieslab® complement assay ELISA kits widely used in complement diagnostics and research for pathway activity determination.[181] This includes also the only currently commercially available lectin (i.e. MBL) pathway kit. Alternatively, QuidelOrtho Corporation also offers complement assay kits for diagnostic purposes.[182] FUJIFILM Wako Chemicals Europe GmbH offers the liposome-based Autokit CH50 for diagnostic classical pathway functional activity determination.[183] Apart from single complement protein detection per assay, more recently also multiplexed formats allowing the simultaneous quantification of up to 10 complement proteins reached the market.[184–186]

Moreover, recent advancements in available and FDA-approved complement inhibitors signify that the entire complement research and diagnostic field is a growth market. Driven by a growing understanding of the complement system's role in various diseases and the successful clinical application of targeted therapies as of now, there are 13 approved complement therapeutics including C1-INH.[187] In addition to these established therapies, the pipeline for complement-targeted treatments includes even more therapeutics over all stages of clinical development.[188–190] Notable companies participating in the development of these innovative therapies include Alexion Pharmaceuticals Inc./AstraZeneca PLC[191], Apellis Pharmaceuticals Inc.[192], Chemocentryx Inc./Amgen Inc.[193], and Omeros Corporation[194], among others.

2.7 Critical factors for successful complement analysis

Successful complement analysis and accurate results can only be obtained when reliable assays are paired with the correct sample handling before complement analysis.[195] *In vivo* complement activation induced through proteolytic cleavage or conformational changes after

protein interactions is regulated by other immune responses such as immune cells and includes consumption of complement activation products.[50] In contrast, *in vitro* activation of the complement system in serum or plasma samples causes raising levels of activation products which remain in the sample, since they are not consumed through other immune responses, and do not reflect to the true *in vivo* levels.[50] Additionally, *in vitro* cleaved complement components cannot be compensated through new expression as it would be the case *in vivo*. *In vitro* complement activation often is caused by elevated temperatures or repeated freeze thaw cycles, since complement is a temperature sensitive system.[195–197] However, bubble formation through rigorous mixing can also induce premature complement activation.[198] Consequently, in the event of *in vitro* complement activation during sample handling prior to analytical measurements, a falsified, i.e. a reduced complement activity would be determined for the respective activated complement pathways in functional assay formats.[50] Therefore, appropriate preanalytical sample handling is of utmost importance for accurate and reliable complement analysis.[50] Furthermore, requirements for sample handling prior to analytical measurements can vary depending on the type of analysis being conducted, i.e. whether the complement function or quantity of individual components is assessed.[199] For complement functionality analyses serum, or hirudin plasma as alternative, is the preferred matrix, since both are free of directly complement inhibiting additives.[199] Hirudin or recombinant hirudin, lepirudin, allows complement activation while preventing coagulation when used at appropriate concentrations.[199–202] For quantification of individual complement components, plasma containing either EDTA or citrate as anticoagulant should be used. These chelate Ca^{2+} and Mg^{2+} ions and consequently minimize artificial complement activation during sample collection by inhibiting the C1 complex and C3 convertase function which are dependent on these ions and responsible for initiation of the complement cascade.[1,199,203,204] This allows lower complement activation product base levels in plasma compared to serum, hence provides more accurate levels, i.e. more comparable to the *in vivo* concentrations.[199,203,204] Heparin is another frequently employed anticoagulant. However, this should be avoided due to its strong interactions with numerous complement proteins and regulators.[205] These interactions affect the complement function and consequently interfere with reliable complement analysis.[204,205]

Since complement is a temperature sensitive system and can thus also be activated through elevated temperatures [195,196], sample collection should be performed according to suitable protocols to avoid premature complement activation. For serum samples it is suggested to let the blood coagulate in the collection tube for around 30 min at RT.[199,201,203] Clotting is initiated through the tube surface, often glass or clot activators such as silica particles or thrombin often contained in PET collection tubes, sometimes also combined with gel separators.[203] Investigations by Andersson et al.[203] focusing on the differences of serum collected in different collection tubes showed that in all cases accurate functional activity could be determined using

functional ELISAs for the classical and alternative pathway. However, elevated complement activation marker levels were observed. Especially the alternative pathway marker C3bBbP, the lectin pathway marker MASP-1/C1-INH and the general C3 activation marker C3bc levels were increased in all collection tubes containing clot activators, except silica particles, in comparison to those without clot activators.[203] Despite that, silica particle based clot activators were also shown to potentially influence complement analysis through depletion of the complement protein ficolin 2 and therefore altering subsequent lectin pathway analyses.[199,204,206,207] Hence, it can be concluded that the appropriate collection tube must always be selected according to the subsequent application and such information is even vital in any publication to ensure comparability. After coagulation, the clot and red blood cells should be centrifuged in a refrigerated centrifuge at 4 °C, 2000 g for 10 min.[199] For storage, serum should be frozen quickly and be stored at -80 °C since higher storage temperatures still promote *in vitro* complement activation.[50,199,201] Especially in the case of functional complement assays, where serum is used as matrix, suitable buffers which meet the requirements of the pH sensitive [208] and Ca^{2+}- and Mg^{2+}-dependent[1] complement system are essential to ensure functionality and to avoid artificial complement activation. Traditional buffers are based on barbitone containing gelatin veronal buffers and contain 0.15 mM Ca^{2+} and 0.5 mM Mg^{2+} with a pH of 7.3. Despite the toxicity of barbitone and its stringent regulations it still persists in many complement assays, even though alternatives based on HEPES were successfully described and implemented.[209]

For plasma production, plasma collection tubes containing the anticoagulants (for EDTA ideally above 10 mM should be used for complete complement inhibition[175]) should be placed on ice quickly.[199] Red blood cells should be removed quickly via centrifugation in a refrigerated centrifuge within 60 minutes after collection.[199] For storage, isolated plasma should again be frozen quickly and be stored at -80 °C.

Besides these matrix dependent requirements, it is generally advisable to avoid elevated temperatures, bubble formation through rigorous mixing and repeated freeze thaw cycles during sample preparation to avoid artificial pre-analytical complement activation.

2.8 Standardization in the complement field

From an analytical point of view, the clear need for standardized complement analysis can be expressed, which asks for standardization in reference materials, evaluation methods and applied assays. Initiation of the EQA through the International Complement Society together with INSTAND[174] provides an opportunity for laboratories to be validated for their applied methods.[176] However, this program is subject to limitations, which include the limited accessibility of appropriate samples and the low number of participating laboratories for some

of the test categories.[176] These factors influence the actual value of the determined laboratory passing quotas. Furthermore, it can generally be stated that the lack of available international calibrators and control materials impedes new assay developments. An international serum standard for the detection of human complement activation products as an internationally available reference material[210] was a first breakthrough development. Yet there is an equal need for internationally available standards applicable to analysis methods focusing on the complement functionality and not on mere protein quantification. Apart from reference samples, assay procedures and assay materials require standardization. While this is more readily achievable for ELISAs, which can also easily be automated, it is very difficult for assays that rely on animal products, such as the erythrocyte hemolysis assay. Animal erythrocytes, including those from sheep, are known to exhibit seasonal differences[211–213] and sheep erythrocytes used for complement assays usually are not recommended to be used after several weeks of storage.[214] This makes reproducible results more than challenging even when following the same sample handling. Here, liposomes could provide a suitable alternative with their flexibility and adjustability of surface characteristics, enabling the preparation of standardized, long-term stable vesicles.[120,138] They can also be produced animal product-free, offer complete chemical control, are suitable for mass production, and are highly adaptable to evolving assay requirements. In addition, liposome-based assays reduce procedural complexity by eliminating the need for handling biological materials, improve batch-to-batch consistency, and hence are much better suited for integration into automated and high-throughput platforms.

Underestimated is the importance of subsequent assay evaluation, especially for functional lysis assays. Efforts to harmonize evaluation through calibration with a normal pooled control sample[176] may help in the simplest case where only one serum concentration is evaluated, but remains a challenge when several sample concentrations have to be reduced to one comparable value, which is highly dependent on the chosen evaluation method. Hence direct comparability between obtained values of the assays would require standardized evaluation protocols and currently means, that the obtained results for the same samples from different assays or laboratories are not necessarily interchangeable.[176]

2.9 References

(1) Merle, N. S.; Church, S. E.; Fremeaux-Bacchi, V.; Roumenina, L. T. Complement System Part I - Molecular Mechanisms of Activation and Regulation. *Front Immunol* **2015**, *6*, 262. DOI: 10.3389/fimmu.2015.00262.

(2) Grumach, A. S.; Kirschfink, M. Are complement deficiencies really rare? Overview on prevalence, clinical importance and modern diagnostic approach. *Mol Immunol* **2014**, *61*, 110–117. DOI: 10.1016/j.molimm.2014.06.030.

(3) Nandakumar, V.; Braun, K. M. P.; Willrich, M. A. V. Challenges for complement functional assays in the clinical laboratory: From test validation to clinical interpretation. *J Immunol Methods* **2025**, *537*, 113824. DOI: 10.1016/j.jim.2025.113824.

(4) Skattum, L. Clinical Complement Analysis-An Overview. *Transfus Med Rev* **2019**, *33*, 207–216. DOI: 10.1016/j.tmrv.2019.09.001.

(5) Yamamoto, S.; Kubotsu, K.; Kida, M.; Kondo, K.; Matsuura, S.; Uchiyama, S.; Yonekawa, O.; Kanno, T. Automated homogeneous liposome-based assay system for total complement activity. *Clin Chem* **1995**, *41*, 586–590. DOI: 10.1093/clinchem/41.4.586.

(6) Ricklin, D.; Hajishengallis, G.; Yang, K.; Lambris, J. D. Complement: a key system for immune surveillance and homeostasis. *Nat Immunol* **2010**, *11*, 785–797. DOI: 10.1038/ni.1923.

(7) Carroll, M. V.; Sim, R. B. Complement in health and disease. *Adv Drug Delivery Rev* **2011**, *63*, 965–975. DOI: 10.1016/j.addr.2011.06.005.

(8) Cerenius, L.; Kawabata, S.; Lee, B. L.; Nonaka, M.; Söderhäll, K. Proteolytic cascades and their involvement in invertebrate immunity. *Trends Biochem Sci* **2010**, *35*, 575–583. DOI: 10.1016/j.tibs.2010.04.006.

(9) West, E. E.; Kemper, C. Complosome - the intracellular complement system. *Nat Rev Nephrol* **2023**, *19*, 426–439. DOI: 10.1038/s41581-023-00704-1.

(10) Merle, N. S.; Noe, R.; Halbwachs-Mecarelli, L.; Fremeaux-Bacchi, V.; Roumenina, L. T. Complement System Part II: Role in Immunity. *Front Immunol* **2015**, *6*, 257. DOI: 10.3389/fimmu.2015.00257.

(11) Bally, I.; Rossi, V.; Lunardi, T.; Thielens, N. M.; Gaboriaud, C.; Arlaud, G. J. Identification of the C1q-binding Sites of Human C1r and C1s: a refined three-dimensional model of the C1 complex of complement. *J Biol Chem* **2009**, *284*, 19340–19348. DOI: 10.1074/jbc.M109.004473.

(12) Reid, K. B. M. Complement Component C1q: Historical Perspective of a Functionally Versatile, and Structurally Unusual, Serum Protein. *Front Immunol* **2018**, *9*, 764. DOI: 10.3389/fimmu.2018.00764.

(13) Beurskens, F. J.; van Schaarenburg, R. A.; Trouw, L. A. C1q, antibodies and anti-C1q autoantibodies. *Mol Immunol* **2015**, *68*, 6–13. DOI: 10.1016/j.molimm.2015.05.010.

(14) Diebolder, C. A.; Beurskens, F. J.; Jong, R. N. de; Koning, R. I.; Strumane, K.; Lindorfer, M. A.; Voorhorst, M.; Ugurlar, D.; Rosati, S.; Heck, A. J. R.; van de Winkel, J. G. J.; Wilson, I. A.; Koster, A. J.; Taylor, R. P.; Saphire, E. O.; Burton, D. R.; Schuurman, J.; Gros, P.; Parren, P. W. H. I. Complement is activated by IgG hexamers assembled at the cell surface. *Science* **2014**, *343*, 1260–1263. DOI: 10.1126/science.1248943.

(15) Bally, I.; Inforzato, A.; Dalonneau, F.; Stravalaci, M.; Bottazzi, B.; Gaboriaud, C.; Thielens, N. M. Interaction of C1q With Pentraxin 3 and IgM Revisited: Mutational Studies With Recombinant C1q Variants. *Front Immunol* **2019**, *10*, 461. DOI: 10.3389/fimmu.2019.00461.

(16) McGrath, F. D. G.; Brouwer, M. C.; Arlaud, G. J.; Daha, M. R.; Hack, C. E.; Roos, A. Evidence that complement protein C1q interacts with C-reactive protein through its

globular head region. *J Immunol* **2006**, *176*, 2950–2957. DOI: 10.4049/jimmunol.176.5.2950.

(17) Roumenina, L. T.; Popov, K. T.; Bureeva, S. V.; Kojouharova, M.; Gadjeva, M.; Rabheru, S.; Thakrar, R.; Kaplun, A.; Kishore, U. Interaction of the globular domain of human C1q with Salmonella typhimurium lipopolysaccharide. *Biochim Biophys Acta* **2008**, *1784*, 1271–1276. DOI: 10.1016/j.bbapap.2008.04.029.

(18) Albertí, S.; Marqués, G.; Hernández-Allés, S.; Rubires, X.; Tomás, J. M.; Vivanco, F.; Benedí, V. J. Interaction between complement subcomponent C1q and the Klebsiella pneumoniae porin OmpK36. *Infect Immun* **1996**, *64*, 4719–4725. DOI: 10.1128/iai.64.11.4719-4725.1996.

(19) Païdassi, H.; Tacnet-Delorme, P.; Garlatti, V.; Darnault, C.; Ghebrehiwet, B.; Gaboriaud, C.; Arlaud, G. J.; Frachet, P. C1q binds phosphatidylserine and likely acts as a multiligand-bridging molecule in apoptotic cell recognition. *J Immunol* **2008**, *180*, 2329–2338. DOI: 10.4049/jimmunol.180.4.2329.

(20) Kapogianni, A.; Radulova, G.; Donev, V.; Videv, P.; Cholakova, G.; Iliev, S.; Ivanova, A.; Bogoeva, V.; Tsacheva, I. Characterization of the binding of the globular domains of the complement component C1q to phosphatidylserine. *Int J Biol Macromol* **2025**, *291*, 139116. DOI: 10.1016/j.ijbiomac.2024.139116.

(21) Païdassi, H.; Tacnet-Delorme, P.; Lunardi, T.; Arlaud, G. J.; Thielens, N. M.; Frachet, P. The lectin-like activity of human C1q and its implication in DNA and apoptotic cell recognition. *FEBS Lett* **2008**, *582*, 3111–3116. DOI: 10.1016/j.febslet.2008.08.001.

(22) Mortensen, S. A.; Sander, B.; Jensen, R. K.; Pedersen, J. S.; Golas, M. M.; Jensenius, J. C.; Hansen, A. G.; Thiel, S.; Andersen, G. R. Structure and activation of C1, the complex initiating the classical pathway of the complement cascade. *PNAS* **2017**, *114*, 986–991. DOI: 10.1073/pnas.1616998114.

(23) Wallis, R.; Mitchell, D. A.; Schmid, R.; Schwaeble, W. J.; Keeble, A. H. Paths reunited: Initiation of the classical and lectin pathways of complement activation. *Immunobiology* **2010**, *215*, 1–11. DOI: 10.1016/j.imbio.2009.08.006.

(24) Gaboriaud, C.; Ling, W. L.; Thielens, N. M.; Bally, I.; Rossi, V. Deciphering the fine details of c1 assembly and activation mechanisms: "mission impossible"? *Front Immunol* **2014**, *5*, 565. DOI: 10.3389/fimmu.2014.00565.

(25) Bohlson, S. S.; Garred, P.; Kemper, C.; Tenner, A. J. Complement Nomenclature-Deconvoluted. *Front Immunol* **2019**, *10*, 1308. DOI: 10.3389/fimmu.2019.01308.

(26) Garred, P.; Genster, N.; Pilely, K.; Bayarri-Olmos, R.; Rosbjerg, A.; Ma, Y. J.; Skjoedt, M.-O. A journey through the lectin pathway of complement-MBL and beyond. *Immunol Rev* **2016**, *274*, 74–97. DOI: 10.1111/imr.12468.

(27) Dobó, J.; Pál, G.; Cervenak, L.; Gál, P. The emerging roles of mannose-binding lectin-associated serine proteases (MASPs) in the lectin pathway of complement and beyond. *Immunol Rev* **2016**, *274*, 98–111. DOI: 10.1111/imr.12460.

(28) Ekdahl, K. N.; Mohlin, C.; Adler, A.; Åman, A.; Manivel, V. A.; Sandholm, K.; Huber-Lang, M.; Fromell, K.; Nilsson, B. Is generation of C3(H2O) necessary for activation of the alternative pathway in real life? *Mol Immunol* **2019**, *114*, 353–361. DOI: 10.1016/j.molimm.2019.07.032.

(29) Fromell, K.; Adler, A.; Åman, A.; Manivel, V. A.; Huang, S.; Dührkop, C.; Sandholm, K.; Ekdahl, K. N.; Nilsson, B. Assessment of the Role of C3(H2O) in the Alternative Pathway. *Front Immunol* **2020**, *11,* No. 530 vols.

(30) Lachmann, P. J. Looking back on the alternative complement pathway. *Immunobiology* **2018**, *223*, 519–523. DOI: 10.1016/j.imbio.2018.02.001.

(31) Nilsson, B.; Nilsson Ekdahl, K. The tick-over theory revisited: is C3 a contact-activated protein? *Immunobiology* **2012**, *217*, 1106–1110. DOI: 10.1016/j.imbio.2012.07.008.

(32) Lachmann, P. J. In Advances in Immunology; Alt, Frederick W., Ed.; Academic Press, 2009; pp. 115–149.

(33) Harboe, M.; Mollnes, T. E. The alternative complement pathway revisited. *J Cell Mol Med* **2008**, *12*, 1074–1084. DOI: 10.1111/j.1582-4934.2008.00350.x.

(34) Pangburn, M. K.; Rawal, N. Structure and function of complement C5 convertase enzymes. *Biochem Soc Trans* **2002**, *30*, 1006–1010. DOI: 10.1042/bst0301006.

(35) Berends, E. T. M.; Gorham, R. D.; Ruyken, M.; Soppe, J. A.; Orhan, H.; Aerts, P. C.; Haas, C. J. C. de; Gros, P.; Rooijakkers, S. H. M. Molecular insights into the surface-specific arrangement of complement C5 convertase enzymes. *BMC Biol* **2015**, *13*, 93. DOI: 10.1186/s12915-015-0203-8.

(36) Morgan, B. P.; Boyd, C.; Bubeck, D. Molecular cell biology of complement membrane attack. *Semin Cell Dev Biol* **2017**, *72*, 124–132. DOI: 10.1016/j.semcdb.2017.06.009.

(37) Menny, A.; Serna, M.; Boyd, C. M.; Gardner, S.; Joseph, A. P.; Morgan, B. P.; Topf, M.; Brooks, N. J.; Bubeck, D. CryoEM reveals how the complement membrane attack complex ruptures lipid bilayers. *Nat Commun* **2018**, *9*, 5316. DOI: 10.1038/s41467-018-07653-5.

(38) Buelli, S.; Imberti, B.; Morigi, M. The Complement C3a and C5a Signaling in Renal Diseases: A Bridge between Acute and Chronic Inflammation. *Nephron* **2024**, *148*, 712–723. DOI: 10.1159/000538241.

(39) Klos, A.; Wende, E.; Wareham, K. J.; Monk, P. N. International Union of Basic and Clinical Pharmacology. corrected. LXXXVII. Complement peptide C5a, C4a, and C3a receptors. *Pharmacol Rev* **2013**, *65*, 500–543. DOI: 10.1124/pr.111.005223.

(40) Coulthard, L. G.; Woodruff, T. M. Is the complement activation product C3a a proinflammatory molecule? Re-evaluating the evidence and the myth. *The Journal of Immunology* **2015**, *194*, 3542–3548. DOI: 10.4049/jimmunol.1403068.

(41) Guo, R.-F.; Ward, P. A. Role of C5a in inflammatory responses. *Annu Rev Immunol* **2005**, *23*, 821–852. DOI: 10.1146/annurev.immunol.23.021704.115835.

(42) Baillie, K.; Davies, H. E.; Keat, S. B. K.; Ladell, K.; Miners, K. L.; Jones, S. A.; Mellou, E.; Toonen, E. J. M.; Price, D. A.; Morgan, B. P.; Zelek, W. M. Complement dysregulation is a prevalent and therapeutically amenable feature of long COVID. *Med* **2024**, *5*, 239-253.e5. DOI: 10.1016/j.medj.2024.01.011.

(43) Cervia-Hasler, C.; Brüningk, S. C.; Hoch, T.; Fan, B.; Muzio, G.; Thompson, R. C.; Ceglarek, L.; Meledin, R.; Westermann, P.; Emmenegger, M.; Taeschler, P.; Zurbuchen, Y.; Pons, M.; Menges, D.; Ballouz, T.; Cervia-Hasler, S.; Adamo, S.; Merad, M.; Charney, A. W.; Puhan, M.; Brodin, P.; Nilsson, J.; Aguzzi, A.; Raeber, M. E.; Messner, C. B.; Beckmann, N. D.; Borgwardt, K.; Boyman, O. Persistent complement dysregulation with signs of thromboinflammation in active Long Covid. *Science* **2024**, *383*, eadg7942. DOI: 10.1126/science.adg7942.

(44) Figueroa, J. E.; Densen, P. Infectious diseases associated with complement deficiencies. *Clin Microbiol Rev* **1991**, *4*, 359–395. DOI: 10.1128/CMR.4.3.359.

(45) Schröder-Braunstein, J.; Kirschfink, M. Complement deficiencies and dysregulation: Pathophysiological consequences, modern analysis, and clinical management. *Mol Immunol* **2019**, *114*, 299–311. DOI: 10.1016/j.molimm.2019.08.002.

(46) Pettigrew, H. D.; Teuber, S. S.; Gershwin, M. E. Clinical significance of complement deficiencies. *Ann N Y Acad Sci* **2009**, *1173*, 108–123. DOI: 10.1111/j.1749-6632.2009.04633.x.

(47) Dahl, M.; Tybjaerg-Hansen, A.; Schnohr, P.; Nordestgaard, B. G. A population-based study of morbidity and mortality in mannose-binding lectin deficiency. *J Exp Med* **2004**, *199*, 1391–1399. DOI: 10.1084/jem.20040111.

(48) El Sissy, C.; Rosain, J.; Vieira-Martins, P.; Bordereau, P.; Gruber, A.; Devriese, M.; Pontual, L. de; Taha, M.-K.; Fieschi, C.; Picard, C.; Frémeaux-Bacchi, V. Clinical and Genetic Spectrum of a Large Cohort With Total and Sub-total Complement Deficiencies. *Front Immunol* **2019**, *10*, 1936. DOI: 10.3389/fimmu.2019.01936.

(49) Eichenfield, L. F.; Johnston, R. B. Secondary disorders of the complement system. *Am J Dis Child* **1989**, *143*, 595–602. DOI: 10.1001/archpedi.1989.02150170097032.

(50) Ekdahl, K. N.; Persson, B.; Mohlin, C.; Sandholm, K.; Skattum, L.; Nilsson, B. Interpretation of Serological Complement Biomarkers in Disease. *Front Immunol* **2018**, *9*, 2237. DOI: 10.3389/fimmu.2018.02237.

(51) Kulasekararaj, A. G.; Kuter, D. J.; Griffin, M.; Weitz, I. C.; Röth, A. Biomarkers and laboratory assessments for monitoring the treatment of patients with paroxysmal nocturnal hemoglobinuria: Differences between terminal and proximal complement inhibition. *Blood Rev* **2023**, *59*, 101041. DOI: 10.1016/j.blre.2023.101041.

(52) Kirschfink, M.; Mollnes, T. E. Modern complement analysis. *Clinical and Diagnostic Laboratory Immunology* **2003**, *10*, 982–989. DOI: 10.1128/cdli.10.6.982-989.2003.

(53) Turley, A. J.; Gathmann, B.; Bangs, C.; Bradbury, M.; Seneviratne, S.; Gonzalez-Granado, L. I.; Hackett, S.; Kutukculer, N.; Alachkar, H.; Hambleton, S.; Ritterbusch, H.; Kralickova, P.; Marodi, L.; Seidel, M. G.; Dueckers, G.; Roesler, J.; Huissoon, A.; Baxendale, H.; Litzman, J.; Arkwright, P. D. Spectrum and management of complement immunodeficiencies (excluding hereditary angioedema) across Europe. *J Clin.Immunol* **2015**, *35*, 199–205. DOI: 10.1007/s10875-015-0137-5.

(54) S Reis, E.; Falcão, D. A.; Isaac, L. Clinical aspects and molecular basis of primary deficiencies of complement component C3 and its regulatory proteins factor I and factor H. *Scand J Immunol* **2006**, *63*, 155–168. DOI: 10.1111/j.1365-3083.2006.01729.x.

(55) Ram, S.; Lewis, L. A.; Rice, P. A. Infections of people with complement deficiencies and patients who have undergone splenectomy. *Clin Microbiol Rev* **2010**, *23*, 740–780. DOI: 10.1128/CMR.00048-09.

(56) Ross, S. C.; Densen, P. Complement deficiency states and infection: epidemiology, pathogenesis and consequences of neisserial and other infections in an immune deficiency. *Medicine (Baltimore)* **1984**, *63*, 243–273.

(57) Bousfiha, A.; Jeddane, L.; Picard, C.; Ailal, F.; Bobby Gaspar, H.; Al-Herz, W.; Chatila, T.; Crow, Y. J.; Cunningham-Rundles, C.; Etzioni, A.; Franco, J. L.; Holland, S. M.; Klein, C.; Morio, T.; Ochs, H. D.; Oksenhendler, E.; Puck, J.; Tang, M. L. K.; Tangye, S. G.; Torgerson, T. R.; Casanova, J.-L.; Sullivan, K. E. The 2017 IUIS Phenotypic Classification for Primary Immunodeficiencies. *J Clin.Immunol* **2018**, *38*, 129–143. DOI: 10.1007/s10875-017-0465-8.

(58) Gupta, K.; Gupta, R. K.; Hajela, K. Disease associations of mannose-binding lectin & potential of replacement therapy. *Indian J Med Res* **2008**, *127*, 431–440.

(59) Eisen, D. P.; Minchinton, R. M. Impact of mannose-binding lectin on susceptibility to infectious diseases. *Clin Infect Dis* **2003**, *37*, 1496–1505. DOI: 10.1086/379324.

(60) Chen, M.; Daha, M. R.; Kallenberg, C. G. M. The complement system in systemic autoimmune disease. *Journal of Autoimmunity* **2010**, *34*, J276-86. DOI: 10.1016/j.jaut.2009.11.014.

(61) Vignesh, P.; Rawat, A.; Sharma, M.; Singh, S. Complement in autoimmune diseases. *Clin Chim Acta* **2017**, *465*, 123–130. DOI: 10.1016/j.cca.2016.12.017.

(62) Bock, M.; Heijnen, I.; Trendelenburg, M. Anti-C1q antibodies as a follow-up marker in SLE patients. *PLoS One* **2015**, *10*, e0123572. DOI: 10.1371/journal.pone.0123572.

(63) Carroll, M. C. A protective role for innate immunity in systemic lupus erythematosus. *Nat Rev Immunol* **2004**, *4*, 825–831. DOI: 10.1038/nri1456.

(64) Macedo, A. C. L.; Isaac, L. Systemic Lupus Erythematosus and Deficiencies of Early Components of the Complement Classical Pathway. *Front Immunol* **2016**, *7*, 55. DOI: 10.3389/fimmu.2016.00055.

(65) Grumach, A. S.; Veronez, C. L.; Csuka, D.; Farkas, H. Angioedema Without Wheals: Challenges in Laboratorial Diagnosis. *Front Immunol* **2021**, *12*, 785736. DOI: 10.3389/fimmu.2021.785736.

(66) Schreiber, A. D.; Kaplan, A. P.; Austen, K. F. Inhibition by C1INH of Hagemann factor fragment activation of coagulation, fibrinolysis, and kinin generation. *J Clin Invest* **1973**, *52*, 1402–1409. DOI: 10.1172/JCI107313.

(67) Gigli, I.; Mason, J. W.; Colman, R. W.; Austen, K. F. Interaction of Plasma Kallikrein with the $C1^-$ Inhibitor. *The Journal of Immunology* **1970**, *104*, 574–581. DOI: 10.4049/jimmunol.104.3.574.

(68) Wuillemin, W. A.; Minnema, M.; Meijers, J. C.; Roem, D.; Eerenberg, A. J.; Nuijens, J. H.; Cate, H. ten; Hack, C. E. Inactivation of factor XIa in human plasma assessed by measuring factor XIa-protease inhibitor complexes: major role for C1-inhibitor. *Blood* **1995**, *85*, 1517–1526. DOI: 10.1182/blood.V85.6.1517.bloodjournal8561517.

(69) Cugno, M.; Bos, I.; Lubbers, Y.; Hack, C. E.; Agostoni, A. In vitro interaction of C1-inhibitor with thrombin. *Blood Coagul Fibrinolysis* **2001**, *12*, 253–260. DOI: 10.1097/00001721-200106000-00005.

(70) Cugno, M.; Zanichelli, A.; Foieni, F.; Caccia, S.; Cicardi, M. C1-inhibitor deficiency and angioedema: molecular mechanisms and clinical progress. *Trends Mol Med* **2009**, *15*, 69–78. DOI: 10.1016/j.molmed.2008.12.001.

(71) Wong, E. K. S.; Kavanagh, D. Diseases of complement dysregulation-an overview. *Semin Immunopathol* **2018**, *40*, 49–64. DOI: 10.1007/s00281-017-0663-8.

(72) Fleckenstein, M.; Keenan, T. D. L.; Guymer, R. H.; Chakravarthy, U.; Schmitz-Valckenberg, S.; Klaver, C. C.; Wong, W. T.; Chew, E. Y. Age-related macular degeneration. *Nat Rev Dis Primers* **2021**, *7*, 31. DOI: 10.1038/s41572-021-00265-2.

(73) Yerigeri, K.; Kadatane, S.; Mongan, K.; Boyer, O.; Burke, L. L. G.; Sethi, S. K.; Licht, C.; Raina, R. Atypical Hemolytic-Uremic Syndrome: Genetic Basis, Clinical Manifestations, and a Multidisciplinary Approach to Management. *J Multidiscip Healthc* **2023**, *16*, 2233–2249. DOI: 10.2147/JMDH.S245620.

(74) Yoshida, Y.; Kato, H.; Ikeda, Y.; Nangaku, M. Pathogenesis of Atypical Hemolytic Uremic Syndrome. *J Atheroscler Thromb* **2019**, *26*, 99–110. DOI: 10.5551/jat.RV17026.

(75) Raina, R.; Krishnappa, V.; Blaha, T.; Kann, T.; Hein, W.; Burke, L.; Bagga, A. Atypical Hemolytic-Uremic Syndrome: An Update on Pathophysiology, Diagnosis, and Treatment. *Ther Apher Dial* **2019**, *23*, 4–21. DOI: 10.1111/1744-9987.12763.

(76) Ponticelli, C.; Calatroni, M.; Moroni, G. C3 glomerulopathies: dense deposit disease and C3 glomerulonephritis. *Front Med (Lausanne)* **2023**, *10*, 1289812. DOI: 10.3389/fmed.2023.1289812.

(77) Smith, R. J. H.; Appel, G. B.; Blom, A. M.; Cook, H. T.; D'Agati, V. D.; Fakhouri, F.; Fremeaux-Bacchi, V.; Józsi, M.; Kavanagh, D.; Lambris, J. D.; Noris, M.; Pickering, M. C.; Remuzzi, G.; Córdoba, S. R. de; Sethi, S.; van der Vlag, J.; Zipfel, P. F.; Nester, C. M. C3 glomerulopathy - understanding a rare complement-driven renal disease. *Nat Rev Nephrol* **2019**, *15*, 129–143. DOI: 10.1038/s41581-018-0107-2.

(78) Meuleman, M.-S.; Grunenwald, A.; Chauvet, S. Complement C3-targeted therapy in C3 glomerulopathy, a prototype of complement-mediated kidney diseases. *Semin Immunol* **2022**, *60*, 101634. DOI: 10.1016/j.smim.2022.101634.

(79) Thomas, C. J.; Mirza, R. G.; Gill, M. K. Age-Related Macular Degeneration. *Med Clin North Am* **2021**, *105*, 473–491. DOI: 10.1016/j.mcna.2021.01.003.

(80) Klein, R. J.; Zeiss, C.; Chew, E. Y.; Tsai, J.-Y.; Sackler, R. S.; Haynes, C.; Henning, A. K.; SanGiovanni, J. P.; Mane, S. M.; Mayne, S. T.; Bracken, M. B.; Ferris, F. L.; Ott, J.; Barnstable, C.; Hoh, J. Complement factor H polymorphism in age-related macular degeneration. *Science* **2005**, *308*, 385–389. DOI: 10.1126/science.1109557.

(81) Hageman, G. S.; Anderson, D. H.; Johnson, L. V.; Hancox, L. S.; Taiber, A. J.; Hardisty, L. I.; Hageman, J. L.; Stockman, H. A.; Borchardt, J. D.; Gehrs, K. M.; Smith, R. J. H.; Silvestri, G.; Russell, S. R.; Klaver, C. C. W.; Barbazetto, I.; Chang, S.; Yannuzzi, L. A.; Barile, G. R.; Merriam, J. C.; Smith, R. T.; Olsh, A. K.; Bergeron, J.; Zernant, J.; Merriam, J. E.; Gold, B.; Dean, M.; Allikmets, R. A common haplotype in the complement regulatory gene factor H (HF1/CFH) predisposes individuals to age-related macular degeneration. *PNAS* **2005**, *102*, 7227–7232. DOI: 10.1073/pnas.0501536102.

(82) Park, Y. G.; Park, Y. S.; Kim, I.-B. Complement System and Potential Therapeutics in Age-Related Macular Degeneration. *Int J Mol Sci* **2021**, *22*. DOI: 10.3390/ijms22136851.

(83) Armento, A.; Ueffing, M.; Clark, S. J. The complement system in age-related macular degeneration. *Cell Mol Life Sci* **2021**, *78*, 4487–4505. DOI: 10.1007/s00018-021-03796-9.

(84) Takeda, J.; Miyata, T.; Kawagoe, K.; Iida, Y.; Endo, Y.; Fujita, T.; Takahashi, M.; Kitani, T.; Kinoshita, T. Deficiency of the GPI anchor caused by a somatic mutation of the PIG-A gene in paroxysmal nocturnal hemoglobinuria. *Cell* **1993**, *73*, 703–711. DOI: 10.1016/0092-8674(93)90250-t.

(85) Brodsky, R. A. Paroxysmal nocturnal hemoglobinuria. *Blood* **2014**, *124*, 2804–2811. DOI: 10.1182/blood-2014-02-522128.

(86) Szlendak, U.; Budziszewska, B.; Spychalska, J.; Drozd-Sokołowska, J.; Patkowska, E.; Nowak, J. Paroxysmal nocturnal hemoglobinuria: advances in the understanding of pathophysiology, diagnosis, and treatment. *Pol Arch Intern Med* **2022**, *132*. DOI: 10.20452/pamw.16271.

(87) Holers, V. M.; Banda, N. K. Complement in the Initiation and Evolution of Rheumatoid Arthritis. *Front Immunol* **2018**, *9*, 1057. DOI: 10.3389/fimmu.2018.01057.

(88) Okroj, M.; Heinegård, D.; Holmdahl, R.; Blom, A. M. Rheumatoid arthritis and the complement system. *Annals of Medicine* **2007**, *39*, 517–530. DOI: 10.1080/07853890701477546.

(89) Chen, M.; Jayne, D. R. W.; Zhao, M.-H. Complement in ANCA-associated vasculitis: mechanisms and implications for management. *Nat Rev Nephrol* **2017**, *13*, 359–367. DOI: 10.1038/nrneph.2017.37.

(90) Kimoto, Y.; Horiuchi, T. The Complement System and ANCA Associated Vasculitis in the Era of Anti-Complement Drugs. *Front Immunol* **2022**, *13*, 926044. DOI: 10.3389/fimmu.2022.926044.

(91) Sun, X.-J.; Li, Z.-Y.; Chen, M. Pathogenesis of anti-neutrophil cytoplasmic antibody-associated vasculitis. *Rheumatology and Immunology Research* **2023**, *4*, 11–21. DOI: 10.2478/rir-2023-0003.

(92) Mayer, M. M. In Experimental immunochemistry, 2nd edn.; Kabat, Elvin A.; Mayer, Manfred Martin, Eds.; Charles C. Thomas: Springfield, Ill., 1961; pp. 133–240.

(93) Harboe, M.; Thorgersen, E. B.; Mollnes, T. E. Advances in assay of complement function and activation. *Adv Drug Delivery Rev* **2011**, *63*, 976–987. DOI: 10.1016/j.addr.2011.05.010.

(94) Platts-Mills, T. A. E.; Ishizaka, K. Activation of the Alternate Pathway of Human Complement by Rabbit Cells. *The Journal of Immunology* **1974**, *113*, 348–358. DOI: 10.4049/jimmunol.113.1.348.

(95) Nilsson, U. R.; Nilsson, B. Simplified assays of hemolytic activity of the classical and alternative complement pathways. *J Immunol Methods* **1984**, *72*, 49–59. DOI: 10.1016/0022-1759(84)90432-0.

(96) Truedsson, L.; Sjöholm, A. G.; Laurell, A. B. Screening for deficiencies in the classical and alternative pathways of complement by hemolysis in gel. *Acta Pathol Microbiol Scand C* **1981**, *89*, 161–166. DOI: 10.1111/j.1699-0463.1981.tb02680.x.

(97) Masaki, T.; Okada, N.; Yasuda, R.; Okada, H. Assay of complement activity in human serum using large unilamellar liposomes. *J Immunol Methods* **1989**, *123*, 19–24. DOI: 10.1016/0022-1759(89)90025-2.

(98) Estapé Senti, M.; Jongh, C. A. de; Dijkxhoorn, K.; Verhoef, J. J. F.; Szebeni, J.; Storm, G.; Hack, C. E.; Schiffelers, R. M.; Fens, M. H.; Boross, P. Anti-PEG antibodies compromise the integrity of PEGylated lipid-based nanoparticles via complement. *J Control Release* **2022**, *341*, 475–486. DOI: 10.1016/j.jconrel.2021.11.042.

(99) Prohászka, Z.; Nilsson, B.; Frazer-Abel, A.; Kirschfink, M. Complement analysis 2016: Clinical indications, laboratory diagnostics and quality control. *Immunobiology* **2016**, *221*, 1247–1258. DOI: 10.1016/j.imbio.2016.06.008.

(100) Nagy, G.; Brózik, M.; Varga, L.; Füst, G.; Kirschfink, M.; Kiss, E.; Gergely, P. Usefulness of detection of complement activation products in evaluating SLE activity. *Lupus* **2000**, *9*, 19–25. DOI: 10.1177/096120330000900105.

(101) Burger, R.; Bader, A.; Kirschfink, M.; Rother, U.; Schrod, L.; Wörner, I.; Zilow, G. Functional analysis and quantification of the complement C3 derived anaphylatoxin C3a with a monoclonal antibody. *Clin Exp Immunol* **1987**, *68*, 703–711.

(102) Falk, R. J.; Dalmasso, A. P.; Kim, Y.; Tsai, C. H.; Scheinman, J. I.; Gewurz, H.; Michael, A. F. Neoantigen of the polymerized ninth component of complement. Characterization of a monoclonal antibody and immunohistochemical localization in renal disease. *J Clin Invest* **1983**, *72*, 560–573. DOI: 10.1172/JCI111004.

(103) Garred, P.; Mollnes, T. E.; Lea, T.; Fischer, E. Characterization of a monoclonal antibody MoAb bH6 reacting with a neoepitope of human C3 expressed on C3b, iC3b, and C3c. *Scand J Immunol* **1988**, *27*, 319–327. DOI: 10.1111/j.1365-3083.1988.tb02353.x.

(104) Ichihara, C.; Nakamura, T.; Nagasawa, S.; Koyama, J. Monoclonal anti-human C4b antibodies: stabilization and inhibition of the classical-pathway C3 convertase. *Mol Immunol* **1986**, *23*, 151–157. DOI: 10.1016/0161-5890(86)90037-4.

(105) Wolbink, G. J.; Bollen, J.; Baars, J. W.; Berge, R. J. ten; Swaak, A. J.; Paardekooper, J.; Hack, C. E. Application of a monoclonal antibody against a neoepitope on activated C4 in an ELISA for the quantification of complement activation via the classical pathway. *J Immunol Methods* **1993**, *163*, 67–76. DOI: 10.1016/0022-1759(93)90240-8.

(106) Seelen, M. A.; Roos, A.; Wieslander, J.; Mollnes, T. E.; Sjöholm, A. G.; Wurzner, R.; Loos, M.; Tedesco, F.; Sim, R. B.; Garred, P.; Alexopoulos, E.; Turner, M. W.; Daha, M. R. Functional analysis of the classical, alternative, and MBL pathways of the complement system: standardization and validation of a simple ELISA. *J Immunol Methods* **2005**, *296*, 187–198. DOI: 10.1016/j.jim.2004.11.016.

(107) Hein, E.; Honoré, C.; Skjoedt, M.-O.; Munthe-Fog, L.; Hummelshøj, T.; Garred, P. Functional analysis of Ficolin-3 mediated complement activation. *PLoS One* **2010**, *5*, e15443. DOI: 10.1371/journal.pone.0015443.

(108) Nilsson, B.; Ekdahl, K. N. Complement diagnostics: concepts, indications, and practical guidelines. *Clin Dev Immunol* **2012**, *2012*, 962702. DOI: 10.1155/2012/962702.

(109) Mancini, G.; Carbonara, A. O.; Heremans, J. F. Immunochemical quantitation of antigens by single radial immunodiffusion. *Immunochemistry* **1965**, *2*, 235–254. DOI: 10.1016/0019-2791(65)90004-2.

(110) Whicher, J. T.; Price, C. P.; Spencer, K. Immunonephelometric and immunoturbidimetric assays for proteins. *Crit Rev Clin Lab Sci* **1983**, *18*, 213–260. DOI: 10.3109/10408368209085072.

(111) Engel, R.; Rensink, I.; Roem, D.; Brouwer, M.; Kalei, A.; Perry, D.; Zeerleder, S.; Wouters, D.; Hamann, D. ELISA to measure neutralizing capacity of anti-C1-inhibitor antibodies in plasma of angioedema patients. *J Immunol Methods* **2015**, *426*, 114–119. DOI: 10.1016/j.jim.2015.08.011.

(112) Watson, R.; Lindner, S.; Bordereau, P.; Hunze, E.-M.; Tak, F.; Ngo, S.; Zipfel, P. F.; Skerka, C.; Dragon-Durey, M.-A.; Marchbank, K. J. Standardisation of the factor H autoantibody assay. *Immunobiology* **2014**, *219*, 9–16. DOI: 10.1016/j.imbio.2013.06.004.

(113) Csorba, K.; Schirmbeck, L.; Dubler, D.; Trendelenburg, M. Anti-C1q Autoantibodies: Standard Quantification and Innovative ELISA. *Methods Mol Biol* **2021**, *2227*, 107–114. DOI: 10.1007/978-1-0716-1016-9_10.

(114) Michels, M. A. H. M.; Volokhina, E. B.; van de Kar, N. C. A. J.; van den Heuvel, L. P. W. J. Challenges in diagnostic testing of nephritic factors. *Front Immunol* **2022**, *13*, 1036136. DOI: 10.3389/fimmu.2022.1036136.

(115) Degn, S. E.; Jensenius, J. C.; Thiel, S. Disease-causing mutations in genes of the complement system. *Am J Hum Genet* **2011**, *88*, 689–705. DOI: 10.1016/j.ajhg.2011.05.011.

(116) Mollnes, T. E.; Jokiranta, T. S.; Truedsson, L.; Nilsson, B.; Rodriguez de Cordoba, S.; Kirschfink, M. Complement analysis in the 21st century. *Mol Immunol* **2007**, *44*, 3838–3849. DOI: 10.1016/j.molimm.2007.06.150.

(117) Willems, E.; Lorés-Motta, L.; Zanichelli, A.; Suffritti, C.; van der Flier, M.; van der Molen, R. G.; Langereis, J. D.; van Drongelen, J.; van den Heuvel, L. P.; Volokhina, E.; van de Kar, N. C.; Keizer-Garritsen, J.; Levin, M.; Herberg, J. A.; Martinon-Torres, F.; Wessels, H. J.; Breuk, A. de; Fauser, S.; Hoyng, C. B.; Hollander, A. I. den; Groot, R. de; van Gool, A. J.; Gloerich, J.; Jonge, M. I. de. Quantitative multiplex profiling of the complement system to diagnose complement-mediated diseases. *Clin Transl Immunology* **2020**, *9*, e1225. DOI: 10.1002/cti2.1225.

(118) Lombardo, D.; Kiselev, M. A. Methods of Liposomes Preparation: Formation and Control Factors of Versatile Nanocarriers for Biomedical and Nanomedicine Application. *Pharmaceutics* **2022**, *14*. DOI: 10.3390/pharmaceutics14030543.

(119) Lasic, D. D. The mechanism of vesicle formation. *Biochem J* **1988**, *256*, 1–11. DOI: 10.1042/bj2560001.

(120) Edwards, K. A.; Baeumner, A. J. Liposomes in analyses. *Talanta* **2006**, *68*, 1421–1431. DOI: 10.1016/j.talanta.2005.08.044.

(121) Nsairat, H.; Khater, D.; Sayed, U.; Odeh, F.; Al Bawab, A.; Alshaer, W. Liposomes: structure, composition, types, and clinical applications. *Heliyon* **2022**, *8*, e09394. DOI: 10.1016/j.heliyon.2022.e09394.

(122) Liu, Q.; Boyd, B. J. Liposomes in biosensors. *Analyst* **2013**, *138*, 391–409. DOI: 10.1039/c2an36140j.

(123) Gulati, M.; Grover, M.; Singh, S.; Singh, M. Lipophilic drug derivatives in liposomes. *Int J Pharm* **1998**, *165*, 129–168. DOI: 10.1016/S0378-5173(98)00006-4.

(124) Pande, S. Liposomes for drug delivery: review of vesicular composition, factors affecting drug release and drug loading in liposomes. *Artif Cells Nanomed Biotechnol* **2023**, *51*, 428–440. DOI: 10.1080/21691401.2023.2247036.

(125) Ferreira, M.; Ogren, M.; Dias, J. N. R.; Silva, M.; Gil, S.; Tavares, L.; Aires-da-Silva, F.; Gaspar, M. M.; Aguiar, S. I. Liposomes as Antibiotic Delivery Systems: A Promising Nanotechnological Strategy against Antimicrobial Resistance. *Molecules* **2021**, *26*, 2047. DOI: 10.3390/molecules26072047.

(126) Zylberberg, C.; Gaskill, K.; Pasley, S.; Matosevic, S. Engineering liposomal nanoparticles for targeted gene therapy. *Gene Ther* **2017**, *24*, 441–452. DOI: 10.1038/gt.2017.41.

(127) O'Connell, J. P.; Campbell, R. L.; Fleming, B. M.; Mercolino, T. J.; Johnson, M. D.; McLaurin, D. A. A highly sensitive immunoassay system involving antibody-coated tubes and liposome-entrapped dye. *Clin Chem* **1985**, *31*, 1424–1426.

(128) Kannuck, R. M.; Bellama, J. M.; Durst, R. A. Measurement of liposome-released ferrocyanide by a dual-function polymer modified electrode. *Anal Chem* **1988**, *60*, 142–147. DOI: 10.1021/ac00153a009.

(129) Colletier, J.-P.; Chaize, B.; Winterhalter, M.; Fournier, D. Protein encapsulation in liposomes: efficiency depends on interactions between protein and phospholipid bilayer. *BMC Biotechnol* **2002**, *2*, 9. DOI: 10.1186/1472-6750-2-9.

(130) Edwards, K. A.; Bolduc, O. R.; Baeumner, A. J. Miniaturized bioanalytical systems: enhanced performance through liposomes. *Current Opinion in Chemical Biology* **2012**, *16*, 444–452. DOI: 10.1016/j.cbpa.2012.05.182.

(131) Bangham, A. D.; Standish, M. M.; Watkins, J. C. Diffusion of univalent ions across the lamellae of swollen phospholipids. *J Mol Biol* **1965**, *13*, 238–252. DOI: 10.1016/s0022-2836(65)80093-6.

(132) Galvain, S.; André, C.; Vatrinet, C.; Villet, B. Safety and efficacy studies of liposomes in specific immunotherapy. *Current Therapeutic Research* **1999**, *60*, 278–294. DOI: 10.1016/S0011-393X(99)80004-6.

(133) He, K.; Tang, M. Safety of novel liposomal drugs for cancer treatment: Advances and prospects. *Chem Biol Interact* **2018**, *295*, 13–19. DOI: 10.1016/j.cbi.2017.09.006.

(134) Zahednezhad, F.; Saadat, M.; Valizadeh, H.; Zakeri-Milani, P.; Baradaran, B. Liposome and immune system interplay: Challenges and potentials. *J Control Release* **2019**, *305*, 194–209. DOI: 10.1016/j.jconrel.2019.05.030.

(135) Dymek, M.; Sikora, E. Liposomes as biocompatible and smart delivery systems - the current state. *Adv Colloid Interface Sci* **2022**, *309*, 102757. DOI: 10.1016/j.cis.2022.102757.

(136) Sforzi, J.; Palagi, L.; Aime, S. Liposome-Based Bioassays. *Biology (Basel)* **2020**, *9*. DOI: 10.3390/biology9080202.

(137) Mazur, F.; Bally, M.; Städler, B.; Chandrawati, R. Liposomes and lipid bilayers in biosensors. *Adv Colloid Interface Sci* **2017**, *249*, 88–99. DOI: 10.1016/j.cis.2017.05.020.

(138) Grit, M.; Crommelin, D. J. Chemical stability of liposomes: implications for their physical stability. *Chem Phys Lipids* **1993**, *64*, 3–18. DOI: 10.1016/0009-3084(93)90053-6.

(139) Sułkowski, W. W.; Pentak, D.; Nowak, K.; Sułkowska, A. The influence of temperature, cholesterol content and pH on liposome stability. *J Mol Struct* **2005**, *744-747*, 737–747. DOI: 10.1016/j.molstruc.2004.11.075.

(140) Stark, B.; Pabst, G.; Prassl, R. Long-term stability of sterically stabilized liposomes by freezing and freeze-drying: Effects of cryoprotectants on structure. *Eur J Pharm Sci* **2010**, *41*, 546–555. DOI: 10.1016/j.ejps.2010.08.010.

(141) Andra, V. V. S. N. L.; Pammi, S. V. N.; Bhatraju, L. V. K. P.; Ruddaraju, L. K. A Comprehensive Review on Novel Liposomal Methodologies, Commercial Formulations, Clinical Trials and Patents. *Bionanoscience* **2022**, *12*, 274–291. DOI: 10.1007/s12668-022-00941-x.

(142) Shah, S.; Dhawan, V.; Holm, R.; Nagarsenker, M. S.; Perrie, Y. Liposomes: Advancements and innovation in the manufacturing process. *Adv Drug Delivery Rev* **2020**, *154-155*, 102–122. DOI: 10.1016/j.addr.2020.07.002.

(143) Luiz, H.; Oliveira Pinho, J.; Gaspar, M. M. Advancing Medicine with Lipid-Based Nanosystems-The Successful Case of Liposomes. *Biomedicines* **2023**, *11*. DOI: 10.3390/biomedicines11020435.

(144) Pöhnl, M.; Trollmann, M. F. W.; Böckmann, R. A. Nonuniversal impact of cholesterol on membranes mobility, curvature sensing and elasticity. *Nat Commun* **2023**, *14*, 8038. DOI: 10.1038/s41467-023-43892-x.

(145) Doole, F. T.; Kumarage, T.; Ashkar, R.; Brown, M. F. Cholesterol Stiffening of Lipid Membranes. *J Membr Biol* **2022**, *255*, 385–405. DOI: 10.1007/s00232-022-00263-9.

(146) Wang, C.; Lan, X.; Zhu, L.; Wang, Y.; Gao, X.; Li, J.; Tian, H.; Liang, Z.; Xu, W. Construction Strategy of Functionalized Liposomes and Multidimensional Application. *Small* **2024**, *20*, e2309031. DOI: 10.1002/smll.202309031.

(147) Liu, G.; Hou, S.; Tong, P.; Li, J. Liposomes: Preparation, Characteristics, and Application Strategies in Analytical Chemistry. *Crit Rev Anal Chem* **2022**, *52*, 392–412. DOI: 10.1080/10408347.2020.1805293.

(148) Stetefeld, J.; McKenna, S. A.; Patel, T. R. Dynamic light scattering: a practical guide and applications in biomedical sciences. *Biophys Rev* **2016**, *8*, 409–427. DOI: 10.1007/s12551-016-0218-6.

(149) Tonggu, L.; Wang, L. Cryo-EM sample preparation method for extremely low concentration liposomes. *Ultramicroscopy* **2020**, *208*, 112849. DOI: 10.1016/j.ultramic.2019.112849.

(150) Bhattacharjee, S. DLS and zeta potential - What they are and what they are not? *J Control Release* **2016**, *235*, 337–351. DOI: 10.1016/j.jconrel.2016.06.017.

(151) Chonn, A.; Cullis, P. R.; Devine, D. V. The role of surface charge in the activation of the classical and alternative pathways of complement by liposomes. *The Journal of Immunology* **1991**, *146*, 4234–4241. DOI: 10.4049/jimmunol.146.12.4234.

(152) Gillet, A.; Compère, P.; Lecomte, F.; Hubert, P.; Ducat, E.; Evrard, B.; Piel, G. Liposome surface charge influence on skin penetration behaviour. *Int J Pharm* **2011**, *411*, 223–231. DOI: 10.1016/j.ijpharm.2011.03.049.

(153) Krasnici, S.; Werner, A.; Eichhorn, M. E.; Schmitt-Sody, M.; Pahernik, S. A.; Sauer, B.; Schulze, B.; Teifel, M.; Michaelis, U.; Naujoks, K.; Dellian, M. Effect of the surface charge of liposomes on their uptake by angiogenic tumor vessels. *Int J Cancer* **2003**, *105*, 561–567. DOI: 10.1002/ijc.11108.

(154) Streif, S.; Neckermann, P.; Spitzenberg, C.; Weiss, K.; Hoecherl, K.; Kulikowski, K.; Hahner, S.; Noelting, C.; Einhauser, S.; Peterhoff, D.; Asam, C.; Wagner, R.; Baeumner, A. J. Liposome-based high-throughput and point-of-care assays toward the quick, simple, and sensitive detection of neutralizing antibodies against SARS-CoV-2 in patient sera. *Anal Bioanal Chem* **2023**, *415*, 1421–1435. DOI: 10.1007/s00216-023-04548-3.

(155) Yahata, S.; Hirose, M.; Ueno, T.; Nagumo, H.; Sakai-Kato, K. Effect of Sample Concentration on Nanoparticle Tracking Analysis of Small Extracellular Vesicles and Liposomes Mimicking the Physicochemical Properties of Exosomes. *Chem Pharm Bull (Tokyo)* **2021**, *69*, 1045–1053. DOI: 10.1248/cpb.c21-00452.

(156) Liu, P.; Chen, G.; Zhang, J. A Review of Liposomes as a Drug Delivery System: Current Status of Approved Products, Regulatory Environments, and Future Perspectives. *Molecules* **2022**, *27*, 1372. DOI: 10.3390/molecules27041372.

(157) Zhou, S.; Luo, Y.; Lovell, J. F. Vaccine approaches for antigen capture by liposomes. *Expert Rev Vaccines* **2023**, *22*, 1022–1040. DOI: 10.1080/14760584.2023.2274479.

(158) Liang, J.; Wang, J.; Zhang, L.; Wang, S.; Yao, C.; Zhang, Z. Glucose oxidase-loaded liposomes for in situ amplified signal of electrochemical immunoassay on a handheld pH meter. *New J. Chem.* **2019**, *43*, 1372–1379. DOI: 10.1039/C8NJ05637D.

(159) Bunyakul, N.; Promptmas, C.; Baeumner, A. J. Microfluidic biosensor for cholera toxin detection in fecal samples. *Anal Bioanal Chem* **2015**, *407*, 727–736. DOI: 10.1007/s00216-014-7947-9.

(160) Zeng, X.; Wang, L.; Liu, C.; Zhang, J.; Shi, H.-W.; Shen, W.; Kong, D.; Huang, C.; Lee, H. K.; Tang, S. An integrated liposome-based microfluidic strategy for rapid colorimetric analysis: A case study of microRNA-21 detection. *Talanta* **2024**, *272*, 125838. DOI: 10.1016/j.talanta.2024.125838.

(161) Rink, S.; Kaiser, B.; Steiner, M.-S.; Duerkop, A.; Baeumner, A. J. Highly sensitive interleukin 6 detection by employing commercially ready liposomes in an LFA format. *Anal Bioanal Chem* **2022**, *414*, 3231–3241. DOI: 10.1007/s00216-021-03750-5.

(162) Khreich, N.; Lamourette, P.; Boutal, H.; Devilliers, K.; Créminon, C.; Volland, H. Detection of Staphylococcus enterotoxin B using fluorescent immunoliposomes as label for immunochromatographic testing. *Anal Biochem* **2008**, *377*, 182–188. DOI: 10.1016/j.ab.2008.02.032.

(163) Wang, C.; Piao, J.; Li, Y.; Tian, X.; Dong, Y.; Liu, D. Construction of Liposomes Mimicking Cell Membrane Structure through Frame-Guided Assembly. *Angew Chem Int Ed* **2020**, *59*, 15176–15180. DOI: 10.1002/anie.202005334.

(164) Adler, A.; Fritsch, M.; Fromell, K.; Leneweit, G.; Ekdahl, K. N.; Nilsson, B.; Teramura, Y. Regulation of the innate immune system by fragmented heparin-conjugated lipids on lipid bilayered membranes in vitro. *J Mater Chem B* **2023**, *11*, 11121–11134. DOI: 10.1039/d3tb01721d.

(165) Bradley, A. J.; Devine, D. V. The complement system in liposome clearance: Can complement deposition be inhibited? *Adv Drug Delivery Rev* **1998**, *32*, 19–29. DOI: 10.1016/s0169-409x(97)00129-4.

(166) Gabizon, A.; Szebeni, J. Complement Activation: A Potential Threat on the Safety of Poly(ethylene glycol)-Coated Nanomedicines. *ACS Nano* **2020**, *14*, 7682–7688. DOI: 10.1021/acsnano.0c03648.

(167) Wang, H.; Lin, S.; Wu, X.; Jiang, K.; Lu, H.; Zhan, C. Interplay between Liposomes and IgM: Principles, Challenges, and Opportunities. *Adv Sci (Weinh)* **2023**, *10*, e2301777. DOI: 10.1002/advs.202301777.

(168) Immordino, M. L.; Dosio, F.; Cattel, L. Stealth liposomes: review of the basic science, rationale, and clinical applications, existing and potential. *Int J Nanomedicine* **2006**, *1*, 297–315.

(169) Milla, P.; Dosio, F.; Cattel, L. PEGylation of proteins and liposomes: a powerful and flexible strategy to improve the drug delivery. *Curr Drug Metab* **2012**, *13*, 105–119. DOI: 10.2174/138920012798356934.

(170) C̆eh, B.; Winterhalter, M.; Frederik, P. M.; Vallner, J. J.; Lasic, D. D. Stealth® liposomes: from theory to product. *Adv Drug Delivery Rev* **1997**, *24*, 165–177. DOI: 10.1016/S0169-409X(96)00456-5.

(171) Zhang, P.; Sun, F.; Liu, S.; Jiang, S. Anti-PEG antibodies in the clinic: Current issues and beyond PEGylation. *J Control Release* **2016**, *244*, 184–193. DOI: 10.1016/j.jconrel.2016.06.040.

(172) Alving, C. R.; Richards, R. L.; Guirguis, A. A. Cholesterol-dependent human complement activation resulting in damage to liposomal model membranes. *J Immunol* **1977**, *118*, 342–347.

(173) Kishimura, M.; Fukuda, H.; Katoh, S.; Sada, E.; Taniguchi, H. Lysis of rabbit γ-globulin-coupled liposomes by the complement system. *J Ferment Bioeng* **1992**, *74*, 81–84. DOI: 10.1016/0922-338X(92)80005-4.

(174) *Homepage - INSTAND e.V,* https://www.instand-ev.de/en/ (accessed 2025/05/15).

(175) Frazer-Abel, A.; Kirschfink, M.; Prohászka, Z. Expanding Horizons in Complement Analysis and Quality Control. *Front Immunol* **2021**, *12*, 697313. DOI: 10.3389/fimmu.2021.697313.

(176) Kirschfink, M.; Frazer-Abel, A.; Balogh, E.; Goseberg, S.; Weiss, N.; Prohászka, Z. External quality assurance program for diagnostic complement laboratories: evaluation of the results of the past seven years. *Front Immunol* **2024**, *15*, 1368399. DOI: 10.3389/fimmu.2024.1368399.

(177) Hycult Biotech. *Hycult Biotech - Let's improve health,* https://www.hycultbiotech.com/ (accessed 2025/05/15).

(178) *Complement Therapeutics - Creative Biolabs,* https://www.creative-biolabs.com/complement-therapeutics/ (accessed 2025/05/15).

(179) *HaemoScan | Laboratory for blood compatibility and biomarker detection,* https://www.haemoscan.com/ (accessed 2025/05/15).

(180) *Thermo Fisher Scientific - DE,* https://www.thermofisher.com/de/de/home.html (accessed 2025/05/15).

(181) Svar Life Science AB. *Svar Life Science - Answers through the drug development value chain,* https://www.svarlifescience.com/ (accessed 2025/05/15).

(182) *MicroVue™ Products,* https://www.quidelortho.com/de/de/products/microvue-assays (accessed 2025/05/15).

(183) *Autokit CH50 Assay | FUJIFILM Wako Chemicals Europe GmbH,* https://www.wako-chemicals.de/produkte/autokit-ch50-assay.php (accessed 2025/05/15).

(184) *MicroVue™ Complement Multiplex,* https://www.quidelortho.com/de/de/products/microvue-assays/complement-multiplex (accessed 2025/05/15).

(185) *MILLIPLEX® Human Complement Expanded Panel 1,* https://www.sigmaaldrich.com/DE/de/product/mm/hcmpex119k (accessed 2025/05/15).

(186) *MILLIPLEX® Human Complement Panel 2 - Immunology Multiplex Assay The Human Complement Panel 2 Bead-Based Multiplex Assay kit, using the Luminex xMAP technology, enables the simultaneous analysis of complement proteins and factors in human serum, plasma and cell culture samples,* https://www.sigmaaldrich.com/DE/de/product/mm/hcmp2mag19k (accessed 2025/05/15).

(187) Ricklin, D. Complement-targeted therapeutics: Are we there yet, or just getting started? *Eur. J. Immunol.* **2024**, *54*, e2350816. DOI: 10.1002/eji.202350816.

(188) West, E. E.; Woodruff, T.; Fremeaux-Bacchi, V.; Kemper, C. Complement in human disease: approved and up-and-coming therapeutics. *Lancet* **2024**, *403*, 392–405. DOI: 10.1016/S0140-6736(23)01524-6.

(189) Kolev, M.; Rao, K. N.; Yeh, M.; Parikh, A.; Deschatelets, P. The future of complement therapeutics. *Explor Immunol* **2024**, 577–615. DOI: 10.37349/ei.2024.00161.

(190) Lamers, C.; Ricklin, D.; Lambris, J. D. Complement-targeted therapeutics: An emerging field enabled by academic drug discovery. *Am J Hematol* **2023**, *98 Suppl 4*, S82-S89. DOI: 10.1002/ajh.26875.

(191) *Alexion – Speziell für Menschen mit seltenen Krankheiten,* https://alexion.de/ (accessed 2025/05/15).

(192) Apellis. *Official Home Page of the Apellis Pharmaceuticals Corporate Site | Apellis Pharmaceuticals,* https://apellis.com/ (accessed 2025/05/15).

(193) Amgen. *Amgen - A Worldwide Pioneer in Biotechnology,* https://www.amgen.com/ (accessed 2025/05/15).

(194) Omeros. *Omeros – Next-generation Therapeutics Transforming Patient Care,* https://www.omeros.com/ (accessed 2025/05/15).

(195) Mollnes, T. E.; Garred, P.; Bergseth, G. Effect of time, temperature and anticoagulants on in vitro complement activation: consequences for collection and preservation of samples to be examined for complement activation. *Clin Exp Immunol* **1988**, *73*, 484–488.

(196) Yang, S.; McGookey, M.; Wang, Y.; Cataland, S. R.; Wu, H. M. Effect of blood sampling, processing, and storage on the measurement of complement activation biomarkers. *Am J Clin Pathol* **2015**, *143*, 558–565. DOI: 10.1309/AJCPXPD7ZQXNTIAL.

(197) Gao, Y.; Tang, L.; Tang, B.; Cao, W.; Sun, X. Effect of Repeated Freeze-Thaw on Serum Biomarkers Associated with Eye Disease. *Med Sci Monit* **2018**, *24*, 4481–4488. DOI: 10.12659/MSM.908567.

(198) Storm, B. S.; Christiansen, D.; Fure, H.; Ludviksen, J. K.; Lau, C.; Lambris, J. D.; Woodruff, T. M.; Brekke, O.-L.; Braaten, T.; Nielsen, E. W.; Mollnes, T. E. Air Bubbles Activate Complement and Trigger Hemostasis and C3-Dependent Cytokine Release Ex Vivo in Human Whole Blood. *The Journal of Immunology* **2021**, *207*, 2828–2840. DOI: 10.4049/jimmunol.2100308.

(199) Brandwijk, R. J. M. G. E.; Michels, M. A. H. M.; van Rossum, M.; Nooijer, A. H. de; Nilsson, P. H.; Bruin, W. C. C. de; Toonen, E. J. M. Pitfalls in complement analysis: A systematic literature review of assessing complement activation. *Front Immunol* **2022**, *13*, 1007102. DOI: 10.3389/fimmu.2022.1007102.

(200) Bexborn, F.; Engberg, A. E.; Sandholm, K.; Mollnes, T. E.; Hong, J.; Nilsson Ekdahl, K. Hirudin versus heparin for use in whole blood in vitro biocompatibility models. *J Biomed Mater Res A* **2009**, *89*, 951–959. DOI: 10.1002/jbm.a.32034.

(201) Lachmann, P. J. Preparing serum for functional complement assays. *J Immunol Methods* **2010**, *352*, 195–197. DOI: 10.1016/j.jim.2009.11.003.

(202) Mollnes, T. E.; Brekke, O.-L.; Fung, M.; Fure, H.; Christiansen, D.; Bergseth, G.; Videm, V.; Lappegård, K. T.; Köhl, J.; Lambris, J. D. Essential role of the C5a receptor in E coli–induced oxidative burst and phagocytosis revealed by a novel lepirudin-based human whole blood model of inflammation. *Blood* **2002**, *100*, 1869–1877. DOI: 10.1182/blood.V100.5.1869.h81702001869_1869_1877.

(203) Andersson, L. I.; Sjöström, D. J.; Brandwijk, R. J. M. G. E.; Toonen, E. J. M.; Mollnes, T. E.; Nilsson, P. H. Complement function and activation in human serum and plasma collected in different blood collection tubes. *J Immunol Methods* **2025**, *538*, 113825. DOI: 10.1016/j.jim.2025.113825.

(204) Moghimi, S. M.; Simberg, D. Critical issues and pitfalls in serum and plasma handling for complement analysis in nanomedicine and bionanotechnology. *Nano Today* **2022**, *44*, 101479. DOI: 10.1016/j.nantod.2022.101479.

(205) Sahu, A.; Pangburn, M. K. Identification of multiple sites of interaction between heparin and the complement system. *Mol Immunol* **1993**, *30*, 679–684. DOI: 10.1016/0161-5890(93)90079-q.

(206) Brady, A. M.; Spencer, B. L.; Falsey, A. R.; Nahm, M. H. Blood collection tubes influence serum ficolin-1 and ficolin-2 levels. *Clin Vaccine Immunol* **2014**, *21*, 51–55. DOI: 10.1128/CVI.00607-13.

(207) Hein, E.; Bay, J. T.; Munthe-Fog, L.; Garred, P. Ficolin-2 reveals different analytical and biological properties dependent on different sample handling procedures. *Mol Immunol* **2013**, *56*, 406–412. DOI: 10.1016/j.molimm.2013.05.233.

(208) Kenawy, H. I.; Boral, I.; Bevington, A. Complement-Coagulation Cross-Talk: A Potential Mediator of the Physiological Activation of Complement by Low pH. *Front Immunol* **2015**, *6*, 215. DOI: 10.3389/fimmu.2015.00215.

(209) Zelek, W. M.; Harris, C. L.; Morgan, B. P. Extracting the barbs from complement assays: Identification and optimisation of a safe substitute for traditional buffers. *Immunobiology* **2018**, *223*, 744–749. DOI: 10.1016/j.imbio.2018.07.016.

(210) Bergseth, G.; Ludviksen, J. K.; Kirschfink, M.; Giclas, P. C.; Nilsson, B.; Mollnes, T. E. An international serum standard for application in assays to detect human complement activation products. *Mol Immunol* **2013**, *56*, 232–239. DOI: 10.1016/j.molimm.2013.05.221.

(211) Khalil, F.; Yapati, H.; Al Blallam, Z.; Jose, R. Seasonal effects on Growth, Physiology, Hematology and Biochemical Profiles of Naeemi Sheep Breed. *AAVS* **2022**, *10*. DOI: 10.17582/journal.aavs/2022/10.10.2160.2170.

(212) Kovacik, A.; Arvay, J.; Tusimova, E.; Harangozo, L.; Tvrda, E.; Zbynovska, K.; Cupka, P.; Andrascikova, S.; Tomas, J.; Massanyi, P. Seasonal variations in the blood concentration of selected heavy metals in sheep and their effects on the biochemical and hematological parameters. *Chemosphere* **2017**, *168*, 365–371. DOI: 10.1016/j.chemosphere.2016.10.090.

(213) Yaqub, Y. Influence of reproductive cycle, sex, age and season on haematologic parameters in domestic animals: A review. *J. Cell Anim. Biol.* **2013**, *7*, 37–43. DOI: 10.5897/JCAB12.063.

(214) Chabannes, M.; Bordereau, P.; Martins, P. V.; Dragon-Durey, M.-A. Sheep Erythrocyte Preparation for Hemolytic Tests Exploring Complement Functional Activities. *Methods Mol Biol* **2021**, *2227*, 61–67. DOI: 10.1007/978-1-0716-1016-9_6.

3 Encapsulants Affect Liposome Surface Interactions with Biological Systems

Graphical Abstract

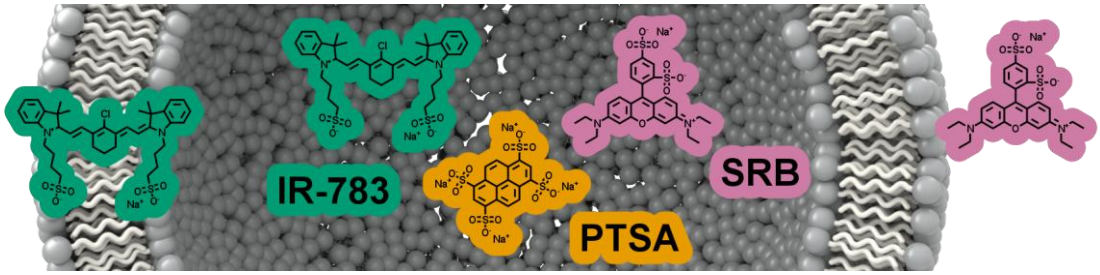

This chapter has been published as an original research article in the journal *Small*.

Reprinted from Spitzenberg, C.; Bruckschlegel, C.; Holzhausen, F.; Boesl-Bichlmeier, S.; Pasquier, C.; Nuernberger, P.; Bauduin, P.; Baeumner, A. J. Encapsulants Affect Liposome Surface Interactions with Biological Systems. *Small* **2025**, *21* (33), e2505312. DOI: https://doi.org/10.1002/smll.202505312.

Author's contributions

Conceptualization of this research article was performed by Antje J. Baeumner and the author and supported by Ferdinand Holzhausen. The methodology was developed by Antje J. Baeumner, Christoph Bruckschlegel, Ferdinand Holzhausen and the author and supported by Pierre Bauduin and Patrick Nuernberger. Christoph Bruckschlegel, Ferdinand Holzhausen and the author contributed equally to the experimental investigations. Christoph Bruckschlegel performed and evaluated the SAXS measurements supported by Coralie Pasquier. Samples for the SAXS measurements were prepared by the author. Ferdinand Holzhausen and the author prepared the samples for spectroscopic investigations performed by Sebastian Boesl-Bichlmeier (Figure 3-1 and 3-4). The author performed and evaluated the liposome-based complement assays and preliminary studies on the fluorophores. Ferdinand Holzhausen, Anna Gebhardt, Michaela Aichinger, Ernst Eberhardt, Sandra Friedrich, Anna-Maria Lauerer and Silvia Haage assisted with the liposome preparation. Funding acquisition was led by Antje J. Baeumner and supported by Pierre Bauduin. Antje J. Baeumner supervised in a leading role and was supported by Pierre Bauduin and Patrick Nuernberger. Antje J. Baeumner contributed by project administration. The author wrote the first draft of the manuscript. Antje J. Baeumner, Christoph Bruckschlegel, Ferdinand Holzhausen, Sebastian Boesl-Bichlmeier, Patrick Nuernberger and Pierre Bauduin revised the manuscript. Antje J. Baeumner is corresponding author.

Abstract

Liposomes are self-assembled lipid bilayer nanostructures with an inner aqueous core used for diagnostic signal amplification, drug delivery and as biomimics. Small molecules and proteins are typically encapsulated. While the lipid composition is used to control liposome and surface characteristics, overlooked is the effect entrapped molecules may have on the outer surface through interface activity. Here, we demonstrate how different dyes not only distribute between aqueous core and bilayer, but also significantly affect the outer surface chemistry thus influencing interactions with reaction partners and sample matrices. Specifically, IR-783, sulforhodamine B (SRB), and 1,3,6,8-pyrenetetrasulfonic acid (PTSA) were encapsulated in liposomes of standard bioanalytical composition. Spectroscopic and small-angle X-ray scattering data indicated interactions of IR-783 with the liposome membrane and its strong influence on the bilayer structure. Increasing SRB concentrations showed potential adsorption at liposome bilayer surfaces, whereas PTSA did not interact with the bilayer itself. Surprising was the correlating effect on biological systems discovered through the complement system as model. Liposomes incubated with serum revealed complement protein interaction with the liposome surface depending on the dye and not only on the lipid composition. This study emphasizes the need for careful selection of both lipid and encapsulant formulations in any biological application.

3.1 Introduction

Liposomes, first described as swollen phospholipid systems by Bangham et al. in 1965[1], have been established as a powerful and versatile tool in modern diagnostics and research. The simplest form of liposomes has been described as a self-assembled structure containing an inner aqueous cavity surrounded by a lipid bilayer.[2] The bilayer is composed predominantly of phospholipids with diversity in the chemical structure and characteristics of their head group and the carbon chain length of their hydrophobic tail. Phosphatidylcholine, phosphatidylethanolamine, phosphatidylserine, and phosphatidylglycerol are the most abundant naturally occurring head groups in biological systems and are also applied in liposome preparation.[3] Increased stability is often achieved by including cholesterol in the lipid composition causing tighter packing of the phospholipids, thereby reducing bilayer permeability and forming more rigid liposomes.[4] Liposomes can be prepared in various sizes, ranging from small vesicles of 25-50 nm to vesicles up to a few millimeters in size, depending on the number of bilayer shells (i.e. the lamellarity), the lipid composition, the preparation procedure and the molecules inside the aqueous compartment.[5] Already in the 1970s, scientists began to explore the use of liposomes as drug or biomolecule carriers.[6] Since then, the cavity has been demonstrated to be suitable for encapsulation of a variety of hydrophilic molecules, including

fluorescent dyes[7], electroactive species[8], oligonucleotides[9], drugs[10], or enzymes[11]. Overall, this flexibility in lipid composition, surface charge and modification, liposome size, and encapsulant allows for a wide versatility in the application of liposomes. These range from signal amplification[12], the use as biomimics of cells or other biological vesicles in bioassays and to the application as drug delivery vesicles in therapeutic contexts.[13] However, the introduction of liposomes into biofluids and biological systems is affected by corona formation, opsonization, or more general deposition of biomolecules on the surface.[14] These reactions to the intruding nanomaterial alter the surface characteristics, which often also hampers their efficacy due to the accelerated clearance rates of such materials.

Small-angle X-ray scattering (SAXS) is a technique used to study such structural and physical properties and their changes of nanomaterials. The method is based on the irradiation of samples with monochromatic, collimated X-rays. The X-rays are scattered depending on the electron density characteristics of the nanomaterial and are subsequently recorded with a 2D-detector.[15] The intensity of the scattered X-rays as a function of the scattering vector q ($q = 4\pi/\lambda \sin(\theta/2)$; with the wavelength of X-rays λ and scattering angle θ) provide information about the form factor (revealing size, shape and size distribution) and the structure factor (revealing structural organization and particle interactions) of the nanomaterial.[16] The scattered X-rays are typically investigated in a range from $q = 10^{-1} - 10^{1}$ nm^{-1}, corresponding to structures in the range of approximately 1 - 100 nm, making SAXS a powerful technique for the study of nanomaterials. While smaller angles (lower q values) are associated with larger features, larger angles (higher q values) refer to smaller structures, as can be seen from the relation $d=2\pi/q$ where d is the distance probed in real space at a given q value.[15] Especially the lipid bilayer of liposomes, with a thickness of roughly 5 nm and with a defined electron density profile, is well-suited for study by SAXS, as binding or accumulation of molecules (including dyes) on the bilayer will lead to changes in the scattering.[17–19]

Due to the frequent application of liposomes in biofluids, most current research focuses on surface characteristics and modifications to circumvent unwanted reactions of biological systems with liposomes. For instance, PEGylation is often mentioned as a suitable surface modification as well as neutral surface charge to prevent protein deposition.[14,20,21] The broad application of PEGylation in pharmaceutical or cosmetical formulations induces anti-PEG antibody production in many individuals, which triggers unwanted immune reactions (e.g. faster clearance of pharmaceuticals) as shown in recent studies.[22,23] However, in this work, rather than intensifying further optimizations on the liposome surface via lipid compositions or modifications, our goal was to investigate the relevance of effects entrapped molecules may have on the lipid bilayer and the characteristics of the outer surface. This has received little attention to date, yet it represents a significant factor which potentially influences the reactivity

of liposomes. In the case of liposomes, the effect entrapped molecules may have on the lipid bilayer and the characteristics of the outer surface has received little attention to date. Therefore, this work focuses on examining how different fluorescent dyes can affect the liposome surface chemistry and, through this influence, interactions with biological systems using the human complement system as an example. Specifically, the fluorophores IR-783, sulforhodamine B (SRB), and 1,3,6,8-pyrenetetrasulfonic acid (PTSA) were encapsulated in liposomes. These were then analyzed for their size, surface charge and spectroscopic characteristics, and SAXS measurements were performed to determine changes in the lipid bilayer structure. Finally, the effect of the different liposomes on the human complement system was investigated in serum samples.

3.2 Materials and Methods

3.2.1 Chemicals and consumables

All chemicals were of analytical grade and used without purification. Sephadex® G-50 (G50150), Lipopolysaccharides (LPS) from Salmonella enteritidis (L6011), Cholesterol from sheep wool (C8667) and tetrasodium ethylenediaminetetraacetic acid (EDTA, EDS), ethylene glycol-bis(2-aminoethyl ether)-*N,N,N′,N′*-tetraacetic acid (EGTA, E4378), sodium hydroxide, methanol and polyclonal goat anti-biotin IgG (B3640) were purchased from Sigma-Aldrich/Merck KGaA (Darmstadt, Germany). Sodium azide and magnesium dichloride hexahydrate were purchased from Merck KGaA (Darmstadt, Germany). The extrusion kit and the phospholipids 1,2-dipalmitoyl-*sn*-glycero-3-phosphocholine (DPPC, 850355P), 1,2-dipalmitoyl-*sn*-glycero-3-phospho-(1′-*rac*-glycerol) (sodium salt) (DPPG, 840455P) and 1,2-dipalmitoyl-*sn*-glycero-3-phosphoethanolamine-*N*-(biotinyl) (DPPE-biotin, 870285P) were purchased from Avanti Polar Lipids (Alabaster, AL, USA). Sulforhodamine B (SRB, S1307) was purchased from Thermo Fisher Scientific (Darmstadt, Germany). Chloroform and nitric acid (HNO_3) were bought from Fisher Chemical (Schwerte, Germany). N-2-hydroxyethylpiperazine-N'-2-ethanesulfonic acid (HEPES, HN78.3), Sodium chloride, sucrose (4621.3), N-octyl-β-d-glucopyranoside (OG, CN23.3) and calcium chloride was bought from Carl Roth (Karlsruhe, Germany). Dialysis membrane Spectra/Por® 4 (MWCO 12 - 14 kDa, 132700) from Spectrum Laboratories and polycarbonate Whatman Nucleopore™ Track-Etched membranes with a pore size of 1.0 µm, 0.4 µm or 0.2 µm (Ø 19 mm) from Whatman were bought from VWR (Darmstadt, Germany). The ICP-OES phosphorus standard solution (10882.0000) was purchased from Bernd Kraft/AnalytiChem GmbH (Duisburg, Germany). Black 96-well flat bottom microtiter plates (MTP, 781608) were purchased from Brand (Wertheim, Germany). Pooled human complement serum was purchased from Innovative Research (ISCER, Novi, Michigan, USA). IR-783 (I1031) was purchased from TCI

Deutschland GmbH (Eschborn, Germany). 1,3,6,8-pyrenetetrasulfonic acid (PTSA, P0021) was purchased from Chemodex AG (St. Gallen, Switzerland).

3.2.2 Liposome synthesis

Liposome synthesis was performed as described earlier[24] using the reverse-phase evaporation method. Standard anionic lipid composition contained 5 %mol. Cholesterol, 73 %mol. DPPC, 20 %mol. DPPG and 2 %mol. DPPE-Biotin for low cholesterol liposomes or 44 %mol. Cholesterol, 34 %mol. DPPC, 20 %mol. DPPG and 2 %mol. DPPE-Biotin for high cholesterol liposomes. For LPS liposomes, LPS from Salmonella enteritidis was added to the lipid mixture. For LPS an estimated molecular weight of 15000 $g \cdot mol^{-1}$ was used for calculations.

60 µmol of the desired lipids were dissolved in chloroform (3 mL) and methanol (0.5 mL). After sonication at 60 °C for 1 min, 2 mL of the preheated (60 °C) encapsulant solution was added. Encapsulant solutions contained 10 mM SRB, 210 mM NaCl or 10 mM IR-783, 210 mM NaCl or 100, 150 or 200 mM PTSA or 280 mM NaCl dissolved in 20 mM HEPES, pH 7.5. Mixture was sonicated again at 60 °C for 4 min. The organic solvents were removed with a rotary evaporator (LABOROTA 4001, Heidolph, Germany) at 60 °C while the pressure was reduced stepwise from 900 to 780 mbar within 40 min (900 mbar for 10 min, 850 mbar for 5 min, 800 mbar for 5 min, 780 mbar for 20 min). The solution was vortexed for 30 s, and another 2 mL of the encapsulant was added. After a second vortexing step for 30 s, the solution was further rotated at 60 °C while the pressure was reduced stepwise starting from 750 to 400 mbar within 60 min (750 mbar for 20 min, 600 mbar for 5 min, 500 mbar for 5 min, 400 mbar for 20 min). The solution was then extruded through polycarbonate membranes with varying membrane pore sizes (1 µm, 0.4 µm or 0.2 µm). Extrusion was done at 65 °C by pushing the solution with the syringes 21 times through each membrane pore size. Excess of encapsulant (i.e. fluorophore and NaCl) was removed by size exclusion chromatography with a Sephadex G-50 column followed by dialysis against the liposome storage buffer (HSS, 10 mM HEPES, 200 mM NaCl, 200 mM sucrose, 0.01 % NaN3, pH 7.5). Liposomes were stored at 4 °C.

For PTSA encapsulating liposomes with a PTSA content of 150 and 200 mM PTSA the NaCl and sucrose content in the HSS buffer was adjusted to 250 mM NaCl, 335 mM sucrose and 400 mM NaCl, 300 mM sucrose respectively.

Smallest membrane pore size during extrusion is mentioned in **Table S 3-1** for each liposome synthesis.

3.2.3 Liposome characterization

Dynamic light scattering (DLS), zeta potential and polydispersity index (PDI) measurements were performed on a Malvern Panalytical Zetasizer Nano-ZS. For size determination

polymethyl methacrylate semi-micro cuvettes (Brand, Germany) and for zeta potential determination disposable folded capillary cells (Malvern Panalytical, Germany) were used. Measurement temperature was set to 25 °C with a 1:100 sample dilution in HSS buffer in both cases. Measurement of size and PDI were conducted with a dispersant refractive index n_D20 of 1.34, a material absorbance of zero, a dispersant viscosity η of 1.1185 mPa s, an angle of 173° and backscattering mode after equilibration for 15 s in three measurement runs with each 13 single measurements. For zeta potential, a dielectric constant ε of 78.5 was used with an equilibration time of 60 s before four measurement runs started with each twenty single measurements.

Phospholipid concentrations were determined via optical emission spectroscopy with inductively coupled plasma (ICP-OES, SpectroBlue TI/EOP) from SPECTRO Analytical Instruments GmbH (Kleve, Germany). Liposomes solutions were diluted 1/150 with a total volume of 3 mL in 0.5 M HNO3. A phosphorus standard diluted in 0.5 M HNO3 from 1 to 100 µM was used for calibration of the device. Phosphorous was detected at a wavelength of 177.495 nm. Before each measurement, 0 µM and 100 µM phosphorus standard dilutions were used to re-calibrate the device. The total lipid concentration (tL) was calculated from the phospholipid concentration and the lipid composition used during synthesis.

The initial fluorescence of the liposomes was determined using a SYNERGY neo2 multi-mode reader from BioTek (Bad Friedrichshall, Germany). The liposome stock solutions were diluted to 50 µM tL concentration in HSS with and without 30 mM OG. Samples were prepared in quadruplicates. The so-called initial fluorescence was calculated as the ratio of the fluorescence intensities of intact (without OG) and lysed liposomes (with OG).

Measurement conditions were λ_{Ex} = 565 (5) nm, λ_{Em} = 585 (5) nm, gain 100 for SRB liposomes, λ_{Ex} = 790 (13) nm, λ_{Em} = 820 (13) nm, gain 150 for IR-783 liposomes, and λ_{Ex} = 375 (5) nm, λ_{Em} = 405 (5) nm, gain 100 for PTSA liposomes.

3.2.4 Fluorophore mixtures and self-quenching

Fluorophores were dissolved in HSS to 100 mM in case of SRB and IR-783 and 200 mM for PTSA. Fluorophore mixtures were prepared out of these stocks with 10 µM of each respective dye. For the fluorophore self-quenching studies each fluorophore was investigated with a concentration titration from 1 µM to 100 mM for SRB and IR-783 and 1 µM to 200 mM for PTSA. Samples prepared in triplicates were measured with a SYNERGY neo2 multi-mode reader from BioTek (Bad Friedrichshall, Germany). Measurement settings: IR-783, λ_{Ex} = 790 (13) nm, λ_{Em} = 820 (13) nm, gain 150; SRB, λ_{Ex} = 565 (8) nm and λ_{Em} = 585 (8) nm, gain 75; PTSA, λ_{Ex} = 375 (5) nm and λ_{Em} = 405 (5) nm, gain 100.

3.2.5 Dialysis experiment

Ghostisome stock solutions were mixed with 100 mM dye stock solutions to reach 6 mM tL and 10 mM dye content in HSS and incubated for 1 hour at room temperature. From each sample a positive control without dialysis was taken. The remaining solutions were dialysed in parallel against pure buffer over 24 hours with two buffer exchanges. Dialysis was stopped at the same time for all samples. Total lipid concentration was determined again for all dialysed samples with the above described procedure.

For spectral investigations the solutions for PTSA and SRB were diluted to 2 µM. For the dialyzed samples a concentration of 200 µM was used. All solutions containing IR-783 were diluted to a concentration of 10 µM. All measurements were carried out with a cuvette with thickness 1 cm. Absorption spectra were recorded with the Cary 60 from Agilent. All spectra were referenced to the HSS buffer solution. The fluorescence measurements were carried out with the fluorimeter Fluorolog-3 from Horiba.

3.2.6 SAXS measurements

For SAXS measurements with lipid-dye mixtures high cholesterol (44 %mol. Cholesterol, 34 %mol. DPPC, 20 %mol. DPPG and 2 %mol. DPPE-Biotin) and low cholesterol (5 %mol. Cholesterol, 73 %mol. DPPC, 20 %mol. DPPG and 2 %mol. DPPE-Biotin) lipid stock solutions were dissolved to 100 mM tL in 20 mM HEPES, pH 7.5 at elevated temperatures while vortexing until a homogeneous mixture was obtained. 100 mM dye stock solutions were prepared in 20 mM HEPES, pH 7.5. Buffer, dye and lipid stock solutions were mixed accordingly to reach 50 mM tL with a varying dye content of 0, 2, 5, 25 or 50 mM.

For SAXS measurements investigating concentrated liposome solutions the respective liposomes were diluted to 5 mM in HSS followed by concentration through evaporation of water at room temperature with a rotary vacuum concentrator (RVC 2-18 CDplus HCl, Martin Christ Gefriertrocknungsanlagen GmbH, Germany). The process was stopped after reducing the volume by approximately 10 times.

SAXS measurements were performed on a bench built by XENOCS. The scattered beam of Mo radiation (λ= 0.071 nm) was collected on a 2D online scanner detector from MAR Research (diameter: 345 mm). Quartz capillaries (diameter: 2 mm) were used as sample containers and silver behenate was used for scattering vector calibration. Data treatment of raw data (integration) was conducted by pySAXS. Furthermore, the exact size of the capillaries was considered and background (empty capillary) as well as aqueous solvent (φ(water)= 50-70%) were subtracted from the liposome/lipid samples. All measurements were conducted at ambient temperature.

3.2.7 Homogeneous liposome-based complement assay

The liposome-based complement assay was performed following a previously established protocol.[24]

Each assay contained four liposome containing samples: liposomes in liposome complement buffer (LCB, 10 mM HEPES, 150 mM NaCl, 135 nM $CaCl_2$, and 1 mM $MgCl_2$ in double distilled H_2O, pH 7.4 prepared according to the HBS buffer of Zelek et al.[25], negative control), liposomes in active serum or in inactivated serum (negative control) containing 1/10 diluted inactivation buffer (iaCB, 200 mM EDTA and 0.5 µM EGTA, diluted in LCB, pH 7.5 – 8) and lysed liposomes by detergent addition as positive control, all prepared in LCB. Serum was inactivated by EDTA and EGTA addition to complex free Ca^{2+} and Mg^{2+} ions essential for the functionality of the complement system. Detergent positive controls contained 30 mM OG and serum in the final well. The final wells contained 100 µL volume, 10 µM tL liposomes and 200 mM sucrose for liposome stability. Final inactivated serum wells contained 20 mM EDTA and 0.05 µM EGTA. Serum content was 10 %vol. in the respective wells. All samples were prepared in triplicates.

Liposomes were prediluted in LCB to 100 µM tL solutions. In case antibodies were used as complement triggers, polyclonal goat anti-biotin antibodies (1.0 mg mL^{-1}) were incubated 15 min at RT with the liposome stock solution prior to dilution to 100 µM tL with LCB. Black 96 well, flat bottom microtiter plates were prepared on ice with LCB, sucrose (1 M sucrose in LCB), iaCB and OG (300 mM OG in double distilled H2O) stock solution additions to the respective wells to reach the desired conditions. Liposomes were added, resulting in a 1/10 dilution in the final well. As last step, serum was added before incubation at 37 °C for 60 min and fluorescence intensity measurements with a SYNERGY neo2 multi-mode reader from BioTek (Bad Friedrichshall, Germany) (SRB: λ_{Ex} = 565 nm and λ_{Em} = 585 nm with bandwidth 8 and gain 125; IR-783: λ_{Ex} = 790 nm and λ_{Em} = 820 nm with bandwidth 13 and gain 175; PTSA: λ_{Ex} = 375 nm and λ_{Em} = 405 nm with bandwidth 5 and gain 150). For each measurement, the plate was read 3 consecutive times to relativize the instrument's influence on the signal.

All obtained fluorescence intensities were background corrected by subtraction of the respective inactivated serum negative control and then normalized to the background corrected fluorescence intensity of the positive control to obtain the liposome lysis. In all cases, gaussian error propagation was used to determine the respective standard deviations.

3.3 Results and Discussion

In bioassays, the simultaneous detection of several analytes in the same sample is often desirable since it allows more data per assay, increases efficiency, reduces reagent

consumption and shortens assay times. Thus, multiplex bioassays are often more cost-effective in diagnostic setups. The selection of the three fluorophores used in this work, which are encapsulated into the liposomes, was aimed exactly at the development of such a multiplex detection system. The fluorophores were carefully selected to allow this simultaneous detection by showing minimal overlap in their optical spectra. Since liposomes encapsulating SRB have already been used for more than two decades[26] with extensive analysis and optimization of encapsulant concentration and lipid composition[24], they were used as standard reference liposomes. Consequently, PTSA was chosen as a fluorophore in the lower wavelength range and IR-783 in the higher wavelength range. Spectral overlap was avoided as much as possible (**Figure 3-1**). In general, simultaneous detection of the free dyes could be confirmed (**Figure 3-2**) and the minimal effects on the mutual emission can be corrected mathematically. Specifically, while the equimolar combination of PTSA and SRB only minimally influenced the fluorescence signal of each other, the presence of IR-783 detectably reduced the fluorescence obtained for the other two dyes, albeit to a small degree. The mixture of PTSA and SRB caused an increase in SRB signal of 10 ± 4 %, while the signal of PTSA showed an insignificant reduction of 3 ± 4 % compared to the pure dyes. Thus, SRB partially reabsorbs PTSA emission, resulting in decreased PTSA and increased SRB intensities. The IR-783 signal intensity was unchanged for all mixtures compared to the pure dye. The PTSA signal intensity dropped by 31 ± 3 % when mixed with IR-783 and by 33 ± 3 % when mixed with both other dyes simultaneously. SRB fluorescence was quenched by 16 ± 2 % when mixed with IR-783 and by 15 ± 3 % when mixed with the other two dyes. Hence, not surprisingly, IR-783 influences the fluorescence intensities of the other two dyes due to its broad absorption bands, due to significant radiative energy transfer at the given concentrations, and possibly by heteromolecular aggregation effects between the fluorophore molecules. The latter could likely be caused by π-π-interactions of the aromatic moieties found in all investigated fluorophores.

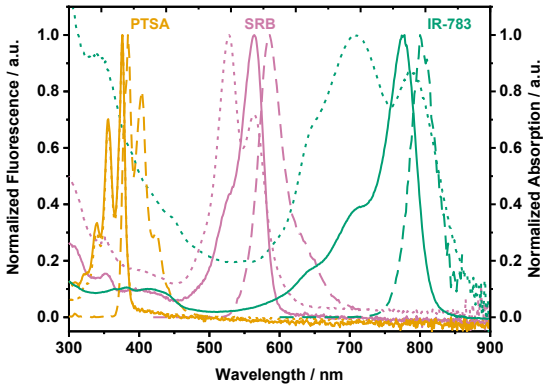

Figure 3-1: Optical spectra of SRB, PTSA and IR-783. Solid lines show absorbance spectra, dashed lines represent fluorescence spectra and dotted lines refer to dyes encapsulated in liposomes (44 %mol. cholesterol lipid mixture, PTSA-Liposome-2, SRB-Liposome-4, IR-Liposome-2). 20 µM total lipid concentration of each dye encapsulating liposome was measured.

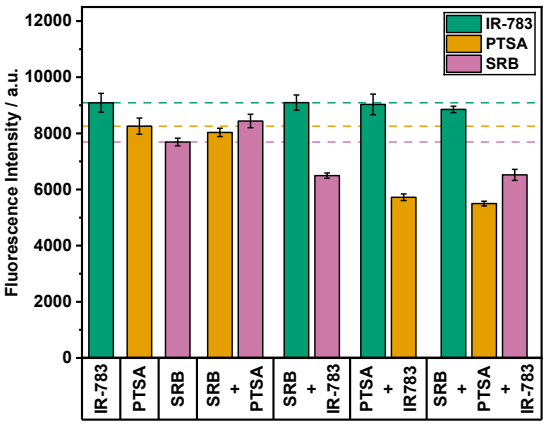

Figure 3-2: Fluorescence intensities of PTSA, SRB and IR-783 in different compositions (each fluorophore at 10 µM). Reference lines and control bars show the fluorescence intensities of pure dyes. IR-783, λ_{Ex}=790 (13) nm, λ_{Em}=820 (13) nm, gain 150; SRB, λ_{Ex}=565 (8) nm and λ_{Em}=585 (8) nm, gain 75; PTSA, λ_{Ex}=375 (5) nm and λ_{Em}=405 (5) nm, gain 100; n=3.

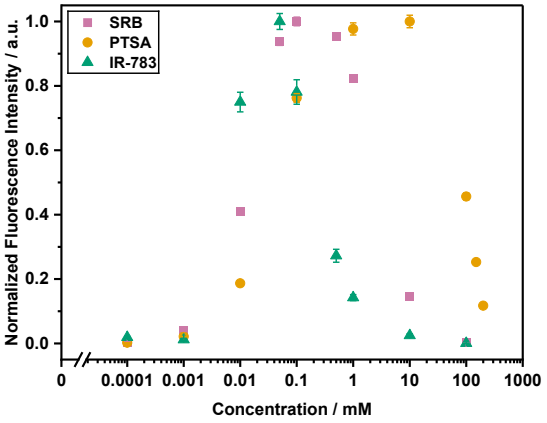

Figure 3-3: Normalized fluorescence intensities for fluorophore titrations in Liposome Complement Buffer (LCB). Normalization to maximum intensity. IR-783, λ_{Ex}=790 (13) nm, λ_{Em}=820 (13) nm, gain 150; SRB, λ_{Ex}=565 (8) nm and λ_{Em}=585 (8) nm, gain 75; PTSA, λ_{Ex}=375 (5) nm and λ_{Em}=405 (5) nm, gain 100; n=3 (except IR-783 0.0001 mM and PTSA 0.01 mM, n=2).

3.3.1 Liposome Preparation and Characterization

High concentrations of fluorescent dyes lead to aggregation. Depending on the relative orientation of the chromophores, H- or J-type molecular aggregates can be formed.[27,28] H-aggregates usually exhibit a blue-shifted absorption and reduced emission compared to the monomeric dye. For both SRB and IR-783, corresponding characteristics are found in the absorption spectrum of the dyes (dotted line in **Figure 3-1**). This is in line with the observation that intact liposomes exhibit no or minimal fluorescence (associated with the common term 'self-quenching'), whereas in their lysed state, when the encapsulants are released and diluted in the surrounding solution, high fluorescence signals are observed, allowing easy quantification of their release.[29]. For SRB, liposome dye concentrations ranging from 10 to 150 mM have been described to show this phenomenon[24,30,31], i.e. efficient self-quenching (as explained above) could be confirmed in this concentration range (**Figure 3-3**). Subsequently, an SRB encapsulant concentration of 10 mM was chosen, which resulted in a signal intensity of 15 ± 1 % when encapsulated compared to the maximum signal upon fluorophore release. The fluorophore IR-783 showed self-quenching due to aggregation with the lowest

concentrations among the investigated dyes starting at 0.05 mM and around 1 mM aggregates are clearly predominant (**Figure 3-3**). Hence, similar to SRB, 10 mM IR-783 was chosen with low background signals of only 2.5 ± 0.5 % of the released maximum signal. For PTSA, higher concentrations were necessary to ensure efficient self-quenching (**Figure 3-3**). Dye concentrations of 150 mM and above were determined to be suitable with residual signal intensities of 25.3 ± 0.5 % for 150 mM and 11.7 ± 0.3 % for 200 mM of the released maximum intensity. In previous work, preparation conditions for liposomes have been established for SRB liposomes with encapsulant concentrations of 10 mM SRB and 210 mM NaCl. Due to the structure of PTSA with its four sulfonic acid groups, concentrations above 100 mM PTSA bear the risk of a too high osmolality inside the liposomes compared to the osmolality of the established buffers for SRB liposome preparation. This can lead to liposome instability or fluorophore leakage if the buffers are not adjusted accordingly. Therefore, although fluorescence signal reduction was not ideal at 100 mM, the concentration range of 100, 150, and 200 mM PTSA was tested as encapsulant. With this, self-quenching in the final system could be investigated and it could be evaluated whether higher concentrations with potential buffer adjustments are mandatory. Ultimately, for multiplex analyses, all types of liposomes must be stable under the same buffer conditions, hence similar osmolalities are mandatory to avoid fluorophore leakage or liposome swelling.

Anionic liposomes were prepared by reverse-phase evaporation following the established method by Edwards et al..[32] Liposome preparation was examined with high (i.e. 44 %mol.) and low (i.e. 5 %mol.) cholesterol lipid mixtures in combination with each dye separately to investigate the effect of the respective dye on the different analytically typical lipid compositions.[24] Liposomes prepared with 10 mM SRB and 210 mM NaCl as encapsulant and extruded through the smallest membrane pore size of 0.2 µm resulted in vesicles with a diameter of 143 ± 2 nm for high cholesterol and 130 ± 1 nm for low cholesterol liposomes with a PDI of 0.10 ± 0.01 and 0.12 ± 0.01, respectively. The surface zeta potential of -25 ± 1 mV for high cholesterol and -16 ± 1 mV for low cholesterol liposomes confirmed the expected anionic characteristics contributing to their colloidal stability. Purification by size exclusion chromatography (SEC) led to a clear separation of the liposome and the excess dye band. Consequently, dialysis as a second step to remove excess encapsulant could be kept short over one night including two buffer exchanges.

Similar results were obtained for PTSA liposomes. Preparation parameters were not changed except for the encapsulant containing either 100, 150 or 200 mM PTSA without additional sodium chloride. The sodium chloride and sucrose content in the respective liposome storage buffer was adjusted from 200 mM NaCl and 200 mM sucrose to 250 mM NaCl and 335 mM sucrose for 150 mM and 400 mM NaCl and 300 mM sucrose for 200 mM PTSA encapsulating

liposomes. The resulting liposomes were slightly larger in diameter with 147 to 165 nm for the high cholesterol and in a similar size range with 118 to 142 nm for the low cholesterol lipid composition compared to SRB liposomes, with no trend regarding the encapsulated PTSA content. The determined PDI was in the range of 0.06 to 0.08 and 0.09 to 0.12, respectively. The surface zeta potential was in a comparable range to SRB liposomes with -19 to -16 mV for the low cholesterol and -22 to -18 mV for the high cholesterol liposome batch. As for SRB liposomes, preparations with PTSA showed a clear separation of liposome and free fluorophore band during SEC, which resulted in the same short dialysis time.

Liposome preparations with IR-783 (i.e. 10 mM IR-783 and 210 mM NaCl) as encapsulant resulted in liposome formation only for the high cholesterol lipid composition. For the low cholesterol preparation, the lack of a second band during SEC indicated an absence of liposomes. This observation was further substantiated through DLS measurements which confirmed the absence of vesicles (data not shown). For high cholesterol compositions, worse separation of excess dye and liposomes was observed during SEC, leading to the use of longer (i.e. about 45 cm instead of about 15 cm in length) and wider (i.e. diameter increased from 1.5 cm to 3.0 cm) columns. In addition, an extended dialysis time of two days compared to preparations with the other two dyes was required to remove all the excess encapsulant. The obtained liposomes extruded through the smallest pore size of 0.4 µm had a diameter of 170 ± 10 nm. The PDI of 0.26 ± 0.01 indicates a broader size distribution compared to the other liposomes, which can be attributed to the use of the larger membrane pore size of 0.4 µm instead of 0.2 µm as for the other liposomes. The measured surface zeta potential for IR-783 containing liposomes of -23 ± 3 mV was in a similar range to liposomes with the other two dyes.

Overall, liposomes could be successfully synthesized with all dyes except the low cholesterol lipid compositions in combination with IR-783 in the encapsulant. This finding gave rise to the assumption that each dye may have unique characteristics as encapsulant that may also influence the lipid arrangement, preventing liposome formation in the case of IR-783. The assumption was further supported by the increased effort needed to separate the excess dye from the liposomes.

3.3.2 Optical Characterization

Encapsulation of 10 mM SRB inside the liposomes resulted in an initial fluorescence of 6 to 12 %, as determined by comparing the fluorescence signal intensity of intact and lysed liposomes by detergent addition. Even lower initial fluorescence values were achieved when IR-783 was encapsulated. Here, values as low as 1 % were obtained. The notable reduction of the fluorescence signal found for the dyes confined in intact liposomes points towards the

formation of H-aggregates. By increasing the amount of PTSA in the encapsulant solution, the initial fluorescence of high cholesterol liposomes was improved from 40 ± 2 **%** (100 mM PTSA) to 25 ± 1 **%** (150 mM PTSA) and 13 ± 1 **%** (200 mM PTSA), resulting in an overall better resolution between lysed and non-lysed liposome signals. Higher concentrations are required for pronounced self-quenching effects with PTSA, as can be seen from **Figure 3-1** where only slight changes in the absorption spectrum for the liposome sample is evident at the given concentration, in contrast to the situation for the other two dyes. However, osmolality-induced lysis in the assay buffer was observed through increased fluorescence signals for 150 mM and 200 mM PTSA liposomes (**Figure S 3-1**). This was partially resolved by increasing the sugar content of the assay buffer from 200 mM to 440 mM for 150 mM PTSA liposomes or to 660 mM for 200 mM PTSA liposomes (**Figure S 3-1**). Conversely, high concentrations of sucrose and thus a high osmolality in the buffer surrounding the liposomes could interfere with the multiplex application combining all liposome types together. Hence, the medium concentration of 150 mM PTSA for the encapsulant was chosen as a compromise to test the interaction with biological systems, in this case the human complement system.

The previously mentioned observations during liposome preparation suggest that the dyes influence the lipid bilayer formation during preparation and thus interact directly with the bilayer. A very simple assay was devised to qualitatively demonstrate the differences between the three dyes. Specifically, liposomes without encapsulated dye (ghostisomes) were incubated with each dye from the outside in the surrounding buffer, followed by dialysis against pure buffer over 24 hours. The assay was performed for both a high and a low cholesterol version of the liposomes.

Ghostisome preparations yielded liposomes with a diameter of 301 ± 7 nm for high cholesterol and 220 ± 11 nm for low cholesterol lipid compositions with a PDI of 0.16 ± 0.02 and 0.20 ± 0.01, respectively. The absorbance spectra measured after incubation with the dye and subsequent dialysis indicate that SRB and PTSA may interact with the membrane, however, they can be completely dialyzed away from the liposomes (**Figure 3-4**). In fact, samples after dialysis were measured 100 times more concentrated than the control sample and still no characteristic absorbance was detected at the respective wavelengths which would be indicative for residual dye, but only scattering background was observed. This leads to the inference that no or only weak and reversible interactions with the lipid membrane are present for both dyes.

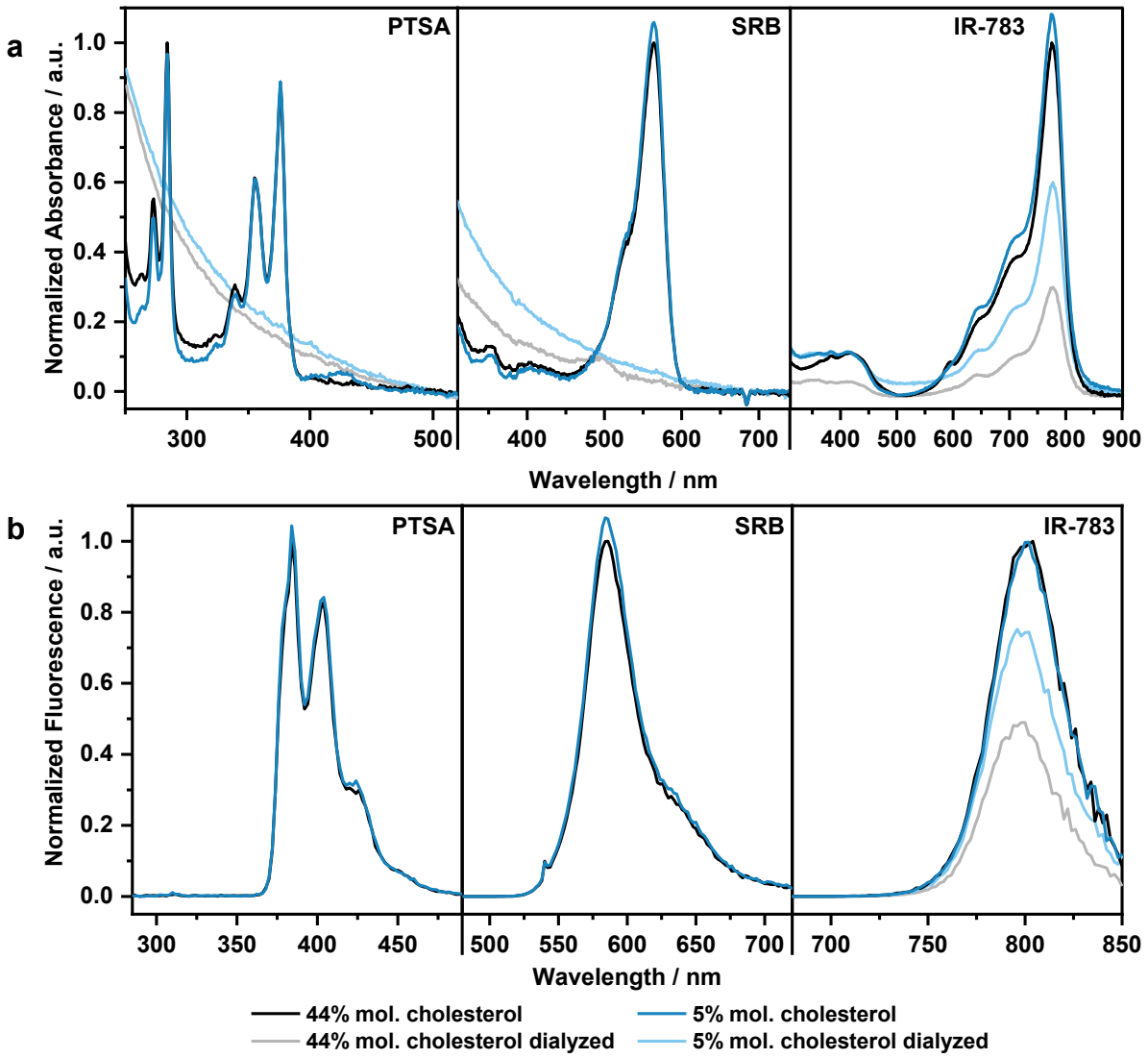

Figure 3-4: Absorption, **a** and emission spectra, **b** of dye-ghostisome (Ghostisome-1 & 3) incubation experiments with different cholesterol content with and without dialysis. Concentrations of PTSA and SRB were 2 µM without dialysis and 200 µM with dialysis. For IR-783 concentrations of 10 µM was chosen for all samples. The excitation wavelengths for all IR-783 samples were λ_{Ex}=777 nm, for PTSA samples λ_{Ex}=284 nm and for SRB-samples λ_{Ex}=540 nm. For PTSA and SRB, no more characteristic dye absorption but rather only scattering signals (as identified by the l^{-4} dependence) were observed for the dialyzed samples, which is why also no emission signals are plotted for them. Note that all curves were normalized with respect to the Ghostisome with 44% mol. Cholesterol (black lines).

In contrast, the fluorophore IR-783 could not be completely removed by dialysis over 24 hours (**Figure 3-4**). Significant absorbance remained in the dialyzed samples of both liposome versions and fluorescence could be detected (**Figure 3-4b**), even given the low quantum yield and short fluorescence lifetime of this dye[33], indicating that a significant amount of it is still present in the dialyzed samples. For the low cholesterol liposomes, the absorbance was reduced by 47 % compared to the non-dialyzed control sample (calculated at the absorbance maximum at 777 nm). For the high cholesterol liposomes, dialysis reduced the absorbance by 66 % (calculated at the absorbance maximum at 777 nm). From this it can be concluded that the fluorophore IR-783 interacts with the lipid bilayer in a non-reversible manner which resists

removal by dialysis. Furthermore, the greater decrease in absorbance for the high cholesterol liposomes suggests a weaker interaction of the fluorophore IR-783 with this lipid composition compared to the low cholesterol liposomes. This finding is consistent with the observation that preparation of low cholesterol liposomes in combination with IR-783 was not achieved, whereas preparation of high cholesterol liposomes was successful. This may be attributed to too excessive interaction of IR-783 with the lipids, which may prevent successful liposome formation.

3.3.3 Lipid Bilayer Characterization by SAXS

Further insight into the dye-lipid bilayer interactions was obtained through SAXS measurements. Specifically, each dye was mixed and investigated at different concentrations ranging from 2 to 50 mM with high and low cholesterol lipid mixtures, maintaining a constant total lipid concentration of 50 mM. The pure lipid samples analyzed as controls showed a form factor typical for lipid bilayer, showing a large oscillation between 0.5 and 2.2 nm^{-1} with a local minimum at 0.5 nm^{-1},and a slightly pronounced Bragg peak around q = 1.06 nm^{-1} (**Figure 3-5**), caused by smectic ordering.[17,34] This peak indicates an interlamellar distance of 5.93 nm, i.e. the lamellar repeat distance in stacked bilayers, which is in accordance with values reported in literature.[35,36] The form factor did not change when SRB was added to the lipid mixtures, regardless of whether the cholesterol content was high or low (**Figure 3-5a**). However, for the low cholesterol compositions, the intensity of the peak (q = 1.06 nm^{-1}) increased with high SRB concentrations (≥25 mM), which can be attributed to a higher order in the multilayer system created by stacking additional bilayers. Furthermore, the peak shifted to a lower q value of 0.88 nm^{-1} at an SRB concentration of 50 mM, indicating that the distance between the bilayers increased from 5.92 nm to 7.13 nm. We hypothesize that this swelling of the multilayers is due to SRB adsorption on the bilayer surface, causing increased electrostatic repulsion between bilayers, as usually observed upon electrostatically charging bilayers.[37] SRB is indeed a charged species, which therefore charges the bilayer when it adsorbs on it. Noteworthy is that the overall bilayer structure (form factor) remains unchanged upon the addition of SRB, informing that SRB adsorbs onto the bilayer surface without significantly altering its electron density profile (bilayer structure). It is likely that the surface concentration of SRB at the bilayer surface is too low to affect significantly the overall electron density at the top bilayer surface.

When PTSA was added to the lipid solutions, results similar to those of SRB lipid mixtures were obtained, with the overall form factor remaining unchanged (**Figure 3-5b**). Especially for the high cholesterol containing sample, no influence of PTSA on the bilayer was found. Lipid mixtures with low cholesterol content partially showed a peak emerging at around 1 nm^{-1}, which is comparable to the one observed with SRB at the same concentration but much less pronounced. However, here no shift in the peak position was observed upon addition of PTSA.

Hence, we can conclude that PTSA does not interact with the lipid membrane, neither by adsorption nor by altering the lipid arrangement in the bilayer.

In contrast, the presence of the fluorophore IR-783 in lipid mixtures had a significant effect on the bilayer form factor in the q-range from 0.3 to 1 changed by increasing IR-783 concentration from 5 to 50 mM (**Figure 3-5c**). For both high and low cholesterol lipid mixtures, a distinct shift in the position of the local scattered intensity minimum of the bilayer form factor from 0.5 down to 0.4 nm^{-1} upon addition of IR-783 and an excess scattering in the region of the large oscillation are observed. This observation indicates that the fluorophore strongly affects the bilayer structure, either by locating in the bilayer surface, i.e. in the polar head region, and/or in the hydrophobic core of the lipid bilayer, thereby substantially altering the electron density profile that produces the pattern probed by SAXS (bilayer form factor). Interestingly, IR-783 has been shown to be membrane-permeable through transport mechanisms only. Specifically, IR-783 enters cells primarily through organic anion transporter polypeptides (OATPs), which are overexpressed in many cancer cells. This mechanism allows IR-783 to selectively accumulate in tumor cells, making it useful for imaging and therapeutic applications.[38,39] Once inside the cells, it localizes to the mitochondria, where it is described to induce mitochondrial fission and to affect cellular processes such as apoptosis and ATP production.[40,41] Based on our data presented here, it needs to be considered that IR-783 may not only enter cells via OATPs but also through the hydrophobic areas of the lipid bilayers.

Subsequently, these results were confirmed for liposomes encapsulating the respective fluorophores. To generate sufficiently high signal intensities, synthesized fluorophore encapsulating 5 mM liposome stock solutions were concentrated approximately 10-fold by water evaporation. Again, a significant change in the form factor of the bilayer was obtained only for liposomes encapsulating IR-783 (**Figure S 3-2**). Differences in signal intensity between the different liposome samples are probably due to slight variations in the lipid concentration of the samples, since the concentration was estimated by eye during the preconcentration step based on the residual volume in the reaction tubes.

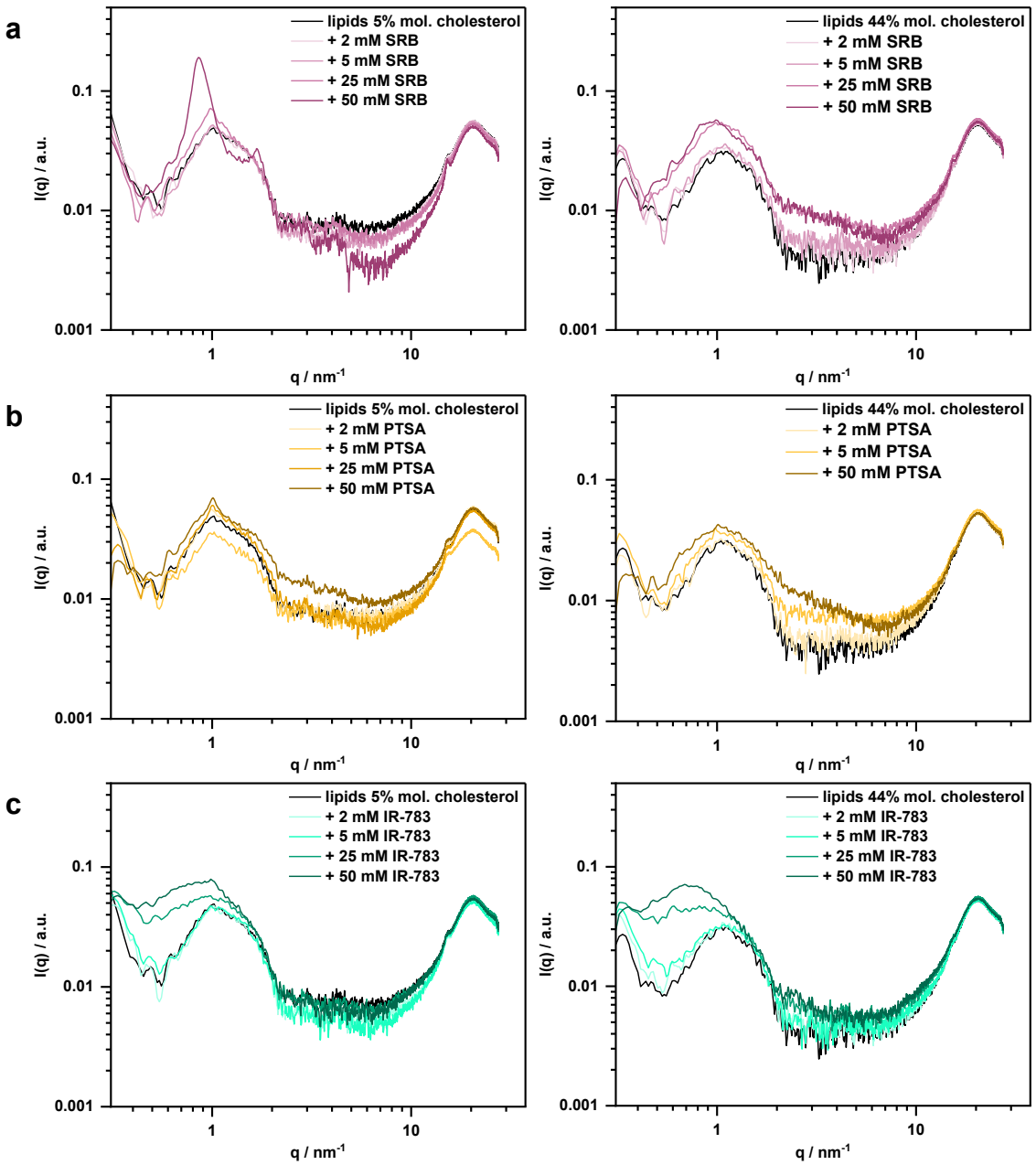

Figure 3-5: SAXS measurements with lipid mixtures (50 mM total lipid concentration, left: 5 %mol. cholesterol lipid mixture, right: 44 %mol. cholesterol lipid mixture) and fluorophore titration from 2 to 50 mM (A: SRB, B: PTSA, C: IR-783).

3.3.4 Reactivity Towards Biological Matrices

The interaction of encapsulants with the lipid bilayer is of relevance in any drug delivery or bioanalytical assay, since the liposome surface chemistry is typically carefully engineered for each specific application. Therefore, to investigate the potential impact these changes in bilayer structure and the interaction of the lipid surfaces with the fluorophores may have, a biological interaction assay was performed which assesses liposome surface interactions with the ever-present complement proteins in human serum. Liposomes can be designed to avoid recognition by the complement system and to remain stable in human serum. However, changes in surface chemistry and the use of ligands can cause the activation of the

complement system, leading to opsonization and ultimately liposome lysis.[24] Here, fluorophore deposition or alterations in the lipid membrane are expected to influence the reactivity of the complement system with these liposomes.

Such a bioassay was developed and optimized for 10 mM SRB encapsulating liposomes. While high cholesterol contents are known to activate the complement system[42–44], a reduction of the cholesterol content results in stable liposomes in serum over the investigated period of 1 hour at 37°C.[24] In addition, surface-bound antibodies in sufficient density on the surface are well known to be complement triggers[45] and are also able to induce a dose-dependent complement activation with low cholesterol SRB liposomes (0.2 %mol. antibody: 24 ± 2 % lysis, 0.5 %mol. antibody: 99 ± 5 % lysis, **Figure 3-6**). Furthermore, lipopolysaccharides (LPS) from bacterial membranes can cause both antibody-mediated and antibody-independent complement activation.[46,47] For this reason, experiments were designed here to study the effect of plain liposomes, LPS-tagged liposomes, and antibody-bound liposomes (**Figure 3-6**). As expected, all low cholesterol liposomes encapsulating SRB or PTSA that did not contain a complement trigger were not lysed, whereas high cholesterol SRB liposomes were lysed. Surprisingly, high cholesterol liposomes entrapping PTSA or IR-783 were stable. This suggests that not cholesterol alone, but in conjunction with SRB, which has been shown to be adsorbed on the bilayer structure by the SAXS analyses, acts as a complement trigger. Consequently, experiments using antibody or LPS triggers exhibited similar responses for the high cholesterol PTSA and IR-783 and the low cholesterol SRB liposomes. Low cholesterol PTSA LPS liposomes were not stable over time and showed fluorophore leakage (data not shown). Therefore, they were only investigated in the complement assay right after preparation with a different serum batch. Nevertheless, the trend of significantly lower responses by the low cholesterol PTSA liposomes, with low antibody concentrations and LPS only being able to activate the complement system very weakly, is still visible and in contrast to low cholesterol SRB liposomes. It can be assumed that the high cholesterol content may be needed to assist the complement response. This may be due to a better surface for complement protein deposition by cholesterol, hence free hydroxy group cluster formation.[48,49] In addition, the cholesterol content also influences membrane characteristics such as membrane fluidity and thickness,[50,51] which effect this has on complement mediated liposome lysis is still unclear.

These findings are important in clarifying statements made in literature regarding the activation of the complement system by cholesterol and in assigning it a more assisting role than a triggering role by itself. More broadly seen, however, these studies emphasize the relevance of gaining an understanding of the interactions encapsulants have with the chosen lipid bilayer, as they will clearly impact the often carefully designed liposome surface chemistry and lead to unexpected interactions with matrix components.

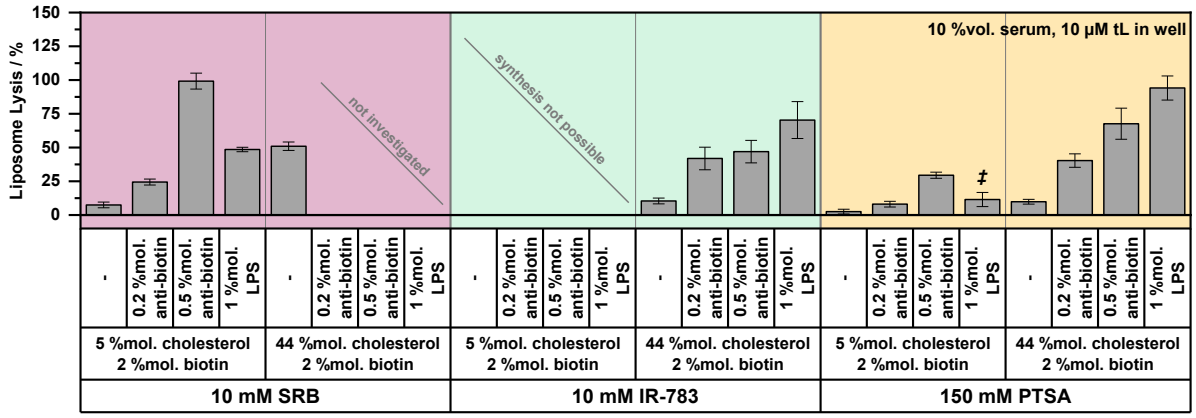

Figure 3-6: Liposome-based complement assays determining reactivity of the human complement system towards varying liposome surfaces and encapsulants (SRB, IR-783 or PTSA). Liposomes with low and high cholesterol content with and without surface modifications (SRB-Liposome-1, 2 & 3, IR-Liposome-1 & 3, PTSA-Liposome-3, 4, 5 & 6). Antibodies were incubated 15 min at RT with the liposomes prior to the complement assay. Lipopolysaccharides were included into the lipid composition during liposome preparation. Fluorescence intensities were corrected by inactive serum controls as background and normalized to a detergent containing positive control (30 mM OG). Liposomes were measured at 10 µM tL. Complement assays were performed in LCB with 200 mM sucrose for SRB and IR-783 liposomes and 440 mM sucrose for PTSA liposomes. Serum content for all liposomes was 10 vol%. per well. ‡ low cholesterol PTSA LPS liposomes were measured with a different serum batch. n=3.

3.4 Conclusion

In summary, the present study demonstrates that it is indeed very relevant to investigate the effects entrapped molecules may have on liposome characteristics and the reactivity of biological systems towards these liposomes. This was demonstrated by examining fluorophores as model liposome loadings, which, besides inducing variability in the optical characteristics, can significantly influence the lipid bilayer membrane characteristics of the liposomes. Consequently, the reactivity of the final liposomes towards biological matrices and also the overall success of liposome preparations is dependent on the encapsulated molecule, in this case the fluorophore. While fluorophore incubation experiments and SAXS measurements confirmed alterations in the lipid arrangements for IR-783, the liposome-based complement assays revealed that lipid compositions or surface modifications cannot be simply transferred between various types of liposomes encapsulating different fluorophores. This generally emphasizes that the encapsulant itself, which initially may seem to have no impact on the outer surface characteristics, indeed plays a crucial role in the biological stability of liposomes. Although the primary focus in assessing liposome stability in biological environments is often limited to the examination of lipid composition, surface modification, and general parameters such as temperature, pH, liposome size, surface charge, or osmolality, a comprehensive evaluation of both surface chemistry and the influence of the encapsulant is essential for the optimization of liposomes tailored to their targeted applications. This aspect is of particular relevance in areas such as drug delivery or diagnostic imaging, where long blood circulation times are critical for liposomal drug efficacy and contrast agent efficiency.

3.5 References

(1) Bangham, A. D.; Standish, M. M.; Watkins, J. C. Diffusion of univalent ions across the lamellae of swollen phospholipids. *J Mol Biol* **1965**, *13*, 238–252. DOI: 10.1016/s0022-2836(65)80093-6.

(2) Akbarzadeh, A.; Rezaei-Sadabady, R.; Davaran, S.; Joo, S. W.; Zarghami, N.; Hanifehpour, Y.; Samiei, M.; Kouhi, M.; Nejati-Koshki, K. Liposome: classification, preparation, and applications. *Nanoscale Res Lett* **2013**, *8*, 102. DOI: 10.1186/1556-276X-8-102.

(3) Dowhan, W. Molecular basis for membrane phospholipid diversity: why are there so many lipids? *Annu Rev Biochem* **1997**, *66*, 199–232. DOI: 10.1146/annurev.biochem.66.1.199.

(4) Briuglia, M.-L.; Rotella, C.; McFarlane, A.; Lamprou, D. A. Influence of cholesterol on liposome stability and on in vitro drug release. *Drug Deliv Transl Res* **2015**, *5*, 231–242. DOI: 10.1007/s13346-015-0220-8.

(5) Liu, G.; Hou, S.; Tong, P.; Li, J. Liposomes: Preparation, Characteristics, and Application Strategies in Analytical Chemistry. *Crit Rev Anal Chem* **2022**, *52*, 392–412. DOI: 10.1080/10408347.2020.1805293.

(6) Gregoriadis, G.; Ryman, B. E. Liposomes as carriers of enzymes or drugs: a new approach to the treatment of storage diseases. *Biochem J* **1971**, *124*, 58P. DOI: 10.1042/bj1240058p.

(7) Streif, S.; Neckermann, P.; Spitzenberg, C.; Weiss, K.; Hoecherl, K.; Kulikowski, K.; Hahner, S.; Noelting, C.; Einhauser, S.; Peterhoff, D.; Asam, C.; Wagner, R.; Baeumner, A. J. Liposome-based high-throughput and point-of-care assays toward the quick, simple, and sensitive detection of neutralizing antibodies against SARS-CoV-2 in patient sera. *Anal Bioanal Chem* **2023**, *415*, 1421–1435. DOI: 10.1007/s00216-023-04548-3.

(8) Edwards, A. J.; Durst, R. A. Flow-injection liposome immunoanalysis (FILIA) with electrochemical detection. *Electroanalysis* **1995**, *7*, 838–845. DOI: 10.1002/elan.1140070909.

(9) Gupta, R.; Salave, S.; Rana, D.; Karunakaran, B.; Butreddy, A.; Benival, D.; Kommineni, N. Versatility of Liposomes for Antisense Oligonucleotide Delivery: A Special Focus on Various Therapeutic Areas. *Pharmaceutics* **2023**, *15*. DOI: 10.3390/pharmaceutics15051435.

(10) Johnston, M. J. W.; Semple, S. C.; Klimuk, S. K.; Edwards, K.; Eisenhardt, M. L.; Leng, E. C.; Karlsson, G.; Yanko, D.; Cullis, P. R. Therapeutically optimized rates of drug release can be achieved by varying the drug-to-lipid ratio in liposomal vincristine formulations. *Biochim Biophys Acta* **2006**, *1758*, 55–64. DOI: 10.1016/j.bbamem.2006.01.009.

(11) Qu, B.; Guo, L.; Chu, X.; Wu, D.-H.; Shen, G.-L.; Yu, R.-Q. An electrochemical immunosensor based on enzyme-encapsulated liposomes and biocatalytic metal deposition. *Anal Chim Acta* **2010**, *663*, 147–152. DOI: 10.1016/j.aca.2010.01.050.

(12) Liu, Q.; Boyd, B. J. Liposomes in biosensors. *Analyst* **2013**, *138*, 391–409. DOI: 10.1039/c2an36140j.

(13) van der Koog, L.; Gandek, T. B.; Nagelkerke, A. Liposomes and Extracellular Vesicles as Drug Delivery Systems: A Comparison of Composition, Pharmacokinetics, and Functionalization. *Adv Healthc Mater* **2022**, *11*, e2100639. DOI: 10.1002/adhm.202100639.

(14) Immordino, M. L.; Dosio, F.; Cattel, L. Stealth liposomes: review of the basic science, rationale, and clinical applications, existing and potential. *Int J Nanomedicine* **2006**, *1*, 297–315.

(15) Li, T.; Senesi, A. J.; Lee, B. Small Angle X-ray Scattering for Nanoparticle Research. *Chem Rev* **2016**, *116*, 11128–11180. DOI: 10.1021/acs.chemrev.5b00690.

(16) Brumberger, H., Ed. *Modern aspects of small-angle scattering*; Kluwer: Dordrecht, London, 1995.

(17) Barba-Bon, A.; El Haitami, A.; Pasquier, C.; Nikšić-Franjić, I.; Diat, O.; Bauduin, P.; Cantin, S.; Nau, W. M. Boron Cluster Anions Dissolve En Masse in Lipids Causing Membrane Expansion and Thinning. *Angew Chem Int Ed Engl* **2024**, *63*, e202412834. DOI: 10.1002/anie.202412834.

(18) Caselli, L.; Conti, L.; Santis, I. de; Berti, D. Small-angle X-ray and neutron scattering applied to lipid-based nanoparticles: Recent advancements across different length scales. *Adv Colloid Interface Sci* **2024**, *327*, 103156. DOI: 10.1016/j.cis.2024.103156.

(19) Konarev, P. V.; Gruzinov, A. Y.; Mertens, H. D. T.; Svergun, D. I. Restoring structural parameters of lipid mixtures from small-angle X-ray scattering data. *J Appl Crystallogr* **2021**, *54*, 169–179. DOI: 10.1107/S1600576720015368.

(20) Campbell, F.; Bos, F. L.; Sieber, S.; Arias-Alpizar, G.; Koch, B. E.; Huwyler, J.; Kros, A.; Bussmann, J. Directing Nanoparticle Biodistribution through Evasion and Exploitation of Stab2-Dependent Nanoparticle Uptake. *ACS Nano* **2018**, *12*, 2138–2150. DOI: 10.1021/acsnano.7b06995.

(21) Papahadjopoulos, D.; Allen, T. M.; Gabizon, A.; Mayhew, E.; Matthay, K.; Huang, S. K.; Lee, K. D.; Woodle, M. C.; Lasic, D. D.; Redemann, C. Sterically stabilized liposomes: improvements in pharmacokinetics and antitumor therapeutic efficacy. *PNAS* **1991**, *88*, 11460–11464. DOI: 10.1073/pnas.88.24.11460.

(22) Tenchov, R.; Sasso, J. M.; Zhou, Q. A. PEGylated Lipid Nanoparticle Formulations: Immunological Safety and Efficiency Perspective. *Bioconjug Chem* **2023**, *34*, 941–960. DOI: 10.1021/acs.bioconjchem.3c00174.

(23) Estapé Senti, M.; Jongh, C. A. de; Dijkxhoorn, K.; Verhoef, J. J. F.; Szebeni, J.; Storm, G.; Hack, C. E.; Schiffelers, R. M.; Fens, M. H.; Boross, P. Anti-PEG antibodies compromise the integrity of PEGylated lipid-based nanoparticles via complement. *J Control Release* **2022**, *341*, 475–486. DOI: 10.1016/j.jconrel.2021.11.042.

(24) Hoecherl, K.; Streif, S.; Spitzenberg, C.; Rink, S.; Behrent, A.; Holzhausen, F.; Griesche, C.; Rogoll, C.; Foedlmeier, M.; Gebhard, A.; Kulikowski, K.; Schaefer, N.; Pauly, D.; Baeumner, A. J. A homogeneous immunoassay technology based on liposomes and the complement system enables one-step, no-wash, rapid diagnostics directly in serum. *Anal Bioanal Chem* **2025**, *417*, 3257–3273. DOI: 10.1007/s00216-025-05882-4.

(25) Zelek, W. M.; Harris, C. L.; Morgan, B. P. Extracting the barbs from complement assays: Identification and optimisation of a safe substitute for traditional buffers. *Immunobiology* **2018**, *223*, 744–749. DOI: 10.1016/j.imbio.2018.07.016.

(26) Vigneault, B.; Percot, A.; Lafleur, M.; Campbell, P. G. C. Permeability Changes in Model and Phytoplankton Membranes in the Presence of Aquatic Humic Substances. *Environ. Sci. Technol.* **2000**, *34*, 3907–3913. DOI: 10.1021/es001087r.

(27) Hestand, N. J.; Spano, F. C. Expanded Theory of H- and J-Molecular Aggregates: The Effects of Vibronic Coupling and Intermolecular Charge Transfer. *Chem Rev* **2018**, *118*, 7069–7163. DOI: 10.1021/acs.chemrev.7b00581.

(28) Kasha, M. Energy Transfer Mechanisms and the Molecular Exciton Model for Molecular Aggregates. *Radiat Res* **1963**, *20*, 55. DOI: 10.2307/3571331.

(29) Bae, W.; Yoon, T.-Y.; Jeong, C. Direct evaluation of self-quenching behavior of fluorophores at high concentrations using an evanescent field. *PLoS One* **2021**, *16*, e0247326. DOI: 10.1371/journal.pone.0247326.

(30) Wen, H.-W.; Borejsza-Wysocki, W.; DeCory, T. R.; Durst, R. A. Development of a competitive liposome-based lateral flow assay for the rapid detection of the allergenic peanut protein Ara h1. *Anal Bioanal Chem* **2005**, *382*, 1217–1226. DOI: 10.1007/s00216-005-3292-3.

(31) Viricel, W.; Mbarek, A.; Leblond, J. Switchable Lipids: Conformational Change for Fast pH-Triggered Cytoplasmic Delivery. *Angew Chem Int Ed Engl* **2015**, *54*, 12743–12747. DOI: 10.1002/anie.201504661.

(32) Edwards, K. A.; Curtis, K. L.; Sailor, J. L.; Baeumner, A. J. Universal liposomes: preparation and usage for the detection of mRNA. *Anal Bioanal Chem* **2008**, *391*, 1689–1702. DOI: 10.1007/s00216-008-1992-1.

(33) Makhal, K.; Maurya, S.; Goswami, D. Excited state absorption and relaxation dynamics in a series of heptamethine dyes under femtosecond and nanosecond excitations. *Phys. Scr.* **2019**, *94*, 95501. DOI: 10.1088/1402-4896/ab0064.

(34) Scott, H. L.; Skinkle, A.; Kelley, E. G.; Waxham, M. N.; Levental, I.; Heberle, F. A. On the Mechanism of Bilayer Separation by Extrusion, or Why Your LUVs Are Not Really Unilamellar. *Biophys J* **2019**, *117*, 1381–1386. DOI: 10.1016/j.bpj.2019.09.006.

(35) Chen, L.; Yu, Z.; Quinn, P. J. The partition of cholesterol between ordered and fluid bilayers of phosphatidylcholine: a synchrotron X-ray diffraction study. *Biochim Biophys Acta* **2007**, *1768*, 2873–2881. DOI: 10.1016/j.bbamem.2007.07.023.

(36) Rand, R. P.; Parsegian, V. A.; Henry, J. A.; Lis, L. J.; McAlister, M. The effect of cholesterol on measured interaction and compressibility of dipalmitoylphosphatidylcholine bilayers. *Can J Biochem* **1980**, *58*, 959–968. DOI: 10.1139/o80-131.

(37) Dubois, M.; Zemb, T. Swelling limits for bilayer microstructures: the implosion of lamellar structure versus disordered lamellae. *Current Opinion in Colloid & Interface Science* **2000**, *5*, 27–37. DOI: 10.1016/S1359-0294(00)00032-7.

(38) Yuan, J.; Yi, X.; Yan, F.; Wang, F.; Qin, W.; Wu, G.; Yang, X.; Shao, C.; Chung, L. W. K. Near-infrared fluorescence imaging of prostate cancer using heptamethine carbocyanine dyes. *Mol Med Rep* **2015**, *11*, 821–828. DOI: 10.3892/mmr.2014.2815.

(39) Duan, L.; Wang, L.; Zhang, C.; Yu, L.; Guo, F.; Sun, Z.; Xu, Y.; Yan, F. Role of near-infrared heptamethine cyanine dye IR-783 in diagnosis of cervical cancer and its mechanism. *Int J Clin Exp Path* **2019**, *12*, 2353–2362.

(40) Tang, Q.; Liu, W.; Zhang, Q.; Huang, J.; Hu, C.; Liu, Y.; Wang, Q.; Zhou, M.; Lai, W.; Sheng, F.; Li, G.; Zhang, R. Dynamin-related protein 1-mediated mitochondrial fission contributes to IR-783-induced apoptosis in human breast cancer cells. *J Cell Mol Med* **2018**, *22*, 4474–4485. DOI: 10.1111/jcmm.13749.

(41) Li, P.; Liu, Y.; Liu, W.; Li, G.; Tang, Q.; Zhang, Q.; Leng, F.; Sheng, F.; Hu, C.; Lai, W.; Liu, Y.; Zhou, M.; Huang, J.; Zhou, H.; Zhang, R.; Zhao, Y. IR-783 inhibits breast cancer cell proliferation and migration by inducing mitochondrial fission. *Int J Oncol* **2019**, *55*, 415–424. DOI: 10.3892/ijo.2019.4821.

(42) Moein Moghimi, S.; Hamad, I.; Bünger, R.; Andresen, T. L.; Jørgensen, K.; Hunter, A. C.; Baranji, L.; Rosivall, L.; Szebeni, J. Activation of the human complement system by cholesterol-rich and PEGylated liposomes-modulation of cholesterol-rich liposome-mediated complement activation by elevated serum LDL and HDL levels. *J Liposome Res* **2006**, *16*, 167–174. DOI: 10.1080/08982100600848801.

(43) Noone, D. P.; Isendoorn, M. M. E.; Hamers, S. M. W. R.; Keizer, M. E.; Wulffelé, J.; van der Velden, T. T.; Dijkstra, D. J.; Trouw, L. A.; Filippov, D. V.; Sharp, T. H. Structural basis for surface activation of the classical complement cascade by the short pentraxin C-reactive protein. *PNAS* **2024**, *121*, e2404542121. DOI: 10.1073/pnas.2404542121.

(44) Samstad, E. O.; Niyonzima, N.; Nymo, S.; Aune, M. H.; Ryan, L.; Bakke, S. S.; Lappegård, K. T.; Brekke, O.-L.; Lambris, J. D.; Damås, J. K.; Latz, E.; Mollnes, T. E.; Espevik, T. Cholesterol crystals induce complement-dependent inflammasome activation and cytokine release. *The Journal of Immunology* **2014**, *192*, 2837–2845. DOI: 10.4049/jimmunol.1302484.

(45) Merle, N. S.; Church, S. E.; Fremeaux-Bacchi, V.; Roumenina, L. T. Complement System Part I - Molecular Mechanisms of Activation and Regulation. *Front Immunol* **2015**, *6*, 262. DOI: 10.3389/fimmu.2015.00262.

(46) Betz, S. J.; Isliker, H. Antibody-independent interactions between Escherichia coli J5 and human complement components. *The Journal of Immunology* **1981**, *127*, 1748–1754. DOI: 10.4049/jimmunol.127.5.1748.

(47) Vukajlovich, S. W.; Hoffman, J.; Morrison, D. C. Activation of human serum complement by bacterial lipopolysaccharides: structural requirements for antibody independent activation of the classical and alternative pathways. *Mol Immunol* **1987**, *24*, 319–331. DOI: 10.1016/0161-5890(87)90173-8.

(48) Elkins, M. R.; Bandara, A.; Pantelopulos, G. A.; Straub, J. E.; Hong, M. Direct Observation of Cholesterol Dimers and Tetramers in Lipid Bilayers. *J Phys Chem B* **2021**, *125*, 1825–1837. DOI: 10.1021/acs.jpcb.0c10631.

(49) Armstrong, C. L.; Marquardt, D.; Dies, H.; Kučerka, N.; Yamani, Z.; Harroun, T. A.; Katsaras, J.; Shi, A.-C.; Rheinstädter, M. C. The Observation of Highly Ordered Domains in Membranes with Cholesterol. *PLoS One* **2013**, *8*, e66162. DOI: 10.1371/journal.pone.0066162.

(50) Doole, F. T.; Kumarage, T.; Ashkar, R.; Brown, M. F. Cholesterol Stiffening of Lipid Membranes. *J Membr Biol* **2022**, *255*, 385–405. DOI: 10.1007/s00232-022-00263-9.

(51) Pöhnl, M.; Trollmann, M. F. W.; Böckmann, R. A. Nonuniversal impact of cholesterol on membranes mobility, curvature sensing and elasticity. *Nat Commun* **2023**, *14*, 8038. DOI: 10.1038/s41467-023-43892-x.

3.6 Supporting Information

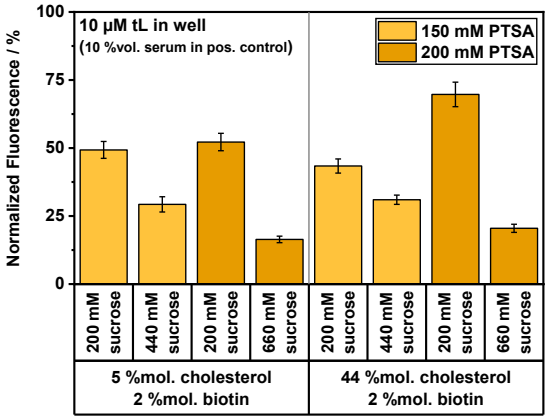

Figure S 3-1: Fluorescence intensities of PTSA encapsulating liposomes (PTSA-Liposome-3, 5, 7 & 8) measured in LCB with varying sucrose content, normalized to a detergent containing positive control (30 mM OG) containing 10 %vol. serum as in liposome complement assays (see materials and methods). Liposomes were measured at 10 µM tL. n=3.

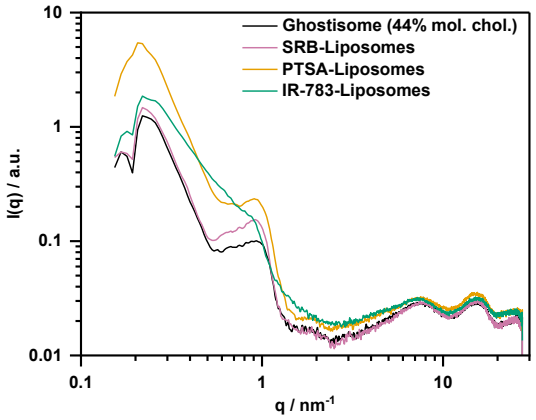

Figure S 3-2: SAXS measurements of fluorophore encapsulating liposomes (44 %mol. cholesterol lipid mixture, ~50 mM total lipid, Ghostisomes-2, SRB-Liposome-4, PTSA-Liposome-2, IR-Liposome-3).

Table S 3-1: Liposome characteristics including lipid composition, encapsulant concentrations in 20 mM HEPES (pH 7.5), smallest membrane pore size during extrusion, Hydrodynamic diameter d(H), polydispersity index PDI, zeta-potential and total lipid concentration tL.

Batch	Lipid composition	Encapsulant & membrane pore size	d(H) / nm	PDI	Zeta potential / mV	tL / mM
SRB-Liposome-1	5 %mol. cholesterol, 74 %mol. DPPC, 19 %mol. DPPG 2 %mol. DPPE-biotin	10 mM SRB 210 mM NaCl 0.2 µm	130.1 ± 0.8	0.12 ± 0.01	-16 ± 1	6.26 ± 0.07
SRB-Liposome-2	5 %mol. cholesterol, 74 %mol. DPPC, 18 %mol. DPPG 2 %mol. DPPE-biotin 1 %mol. LPS	10 mM SRB 210 mM NaCl 0.4 µm	154 ± 4	0.169 ± 0.007	-8 ± 1	7.22 ± 0.04
SRB-Liposome-3	44 %mol. cholesterol, 34 %mol. DPPC, 20 %mol. DPPG 2 %mol. DPPE-biotin	10 mM SRB 210 mM NaCl 0.2 µm	143 ± 2	0.103 ± 0.005	-25 ± 1	9.42 ± 0.03
SRB-Liposome-4	44 %mol. cholesterol, 34 %mol. DPPC, 20 %mol. DPPG 2 %mol. DPPE-biotin	10 mM SRB 210 mM NaCl 0.4 µm	275 ± 5	0.17 ± 0.02	-24 ± 2	8.52 ± 0.03
IR-Liposome-1	44 %mol. cholesterol, 34 %mol. DPPC, 20 %mol. DPPG 2 %mol. DPPE-biotin	10 mM IR-783 210 mM NaCl 0.4 µm	170 ± 10	0.264 ± 0.006	-23 ± 3	4.45 ± 0.02
IR-Liposome-2	44 %mol. cholesterol, 34 %mol. DPPC, 20 %mol. DPPG 2 %mol. DPPE-biotin	10 mM IR-783 210 mM NaCl 0.4 µm	180 ± 6	0.255 ± 0.006	-23 ± 2	8.22 ± 0.04
IR-Liposome-3	44 %mol. cholesterol, 34 %mol. DPPC, 19 %mol. DPPG 2 %mol. DPPE-biotin 1 %mol. LPS	10 mM IR-783 210 mM NaCl 0.4 µm	140.7 ± 0.3	0.22 ± 0.01	-6 ± 1	6.6 ± 0.04
PTSA-Liposome-1	5 %mol. cholesterol, 73 %mol. DPPC, 20 %mol. DPPG 2 %mol. DPPE-biotin	100 mM PTSA 0.2 µm	136 ± 5	0.089 ± 0.007	-16 ± 1	10.62 ± 0.08
PTSA-Liposome-2	44 %mol. cholesterol, 34 %mol. DPPC, 20 %mol. DPPG 2 %mol. DPPE-biotin	100 mM PTSA 0.2 µm	165 ± 7	0.06 ± 0.03	-22 ± 2	7.30 ± 0.03
PTSA-Liposome-3	5 %mol. cholesterol, 73 %mol. DPPC, 20 %mol. DPPG 2 %mol. DPPE-biotin	150 mM PTSA 0.2 µm	118 ± 2	0.12 ± 0.03	-19 ± 2	9.12 ± 0.06

Table S 3-1 - continued: Liposome characteristics including lipid composition, encapsulant concentrations in 20 mM HEPES (pH 7.5), smallest membrane pore size during extrusion, Hydrodynamic diameter d(H), polydispersity index PDI, zeta-potential and total lipid concentration tL.

Batch	Lipid composition	Encapsulant & membrane pore size	d(H) / nm	PDI	Zeta potential / mV	tL / mM
PTSA-Liposome-4	5 %mol. cholesterol, 74 %mol. DPPC, 20 %mol. DPPG 1 %mol. LPS	150 mM PTSA 0.4 µm	145 ± 4	0.16 ± 0.03	-9 ± 4	3.26 ± 0.01
PTSA-Liposome-5	44 %mol. cholesterol, 35 %mol. DPPC, 20 %mol. DPPG 2 %mol. DPPE-biotin	150 mM PTSA 0.2 µm	147.3 ± 0.9	0.08 ± 0.02	-22 ± 2	10.16 ± 0.07
PTSA-Liposome-6	44 %mol. cholesterol, 35 %mol. DPPC, 20 %mol. DPPG 1 %mol. LPS 0.4 µm	150 mM PTSA 0.4 µm	176 ± 6	0.21 ± 0.01	-6 ± 2	4.89 ± 0.08
PTSA-Liposome-7	5 %mol. cholesterol, 73 %mol. DPPC, 20 %mol. DPPG 2 %mol. DPPE-biotin	200 mM PTSA 0.2 µm	141.9 ± 0.4	0.08 ± 0.01	-16 ± 3	10.73 ± 0.08
PTSA-Liposome-8	44 %mol. cholesterol, 34 %mol. DPPC, 20 %mol. DPPG 2 %mol. DPPE-biotin	200 mM PTSA 0.2 µm	155 ± 1	0.07 ± 0.02	-18 ± 3	10.80 ± 0.08
Ghostisome-1	5 %mol. cholesterol, 73 %mol. DPPC, 20 %mol. DPPG 2 %mol. DPPE-biotin	280 mM NaCl 0.4 µm	220 ± 11	0.20 ± 0.01	-19.1 ± 0.8	11.66 ± 0.05
Ghostisome-2	44 %mol. cholesterol, 34 %mol. DPPC, 20 %mol. DPPG 2 %mol. DPPE-biotin	280 mM NaCl 0.4 µm	181 ± 7	0.23 ± 0.02	-25 ± 2	10.3 ± 0.2
Ghostisome-3	44 %mol. cholesterol, 34 %mol. DPPC, 20 %mol. DPPG 2 %mol. DPPE-biotin	280 mM NaCl 0.4 µm	301 ± 7	0.16 ± 0.02	-24 ± 2	6.52 ± 0.03

4 Liposomes enable the functional assessment of each complement pathway

Graphical Abstract

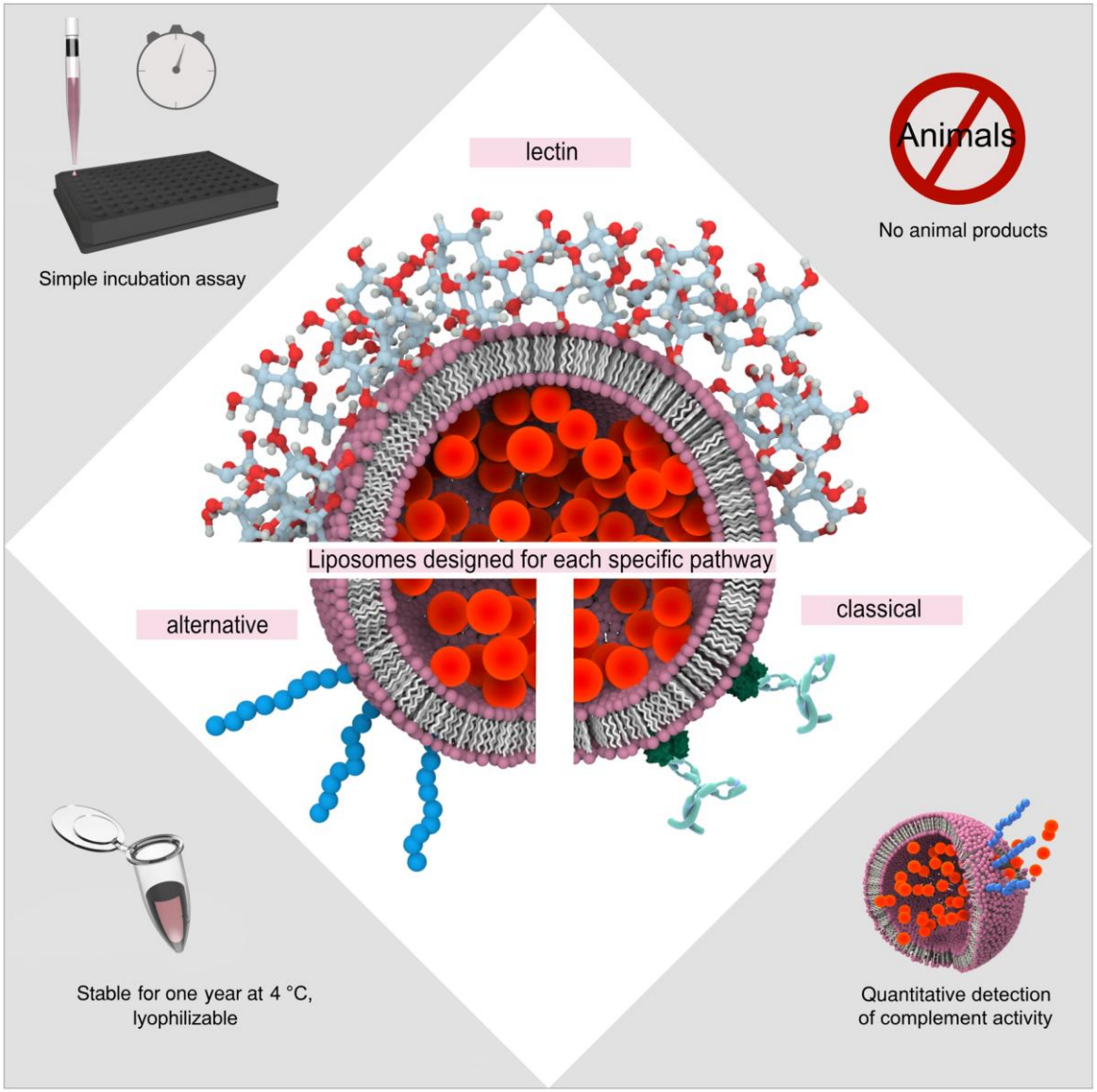

This chapter will be further used as manuscript that is intended to be submitted as an original research article in *ACSnano*.

Author's contributions

Conceptualization of this research article was performed by Antje J. Baeumner, Diana Pauly and the author. The methodology was developed by Antje J. Baeumner, Diana Pauly and the author and supported by Felix Poppelaars and Richard Pouw. Most of the experimental work was done by the author. Michaela Aichinger contributed with experimental work within the

scope of her master's thesis (including in parts inhibitor studies and liposome mannan modification optimizations, the bystander complement lysis assay, the LPS-Liposome content titration and supporting in the donor sera screenings), which is marked with an asterisk [*] in the respective figure caption. Her master's thesis is entitled "Development and Optimization of Liposomes for the Detection of Three Complement Pathways" and was submitted in September 2024 to the Faculty of Chemistry and Pharmacy at the University of Regensburg. This data was reformatted to fit this thesis. Mieke C. Brouwer contributed with performing the ELISA measurements. Anna Gebhart, Christian Griesche, Ernst Eberhardt, Ferdinand Holzhausen, Katharina Weiß, Kilian Höcherl and Michaela Aichinger assisted with liposome synthesis. Richard B. Pouw supported by providing the inhibitors and donor sera. Ernst Eberhardt assisted in experimental investigations of high 4-APM-Liposomes under the supervision of the author. Funding was acquired by Antje J. Baeumner, Diana Pauly and Felix Poppelaars. Antje J. Baeumner and Diana Pauly contributed by project administration. Antje J. Baeumner supervised the project. The author wrote the first draft of the manuscript. Antje J. Baeumner, Diana Pauly, Felix Poppelaars, Ferdinand Holzhausen, Richard Pouw and Michaela Aichinger revised the manuscript. Antje J. Baeumner is corresponding author.

Abstract

The complement system is a key defense mechanism of the human immune system[1,2], with much to be discovered about its function and disease relations. Its lectin pathway, a crucial yet understudied activation pathway, surprisingly lacks reliable, specific functional assays, limiting both fundamental research and clinical application. Thus, developed here are chemically tailored liposomes serving as biomimetic platform to independently quantify activation of all three complement pathways, providing sensitive endpoint and time-resolved measurements, hence facilitating kinetic analyses. Focus on the lectin pathway showed that novel surface functionalization of liposomes with mannan enabled its selective activation, confirmed via inhibitor-based validation using specific complement proteins including C1q, C1s, MBL, MASP-2, Factor B, and C5. Reliability and clinical relevance were proven by application to a cohort of 97 human sera revealing a strong correlation with the established ELISA-based method which itself merely quantifies complement proteins and cannot demonstrate final function. Liposome surface adaptation with antibodies or lipopolysaccharides enabled strikingly easy expansion to classical and alternative pathway functional analysis, respectively. This liposome-based platform represents an impactful new tool for fundamental complement research enabling precise mechanistic studies, biomarker discovery, therapeutic development, and diagnostic monitoring at a time when complement-targeted therapies are increasingly reaching clinical approval[3].

4.1 Introduction

The complement system as part of the innate immune system is responsible for several important tasks such as recognition and elimination of invading pathogens or connecting innate and adaptive immune responses[1,2]. The importance of the complement system in various diseases including age-related macular degeneration[4], atypical hemolytic uremic syndrome[5] or autoimmune diseases[6,7] and its potential as target for new drug development highlights the importance of research gaining fundamental understanding of the functional roles of its participating proteins. Activation of the complement system mostly follows a similar and straightforward cascade that includes particle recognition and its opsonization, self-amplification, generation of effector molecules (for example the pore forming membrane-attack-complex (MAC)) and induction of other immune responses[8,9] (**Figure S 4-1**). The formation of the MAC as terminal product of the complement cascade can be initiated by three distinct pathways, the classical, lectin and alternative pathway[8,9]. Current research and diagnostics on the functionality of the cascade and its participating proteins mainly revolves around classical and alternative pathway screenings based on widely established fresh animal erythrocyte hemolysis[10] or liposome assays[11]. Since there are no erythrocytes from any species identified or liposomes developed that specifically trigger the lectin pathway its specific readout is limited to protein quantification via ELISAs, lacking any information on functional pore-mediated lysis. Furthermore, erythrocyte-based assays are time and cost intensive and show high setup variability from lab to lab.

Already in the 1980s liposomes were identified to serve as cell mimics harnessing their natural membrane structure, size, stability and reproducibility afforded through chemical synthesis protocols[12–14]. Liposomes are self-assembled nanovesicles, containing an inner aqueous cavity surrounded by a lipid bilayer. The bilayer is typically composed of phospholipids with varying head group and carbon chain lengths[15], cholesterol is added to stabilize the liposomes, inducing tighter packing of the phospholipids, reducing bilayer permeability and formation of more rigid liposomes[16]. The inner aqueous compartment can be used to encapsulate several different hydrophilic molecules, including fluorescent dyes[17,18], electroactive species[19,20], DNA[21,22] or enzymes[23,24]. Extensively utilized as signal amplification means in bioanalysis[25–27], they have also been used as a biomimic replacing animal-derived erythrocytes[28,29]. When entrapping enzymes[11] or fluorescent dyes[29,30] inside the liposomes, their complement-induced lysis can easily be monitored in high-throughput assays.

Each complement pathway is initiated by pattern recognizing receptors binding to specific ligands. This results in activation of associated serine proteases which in turn triggers a cascading reaction of this system[8,9] (**Figure S 4-1**). In a hypothesis-driven approach,

liposomes were hence modified with lectin pathway specific activators. Rigorous specificity testing and application to a cohort of patient sera demonstrated the potential for generating an assay format that allows standardization. Subsequently, the same hypothesis was demonstrated to hold true for classical and alternative pathway assays in the same platform.

4.2 Materials and Methods

4.2.1 Chemicals and consumables

All chemicals were of analytical grade and were used without purification. Mannan from *Saccharomyces cerevisiae* (M7504) and methanol, Sephadex® G-50 (G50150), lipopolysaccharides (LPS) from *Salmonella enteritidis* (L6011), cholesterol from sheep wool (C8667), tetrasodium ethylenediaminetetraacetic acid (EDTA, EDS), ethylene glycol-bis(2-aminoethyl ether)-*N*,*N*,*N*′,*N*′-tetraacetic acid (EGTA, E4378), polyclonal goat anti-biotin IgG (B3640) and sodium hydroxide were purchased from Sigma-Aldrich/Merck KGaA (Darmstadt, Germany). The extrusion kit and the phospholipids 1,2-dipalmitoyl-*sn*-glycero-3-phosphocholine (DPPC, 850355P), 1,2-dipalmitoyl-*sn*-glycero-3-phospho-(1′-*rac*-glycerol) (sodium salt) (DPPG, 840455P) and 1,2-dipalmitoyl-*sn*-glycero-3-phosphoethanolamine-N-(biotinyl) (DPPE-biotin, 870285P) were purchased from Avanti Polar Lipids (Alabaster, AL, USA). Sodium azide, magnesium dichloride hexahydrate, disodium hydrogen phosphate, potassium dihydrogen phosphate and glycine were purchased from Merck KGaA (Darmstadt, Germany). Sulforhodamine B (SRB, S1307), 1-Ethyl-3-(3-dimethylaminopropyl) carbodiimide hydrochloride (EDC, 22980) and sulfosuccinimidyl acetate (sNHS-acetate, 26777) were purchased from Thermo Fisher Scientific (Darmstadt, Germany). 2-Bromoethylamine hydrobromide (BEA, A17625.18) was purchased from Thermo Fisher Scientific (Darmstadt, Germany) or Sigma-Aldrich/Merck KGaA (B65705, Darmstadt, Germany). *N*-Hydroxysulfosuccinimide sodium salt (sNHS) was bought from Sigma-Aldrich/Merck KGaA (56485, Darmstadt, Germany) or TCI Deutschland GmbH (H1304, Frankfurt am Main, Germany). Concentrated hydrochloric acid, chloroform and nitric acid (HNO_3, N/2185/PB15) were bought from Fisher Chemical (Schwerte, Germany). *N*-2-hydroxyethylpiperazine-*N*′-2-ethanesulfonic acid (HEPES), sodium chloride, sucrose, *N*-octyl-β-D-glucopyranoside (OG, CN23.3), 2-(*N*-morpholino) ethanesulfonic acid (MES) and calcium chloride was bought from Carl Roth (Karlsruhe, Germany). Dialysis membrane (Spectra/Por® 4 with a MWCO of 12 - 14 kDa) was purchased from Spectrum Laboratories and polycarbonate Whatman Nucleopore™ Track-Etched membranes with a pore size of 1.0 µm, 0.4 µm or 0.2 µm (each Ø19 mm) were bought from VWR (Darmstadt, Germany). 1,2-dipalmitoyl-*sn*-glycero-3-phosphoethanolamine-*N*-(glutaryl) (sodium salt) (*N*-glutaryl-DPPE, FE-6060GL) was purchased from Coatsome. The ICP phosphorus standard solution (10882.0000) was purchased from Bernd Kraft/AnalytiChem GmbH (Duisburg, Germany). Black 96-well flat

bottom microtiter plates (MTP, 781608) were purchased from Brand (Wertheim, Germany). Narsoplimab was purchased from TargetMol Chemicals Inc (T76870, Boston, MA, USA). Complement inhibitors anti-C1q.85[31], anti-FB.1[32] and anti-MBL.1[33] were provided by Sanquin Research (Amsterdam, The Netherlands). Eculizumab and sutimlimab were collected from used injection bottles (Sanquin Research). The cohort of healthy human sera was collected as part of a previous study[34]. The pool of healthy human serum was collected from anonymous healthy donors at Sanquin Blood Supply Foundation with written consent according to Dutch regulations and the Declaration of Helsinki, approved by the internal medical ethical committee (NVT0185.05). Before collecting the serum, blood was clotted for one hour at room temperature (RT). Serum was obtained after centrifugation at 1.600 x g at 4 °C for ten min. All samples and the pool were aliquoted and stored at -80°C until use. Characteristics of the inhibitors used to determine the specificity of the three complement pathway liposomes are listed in **Table S 4-1**. Pooled human complement serum was purchased from Innovative Research (ISCER, Novi, Michigan, USA).

4.2.2 Mannan amination

The subsequent method for mannan amination was systematically developed and optimized[35]. Carboxylation was exchanged for amination. For initial optimizations small scale batches aminating 25 mg mannan were performed.

25 mg mannan was dissolved in NaOH (6 M) and mixed ensuring alkalization. The alkaline mannan solution was added under vigorous mixing to respective amounts of BEA at RT. The mixture was heated to 55 °C and shaken overnight. The solution was cooled down and pH adjusted to neutral by adding HCl. The mixture was dialyzed against water and then water was evaporated until dry. Aminated mannan was precipitated by addition of methanol. Finally, solid aminated mannan was dried in the vacuum oven.

For the large-scale synthesis, batches of 10x the amount of mannan were carried out following the same process.

4.2.3 Liposome synthesis

Liposome preparation was performed as described earlier[36] using the reverse-phase evaporation method. Standard complement stable anionic lipid composition contained 5 %mol. cholesterol, 73 %mol. DPPC, 20 %mol. DPPG and 2 %mol. DPPE-biotin. For mannan modified liposomes, 4 %mol. *N*-glutaryl-DPPE was added to the lipid mixture to allow coupling of mannan to the surface via carbodiimide chemistry. For LPS-Liposomes, LPS from *Salmonella enteritidis* was added to the lipid mixture. For LPS an estimated molecular weight of 15000 $g \cdot mol^{-1}$ was used for calculations.

60 µmol of the desired lipids were dissolved in chloroform (3 mL) and methanol (0.5 mL). After sonication at 60 °C for 1 min, 2 mL of a preheated sulforhodamine B (SRB) solution was added as encapsulant (10 mM SRB, 210 mM NaCl, dissolved in 20 mM HEPES, pH 7.5, 60 °C). The mixture was sonicated again at 60 °C for 4 min. The organic solvents were removed with a rotary evaporator (LABOROTA 4001, Heidolph, Germany) at 60 °C with stepwise reduced pressure from 900 to 780 mbar within 40 min (900 mbar for 10 min, 850 mbar for 5 min, 800 mbar for 5 min, 780 mbar for 20 min). The solution was vortexed for 30 s, and another 2 mL of the encapsulant was added. After a second vortexing step for 30 s, the solution was further rotated at 60 °C with stepwise reducing pressure starting from 750 to 400 mbar within 60 min (750 mbar for 20 min, 600 mbar for 5 min, 500 mbar for 5 min, 400 mbar for 20 min). The solution was then extruded through polycarbonate membranes with varying membrane pore sizes (1 µm, 0.4 µm or 0.2 µm). Extrusion was done at 65 °C by forcing the mixture in the syringes 21 times through each membrane pore size. Excess of encapsulant (i.e. SRB and NaCl) was removed by size exclusion chromatography with a Sephadex G-50 column followed by dialysis against HSS buffer (10 mM HEPES, 200 mM NaCl, 200 mM sucrose, 0.01 % NaN_3, pH 7.5). Liposomes were stored at 4 °C.

The smallest membrane pore size for LPS-liposomes was 0.4 µm, all other liposomes were also extruded through the pore size of 0.2 µm.

4.2.4 Liposome characterization

Size, zeta potential and lipid concentration of liposomes were characterized. Dynamic light scattering (DLS) and zeta potential measurements were performed on a Malvern Panalytical Zetasizer Nano-ZS. For size determination polymethyl methacrylate semi-micro cuvettes (Brand, Germany) and for zeta potential determination disposable folded capillary cells (Malvern Panalytical, Germany) were used. Measurement temperature was set in both cases to 25 °C with 50 µM tL (or 25 µM tL for small-scale mannan modified liposome batches) sample dilutions in HSS buffer. Measurement of size was conducted with a dispersant refractive index n_D^{20} of 1.34, a material absorbance of zero, a dispersant viscosity η of 1.1185 mPa s, an angle of 173° and backscattering mode after equilibration for 15 s in three measurement runs with each 13 single measurements. For zeta potential, a dielectric constant ε of 78.5 was used with an equilibration time of 60 s before four measurement runs started with each twenty single measurements.

Phospholipid concentrations were determined via optical emission spectroscopy with inductively coupled plasma (ICP-OES, SpectroBlue TI/EOP) from SPECTRO Analytical Instruments GmbH (Kleve, Germany). Liposomes solutions were diluted 1/150 with a total volume of 3 mL in 0.5 M HNO_3. A phosphorus standard diluted in 0.5 M HNO_3 from 1 to 100 µM

was used for calibration of the device. Phosphorous was detected at a wavelength of 177.495 nm. Before each measurement, 0 µM and 100 µM phosphorus standard dilutions were used to re-calibrate the device. The total lipid concentration (tL) was calculated from the phospholipid concentration and the lipid composition used during liposome preparation.

Lipid concentrations of mannan coupled liposomes could not easily be determined via ICP-OES determining the phosphorous content since mannan itself contains phosphate groups. Consequently, determination via fluorescence measurements using the non-coupled liposomes with known concentration was used. For this, a calibration curve between 0 and 10 µM tL in presence of 30 mM OG of the non-coupled liposomes in HSS was prepared. A 1/50 diluted sample of the coupled liposomes was prepared with HSS in presence of 30 mM OG. Samples were prepared in triplicates. Fluorescence was determined using a SYNERGY neo2 multi-mode reader (Reader-1) from BioTek (Bad Friedrichshall, Germany). The measurements were taken at λ_{Ex} = 565 (8) nm, λ_{Em} = 585 (8) nm, and gain 125. The total lipid concentration of the coupled liposomes was calculated using the calibration curve and considering the dilution factors.

The initial fluorescence of the liposomes was determined using Reader-1 and its stability was monitored over time. The liposome stock solutions were diluted to 50 µM tL concentration in HSS with and without 30 mM OG. Samples were prepared in quadruplicates. Measurement conditions were λ_{Ex} = 565 (5) nm, λ_{Em} = 585 (5) nm, and gain 100. The so-called initial fluorescence was calculated as the ratio of the fluorescence intensities of intact (without OG) and lysed liposomes (with OG) and was used as a marker for liposome stability, i.e. fluorophore leakage over time.

4.2.5 Liposome modification/coupling

Aminated mannan was conjugated to carboxylated liposomes via EDC/NHS chemistry. For this EDC, sNHS, and aminated mannan were individually dissolved in 0.05 M MES buffer (pH 5.5) to achieve final concentrations of 10 mg·mL^{-1} for each component. A sNHS-acetate solution was prepared freshly right before use by dissolving 100 mg·mL^{-1} in 0.05 M MES buffer (pH 5.5). Liposomes were incubated with respective amounts of EDC and sNHS solution (1:100:180 ratio of carboxyl groups: EDC:sNHS) for 1 hour at room temperature (RT) and 300 rpm. The desired amount of aminated mannan (calculated on monomer subunit) was added, and the solution was incubated for another 1.5 hours at RT and 300 rpm. Remaining activated carboxy groups were not quenched. Non-reacted amino groups were quenched by addition of varying amounts of sNHS-acetate at RT for additional 1.5 hours and 300 rpm. For final optimized conditions equimolar amounts compared to mannan monomers were used. Finally, small liposome batches were cleaned up via size exclusion chromatography with a

Sephadex G-50 column. Large coupled batches were dialyzed against HSS buffer overnight with two buffer exchanges in a Spectra-Por® dialysis membrane, MWCO: 1000 kDa. Purified coupled liposomes were stored at 4 °C.

4.2.6 Liposome-based complement assay

The exact conditions of this assay were adjusted and varied throughout the development and are directly mentioned in each respective data set. Nevertheless, two procedures can be described following an established protocol[36].

4.2.6.1 Research and development procedure:

A liposome complement buffer (LCB) was prepared using 10 mM HEPES, 150 mM NaCl, 135 nM $CaCl_2$, and 1 mM $MgCl_2$ in double distilled H_2O, pH 7.4, according to the HBS buffer of Zelek et al.[37]. Each assay contained four liposome containing samples: liposomes in liposome complement buffer (LCB, negative control), liposomes in active serum or in inactivated serum (negative control) containing 1/10 diluted inactivation buffer (iaCB, 400 mM EDTA and 1 µM EGTA, diluted in LCB, pH 7.5 – 8) and lysed liposomes by detergent addition as positive control, all prepared in LCB. Serum was inactivated by EDTA and EGTA addition to complex free Ca^{2+} and Mg^{2+} ions essential for the functionality of the complement system. Detergent positive controls contained 30 mM OG and serum in the final well. The final wells contained 100 µL volume, 1 or 5 µM tL liposomes, 200 mM glycine for liposome stability and inactivated serum wells contained 40 mM EDTA and 0.1 µM EGTA, if not mentioned differently in the respective experiment. Wherever needed, a Mg^{2+}/EGTA solution (100 mM EGTA and 100 mM $MgCl_2$ in bidest. H_2O, pH 7.5 - 8) was added in appropriate amounts to work under alternative pathway conditions, this is explicitly mentioned for each experiment (mostly 8 mM Mg^{2+}/EGTA in well was used). EGTA effectively removes free Ca^{2+} ions out of the solution which are needed for classical and lectin pathway functionality. All samples were prepared in triplicates.

Liposomes were prediluted in LCB to 10 or 50 µM total lipid (tL) content depending on the desired liposome content in each well. In case antibodies were used as complement trigger, polyclonal goat anti-biotin antibodies (1.0 $mg \cdot mL^{-1}$) were incubated 1 hour at RT with the liposome stock solution prior to predilution to the desired total lipid content with LCB. Black 96 well, flat bottom MTPs were prepared on ice with LCB, glycine (1 M glycine in LCB), iaCB and OG (300 mM OG in double distilled H_2O) stock solution additions to the respective wells to reach the desired conditions. Liposomes were added, resulting in a 1/10 dilution in the final well. In case inhibitors were used, serum was premixed with respective inhibitor dilutions in LCB for 15 min on ice prior to well addition. As last step, serum was added in respective amounts (mentioned in each experiment) before incubation at 37 °C for 60 min and

fluorescence intensity measurements with Reader-1 or a SYNERGY 2 multi-mode reader (Reader-2) from BioTek (Bad Friedrichshall, Germany). The wavelengths for Reader-1 were λ_{Ex} = 565 nm, λ_{Em} = 585 nm with bandwidth 8. Depending on the liposome content the gain was adjusted to 140 (for 5 µM tL) or 150 (for 1 µM tL). The wavelengths for Reader-2 were λ_{Ex} = 540 nm, bandwith 25 and λ_{Em} = 620 nm, bandwith 40 with a gain of 85 only used for 1 µM tL measurements. Time-resolved measurements were performed starting with a 1.5-minute interval for 15 min followed by another 45 min with a 5-minute measurement interval at constant 37 °C. For each measurement, the plate was read 3 consecutive times to relativize the instrument's influence on the signal.

4.2.6.2 High throughput format

For this format, the procedure from above was followed with some adjustments. Instead of triplicates only duplicates were measured. Instead of measuring an inactive serum control for all measured serum concentrations, only the highest serum concentration was investigated with inactive serum. The positive control with detergent (OG) was not included on the plate, but each well was lysed by OG addition after the 60-minute measurement time. For this 10 µL of the 300 mM OG stock was added to each well followed by shaking and 10 min incubation at 37 °C before a final readout. Readout settings had to be the same as the preceding time-resolved measurement.

4.2.6.3 Data evaluation

For data evaluation, mean and standard deviation were calculated for all samples. Each sample signal intensity after 10.5 min was subtracted as background. This subtracts the background fluorescent signal of intact liposomes. Resulting intensities were normalized to detergent containing positive controls at time point "60 min". In all cases, gaussian error propagation was used to determine the normalized standard deviations. Negative endpoint values between 0 and -5 % after background correction and normalization were changed to 0 %.

4.2.6.4 Screening of healthy donor sera and normalization to pooled human serum

Normalization to a pooled human serum control (PHS) of healthy donor sera measured in the high-throughput format was done for easier correlation to the ELISA data. For this, PHS was measured in a serum titration as control followed by determination of the linear range which was then fitted with a linear regression. Each donor sample was measured in duplicates at 4 and 8 %vol. serum. For each of the serum dilutions of the donor samples a respective reference dilution on the linear control regression was imputed based on the measured liposome lysis and using the linear regression of the pooled human serum control. Then, the fold difference between imputed serum dilution and actual serum dilution was calculated. The

calculated fold difference of the dependent dilutions of each sample had to be within 25 % of their combined average. Activity of the pooled human control used for calibration was then set to 100% activity. Finally, the 100% activity was corrected with the calculated fold difference for each sample.

4.2.7 Complement activity ELISAs

Classical pathway activity on aggregated human IgG, alternative pathway activity on zymosan and lectin pathway activity on mannan was determined by ELISA as described previously[32,38]. All assays measured C3 deposition as readout of complement activity, using biotinylated anti-C3.19 (Sanquin Research) as previously described[32].

4.3 Results and Discussion

4.3.1 The liposome assay technology

A general liposome-based time-resolved fluorescence assay needs to provide low background signals, negative and positive controls, and hence enable reliable and quantitative assessment of lysis levels (**Figure 4-1a**). This is achieved through selection of appropriate concentration ranges of additives, liposomes and serum. In general, liposomes can be synthesized to remain stealth in human serum under physiological conditions when no complement triggering ligands are present on their surface[39]. However, certain conditions must be met to avoid unwanted complement activation or liposome instability in serum. These include the presence of high concentrations of cholesterol, surface pegylation as it increases the risk for patient anti-PEG antibody binding and thus for classical pathway activation, and too high encapsulated fluorophore concentrations[36]. Similarly, assay buffer additives can influence liposome stability and hence cause unwanted background signals[36]. Pathway specificity of an assay will here be achieved through careful stealth liposome surface design via modification with well-known pathway activators, i.e. antibody-based classical pathway, LPS alternative pathway and mannan lectin pathway triggers, but also high cholesterol content could be investigated for the classical pathway. Important for pathway specificity and quantitative complement functionality assessment will also be to avoid any exhaustion by buffer additives. Since the standard additive sucrose used as liposome stabilizer could be identified in the assay set-up to cause such exhaustion to a measurable degree for LPS-Liposomes (**Figure 4-1a,b**), substitutes were studied early on. This led to glycine as a suitable stabilizer for low background signals (**Figure S 4-2a**) without affecting regulatory effects on any of the pathway specific liposome assays (**Figure S 4-2b**).

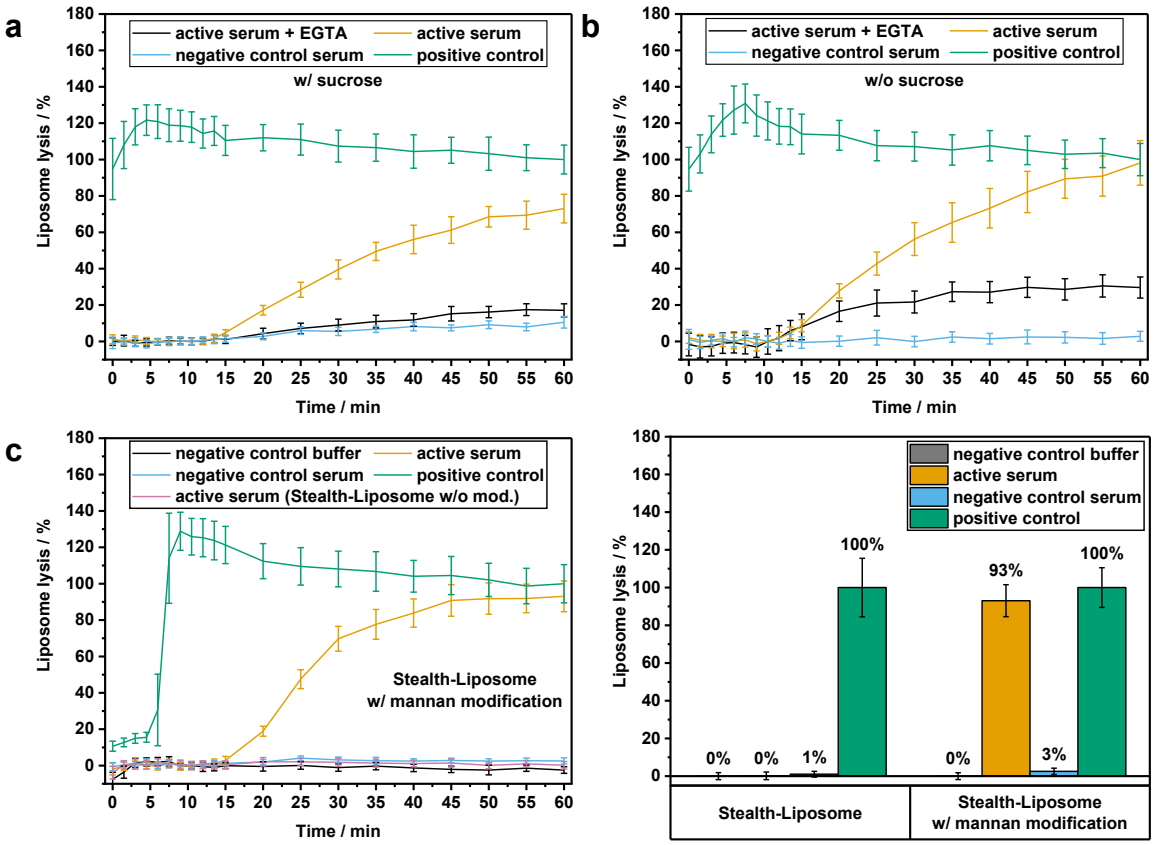

Figure 4-1: Liposome-based complement assays examining additives and mannan modification. Time-resolved complement assays investigating LPS-Liposome (1 % LPS, 10 µM total lipid (tL) in well) with, **a** and without, **b** 200 mM sucrose addition (final well concentration). Complement assays were performed in liposome complement buffer containing a sample with EGTA addition (0.4 mM EGTA final well concentration, active serum + EGTA, see materials and methods). Negative control serum contained inactivation complement buffer (iaCB) to a final concentration of 20 mM EDTA and serum. Positive control contained 30 mM OG and serum. Pooled human serum content was 10 %vol. per well. λ_{Ex}=565 (5) nm and λ_{Em}=585 (5) nm, Reader-1, 37 °C, gain=150, n=3 (except serum + EGTA w/o sucrose, n=2). **c**, Complement assays investigating Stealth-Liposomes (1 µM tL in well) with and without aminated mannan modification (see materials and methods, 3000 %mol. mannan monomer, 100 %wt. bromoethylamine (BEA) version). Complement assays were performed in liposome complement buffer with 200 mM glycine addition. Negative control serum contained iaCB to a final concentration of 20 mM EDTA and serum. Positive control contained 30 mM OG and serum. Pooled human serum content was 10 %vol. per well. λ_{Ex}=565 (8) nm and λ_{Em}=585 (8) nm, Reader-1, 37 °C, gain=150, n=3.

4.3.1.1 Development of lectin pathway specific liposome surface chemistry

Mannan, a polysaccharide derived from mannose, causes lectin pathway activation by mannose binding lectin (MBL), and has been applied in ELISA-based protein assays[40–42]. Other known triggers include acetylated BSA[43] and bare mannose[44]. Thus, BSA was acetylated and mannose was used as mannosamine or 4-aminophenyl mannopyranoside for the coupling to amine or carboxylic acid groups on the liposome surface. However, in no instance, lectin specific complement activation could be accomplished through these modifications (data not shown). As the mannose density was likely too low, the polymer mannan was used instead. First, amine groups were introduced into its structure[35] (see materials and methods). This was followed by standard carbodiimide chemistry for attachement to the liposome surface under conditions ensuring liposome stability. Successfully, the resulting surface caused complement-mediated liposome lysis (**Figure 4-1c**)

whereas non-modified liposomes remained intact. Dynamic light scattering (DLS) and zeta potential analyses indicated aggregation of the mannan-modified liposomes (**Figure S 4-3**), caused by electrostatic interactions between the negatively charged liposomes and positively charged aminated mannan. Therefore, the modification of liposomes with mannan, i.e. activation and coupling, was optimized with respect to coupling efficiency, liposome aggregation and complement activation, with the goal of achieving maximum complement-mediated liposome lysis with minimal material consumption and lowest liposome aggregation.

In the case of the mannan amination chemistry, a balance had to be found between a lower limit of amine concentration needed to enable reliable coupling to liposomes and hence activation of the complement system, and a higher limit that would help avoid liposome aggregation. By varying the bromoethylamine (BEA) amount used in the reaction, the lower limit could easily be identified, i.e. all versions caused liposome aggregation (**Figure S 4-4a,i**), yet the lowest concentration tested (40 %wt. BEA) led to reduced complement activation (**Figure S 4-4a,ii**). The amount of mannan per liposome was studied using optimized amination condition, (50 %wt. BEA). Here, 500 %mol. (monomer content) was determined as the most suitable condition inducing maximum complement-mediated lysis (**Figure S 4-4b,ii**) as lower mannan content had lower complement triggering capability. To avoid mannan-liposome aggregation (**Figure S 4-4b,i**), and to take advantage of acetylated groups to trigger the lectin pathways via ficolins[43] the free amine groups of the mannan-modified liposomes were acetylated using NHS-acetate. It was found that timing of acetate addition to the reaction mixture had more of an effect than the concentration itself. The earlier NHS-acetate could compete with the coupling of mannan to liposomes, the less mannan was coupled to the liposomes as determined by aggregate size (**Figure S 4-4c,i**) and by complement activation (**Figure S 4-4c,ii**). To ensure 100% liposome lysis signals, NHS-acetate addition after 60 minutes was chosen and reagent use reduced from previous ten molar equivalents of aminated mannan monomer with no negative effect on any condition (**Figure S 4-4d**). As a final fine-tuning step, mannan amination batch sizes were varied and a better mixing condition of larger batch sizes allowed a reliable modification of liposomes with aminated mannan resulting in full complement triggering (**Figure S 4-5b**) and no aggregation (**Figure S 4-5a**). Under the final conditions chosen, the acetylation reaction has no effect on either parameter, the reaction can be fully controlled including varying amounts of mannan per liposome (**Figure S 4-5c,d**), allowing triggering of the lectin pathway. The final optimized mannan liposomes (Man-Liposomes) comprised 500 %mol. mannan monomer modification with 50 %wt. BEA large batch amination followed by acetylation with 1x molar equivalents of mannan monomer.

4.3.1.2 Verifying lectin pathway specificity of mannan liposomes

Man-Liposomes were characterized for their specificity in activating solely the lectin pathway. Assay conditions were optimized to reduce liposome and serum amounts needed resulting in maximum lysis at 1 µM total lipid (tL) liposomes (**Figure S 4-5e**). Thus, depending on the serum used, a full titration from no to full lysis could be achieved between 1 and 10 %vol. serum (**Figure S 4-5f**). Furthermore, it was demonstrated that covalent surface modification with mannan was necessary because bystander lysis, in which 500 %mol. aminated mannan monomers were merely added to the assay and not covalently coupled to liposomes, was not observed. (**Figure S 4-6**)

A refined analysis of inhibitors provided mechanistic insight into the lectin pathway activation by the Man-Liposomes. General proof that Man-Liposomes activate the complement system which subsequently results in MAC formation and liposome lysis, was obtained through the use of an anti-C5 antibody (eculizumab). The antibody targets C5 to block the formation of the MAC[45,46] which in turn led to a complete blocking of all liposome lysis (≥9.6 µg/mL, EC50 = 5 ± 2 µg/mL) (**Figure 4-2 and Table S 4-2**). General activation by the alternative pathway could clearly be ruled out as 8 mM Mg^{2+}/EGTA addition fully blocked liposome lysis (**Figure S 4-7**). Activation by the classical pathway was dismissed because adding anti-C1q[31] or anti-C1s antibodies (sutimlimab), respectively (**Figure 4-2 and Table S 4-2**) had no effect on complement activation followed by lysis of the Man-Liposomes. The former targets the globular head region of C1q and thus effectively blocks the classical pathway complement activation at the trigger recognition element[31]. Sutimlimab targets C1s one step later in the classical pathway cascade[47]. Proof, that the Man-Liposomes in fact activate and initiate complement lysis via the lectin pathway specifically was gained by anti-MBL[33] and anti-MASP2 (narsoplimab) antibody additions, respectively (**Figure 4-2 and Table S 4-2**). These antibodies specifically inhibit MBL or more generally the lectin pathway by binding their specific targets, essential for a functional MBL/lectin pathway cascade[48]. Both antibodies showed the expected inhibition of liposome lysis where the anti-MBL antibody (≥0.8 µg/mL, EC50 = 0.14 ± 0.01 µg/mL) prevented lysis completely and the anti-MASP2 antibody (≥1.2 µg/mL, EC50 = 0.35 ± 0.06 µg/mL) reduced the lysis significantly. Furthermore, since lysis is inhibited completely with the anti-MBL antibody it can be concluded that only the MBL and not also the ficolin pathway is involved in Man-Liposome lysis. Through the use of an anti-FB antibody[32] which inhibits Factor B (FB), more in-depth analysis of the complement reaction cascade investigated the role of the amplification loop (**Figure 4-2 and Table S 4-2**). Specifically, other studies show that the alternative pathway can not only initiate the complement cascade but separately from that also amplify the classical and lectin pathway activation by the so-called amplification loop, contributing up to ~80% of total complement

activation[49,50]. Factor B is necessary for the formation of the alternative pathway C3 convertase (C3bBb), relevant for further downstream complement activation. The anti-FB antibody (≥25 µg/mL, EC50 = 12.6 ± 0.4 µg/mL) reduced the complement lysis which stands out and indicates participation of the alternative pathway. This was confirmed to be solely due to the amplification loop further downstream of the initial activation, since under alternative pathway conditions, i.e. in presence of 8 mM Mg^{2+}/EGTA (see materials and methods) no liposome lysis is obtained (**Figure S 4-7**).

All of these data conclude that the mannan liposomes specifically initiate complement-mediated liposome lysis via the MBL-derived lectin pathway with contribution of the alternative pathway amplification loop at a later stage in the reaction cascade.

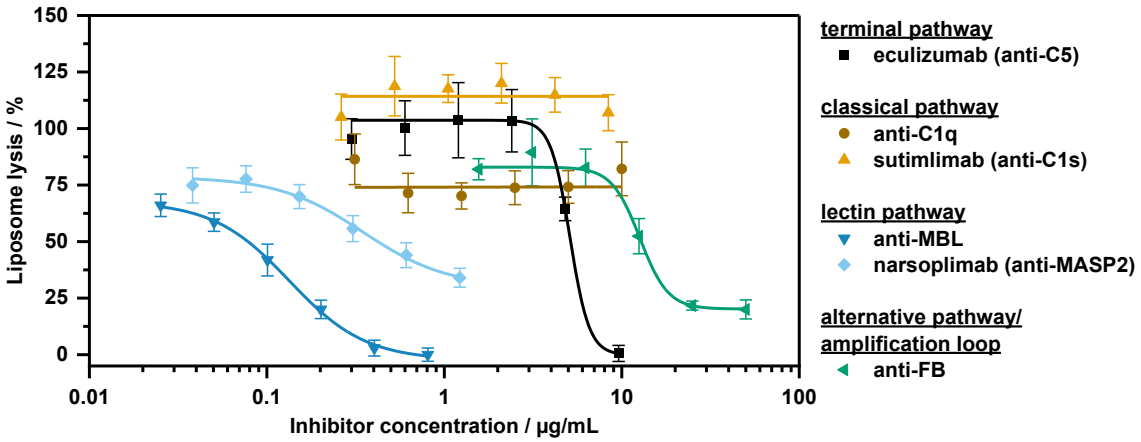

Figure 4-2: Inhibitor screen with Man-Liposomes in the complement assay. Inhibitor titrations in complement assays investigating lysis obtained for Man-Liposomes (1 µM tL in well, 500 %mol. mannan monomer modification, 50 %wt. BEA large batch synthesis version, acetylation with 1x molar equivalents of mannan monomer. Anti-C1q, sutimlimab (anti-C1s), anti-FB, narsoplimab (anti-MASP2), anti-MBL and eculizumab (anti-C5) were examined. Complement assays were performed in liposome complement buffer with 200 mM glycine addition. Positive control contained 30 mM OG and serum. Pooled human serum content was 4 %vol. per well. λ_{Ex}=565 (8) nm and λ_{Em}=585 (8) nm, Reader-1, 37 °C, gain=150, n=2. [* executed by Michaela Aichinger and the author]

4.3.1.3 Long-term stability of the lectin pathway liposomes

While aggregation of liposomes or nanoparticles is generally undesirable to maintain stability in terms of fusion and functionality, even aggregated non-optimized Man-Liposomes demonstrated storage stability and full functionality for over twelve months suggesting that the risk of liposome fusion is minimized in this specific case due to steric hindrance of covalently attached mannan on the liposome surface (**Figure S 4-8a**). Furthermore, at this point the optimized Man-Liposomes additionally showed long term storage stability in size, zeta-potential and sulforhodamine B (SRB) leakage for over seven months (**Figure S 4-8b,c**).

4.3.2 Testing a healthy cohort and correlating it to an ELISA

The suitability of the liposome-based assay for the determination of lectin pathway activity was tested on a random selection of 97 healthy human donor sera and compared to a mannan-triggered protein ELISA in which deposition of the complement activation product C3b is

detected. The liposome assay as research tool can be designed for high-throughput screening by choosing a two-data point analysis rather than a full serum titration curve with seven data points. Such an approach saves time, consumables and patient sera while maintaining its statistical significance and biological value. For this purpose, two data points with 4 and 8 %vol. serum content were selected by first titrating a full concentration range of a pooled human serum (**Figure S 4-5f**), and then refining the ideal serum content by screening six donor sera at 4, 5 and 8 %vol. This two-point assay can now provide highly reliable data interpretation, because the full range of complement activity is covered including weak and strong signals (**Figure S 4-9**). Consequently, a complement activity screening of the 97 human donor sera with the liposome-based assay (**Figure S 4-11**) correlated to the ELISA method with a Pearson's r of 0.77 (**Figure 4-3**). Differences may result from the two different assay strategies, i.e. liposomes require the full complement cascade activity, whereas the ELISA only quantifies the onset of the cascade and cannot provide any correlation to activities beyond the C3b stage.

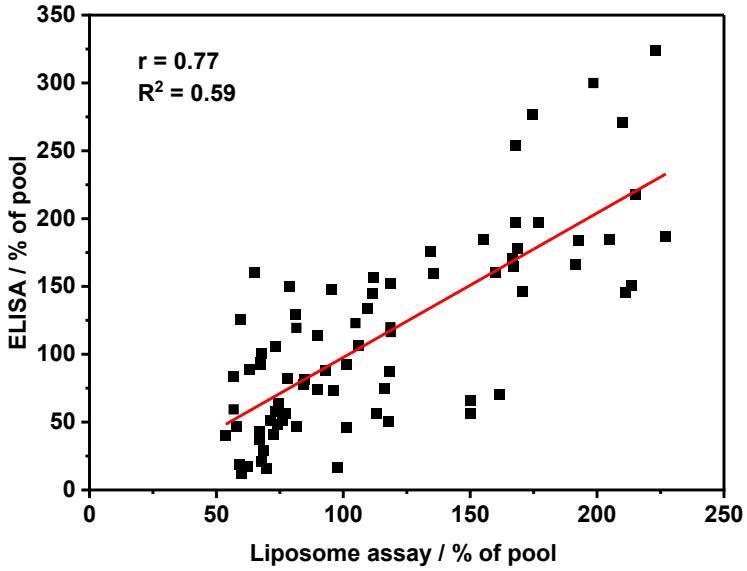

Figure 4-3: Correlation of liposome complement assay to C3b-ELISA. Correlation of healthy donor samples measured once in the liposome complement assay and once with the C3b-deposition ELISA triggered by immobilized mannan (see materials and methods).

4.3.3 Adaptability of SRB liposomes to the classical and alternative pathway

The true value of the lectin pathway specific liposome assay lies in the fact that it stands for a new platform technology that can easily be adapted to the classical and alternative pathways by simple liposome surface modifications. In the case of the classical pathway it has long been known that antibodies bound to liposomes activate the classical pathway[51]. In fact, we also have previously used biotin-modified liposomes as signal generation means in homogeneous bioanalytical assays[36]. Here, we now prove the antibody modified Biot-Liposome specificity for the classical pathway using the same range of inhibitors employed above (**Figure 4-2**). Specifically, only the classical pathway responsive inhibitors anti-C1q and sutimlimab (anti-C1s) as well as the terminal pathway inhibitor eculizumab (anti-C5) influenced liposome

lysis (**Figure 4-4a**). The inhibitors anti-C1q and eculizumab (anti-C5) prevented lysis completely upon a certain concentration (anti-C1q: ≥7.5 µg/mL, EC50 = 2.0 ± 0.1 µg/mL, eculizumab (anti-C5): ≥3.6 µg/mL, EC50 = 3.9 ± 0.2 µg/mL for 3 %vol. serum). Sutimlimab (anti-C1s) was less effective in inhibiting the liposome lysis leading to a remaining lysis of 20 % for the investigated concentration range (up to 6.3 µg/mL, EC50 = 1.1 ± 0.1 µg/mL). As expected, all other investigated inhibitors had no effect on the liposome lysis suggesting no contribution of the lectin and alternative pathway.

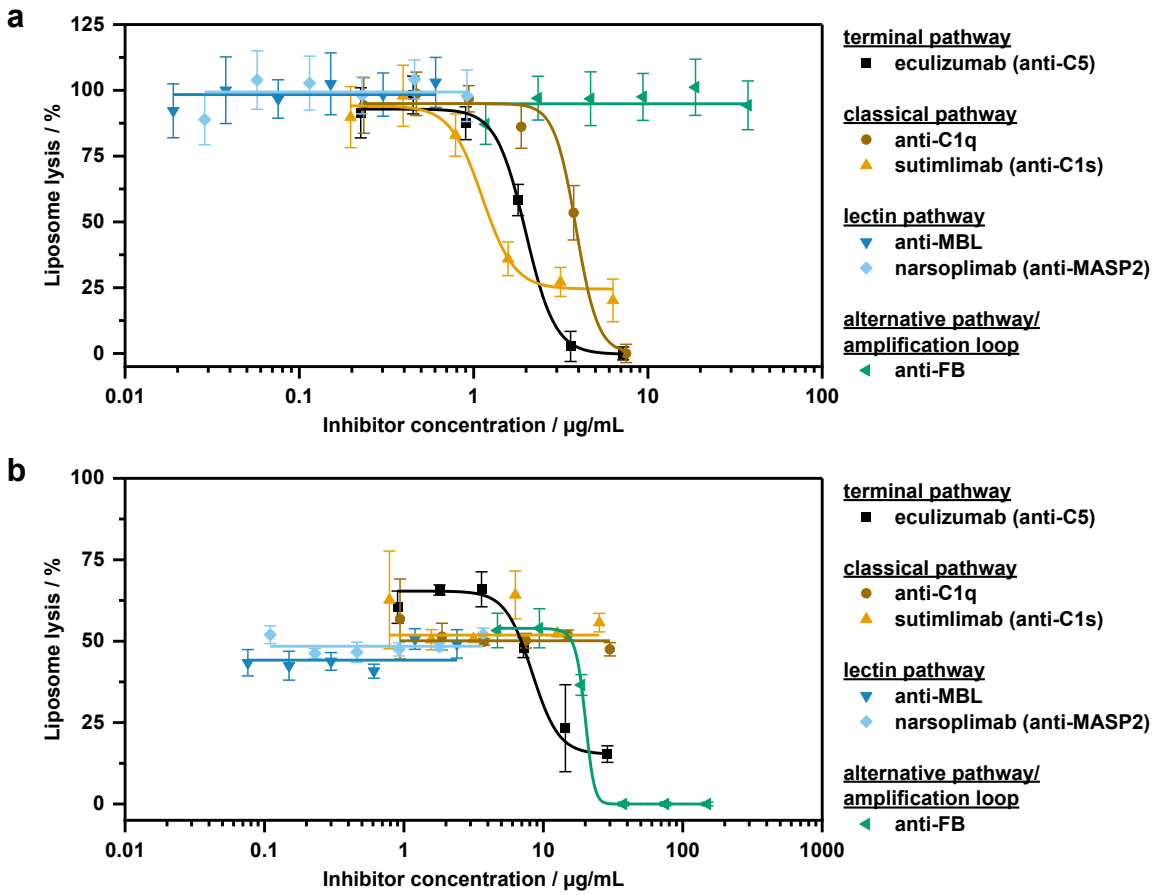

Figure 4-4: Inhibitor screen with antibody modified Biot-Liposomes and LPS-Liposomes. Inhibitor titrations in complement assays investigating lysis obtained for **a**, antibody modified Biot-Liposomes (1 µM tL in well, 0.5 %mol. anti-biotin) and **b**, LPS-Liposomes (2 %mol. LPS, 5 µM tL in well). Anti-C1q, sutimlimab (anti-C1s), anti-FB, narsoplimab (anti-MASP2), anti-MBL and eculizumab (anti-C5) were examined. Complement assays were performed in liposome complement buffer with 200 mM glycine addition. Positive control contained 30 mM OG and serum. In **b** all samples contained 8 mM Mg^{2+}/EGTA in well. Pooled human serum content was **a**, 3 %vol. or **b**, 12 %vol. per well. λ_{Ex}=565 (8) nm and λ_{Em}=585 (8) nm, Reader-1, 37 °C, **a**, gain=150 or **b**, gain=140, n=2. [**b**, * executed by Michaela Aichinger]

For alternative pathway mediated lysis lipopolysaccharides (LPS) are well-known complement triggers and in combination with Mg^{2+} supplemented EGTA (Mg^{2+}/EGTA) containing buffers are widely accepted for alternative pathway mediated lysis investigations. EGTA effectively removes free Ca^{2+} ions out of the solution which are needed for classical and lectin pathway functionality[52,53]. Modification of liposomes with LPS is easily achieved by its addition during liposome preparation as the lipid A moiety of the molecule can anchor within the liposomal membrane. The smooth LPS variant from *Salmonella enteritidis* led to complement activation

(**Figure S 4-10**), and its pathway specificity was confirmed via all aforementioned inhibitors in the presence of 8 mM Mg^{2+}/EGTA. Specifically, complement lysis was not influenced using the anti-MBL antibody, narsoplimab (anti-MASP2), the anti-C1q antibody or sutimlimab (anti-C1s) as inhibitors, respectively. Yet, as expected. the inhibitors anti-FB and eculizumab (anti-C5) showed inhibitory effects on LPS-liposome lysis. For eculizumab (≥14.4 µg/mL, EC50 = 8 ± 1 µg/mL) it was reduced significantly, while for anti-FB (≥27.5 µg/mL, EC50 = 20 ± 1 µg/mL) it was prevented completely (**Figure 4-4b**).

4.4 Conclusion

The biomimic characteristic of liposomes paired with specific surface modification of otherwise stealth liposomes, and the full control over lipid, encapsulant and buffer additive concentrations enabled the development of a novel, reliable platform technology that allows pathway specific complement functionality assessment for the first time. It not only enables dose-response titrations for research studies and 2-point assessments for high-throughput screening, but also has a strikingly high potential for companion diagnostics in the point-of-care considering the superior performance of liposomes in rapid tests. Thus, since liposomes provide full-scale complement functionality analysis including the terminal pathway and the formation of the membrane attack complex, they can form the solid basis for further complement-related assays in the future including ligand, inhibitor and complement protein functional analyses. Long hampered by the impossibility to standardize an erythrocyte-based functional assay, such a flexible, easy-to-perform and standardizable platform technology can hence serve the pharmaceutical, medical and research communities. Its reliable functionality assessment complements protein-based ELISA and omics-based MS studies to further our understanding of this relevant part of our innate immune system and help advance knowledge related to complement-associated diseases.

4.5 References

(1) Merle, N. S.; Noe, R.; Halbwachs-Mecarelli, L.; Fremeaux-Bacchi, V.; Roumenina, L. T. Complement System Part II: Role in Immunity. *Front Immunol* **2015**, *6*, 257. DOI: 10.3389/fimmu.2015.00257.

(2) Rus, H.; Cudrici, C.; Niculescu, F. The role of the complement system in innate immunity. *Immunol Res* **2005**, *33*, 103–112. DOI: 10.1385/IR:33:2:103.

(3) Ricklin, D. Complement-targeted therapeutics: Are we there yet, or just getting started? *Eur. J. Immunol.* **2024**, *54*, e2350816. DOI: 10.1002/eji.202350816.

(4) Anderson, D. H.; Radeke, M. J.; Gallo, N. B.; Chapin, E. A.; Johnson, P. T.; Curletti, C. R.; Hancox, L. S.; Hu, J.; Ebright, J. N.; Malek, G.; Hauser, M. A.; Rickman, C. B.; Bok, D.; Hageman, G. S.; Johnson, L. V. The pivotal role of the complement system in aging and age-related macular degeneration: hypothesis re-visited. *Prog Retin Eye Res* **2010**, *29*, 95–112. DOI: 10.1016/j.preteyeres.2009.11.003.

(5) Kavanagh, D.; Goodship, T. H. J.; Richards, A. Atypical haemolytic uraemic syndrome. *Br Med Bull* **2006**, *77-78*, 5–22. DOI: 10.1093/bmb/ldl004.

(6) Chen, M.; Jayne, D. R. W.; Zhao, M.-H. Complement in ANCA-associated vasculitis: mechanisms and implications for management. *Nat Rev Nephrol* **2017**, *13*, 359–367. DOI: 10.1038/nrneph.2017.37.

(7) Howard, J. F. Myasthenia gravis: the role of complement at the neuromuscular junction. *Ann N Y Acad Sci* **2018**, *1412*, 113–128. DOI: 10.1111/nyas.13522.

(8) Merle, N. S.; Church, S. E.; Fremeaux-Bacchi, V.; Roumenina, L. T. Complement System Part I - Molecular Mechanisms of Activation and Regulation. *Front Immunol* **2015**, *6*, 262. DOI: 10.3389/fimmu.2015.00262.

(9) Ricklin, D.; Hajishengallis, G.; Yang, K.; Lambris, J. D. Complement: a key system for immune surveillance and homeostasis. *Nat Immunol* **2010**, *11*, 785–797. DOI: 10.1038/ni.1923.

(10) Mayer, M. M. In Experimental immunochemistry, 2nd edn.; Kabat, Elvin A.; Mayer, Manfred Martin, Eds.; Charles C. Thomas: Springfield, Ill., 1961; pp. 133–240.

(11) Yamamoto, S.; Kubotsu, K.; Kida, M.; Kondo, K.; Matsuura, S.; Uchiyama, S.; Yonekawa, O.; Kanno, T. Automated homogeneous liposome-based assay system for total complement activity. *Clin Chem* **1995**, *41*, 586–590. DOI: 10.1093/clinchem/41.4.586.

(12) Schaeffer, H. E.; Krohn, D. L. Liposomes in topical drug delivery. *Invest Ophthalmol Vis Sci* **1982**, *22*, 220–227.

(13) Szoka, F.; Papahadjopoulos, D. Comparative properties and methods of preparation of lipid vesicles (liposomes). *Annu Rev Biophys Bioeng* **1980**, *9*, 467–508. DOI: 10.1146/annurev.bb.09.060180.002343.

(14) Russell, D. G.; Alexander, J. Effective immunization against cutaneous leishmaniasis with defined membrane antigens reconstituted into liposomes. *The Journal of Immunology* **1988**, *140*, 1274–1279. DOI: 10.4049/jimmunol.140.4.1274.

(15) Akbarzadeh, A.; Rezaei-Sadabady, R.; Davaran, S.; Joo, S. W.; Zarghami, N.; Hanifehpour, Y.; Samiei, M.; Kouhi, M.; Nejati-Koshki, K. Liposome: classification, preparation, and applications. *Nanoscale Res Lett* **2013**, *8*, 102. DOI: 10.1186/1556-276X-8-102.

(16) Briuglia, M.-L.; Rotella, C.; McFarlane, A.; Lamprou, D. A. Influence of cholesterol on liposome stability and on in vitro drug release. *Drug Deliv Transl Res* **2015**, *5*, 231–242. DOI: 10.1007/s13346-015-0220-8.

(17) Sum, R.; Swaminathan, M.; Rastogi, S. K.; Piloto, O.; Cheong, I. Beta-Hemolytic Bacteria Selectively Trigger Liposome Lysis, Enabling Rapid and Accurate Pathogen Detection. *ACS Sens* **2017**, *2*, 1441–1451. DOI: 10.1021/acssensors.7b00333.

(18) Streif, S.; Neckermann, P.; Spitzenberg, C.; Weiss, K.; Hoecherl, K.; Kulikowski, K.; Hahner, S.; Noelting, C.; Einhauser, S.; Peterhoff, D.; Asam, C.; Wagner, R.; Baeumner, A. J. Liposome-based high-throughput and point-of-care assays toward the quick, simple, and sensitive detection of neutralizing antibodies against SARS-CoV-2 in patient sera. *Anal Bioanal Chem* **2023**, *415*, 1421–1435. DOI: 10.1007/s00216-023-04548-3.

(19) Viswanathan, S.; Wu, L.-C.; Huang, M.-R.; Ho, J.-A. A. Electrochemical immunosensor for cholera toxin using liposomes and poly(3,4-ethylenedioxythiophene)-coated carbon nanotubes. *Anal Chem* **2006**, *78*, 1115–1121. DOI: 10.1021/ac051435d.

(20) Edwards, A. J.; Durst, R. A. Flow-injection liposome immunoanalysis (FILIA) with electrochemical detection. *Electroanalysis* **1995**, *7*, 838–845. DOI: 10.1002/elan.1140070909.

(21) Levine, R. M.; Pearce, T. R.; Adil, M.; Kokkoli, E. Preparation and characterization of liposome-encapsulated plasmid DNA for gene delivery. *Langmuir* **2013**, *29*, 9208–9215. DOI: 10.1021/la400859e.

(22) Ou, L.-J.; Liu, S.-J.; Chu, X.; Shen, G.-L.; Yu, R.-Q. DNA encapsulating liposome based rolling circle amplification immunoassay as a versatile platform for ultrasensitive detection of protein. *Anal Chem* **2009**, *81*, 9664–9673. DOI: 10.1021/ac901786m.

(23) Ge, S.; Jiao, X.; Chen, D. Ultrasensitive electrochemical immunosensor for CA 15-3 using thionine-nanoporous gold-graphene as a platform and horseradish peroxidase-encapsulated liposomes as signal amplification. *Analyst* **2012**, *137*, 4440–4447. DOI: 10.1039/c2an35751h.

(24) Chaize, B.; Colletier, J.-P.; Winterhalter, M.; Fournier, D. Encapsulation of enzymes in liposomes: high encapsulation efficiency and control of substrate permeability. *Artificial Cells, Blood Substitutes, and Biotechnology* **2004**, *32*, 67–75. DOI: 10.1081/bio-120028669.

(25) Esch, M. B.; Locascio, L. E.; Tarlov, M. J.; Durst, R. A. Detection of viable Cryptosporidium parvum using DNA-modified liposomes in a microfluidic chip. *Anal Chem* **2001**, *73*, 2952–2958. DOI: 10.1021/ac001508n.

(26) Gerstl, F.; Pongkitdachoti, U.; Unob, F.; Baeumner, A. J. Miniaturized sensor for electroanalytical and electrochemiluminescent detection of pathogens enabled through laser-induced graphene electrodes embedded in microfluidic channels. *Lab Chip* **2022**, *22*, 3721–3733. DOI: 10.1039/d2lc00593j.

(27) Genç, R.; Murphy, D.; Fragoso, A.; Ortiz, M.; O'Sullivan, C. K. Signal-enhancing thermosensitive liposomes for highly sensitive immunosensor development. *Anal Chem* **2011**, *83*, 563–570. DOI: 10.1021/ac1023765.

(28) Kishimura, M.; Fukuda, H.; Katoh, S.; Sada, E.; Taniguchi, H. Lysis of rabbit γ-globulin-coupled liposomes by the complement system. *J Ferment Bioeng* **1992**, *74*, 81–84. DOI: 10.1016/0922-338X(92)80005-4.

(29) Masaki, T.; Okada, N.; Yasuda, R.; Okada, H. Assay of complement activity in human serum using large unilamellar liposomes. *J Immunol Methods* **1989**, *123*, 19–24. DOI: 10.1016/0022-1759(89)90025-2.

(30) Chen, R. F.; Knutson, J. R. Mechanism of fluorescence concentration quenching of carboxyfluorescein in liposomes: energy transfer to nonfluorescent dimers. *Anal Biochem* **1988**, *172*, 61–77. DOI: 10.1016/0003-2697(88)90412-5.

(31) McGrath, F. D. G.; Brouwer, M. C.; Arlaud, G. J.; Daha, M. R.; Hack, C. E.; Roos, A. Evidence that complement protein C1q interacts with C-reactive protein through its

globular head region. *J Immunol* **2006**, *176*, 2950–2957. DOI: 10.4049/jimmunol.176.5.2950.

(32) Boer, E. C. de; Thielen, A. J.; Langereis, J. D.; Kamp, A.; Brouwer, M. C.; Oskam, N.; Jongsma, M. L.; Baral, A. J.; Spaapen, R. M.; Zeerleder, S.; Vidarsson, G.; Rispens, T.; Wouters, D.; Pouw, R. B.; Jongerius, I. The contribution of the alternative pathway in complement activation on cell surfaces depends on the strength of classical pathway initiation. *Clin Transl Immunology* **2023**, *12*, e1436. DOI: 10.1002/cti2.1436.

(33) Bultink, I. E. M.; Hamann, D.; Seelen, M. A.; Hart, M. H.; Dijkmans, B. A. C.; Daha, M. R.; Voskuyl, A. E. Deficiency of functional mannose-binding lectin is not associated with infections in patients with systemic lupus erythematosus. *Arthritis Res Ther* **2006**, *8*, R183. DOI: 10.1186/ar2095.

(34) Veuskens, B. R. J.; Brouwer, M. C.; van Mierlo, G.; Geissler, J.; van Leeuwen, K.; Derlagen, M.; Keijzer, N. C. H.; Hoogenboezem, M.; Kuijpers, T. W.; Pouw, R. B. Factor H-related 2 levels dictate FHR dimer composition. *Sci Rep* **2025**, *15*, 10669. DOI: 10.1038/s41598-025-94064-4.

(35) Machová, E.; Bystrický, P.; Malovíková, A.; Bystrický, S. Preparation and characterization of carboxymethyl derivatives of yeast mannans in aqueous solutions. *Carbohydr Polym* **2014**, *110*, 219–223. DOI: 10.1016/j.carbpol.2014.03.079.

(36) Hoecherl, K.; Streif, S.; Spitzenberg, C.; Rink, S.; Behrent, A.; Holzhausen, F.; Griesche, C.; Rogoll, C.; Foedlmeier, M.; Gebhard, A.; Kulikowski, K.; Schaefer, N.; Pauly, D.; Baeumner, A. J. A homogeneous immunoassay technology based on liposomes and the complement system enables one-step, no-wash, rapid diagnostics directly in serum. *Anal Bioanal Chem* **2025**, *417*, 3257–3273. DOI: 10.1007/s00216-025-05882-4.

(37) Zelek, W. M.; Harris, C. L.; Morgan, B. P. Extracting the barbs from complement assays: Identification and optimisation of a safe substitute for traditional buffers. *Immunobiology* **2018**, *223*, 744–749. DOI: 10.1016/j.imbio.2018.07.016.

(38) Keizer, M. P.; Pouw, R. B.; Kamp, A. M.; Patiwael, S.; Marsman, G.; Hart, M. H.; Zeerleder, S.; Kuijpers, T. W.; Wouters, D. TFPI inhibits lectin pathway of complement activation by direct interaction with MASP-2. *Eur. J. Immunol.* **2015**, *45*, 544–550. DOI: 10.1002/eji.201445070.

(39) Bradley, A. J.; Devine, D. V. The complement system in liposome clearance: Can complement deposition be inhibited? *Adv Drug Delivery Rev* **1998**, *32*, 19–29. DOI: 10.1016/s0169-409x(97)00129-4.

(40) Seelen, M. A.; Roos, A.; Wieslander, J.; Mollnes, T. E.; Sjöholm, A. G.; Wurzner, R.; Loos, M.; Tedesco, F.; Sim, R. B.; Garred, P.; Alexopoulos, E.; Turner, M. W.; Daha, M. R. Functional analysis of the classical, alternative, and MBL pathways of the complement system: standardization and validation of a simple ELISA. *J Immunol Methods* **2005**, *296*, 187–198. DOI: 10.1016/j.jim.2004.11.016.

(41) Kuipers, S.; Aerts, P. C.; Sjöholm, A. G.; Harmsen, T.; van Dijk, H. A hemolytic assay for the estimation of functional mannose-binding lectin levels in human serum. *J Immunol Methods* **2002**, *268*, 149–157. DOI: 10.1016/s0022-1759(02)00192-8.

(42) Suankratay, C.; Zhang, X.-H.; Zhang, Y.; Lint, T. F.; Gewurz, H. Requirement for the Alternative Pathway as Well as C4 and C2 in Complement-Dependent Hemolysis Via the Lectin Pathway. *The Journal of Immunology* **1998**, *160*, 3006–3013. DOI: 10.4049/jimmunol.160.6.3006.

(43) Hein, E.; Honoré, C.; Skjoedt, M.-O.; Munthe-Fog, L.; Hummelshøj, T.; Garred, P. Functional analysis of Ficolin-3 mediated complement activation. *PLoS One* **2010**, *5*, e15443. DOI: 10.1371/journal.pone.0015443.

(44) Fujita, T.; Matsushita, M.; Endo, Y. The lectin-complement pathway--its role in innate immunity and evolution. *Immunol Rev* **2004**, *198*, 185–202. DOI: 10.1111/j.0105-2896.2004.0123.x.

(45) Thomas, T. C.; Rollins, S. A.; Rother, R. P.; Giannoni, M. A.; Hartman, S. L.; Elliott, E. A.; Nye, S. H.; Matis, L. A.; Squinto, S. P.; Evans, M. J. Inhibition of complement activity by humanized anti-C5 antibody and single-chain Fv. *Mol Immunol* **1996**, *33*, 1389–1401. DOI: 10.1016/s0161-5890(96)00078-8.

(46) Hillmen, P.; Young, N. S.; Schubert, J.; Brodsky, R. A.; Socié, G.; Muus, P.; Röth, A.; Szer, J.; Elebute, M. O.; Nakamura, R.; Browne, P.; Risitano, A. M.; Hill, A.; Schrezenmeier, H.; Fu, C.-L.; Maciejewski, J.; Rollins, S. A.; Mojcik, C. F.; Rother, R. P.; Luzzatto, L. The complement inhibitor eculizumab in paroxysmal nocturnal hemoglobinuria. *N Engl J Med* **2006**, *355*, 1233–1243. DOI: 10.1056/NEJMoa061648.

(47) Bartko, J.; Schoergenhofer, C.; Schwameis, M.; Firbas, C.; Beliveau, M.; Chang, C.; Marier, J.-F.; Nix, D.; Gilbert, J. C.; Panicker, S.; Jilma, B. A Randomized, First-in-Human, Healthy Volunteer Trial of sutimlimab, a Humanized Antibody for the Specific Inhibition of the Classical Complement Pathway. *Clin Pharmacol Ther* **2018**, *104*, 655–663. DOI: 10.1002/cpt.1111.

(48) Dudler, T.; Yaseen, S.; Cummings, W. J. Development and characterization of narsoplimab, a selective MASP-2 inhibitor, for the treatment of lectin-pathway-mediated disorders. *Front Immunol* **2023**, *14*, 1297352. DOI: 10.3389/fimmu.2023.1297352.

(49) Harboe, M.; Garred, P.; Borgen, M. S.; Stahl, G. L.; Roos, A.; Mollnes, T. E. Design of a complement mannose-binding lectin pathway-specific activation system applicable at low serum dilutions. *Clin Exp Immunol* **2006**, *144*, 512–520. DOI: 10.1111/j.1365-2249.2006.03072.x.

(50) Harboe, M.; Ulvund, G.; Vien, L.; Fung, M.; Mollnes, T. E. The quantitative role of alternative pathway amplification in classical pathway induced terminal complement activation. *Clin Exp Immunol* **2004**, *138*, 439–446. DOI: 10.1111/j.1365-2249.2004.02627.x.

(51) Diebolder, C. A.; Beurskens, F. J.; Jong, R. N. de; Koning, R. I.; Strumane, K.; Lindorfer, M. A.; Voorhorst, M.; Ugurlar, D.; Rosati, S.; Heck, A. J. R.; van de Winkel, J. G. J.; Wilson, I. A.; Koster, A. J.; Taylor, R. P.; Saphire, E. O.; Burton, D. R.; Schuurman, J.; Gros, P.; Parren, P. W. H. I. Complement is activated by IgG hexamers assembled at the cell surface. *Science* **2014**, *343*, 1260–1263. DOI: 10.1126/science.1248943.

(52) Des Prez, R. M.; Bryan, C. S.; Hawiger, J.; Colley, D. G. Function of the classical and alternate pathways of human complement in serum treated with ethylene glycol tetraacetic acid and MgCl2-ethylene glycol tetraacetic acid. *Infect Immun* **1975**, *11*, 1235–1243. DOI: 10.1128/iai.11.6.1235-1243.1975.

(53) Morgan, B. P. Measurement of complement hemolytic activity, generation of complement-depleted sera, and production of hemolytic intermediates. *Methods Mol Biol* **2000**, *150*, 61–71. DOI: 10.1385/1-59259-056-X:61.

4.6 Supporting Information

4.6.1 Supporting text to the main article

Signal intensities above 100 % liposome lysis

Normalization to the positive control at 10 min disregards quenching effects of the detergent and the enhancement effects high concentrations of serum proteins have on SRB[1]. This may result in lysis values above 100 % and is a mere mathematical oddity. However, normalization allows the standardization across all experiments.

Negative values lysis values after evaluation of the liposome-based complement assay

Negative lysis values obtained for healthy donor sera (**Figure S 4-9** and **Figure S 4-11**) were caused by the chosen background evaluation. This method does not take into account general fluorescence intensity decay over time so that a non-reactive sample has lower fluorescence signals after 60-minute incubation in comparison to its 10-minute data point. Specifically, to minimize the amount of patient serum needed per analysis, no negative controls were performed for each individual serum. Instead, for each serum signal intensities that were reached after 10.5 min of each sample was used as background. When this is subtracted from the 60-min final value, it can cause negative values when the fluorescence intensity decreases over time. This was also seen for the negative control serum (shown as reference in **Figure S 4-9**). The general negative control was pooled human serum.

4.6.2 Supporting Figures and Tables to the main article

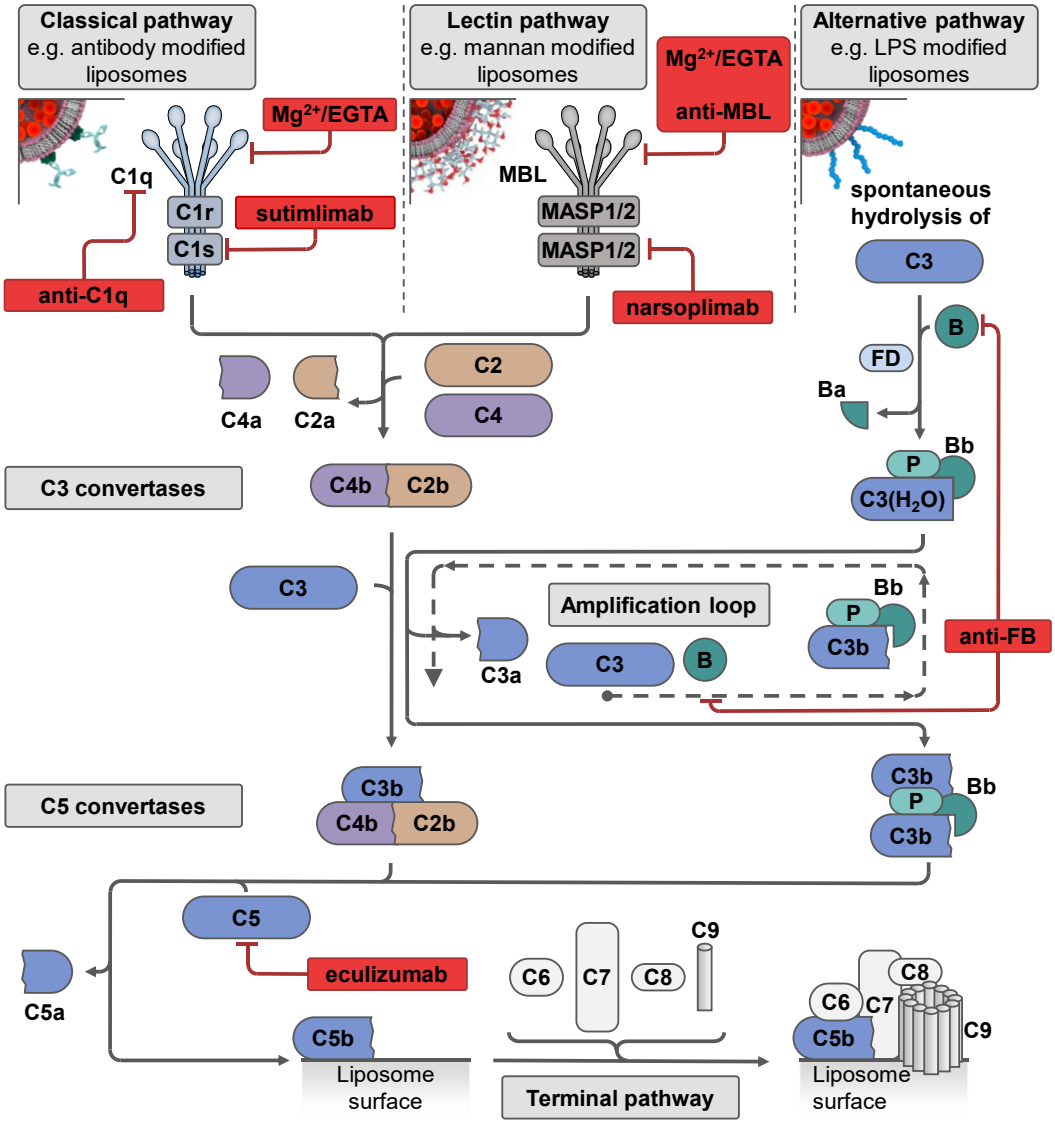

Figure S 4-1: Complement system cascade scheme. An overview over the cascade of the complement system. Inhibitors used are marked in red and indicate their respective target.

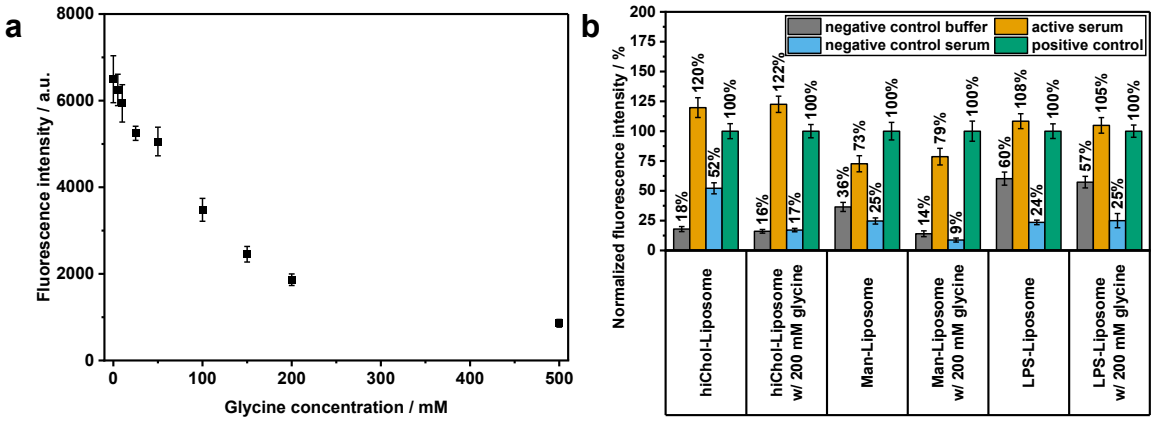

Figure S 4-2: Background fluorescence reduction through glycine addition as stabilizing agent. a, Assay investigating the non-lysed liposome background fluorescence in liposome complement buffer samples of Stealth-Liposomes (1 µM tL in well) with varying glycine concentrations in well. λ_{Ex}=565 (8) nm and λ_{Em}=585 (8) nm, 37 °C, gain=150, Reader-1, n=3. **b**, Complement assays investigating hiChol-Liposome with increased cholesterol content (44 %mol.), preliminary Man-Liposome (500 %mol. mannan monomer modification, 60 %wt. BEA small scale synthesis version, no acetylation) and LPS-Liposome (1 %mol. LPS, all with 10 µM tL in well) with and without 200 mM glycine addition for background signal optimization. Complement assays were performed in liposome complement buffer. Negative control serum contained iaCB to a final concentration of 20 mM EDTA and serum. Positive control contained 30 mM OG and serum. Pooled human serum content was 10 %vol. per well. λ_{Ex}=565 (5) nm and λ_{Em}=585 (5) nm, Reader-1, 37 °C, gain=150, n=3.

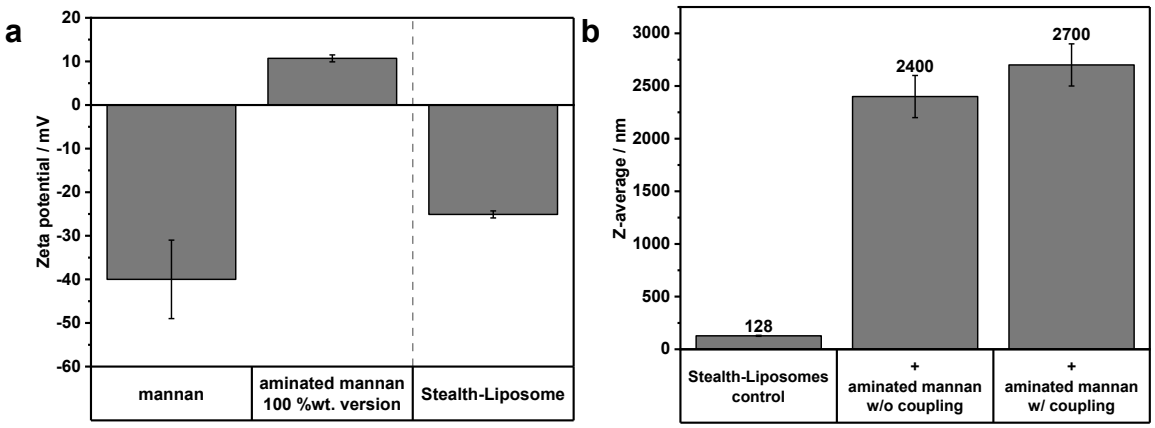

Figure S 4-3: Electrostatic interaction of aminated mannan and anionic liposomes. a, Zeta potential measurements investigating mannan before and after amination (aminated mannan version 100 %wt. BEA) and Stealth-Liposomes. n=1, three consecutive measurements. **b**, Size evaluation via DLS investigating Stealth-Liposomes in presence of aminated mannan (100 %wt. BEA version, 3000 %mol. mannan monomer) once with and once without covalent coupling to the liposome surface. n=1, three consecutive measurements.

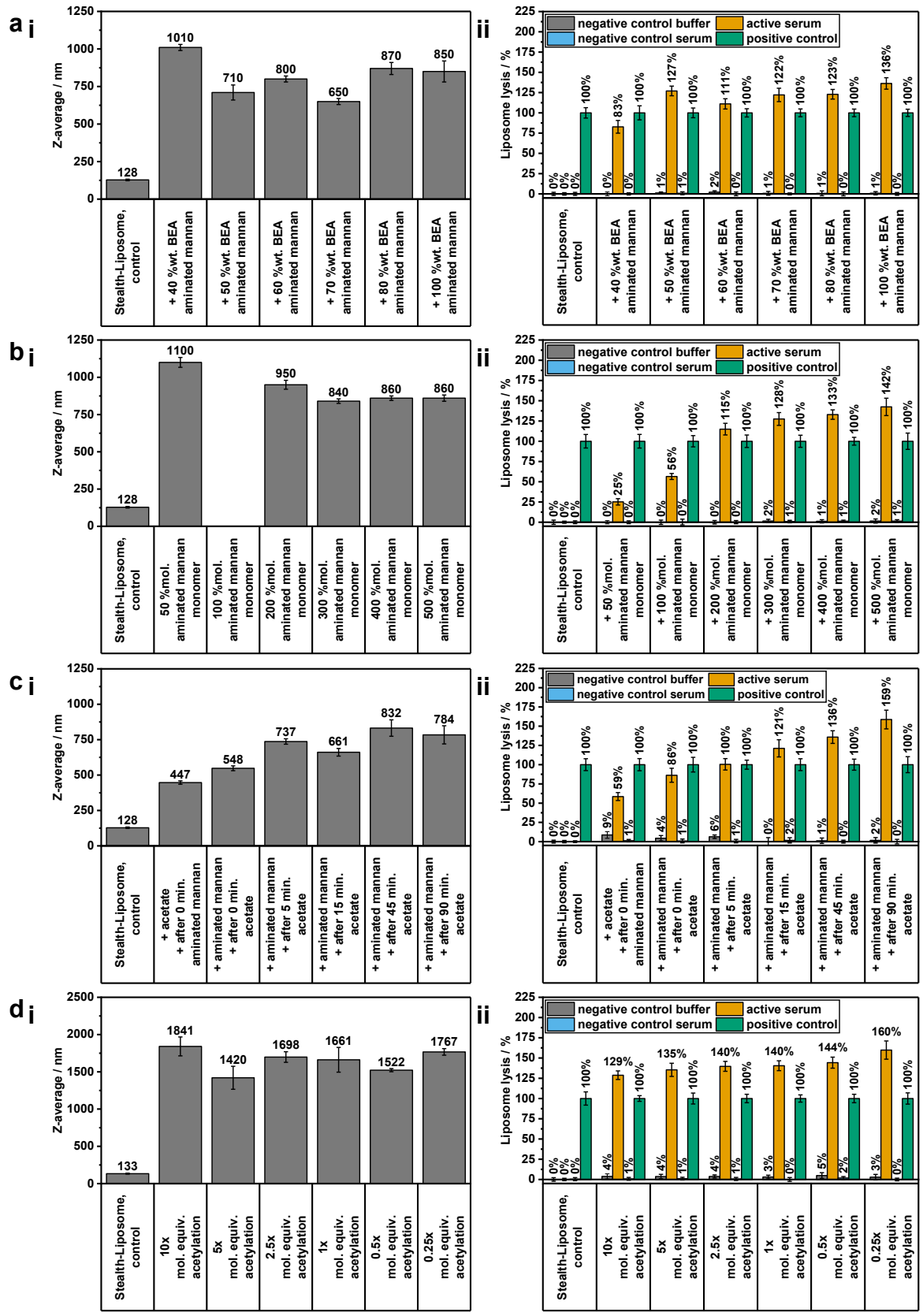

Figure S 4-4: Optimizations of liposome mannan modification. i, Size evaluation of mannan modified Stealth-Liposomes via DLS (25 µM tL in HSS-buffer). n=1, three consecutive measurements. **ii**, Complement assays investigating mannan modified Stealth-Liposomes (1 µM tL in well). Complement assays were performed in liposome complement buffer with 200 mM glycine addition. Negative control serum contained iaCB to a final concentration of 20 mM EDTA and serum. Positive control contained 30 mM OG and serum. Pooled human serum content was 10 %vol. per well. λ_{Ex}=565 (8) nm and λ_{Em}=585 (8) nm, Reader-1, 37 °C, gain=150, n=3. **a**, Stealth-Liposomes modified with aminated mannan with varying amination content (see materials and methods,

aminated mannan versions 40-100 %wt. BEA, 500 %mol. mannan monomer) with followed acetylation (10x molar equivalents of mannan monomer). **b**, Stealth-Liposomes modified with varying aminated mannan content (see materials and methods, 50-500 %mol. mannan monomer, 50 %wt. BEA version) with followed acetylation (10x molar equivalents of mannan monomer). **c**, Stealth-Liposomes with aminated mannan modification (see materials and methods, 500 %mol. mannan monomer, 50 %wt. BEA version) followed by varying addition times for acetylation (10x molar equivalents of mannan monomer, acetate addition 0-90 min after aminated mannan addition). **d**, Stealth-Liposomes with aminated mannan modification (see materials and methods, 500 %mol. mannan monomer, 50 %wt. BEA version) followed by varying acetylation content (0.25-10x molar equivalents of mannan monomer). [**c, d** * executed by Michaela Aichinger]

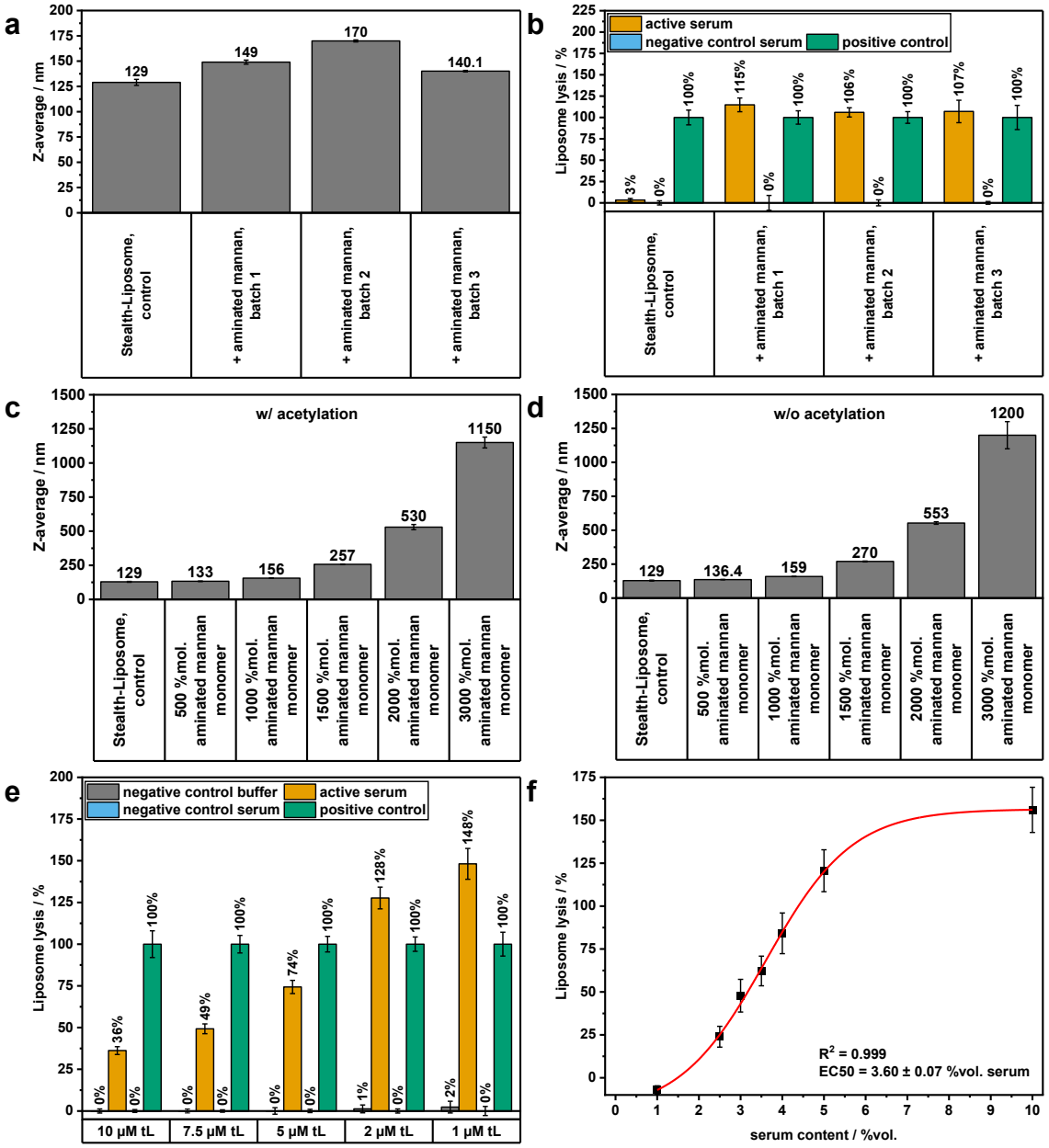

Figure S 4-5: Final optimizations of liposome mannan modification including reproducibility studies and optimizations of the Man-Liposome complement assay. a, b, Reproducibility of the final aminated mannan synthesis and liposome modification protocol. Stealth-Liposomes were modified with aminated mannan (see materials and methods, 500 %mol. mannan monomer, 50 %wt. BEA large batch synthesis versions) followed by acetylation content (1x molar equivalents of mannan monomer). a, Size evaluation via DLS. Liposome concentration was 25 µM total lipid in HSS-buffer. n=1, three consecutive measurements. **b,** Complement assays investigating the final aminated mannan synthesis and liposome modification protocol. Complement assays were performed in liposome complement buffer with 200 mM glycine addition. Negative control serum contained iaCB to a final concentration of 20 mM EDTA and serum. Positive control contained 30 mM OG and serum. Pooled human serum content was 10 %vol. per well. λ_{Ex}=565 (8) nm and λ_{Em}=585 (8) nm, Reader-1, 37 °C, gain=150, n=3. **c, d,** Size evaluation via DLS investigating Stealth-Liposomes modified with varying optimized aminated mannan content (see materials and methods, 500-3000 %mol. mannan monomer, 50 %wt. BEA large batch synthesis version) with, c and without, d acetylation (1x molar equivalents of mannan monomer). Liposome concentration was 25 µM total lipid in HSS-buffer. n=1, three consecutive measurements. **e,** Complement assays investigating the final Man-Liposomes (500 %mol. mannan monomer modification, 50 %wt. BEA large batch synthesis version, acetylation with 1x molar equivalents of mannan monomer) with varying liposome content in well (1-10 µM tL in well). Complement assays were performed in liposome complement buffer with 200 mM glycine addition. Negative control serum contained iaCB to a final concentration of 20 mM EDTA and serum. Positive control contained 30 mM OG and serum. Pooled human serum content was 10 %vol. per well. λ_{Ex}=565 (8) nm and λ_{Em}=585 (8) nm, Reader-1, 37 °C, gain=140, n=3. **f,** Pooled human serum content titration (1-10 %vol.) with Man-Liposomes (1 µM tL in well, 500 %mol. mannan monomer modification, 50 %wt. BEA large batch synthesis version, acetylation with 1x molar equivalents of mannan monomer) Complement assays were performed in liposome complement buffer with 200 mM glycine addition. Positive control contained 30 mM OG and serum. λ_{Ex}=565 (8) nm and λ_{Em}=585 (8) nm, Reader-1, 37 °C, gain=150, n=3.

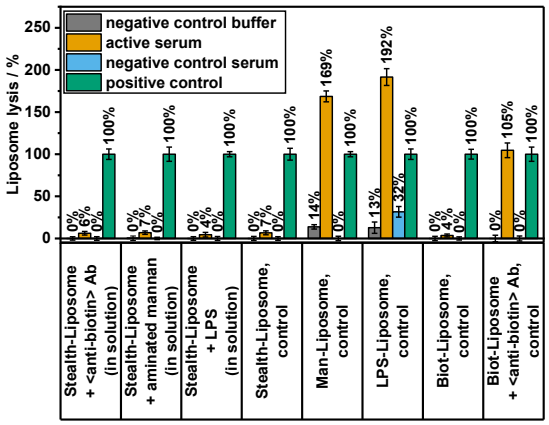

Figure S 4-6: Bystander complement lysis assay. Complement assays investigating bystander complement lysis of Stealth-Liposomes (1 µM tL in well) in presence of anti-biotin antibodies (0.5 %mol.), aminated mannan (500 %mol. mannan monomer) or LPS (2 %mol.) in the solution. As positive control Biot-Liposomes with and without 0.5 %mol. anti-biotin antibodies, Man-Liposomes (500 %mol. mannan monomer modification, 50 %wt. BEA large batch synthesis version, acetylation with 1x molar equivalents of mannan monomer) and LPS-Liposome (2 %mol. LPS) were measured. Complement assays were performed in liposome complement buffer with 200 mM glycine addition. Negative control serum contained iaCB to a final concentration of 20 mM EDTA and serum. Positive control contained 30 mM OG and serum. Pooled human serum content was 10 %vol. per well. λ_{Ex}=565 (8) nm and λ_{Em}=585 (8) nm, Reader-1, 37 °C, gain=150, n=3 (except active serum of Biot-Liposome + anti-biotin antibodies, n=2). [* executed by Michaela Aichinger]

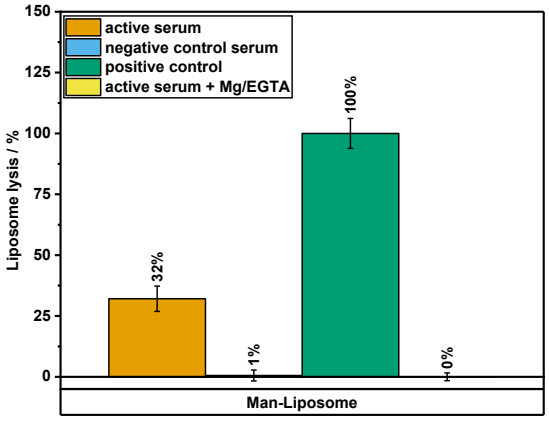

Figure S 4-7: Man-Liposome lysis initiation under Mg^{2+}/EGTA conditions. Complement assay investigating lysis obtained for Man-Liposomes (1 µM tL in well, 500 %mol. mannan monomer modification, 50 %wt. BEA large batch synthesis version, acetylation with 1x molar equivalents of mannan monomer) in presence of Mg^{2+}/EGTA (active serum + Mg/EGTA). Complement assays were performed in liposome complement buffer with 200 mM glycine addition. Negative control serum contained iaCB to a final concentration of 40 mM EDTA and serum. Active serum + Mg/EGTA contained 8 mM Mg^{2+}/EGTA in well and serum. Positive control contained 30 mM OG and serum. Pooled human serum content was 10 %vol. per well. λ_{Ex}=565 (8) nm and λ_{Em}=585 (8) nm, Reader-1, 37 °C, gain=150, n=3. [* executed by Michaela Aichinger]

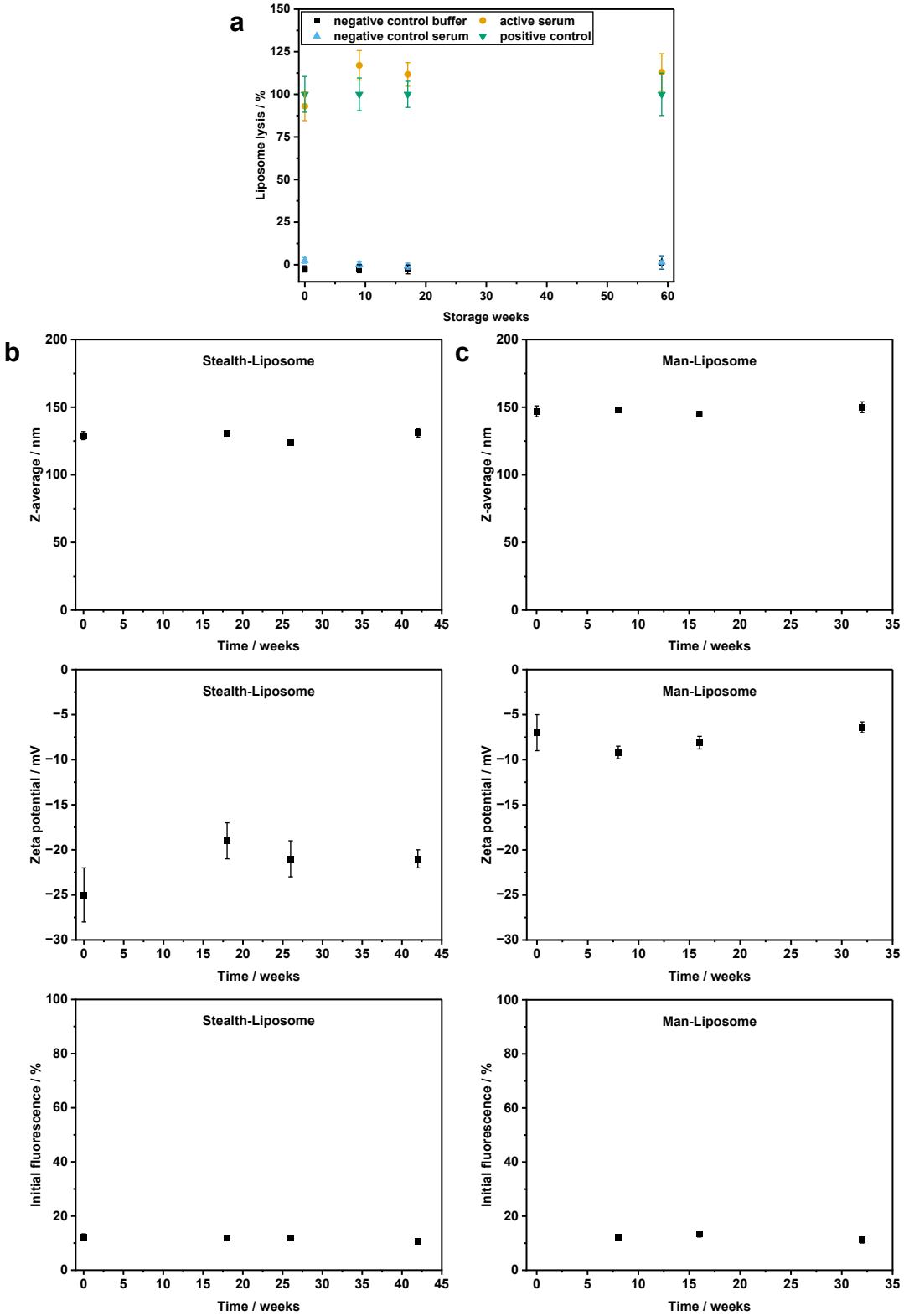

Figure S 4-8: Long-term stability in of Stealth- and Man-Liposomes. a, Long-term stability investigations via complement assay of aggregated non-optimized Man-Liposomes (1 µM tL in well, 3000 %mol. mannan monomer modification, 100 %wt. BEA small batch synthesis version, no acetylation) stored at 4 °C. Complement assays were performed in liposome complement buffer with 200 mM glycine addition. Negative control serum contained iaCB to a final concentration of 20 mM EDTA and serum. Positive control contained 30 mM OG and serum. Pooled human serum content was 10 %vol. per well. λ_{Ex}=565 (8) nm and λ_{Em}=585 (8) nm, Reader-1, 37 °C, gain=150, n=3. **b**, **c**, Long-term stability investigations with DLS, zeta potential and SRB-leakage over time via fluorescence measurements of **b**, non-coupled, Stealth- and **c**, aminated mannan coupled Man-Liposomes (500 %mol. mannan monomer modification, 50 %wt. BEA large batch synthesis version, acetylation with 1x molar equivalents of mannan monomer) stored at 4 °C. For DLS and zeta potential liposome concentration was 50 µM tL in HSS-buffer. n=1, three consecutive measurements. Initial fluorescence is determined as described in the materials and methods, λ_{Ex}=565 (5) nm and λ_{Em}=585 (5) nm, Reader-1, gain=100, n=4.

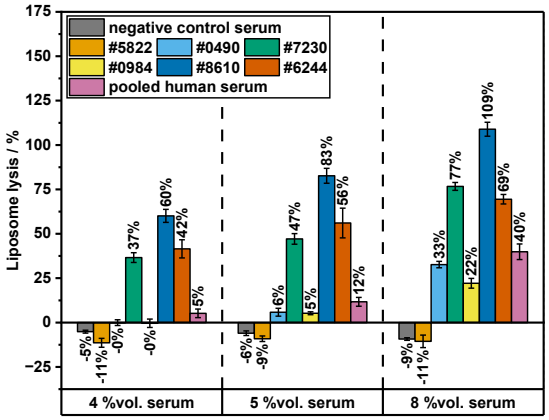

Figure S 4-9: Serum content validation for high-throughput format using Man-Liposomes. Complement assay investigating 4, 5 and 6 %vol. serum of healthy donors with Man-Liposomes (1 µM tL in well, 500 %mol. mannan monomer modification, 50 %wt. BEA large batch synthesis version, acetylation with 1x molar equivalents of mannan monomer) in presence of Mg^{2+}/EGTA (active serum + Mg/EGTA). Complement assays were performed in liposome complement buffer with 200 mM glycine addition. Negative control serum contained iaCB to a final concentration of 40 mM EDTA and pooled human serum. Positive control contained 30 mM OG and serum. See supplementary text for negative lysis values. λ_{Ex}=540 (25) nm and λ_{Em}=620 (40) nm, Reader-2, 37 °C, gain=85, n=2.

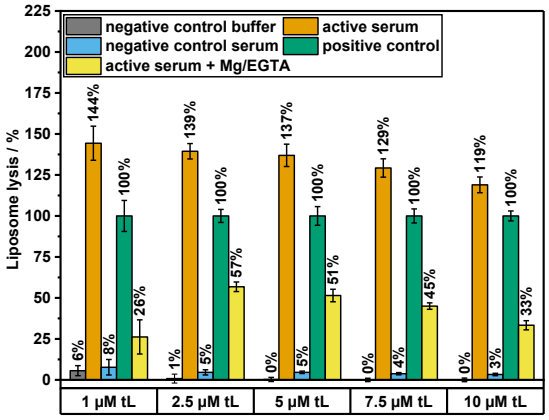

Figure S 4-10: LPS-Liposome content titration in the complement assay. Complement assays investigating LPS-Liposomes (2 %mol. LPS) at varying total lipid concentration (1-10 µM tL in well) with and without Mg^{2+}/EGTA buffer. Complement assays were performed in liposome complement buffer with 200 mM glycine addition. Negative control serum contained iaCB to a final concentration of 20 mM EDTA and serum. Active serum + Mg/EGTA contained 8 mM Mg^{2+}/EGTA in well and serum. Positive control contained 30 mM OG and serum. Pooled human serum content was 10 %vol. per well. λ_{Ex}=565 (8) nm and λ_{Em}=585 (8) nm, Reader-1, 37 °C, gain=130, n=3. [* executed by Michaela Aichinger]

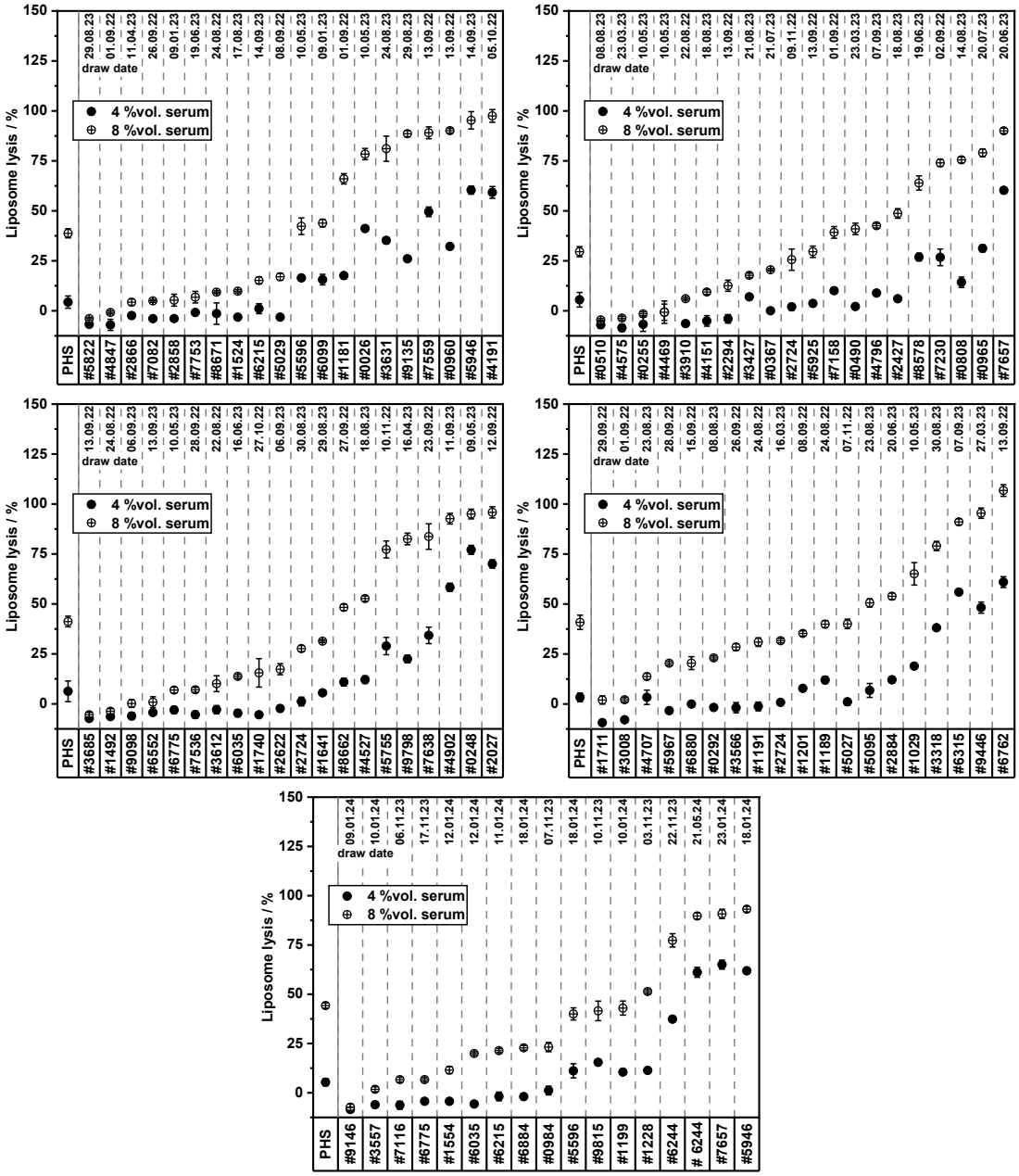

Figure S 4-11: Healthy human donor sera screening with the Man-Liposome complement assay. Complement assays screening lysis of Man-Liposomes (1 µM tL in well, 500 %mol. mannan monomer modification, 50 %wt. BEA large batch synthesis version, acetylation with 1x molar equivalents of mannan monomer) induced by healthy human donor sera and a pooled human serum (PHS) as control. Complement assays were performed in liposome complement buffer with 200 mM glycine addition. Positive control contained 30 mM OG and serum. Human serum content was 4 and 8 %vol. per well. See supplementary text for negative lysis values. λ_{Ex}=540 (25) nm and λ_{Em}=620 (40) nm, Reader-2, 37 °C, gain=85, n=2.

Table S 4-1: Complement inhibitor antibody characteristics

Antibody	Target	Inhibited Pathway	Host	Isotype
anti-C1q.85	C1q	Classical	mouse	IgG1, kappa
sutimlimab	C1s	Classical	humanized	IgG4
anti-FB.1	Factor B	Alternative	mouse	IgG1, kappa
anti-MBL.1	MBL	Lectin	mouse	IgG1, kappa
narsoplimab	MASP-2	Lectin	humanized	IgG4
eculizumab	C5	all three	humanized	IgG2/4

Table S 4-2: Dose-Response complement inhibitor fit EC50 and R^2 values

Man-Liposome		
Antibody	EC50 / µg/mL	R^2
eculizumab (anti-C5)	5 ± 2	0.996
anti-C1q	-	-
sutimlimab (anti-C1s)	-	-
anti-MBL	0.14 ± 0.01	0.999
narsoplimab (anti-MASP2)	0.35 ± 0.06	0.994
anti-FB	12.6 ± 0.4	0.999
anti-biotin modified Biot-Liposomes		
Antibody	EC50 / µg/mL	R^2
eculizumab (anti-C5)	2.0 ± 0.1	0.997
anti-C1q	3.9 ± 0.2	0.996
sutimlimab (anti-C1s)	1.1 ± 0.1	0.991
anti-MBL	-	-
narsoplimab (anti-MASP2)	-	-
anti-FB	-	-
LPS-Liposome		
Antibody	EC50 / µg/mL	R^2
eculizumab (anti-C5)	8 ± 1	0.996
anti-C1q	-	-
sutimlimab (anti-C1s)	-	-
anti-MBL	-	-
narsoplimab (anti-MASP2)	-	-
anti-FB	20 ± 1	1.000

4.6.3 Supplementary Materials and Methods to the main article

4.6.3.1 Chemicals and Consumables

All chemicals were of analytical grade and were used without purification. 4-Aminophenyl α-D-mannopyranoside (4-APM, sc-220930) was purchased from Santa Cruz Biotechnology, Inc., Heidelberg, Germany). Cholesteryl hemisuccinate (Cay25698-1) was bought from Cayman Chemical Company, Michigan, USA. 1,2-dimyristoyl-sn-glycero-3-phosphoethanolamine (DMPE, 850745P) was purchased from Avanti Polar Lipids (Alabaster, AL, USA). D-Mannosamine-hydrochlorid (M4670) and bovine serum albumin (BSA) was purchased from Sigma-Aldrich/Merck KGaA (Darmstadt, Germany).

4.6.3.2 Liposome synthesis

For liposomes with high cholesterol (hiChol-Liposomes) or cholesteryl hemisuccinate content, 44 %mol. cholesterol or cholesteryl hemisuccinate was used in the lipid mixture and the DPPC content reduced respectively. For liposomes with amine groups, 5 %mol. DMPE was added to the lipid mixture.

4.6.3.3 Liposome modification/coupling

4-APM, mannosamine and BSA were conjugated to carboxylated liposomes via EDC/NHS chemistry as described in the main article. For acetylation of liposomes with amine functionality, liposomes were incubated with a 25 times molar excess of sNHS-acetate in 0.05 M MES buffer (pH 5.5) compared to the amine groups on the liposomes for 2.5 hours at RT and 300 rpm. Liposomes were dialyzed against HSS buffer overnight with two buffer exchanges in a Spectra-Por® Float-A-Lyzer® G2 (1 mL, MWCO: 1000 kDa). Purified coupled liposomes were stored at 4 °C.

4.6.4 Supplementary Results and Discussion to the main article

4.6.4.1 Investigations on potential lectin pathway triggers apart from mannan

Before the more complex amination of mannan and subsequent liposome modification was initiated, simpler approaches were investigated. These included known lectin pathway triggers, i.e. acetylated BSA[2] and the mannan subunit, mannose[3]. BSA was coupled to glutaryl group bearing liposomes followed by subsequent acetylation with sNHS-acetate. In addition, since it was shown that the acetylation is the crucial part for activation of the lectin pathway for acetylated BSA in literature[2], direct acetylation of the liposome surface was investigated with amine group bearing liposomes (**Figure S 4-12**). In both cases, no complement-mediated liposome lysis could be observed which suggests that a simple transfer of triggers, which were confirmed in ELISA-based approaches[2] is not necessarily possible to a liposome lysis-based assay. Similarly, mannosamine did not induce liposome lysis (**Figure S 4-12**), which was tested as low molecular alternative to mannan and coupled to the liposome surface in excess (16 %mol.) compared to the amount of carboxyl groups in the liposomal membrane (4 %mol) with subsequent purification of the excess. The introduction of a spacer between the sugar moiety and the liposome surface in conjunction with coupling to the opposite site from the hydroxyl groups on carbon atoms C3 and C4 of mannose, which are relevant for MBL interaction[4], by the use of 4-aminophenyl mannopyranoside (4-APM) initially indicated minimally increased liposome lysis levels compared to the bare liposome control (**Figure S 4-13**). However, increased 4-APM content, achieved through excess coupling (200 %mol. 4-APM) to 44 %mol. cholesterol-hemisuccinate containing liposomes, could not confirm lectin pathway mediated liposome lysis. Here, the control liposomes with high cholesterol-hemisuccinate content already caused complement lysis due to the high cholesterol content, which is known to activate the complement system[5–8]. While additional 4-APM modification again increased the lysis from 53 ± 4 % to 69 ± 7 %, this lysis did not occur under C1q inhibition with the anti-C1q85 antibody. Therefore, all observed lysis had to be attributed to lysis via the classical pathway of the complement system. Overall, this indicated that the mannose density on the liposome surface was likely too low and higher molecular mannose sugars are needed to successfully induce lectin pathway specific liposome lysis.

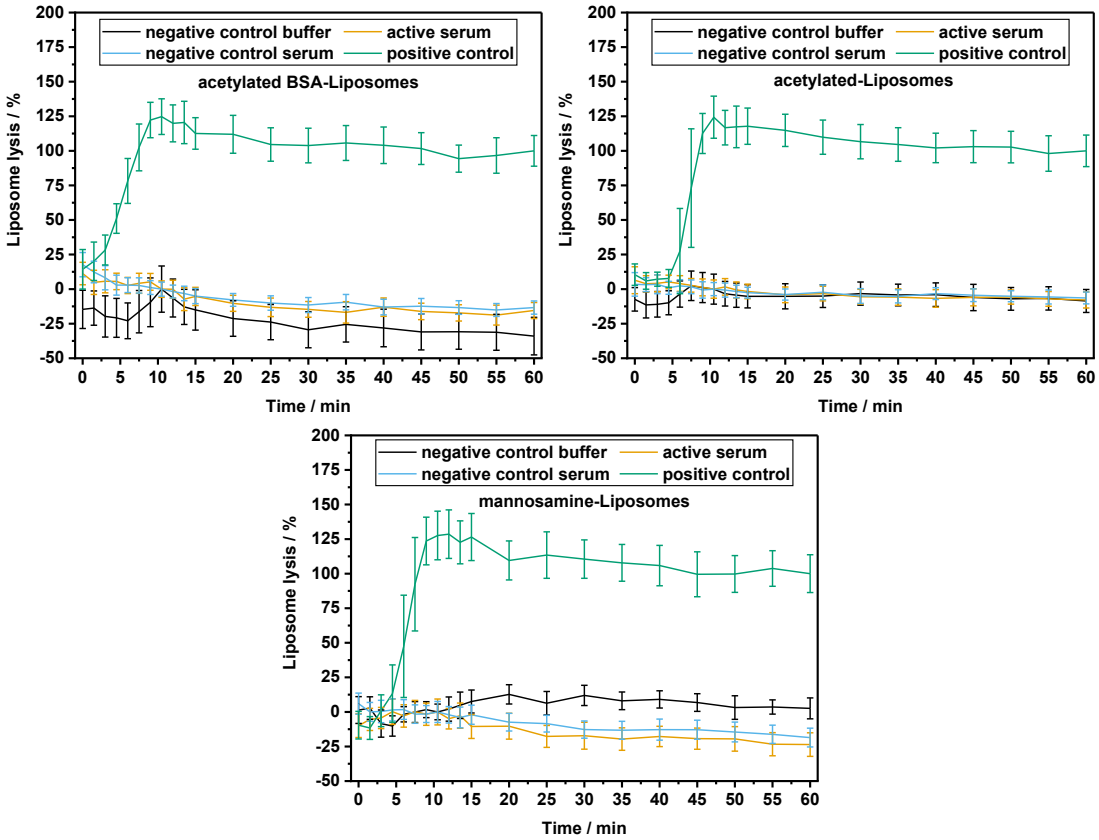

Figure S 4-12: Liposome-based complement assays examining low molecular alternatives to mannan modification. Time-resolved complement assays investigating acetylated BSA-Liposomes (0.5 %mol. BSA, 25x excess of NH_2 groups), acetylated-Liposomes (25x excess of NH_2 groups, 5 %mol. DMPE Liposomes) and mannosamine-Liposomes (16 %mol. mannosamine, 4 %mol. glutaryl-Liposomes) (10 µM total lipid (tL) in well). Complement assays were performed in liposome complement buffer. Negative control serum contained inactivation complement buffer (iaCB) to a final concentration of 20 mM EDTA and serum. Positive control contained 30 mM OG and serum. Pooled human serum content was 10 %vol. per well. λ_{Ex}=565 (5) nm and λ_{Em}=585 (5) nm, Reader-1, 37 °C, gain=150, n=3.

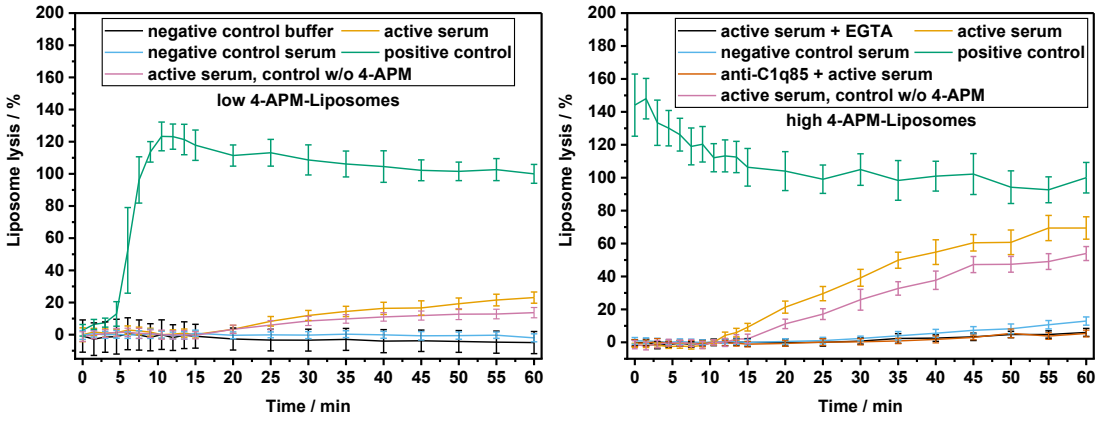

Figure S 4-13: Liposome-based complement assays examining 4-APM as alternative to mannan modification. Time-resolved complement assays investigating 4-APM modified liposomes with low (16 %mol. 4-APM, 4 %mol. glutaryl-Liposomes) or high 4-APM content (200 %mol. 4-APM, 44 %mol. cholesterol-hemisuccinate-Liposomes) (10 µM total lipid (tL) in well). Complement assays were performed in liposome complement buffer with 200 mM glycine addition. Samples with EGTA addition contained 0.4 mM EGTA in the final well (active serum + EGTA, see materials and methods). Anti-C1q containing samples contained 25 µg/mL anti-C1q85 final well (see materials and methods). Negative control serum contained inactivation complement buffer (iaCB) to a final concentration of 20 mM EDTA and serum. Positive control contained 30 mM OG and serum. Pooled human serum content was 10 %vol. per well. λ_{Ex}=565 (5) nm and λ_{Em}=585 (5) nm, Reader-1, 37 °C, gain=150, n=3.

4.6.4.2 Classical pathway specificity and ELISA correlation studies of high cholesterol containing liposomes

For the classical pathway readout, a simpler alternative that circumvents the incubation steps needed during assay preparations for liposomes modified with antibodies was sought. This was envisioned to be achieved through high cholesterol content containing liposomes (hiChol-Liposomes). In previous work[8], complement-mediated lysis was described for hiChol-Liposomes already. However, cholesterol as complement trigger was not yet thoroughly investigated in literature and it was therefore of great interest, to determine the pathways involved during complement activation triggered by high cholesterol levels in liposomal membranes. Analysis of the complement lysis initiated by hiChol-Liposomes with the full range of complement inhibitors, i.e. eculizumab (anti-C5), anti-C1q, sutimlimab (anti-C1s), anti-MBL, narsoplimab (anti-MASP) and anti-FB, determined the obtained lysis as classical pathway specific. Only the classical pathway responsive inhibitors anti-C1q and sutimlimab as well as the general inhibitor eculizumab influenced the liposome lysis (**Figure S 4-14**). All three inhibitors prevent lysis completely upon a certain concentration (anti-C1q: ≥6.25 µg/mL, EC50 = 3.3 ± 0.4 µg/mL, eculizumab (anti-C5): ≥3 µg/mL, EC50 = 1.74 ± 0.08 µg/mL, sutimlimab (anti-C1s): ≥2.63 µg/ml, EC50 = 0.87 ± 0.02 µg/mL for 2.5 %vol. serum), while all other investigated inhibitors had no effect on the liposome lysis suggesting no contribution of the lectin and alternative pathway.

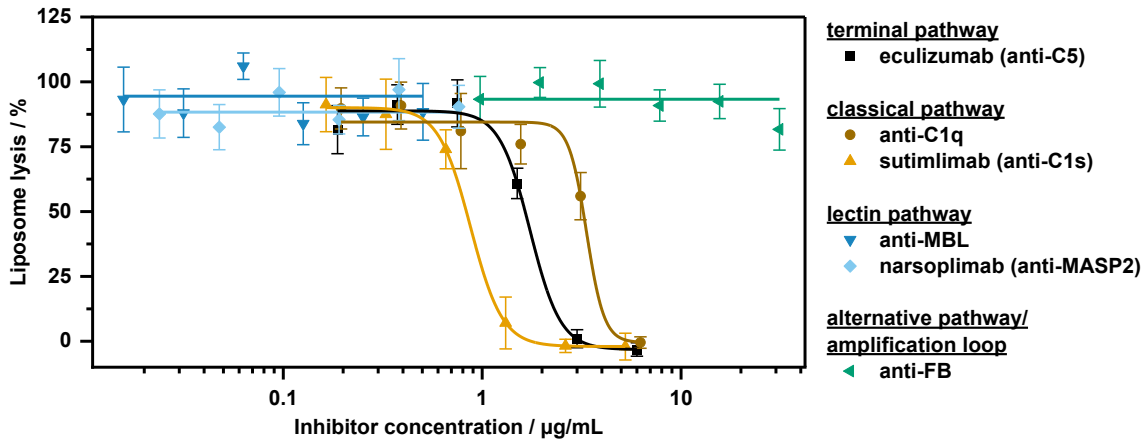

Figure S 4-14: Inhibitor screen with hiChol-Liposomes in the complement assay. Inhibitor titrations in complement assays investigating lysis obtained for hiChol-Liposomes (1 µM tL in well, 44 %mol. cholesterol). Anti-C1q, sutimlimab, anti-FB, narsoplimab, anti-MBL and eculizumab were examined. Complement assays were performed in liposome complement buffer with 200 mM glycine addition. Positive control contained 30 mM OG and serum. Pooled human serum content was 2.5 %vol. per well. λ_{Ex}=565 (8) nm and λ_{Em}=585 (8) nm, Reader-1, 37 °C, gain=150, n=2. [* executed by Michaela Aichinger]

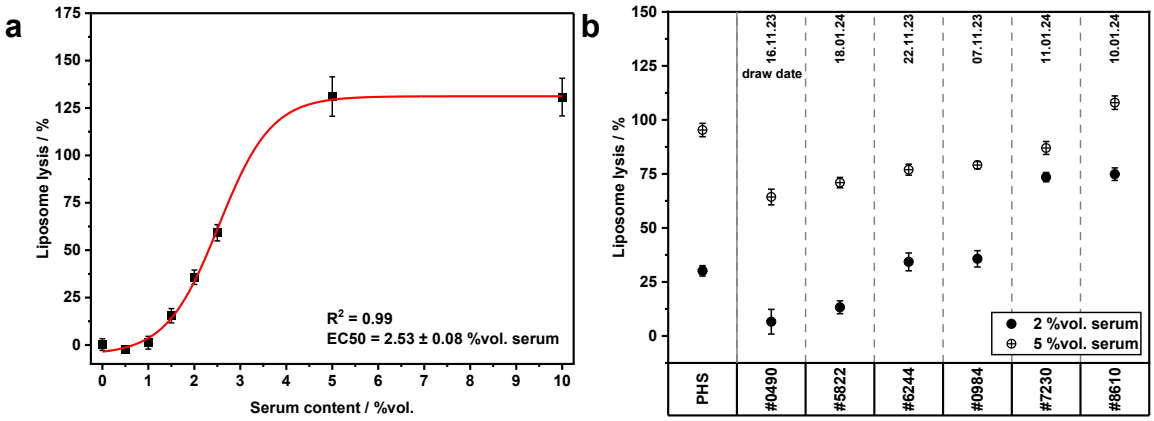

Figure S 4-15: Preparation studies for high-throughput format using hiChol-Liposomes. a, Pooled human serum content titration (1-10 %vol.) with hiChol-Liposomes (1 µM tL in well) Complement assays were performed in liposome complement buffer with 200 mM glycine addition. Positive control contained 30 mM OG and serum. λ_{Ex}=565 (8) nm and λ_{Em}=585 (8) nm, Reader-1, 37 °C, gain=150, n=3. **b**, Complement assay investigating 2 and 5 %vol. serum of healthy donors with hiChol-Liposomes (1 µM tL in well). Complement assays were performed in liposome complement buffer with 200 mM glycine addition. Negative control serum contained iaCB to a final concentration of 40 mM EDTA and pooled human serum. Positive control contained 30 mM OG and serum. λ_{Ex}=540 (25) nm and λ_{Em}=620 (40) nm, Reader-2, 37 °C, gain=85, n=2.

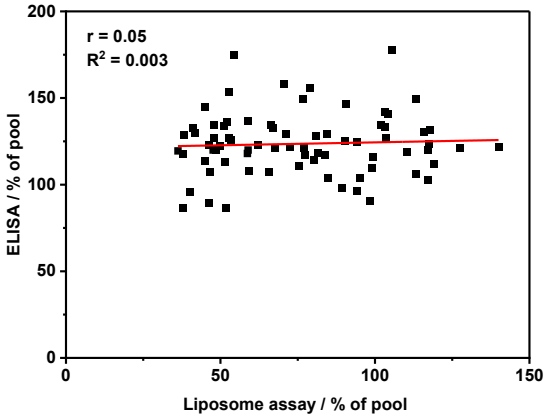

Figure S 4-16: Correlation of hiChol-Liposome complement assay to classical pathway C3b-ELISA. Correlation of healthy donor samples measured once in the hiChol-Liposome complement assay and once with the C3b-deposition ELISA triggered by immobilized antibodies (see materials and methods).

Consequently, hiChol-Liposomes were hypothesized as ideal candidates to serve as classical pathway specific readout vesicles which would facilitate the assay by reducing the assay protocol by one incubation step compared to antibody triggered liposomes. A serum titration covering the full range of complement lysis was performed to determine the two suitable serum concentrations for the high-throughput format, which should be applied in the subsequent validation of the hiChol-Liposomes on healthy human donor sera (**Figure S 4-15a**). 2 and 5 %vol. serum were selected as suitable and further confirmed by an initial screening of six donor sera together with a pooled human serum as control. These sera covered the full range of complement-mediated liposome lysis varying from below 10 to about 75 % for 2 %vol. serum and from 64 to 108 % for 5 %vol. serum (**Figure S 4-15b**). Subsequent validation on healthy human donor sera in the high-throughput format showed a broad range of activity among the tested individuals (**Figure S 4-16**). However, no correlation to a C3b-deposition ELISA based on immobilized antibodies as complement triggers could be confirmed (**Figure S 4-16**). Similar

to the Man-Liposomes it is important to note that differences between the two assay formats may influence the correlation quality, i.e. the liposome format investigates the full complement cascade activity, whereas the ELISA format only quantifies the onset of the cascade and can not provide any correlation to activities beyond the C3b stage. However, the lack of any observed correlation is expected to be attributed to more fundamental divergences between antibody- and cholesterol-triggered complement activation. Complement activation of antibodies is well characterized and based on the interaction of the antibody's Fc-fragment and the globular head region of C1q[9,10] followed by classical pathway complement activation[11]. However, the activation through high membrane cholesterol levels is less studied. It is suggested that C-reactive protein (CRP) might be involved through interaction with high cholesterol containing membrane surfaces and its ability of direct C1q binding[12,13] with subsequent classical pathway activation. Additionally, individual lipoprotein levels might as well influence the resulting liposome lysis initiated through high cholesterol content[5]. These additional factors may provide a comprehensive explanation to the discrepancies observed in the correlation of these two systems, i.e. antibody triggered C3b-deposition ELISA and hiChol-Liposome-based complement assay. Consequently, antibody triggered liposomes were chosen as more suitable material to screen the classical pathway activity due to its well investigated, widely applied and accepted approach.

4.6.4.3 Alternative pathway LPS-Liposome ELISA correlation studies

After confirming the pathway specificity of the LPS-Liposomes, also for those, a correlation study to the C3b-deposition ELISA was conducted. The determination of a suitable serum concentration range was conducted in advance through titrations of a pooled serum control under Mg^{2+}/EGTA conditions (**Figure S 4-17**). Compared to the other pathways much higher serum concentrations of 15 and 20 %vol. were selected for the subsequent donor serum screening. This was at first attributed to a missing pattern recognition element for the alternative pathway. In contrast, the classical or lectin pathway are initiated by such a trigger recognition element, i.e. C1q or MBL, ficolins or collectin respectively. Hence the alternative pathway relies on spontaneous hydrolysis of C3, which is more likely the more serum is used. However, subsequent screening of 40 donor sera revealed that many of the investigated sera did not cause liposome lysis in case of LPS modification (**Figure S 4-18**). This was surprising, since LPS is often described as alternative pathway trigger[14,15] and commonly applied in alternative pathway activity determining ELISAs[16]. Subsequent analysis and correlation to the C3b-deposition ELISA revealed that for the majority of investigated sera activities closer to the pooled control were found in the ELISA (**Figure S 4-19**). This demonstrates, that there are substantial discrepancies, particularly for those sera that did not induce alternative pathway LPS-Liposome lysis. Nevertheless, even though these noticeable differences were observed,

a Pearson's r of 0.60 suggests a correlation between the two assays (**Figure S 4-19**). This indicates that, in the event of liposome lysis, the obtained lysis level exhibited a correlation with the respective C3b levels. Similar to the correlation studies for the other two pathways, a certain level of inaccuracy has to be attributed to the two different investigated time points of the cascade, i.e. C3b compared to MAC formation. Furthermore, the here applied C3b-ELISA assay used zymosan to induce alternative pathway activation. Varying degrees of complement activation due to different trigger properties between the two assays can not be excluded. However, the significant proportion of sera that were unable to lyse the LPS-Liposomes still suggests shortcomings of the liposome-based assay. In literature it has been described that bacteria use LPS as protective barrier against complement attack via steric hinderance.[17] If this can be transferred to the here applied assay, this offers a potential explanation for the observed discrepancy in the efficacy of LPS application in both formats. LPS may efficiently activate the alternative pathway in both formats, yet the activation is only detected in the ELISA format. The reason for this is that the ELISA format focuses on the mere quantification of complement activation, often by measuring the soluble MAC complex or C3b, but in the liposome lysis-based assay the readout is compromised by ineffective complement deposition on the liposome surface, which is required for MAC assembly within the lipid bilayer and liposome lysis. However, the characteristics that differentiate the sera which were capable of inducing liposome lysis from those that were unable to do so remain unclear. According to the C3b-levels, sufficient alternative pathway complement activity should have been present for all sera to theoretically be capable to lyse the liposomes. To facilitate the deposition of complement proteins and subsequent MAC assembly in the future it is suggested to study the influence of liposome surface characteristics. It is described that the presence of amine groups and a more positive surface charge on liposomes are beneficial for alternative pathway complement activation.[18,19] However these studies must be interpreted with care since also in those no liposome lysis but C3 deposition or remaining erythrocyte hemolysis was measured. Nevertheless, the current anionic liposome characteristics and lack of potential binding sites for complement protein deposition should be investigated in systematic studies including variations in surface charge and exposed functional groups.

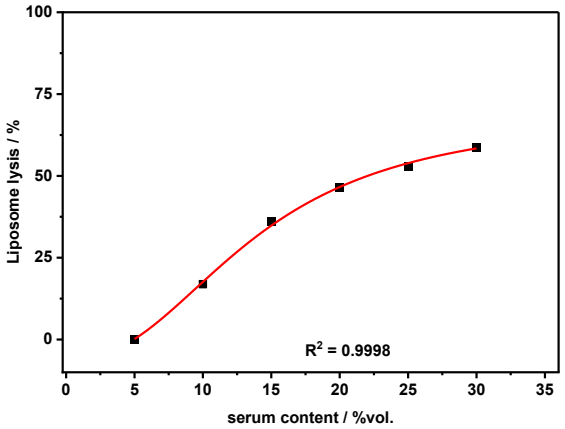

Figure S 4-17: Serum titration study using LPS-Liposomes. Pooled human serum content titration (5-30 %vol.) with LPS-Liposomes (2 %mol. LPS, 5 µM tL in well). Complement assays were performed in liposome complement buffer with 200 mM glycine addition and contained 8 mM Mg^{2+}/EGTA in well. Positive control contained 30 mM OG and serum. λ_{Ex}=540 (25) nm and λ_{Em}=620 (40) nm, Reader-2, 37 °C, gain=85, n=2.

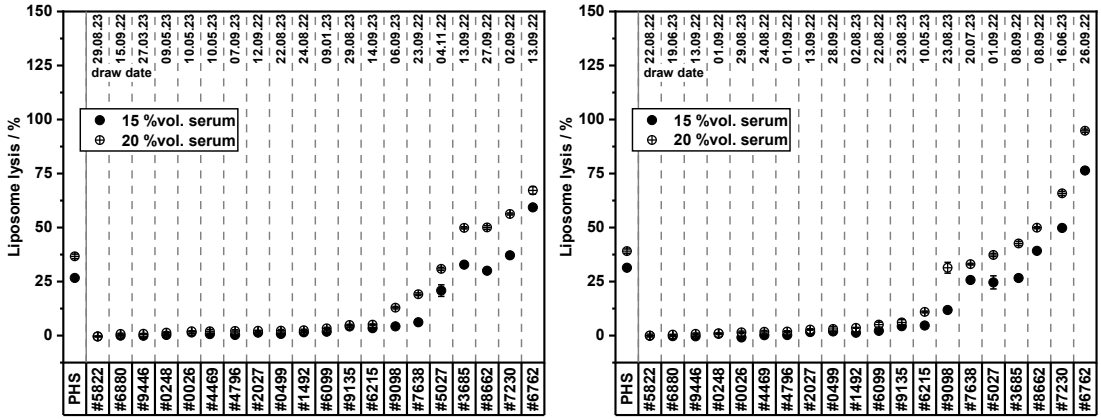

Figure S 4-18: Healthy human donor sera screening with the LPS-Liposome complement assay. Complement assays screening lysis of LPS-Liposomes (2 %mol. LPS, 5 µM tL in well) induced by healthy human donor sera and a pooled human serum (PHS) as control. Complement assays were performed in liposome complement buffer with 200 mM glycine addition and contained 8 mM Mg^{2+}/EGTA in well. Positive control contained 30 mM OG and serum. Human serum content was 15 and 20 %vol. per well λ_{Ex}=540 (25) nm and λ_{Em}=620 (40) nm, Reader-2, 37 °C, gain=85, n=2.

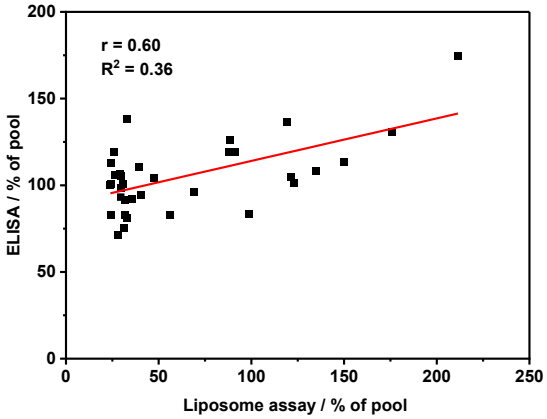

Figure S 4-19: Correlation of LPS-Liposome complement assay to classical pathway C3b-ELISA. Correlation of healthy donor samples measured once in the LPS-Liposome (2 %mol. LPS) complement assay and once with the C3b-deposition ELISA triggered by immobilized zymosan (see materials and methods).

4.6.5 References

(1) Kitamura, M.; Murakami, K.; Yamada, K.; Kawai, K.; Kunishima, M. Binding of sulforhodamine B to human serum albumin: A spectroscopic study. *Dyes Pigm* **2013**, *99*, 588–593. DOI: 10.1016/j.dyepig.2013.06.011.

(2) Hein, E.; Honoré, C.; Skjoedt, M.-O.; Munthe-Fog, L.; Hummelshøj, T.; Garred, P. Functional analysis of Ficolin-3 mediated complement activation. *PLoS One* **2010**, *5*, e15443. DOI: 10.1371/journal.pone.0015443.

(3) Fujita, T.; Matsushita, M.; Endo, Y. The lectin-complement pathway--its role in innate immunity and evolution. *Immunol Rev* **2004**, *198*, 185–202. DOI: 10.1111/j.0105-2896.2004.0123.x.

(4) Weis, W. I.; Drickamer, K.; Hendrickson, W. A. Structure of a C-type mannose-binding protein complexed with an oligosaccharide. *Nature* **1992**, *360*, 127–134. DOI: 10.1038/360127a0.

(5) Moein Moghimi, S.; Hamad, I.; Bünger, R.; Andresen, T. L.; Jørgensen, K.; Hunter, A. C.; Baranji, L.; Rosivall, L.; Szebeni, J. Activation of the human complement system by cholesterol-rich and PEGylated liposomes-modulation of cholesterol-rich liposome-mediated complement activation by elevated serum LDL and HDL levels. *J Liposome Res* **2006**, *16*, 167–174. DOI: 10.1080/08982100600848801.

(6) Noone, D. P.; Isendoorn, M. M. E.; Hamers, S. M. W. R.; Keizer, M. E.; Wulffelé, J.; van der Velden, T. T.; Dijkstra, D. J.; Trouw, L. A.; Filippov, D. V.; Sharp, T. H. Structural basis for surface activation of the classical complement cascade by the short pentraxin C-reactive protein. *PNAS* **2024**, *121*, e2404542121. DOI: 10.1073/pnas.2404542121.

(7) Samstad, E. O.; Niyonzima, N.; Nymo, S.; Aune, M. H.; Ryan, L.; Bakke, S. S.; Lappegård, K. T.; Brekke, O.-L.; Lambris, J. D.; Damås, J. K.; Latz, E.; Mollnes, T. E.; Espevik, T. Cholesterol crystals induce complement-dependent inflammasome activation and cytokine release. *The Journal of Immunology* **2014**, *192*, 2837–2845. DOI: 10.4049/jimmunol.1302484.

(8) Hoecherl, K.; Streif, S.; Spitzenberg, C.; Rink, S.; Behrent, A.; Holzhausen, F.; Griesche, C.; Rogoll, C.; Foedlmeier, M.; Gebhard, A.; Kulikowski, K.; Schaefer, N.; Pauly, D.; Baeumner, A. J. A homogeneous immunoassay technology based on liposomes and the complement system enables one-step, no-wash, rapid diagnostics directly in serum. *Anal Bioanal Chem* **2025**, *417*, 3257–3273. DOI: 10.1007/s00216-025-05882-4.

(9) Diebolder, C. A.; Beurskens, F. J.; Jong, R. N. de; Koning, R. I.; Strumane, K.; Lindorfer, M. A.; Voorhorst, M.; Ugurlar, D.; Rosati, S.; Heck, A. J. R.; van de Winkel, J. G. J.; Wilson, I. A.; Koster, A. J.; Taylor, R. P.; Saphire, E. O.; Burton, D. R.; Schuurman, J.; Gros, P.; Parren, P. W. H. I. Complement is activated by IgG hexamers assembled at the cell surface. *Science* **2014**, *343*, 1260–1263. DOI: 10.1126/science.1248943.

(10) Reid, K. B. M. Complement Component C1q: Historical Perspective of a Functionally Versatile, and Structurally Unusual, Serum Protein. *Front Immunol* **2018**, *9*, 764. DOI: 10.3389/fimmu.2018.00764.

(11) Merle, N. S.; Church, S. E.; Fremeaux-Bacchi, V.; Roumenina, L. T. Complement System Part I - Molecular Mechanisms of Activation and Regulation. *Front Immunol* **2015**, *6*, 262. DOI: 10.3389/fimmu.2015.00262.

(12) McGrath, F. D. G.; Brouwer, M. C.; Arlaud, G. J.; Daha, M. R.; Hack, C. E.; Roos, A. Evidence that complement protein C1q interacts with C-reactive protein through its globular head region. *J Immunol* **2006**, *176*, 2950–2957. DOI: 10.4049/jimmunol.176.5.2950.

(13) Richards, R. L.; Gewurz, H.; Siegel, J.; Alving, C. R. Interactions of C-Reactive Protein and Complement with Liposomes. *The Journal of Immunology* **1979**, *122*, 1185–1189. DOI: 10.4049/jimmunol.122.4.1185.

(14) Grossman, N.; Leive, L. Complement activation via the alternative pathway by purified Salmonella lipopolysaccharide is affected by its structure but not its O-antigen length. *The Journal of Immunology* **1984**, *132*, 376–385. DOI: 10.4049/jimmunol.132.1.376.

(15) Vukajlovich, S. W.; Hoffman, J.; Morrison, D. C. Activation of human serum complement by bacterial lipopolysaccharides: structural requirements for antibody independent activation of the classical and alternative pathways. *Mol Immunol* **1987**, *24*, 319–331. DOI: 10.1016/0161-5890(87)90173-8.

(16) Seelen, M. A.; Roos, A.; Wieslander, J.; Mollnes, T. E.; Sjöholm, A. G.; Wurzner, R.; Loos, M.; Tedesco, F.; Sim, R. B.; Garred, P.; Alexopoulos, E.; Turner, M. W.; Daha, M. R. Functional analysis of the classical, alternative, and MBL pathways of the complement system: standardization and validation of a simple ELISA. *J Immunol Methods* **2005**, *296*, 187–198. DOI: 10.1016/j.jim.2004.11.016.

(17) Rautemaa, R.; Meri, S. Complement-resistance mechanisms of bacteria. *Microbes and Infection* **1999**, *1*, 785–794. DOI: 10.1016/s1286-4579(99)80081-1.

(18) Chonn, A.; Cullis, P. R.; Devine, D. V. The role of surface charge in the activation of the classical and alternative pathways of complement by liposomes. *The Journal of Immunology* **1991**, *146*, 4234–4241. DOI: 10.4049/jimmunol.146.12.4234.

(19) Mold, C. Effect of membrane phospholipids on activation of the alternative complement pathway. *The Journal of Immunology* **1989**, *143*, 1663–1668. DOI: 10.4049/jimmunol.143.5.1663.

5 Feasibility Study for the Applicability of Human Plasma and Animal Sera in the Liposome-Based Complement Assay

Graphical Abstract

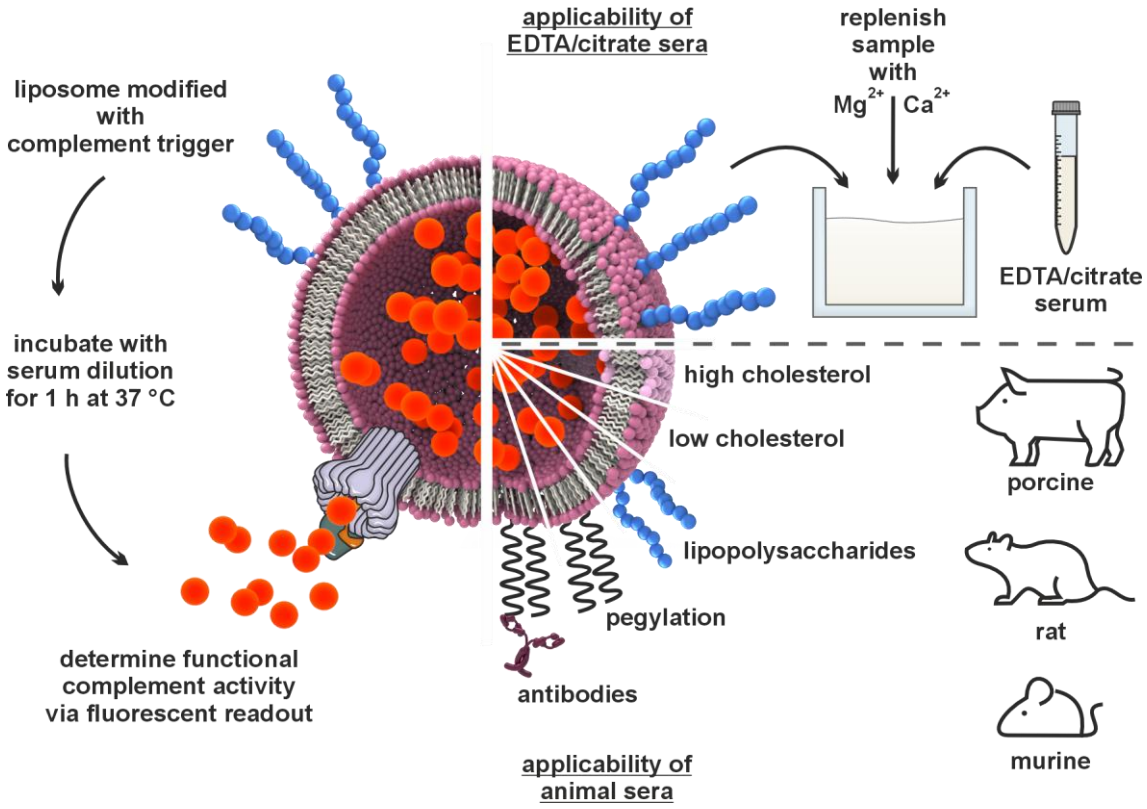

Author contributions

Most of the experimental work was solely done by the author. This chapter originated from a collaboration with Diana Pauly. Anna Gebhardt, Kilian Hoecherl, Cornelia Rogoll and Simon Streif assisted in liposome preparation. Antje J. Baeumner contributed with strategic discussions. The chapter was written by the author.

Abstract

The human complement system is essential for immunity and inflammation, helping to prevent infection by pathogens. Functional complement activity is typically assessed in complement-preserved serum, requiring strict handling to avoid unintentional premature activation. Plasma, containing anticoagulants such as EDTA or citrate, minimizes artificial activation by chelating essential calcium (Ca^{2+}) and magnesium (Mg^{2+}) ions, which, however, also prevents functional activity determination. Replenishing these ions potentially restores complement functionality. Moreover, animal models are used for mechanistic and therapeutic studies on the complement system, facing ethical constraints and limitations in replicating human physiology. It is shown here that EDTA and citrate addition to complement-preserved serum, combined with replenished bivalent ion levels directly in the assay buffer, is applicable in a liposome-based complement assay measuring functional activity, thus indicating the applicability of plasma in this assay. Furthermore, this study examines the applicability and reactivity of animal sera towards different liposome surfaces. Findings indicate that EDTA plasma, when replenished with Ca^{2+} and Mg^{2+}, better suits the assay, restoring about 90 % of control levels, compared to citrate plasma, which restored liposome lysis to about 71 % of control levels. Animal serum was generally well suited for this assay but showed expected high variability between species. Only murine serum, which exhibited no complement response, was unsuitable for the assay setup used. This study highlights the potential of using EDTA plasma for functional complement activity analysis, offering flexibility in sample matrix in diagnostic settings, and of using animal sera in this assay to reduce the number of animal model studies by allowing mechanistic studies and advancing the understanding of inter-species complement system variations.

5.1 Introduction

The complement system, initially described as complementary mechanism supporting antibodies in pathogen defense, is now recognized as a versatile and crucial part of the innate immune system.[1,2] Complement proteins, whose origins date back over 600 million years[3], represent one of the oldest innate immune systems, predating mammals[3]. The system is comprised of more than 50 components found mainly in the blood and on cell surfaces.[4,5] It plays a key role in pathogen recognition and elimination, linking innate and adaptive immunity, immune surveillance, homeostasis, and the removal of immune complexes, cellular debris, and apoptotic cells.[5,6] The complement system activates through a series of enzymatic reactions involving particle recognition, opsonization, self-amplification, generation of effector molecules (e.g., membrane-attack-complex, MAC), and induction of other immune responses[1,5]. Activation occurs via three pathways, the classical, lectin, and alternative

pathway, which converge in the terminal pathway generating approximately 10 nm wide pores in target membranes through MAC formation[5,7,8].

Liposomes are described in literature as highly versatile tool in research, diagnostics and therapy due to their self-assembled lipid bilayer structure containing an inner aqueous cavity.[9,10] The lipid bilayer is primarily composed of phospholipids, such as phosphatidylcholine, phosphatidylethanolamine, phosphatidylserine, and phosphatidylglycerol[11] allowing for flexibility in liposome characteristics such as surface charge and functionality or liposome size. Cholesterol is frequently incorporated into the mixture to influence membrane fluidity, thickness and bilayer permeability reduction.[12–14] Since the 1970s, liposomes have evolved as effective carriers for hydrophilic compounds within the aqueous cavity and hydrophobic compounds within the lipid bilayer.[15–18] In clinical settings, a range of compounds have been encapsulated, including anticancer drugs[16], antibiotics[19] and genetic materials[20]. Apart from clinically relevant molecules also molecules such as fluorescent dyes[21], electroactive species[22] or enzymes[23,24] have been incorporated for bioanalytical or biosensing applications[25,26]. Likewise, liposomes have been successfully employed in the field of complement system analysis as substitutes for animal erythrocytes to analyze the complement cascade function.[27–29]

The suggested matrix for the analysis of the complement system function is serum, since it is free of complement-inhibiting additives[30], which are typically added as anticoagulants in plasma samples. However, since complement is a temperature-sensitive system, it can be artificially activated *in vitro* through elevated temperatures, which can falsify the subsequent analysis, especially in serum.[31,32] To prevent unintentional premature complement activation, it would be advantageous to use plasma as the sample matrix, containing anticoagulants that chelate calcium (Ca^{2+}) and magnesium (Mg^{2+}) ions. Due to these anticoagulants, artificial complement activation is minimized, since the C1, MBL and ficolin complex and C3 convertase function are dependent on both Ca^{2+} and Mg^{2+} ions, minimizing complement activation early in the cascade.[5,30,33,34] However, in order to access the complement activity and function of plasma, Ca^{2+} and Mg^{2+} ions would need to be replenished into the plasma sample prior to the assay. Furthermore, not all anticoagulants that complex these bivalent ions are suited for subsequent complement analysis. For example, heparin is known for its strong interactions with numerous complement proteins and regulators apart from ion complexation.[35] These interactions affect the complement function and consequently interfere with reliable complement analysis.[34,35] However, EDTA and citrate, which are commonly used in clinical diagnostics, may be suitable candidates. Along with higher sample robustness, functional complement analysis, such as the previously developed liposome-based assay platform

applied here[28], would benefit from greater flexibility with regard to the often limited availability of appropriate samples.

Animal models, often applied in preclinical complement system research to study its role in immunity, inflammation, and disease pathogenesis,[34,36,37] allow the investigation of the complex interactions of complement proteins *in vivo*, which can be challenging to fully replicate *in vitro*. Especially murine models are widely used due to their genetic tractability and availability of knockout strains, enabling precise manipulation of complement components like C3 and Factor H.[36,38] They assist in identifying the mechanisms of complement activation, its dual roles in protection and pathology, and potential therapeutic targets. However, ethical constraints and limitations in replicating human physiology in animal models remain a challenge,[34,39] requesting alternative methods and models that more closely resemble the human complement system and are less problematic from an ethical point of view.

Here, we investigate the applicability of EDTA and citrate addition to complement-reserved serum in combination with replenished bivalent ion levels directly in the assay buffer as a measure for the applicability of plasma, as well as the applicability and the inter-species variability of animal serum (i.e. murine, rat and porcine serum) in a previously described liposome-based assay platform to examine complement activity[28]. This study should gain fundamental knowledge about the limitations of the mentioned matrices to enable a refined development of the applied liposome-based assay in further research.

5.2 Materials and Methods

5.2.1 Chemicals and Consumables

All chemicals were of analytical grade and were used without purification. Methanol, Sephadex® G-50 (G50150), lipopolysaccharides (LPS) from *Salmonella enteritidis* (L6011), cholesterol from sheep wool (C8667), tetrasodium ethylenediaminetetraacetic acid (EDTA, EDS), ethylene glycol-bis(2-aminoethyl ether)-*N*,*N*,*N*′,*N*′-tetraacetic acid (EGTA, E4378), polyclonal goat anti-biotin IgG (B3640) and sodium hydroxide were purchased from Sigma-Aldrich/Merck KGaA (Darmstadt, Germany). The extrusion kit and the phospholipids 1,2-dipalmitoyl-*sn*-glycero-3-phosphocholine (DPPC, 850355P), 1,2-dipalmitoyl-*sn*-glycero-3-phospho-(1′-*rac*-glycerol) (sodium salt) (DPPG, 840455P), 1,2-dipalmitoyl-*sn*-glycero-3-phosphoethanolamine-N-(biotinyl) (DPPE-biotin, 870285P) and 1,2-dimyristoyl-*sn*-glycero-3-phosphoethanolamine-N-[methoxy(polyethylene glycol)-2000] (ammonium salt) (DMPE-PEG2000, 880150P) were purchased from Avanti Polar Lipids (Alabaster, AL, USA). Sodium azide, magnesium dichloride hexahydrate and trisodium citrate dihydrate were purchased from Merck KGaA (Darmstadt, Germany). Sulforhodamine B (SRB, S1307) was

purchased from Thermo Fisher Scientific (Darmstadt, Germany). Chloroform and nitric acid (HNO_3, N/2185/PB15) were bought from Fisher Chemical (Schwerte, Germany). *N*-2-hydroxyethylpiperazine-*N'*-2-ethanesulfonic acid (HEPES), sodium chloride, sucrose, *N*-octyl-β-D-glucopyranoside (OG, CN23.3) and calcium chloride was bought from Carl Roth (Karlsruhe, Germany). Dialysis membrane (Spectra/Por® 4 with a MWCO of 12 - 14 kDa) was purchased from Spectrum Laboratories and polycarbonate Whatman Nucleopore™ Track-Etched membranes with a pore size of 1.0 µm, 0.4 µm or 0.2 µm (each Ø19 mm) were bought from VWR (Darmstadt, Germany). 1,2- dimyristoyl-*sn*-glycero-3-phosphoethanolamine-N-[biotinyl(polyethylene glycol)-2000] (DMPE-PEG2000-biotin, PG2-BNDM-2k) was purchase from Nanocs Inc. (New York, USA). The ICP phosphorus standard solution (10882.0000) was purchased from Bernd Kraft/AnalytiChem GmbH (Duisburg, Germany). Black 96-well flat bottom microtiter plates (MTP, 781608) were purchased from Brand (Wertheim, Germany). Pooled human (ISCER), mouse CD1 (IGMSCD1CSER), porcine (IGPCCSER), rat Sprague Dawley (IGRTSDCSER), rat Wistar (IGRTWICSER) and rat Wistar Hannover (IGRTWHCSER) complement serum was purchased from Innovative Research (Novi, Michigan, USA).

5.2.2 Liposome preparation

Liposome preparation was performed as described earlier[28] using the reverse-phase evaporation method. Standard lipids contained in the anionic liposome composition were cholesterol, DPPC, DPPG and DPPE-biotin. Depending on the respective liposome batch, LPS from *Salmonella enteritidis*, the pegylated lipids DMPE-PEG2000 and DMPE-PEG2000-biotin as well as varying lipid ratios were applied in the lipid mixture. For LPS, an estimated molecular weight of 15000 $g \cdot mol^{-1}$ was used for calculations. The exact liposome compositions are listed in **Table S 5-1**.

60 µmol of the desired lipids were dissolved in chloroform (3 mL) and methanol (0.5 mL). After sonication at 60 °C for 1 min, 2 mL of a preheated sulforhodamine B (SRB) solution was added as encapsulant (10 mM SRB, 210 mM NaCl, dissolved in 20 mM HEPES, pH 7.5, 60 °C). The mixture was sonicated again at 60 °C for 4 min. The organic solvents were removed with a rotary evaporator (LABOROTA 4001, Heidolph, Germany) at 60 °C with stepwise reduced pressure from 900 to 780 mbar within 40 min (900 mbar for 10 min, 850 mbar for 5 min, 800 mbar for 5 min, 780 mbar for 20 min). The solution was vortexed for 30 s, and another 2 mL of the encapsulant was added. After a second vortexing step for 30 s, the solution was further rotated at 60 °C with stepwise reducing pressure starting from 750 to 400 mbar within 60 min (750 mbar for 20 min, 600 mbar for 5 min, 500 mbar for 5 min, 400 mbar for 20 min). The solution was then extruded through polycarbonate membranes with varying membrane pore sizes (1 µm, 0.4 µm or 0.2 µm). Extrusion was done at 65 °C by forcing the mixture in the

syringes 21 times through each membrane pore size. Excess of encapsulant (i.e. SRB and NaCl) was removed by size exclusion chromatography with a Sephadex G-50 column, followed by dialysis against HSS buffer (10 mM HEPES, 200 mM NaCl, 200 mM sucrose, 0.01 % NaN_3, pH 7.5). Liposomes were stored at 4 °C. The smallest membrane pore size during extrusion is mentioned in **Table S 5-1** for each liposome synthesis.

5.2.3 Liposome characterization

Size and polydispersity index (PDI) measurements via dynamic light scattering (DLS) as well as zeta potential measurements via electrophoretic light scattering (ELS) were performed on a Malvern Panalytical Zetasizer Nano-ZS. Polymethyl methacrylate semi-micro cuvettes (Brand, Germany) were used for size and PDI determination, and disposable folded capillary cells (Malvern Panalytical, Germany) were used for zeta potential determination. The measurement temperature was set to 25 °C with a 1/100 sample dilution in HSS buffer in both cases. Measurements of size and PDI were conducted with a dispersant refractive index n_D^{20} of 1.34, a material absorbance of zero, a dispersant viscosity η of 1.1185 mPa s, an angle of 173° and in backscattering mode after equilibration for 15 s in three measurement runs, each with 13 single measurements. For zeta potential, a dielectric constant ε of 78.5 was used with an equilibration time of 60 s before the start of four measurement runs, each with 20 single measurements.

Phospholipid concentrations were determined via optical emission spectroscopy with inductively coupled plasma (ICP-OES, SpectroBlue TI/EOP) from SPECTRO Analytical Instruments GmbH (Kleve, Germany). Liposome solutions were diluted 1/150 with a total volume of 3 mL in 0.5 M HNO_3. A phosphorus standard diluted in 0.5 M HNO_3 from 1 to 100 µM was used for calibration of the device. Phosphorus was detected at a wavelength of 177.495 nm. Before each measurement, 0 µM and 100 µM phosphorus standard dilutions were used to recalibrate the device. The total lipid concentration (tL) was calculated from the phospholipid concentration and the lipid composition used during synthesis.

5.2.4 Homogeneous liposome-based complement assay

5.2.4.1 EDTA and citrate studies

The liposome-based complement assays containing EDTA and citrate were performed mostly following a previously established protocol.[25] Each assay contained a) a sample with liposomes in liposome complement buffer (LCB, 10 mM HEPES, 150 mM NaCl, 135 nM $CaCl_2$, and 1 mM $MgCl_2$ in double distilled H_2O, pH 7.4 prepared according to the HBS buffer of Zelek et al.[51], negative control), b) a sample with liposomes in active serum or in EDTA- or citrate-containing serum and c) a sample with lysed liposomes by detergent addition (positive control), all prepared in LCB. Serum was inhibited by EDTA or citrate addition to complex free Ca^{2+} and

Mg^{2+} ions essential for the functionality of the complement system. Detergent positive controls contained 30 mM OG and serum in the final well. The final wells contained a volume of 100 µL, 10 µM tL liposomes and 200 mM sucrose to ensure liposome stability. Final EDTA and citrate levels per well are stated in each respective experiment but were always added as a 10x stock solution, resulting in a 1/10 dilution in the final well. The serum content was 10 %vol. in the respective wells. All samples were prepared in triplicate. Spiking of respective Ca^{2+} and Mg^{2+} levels were performed with spike-LCB containing elevated Mg^{2+} or Ca^{2+} levels and diluted 1/10 in the final well to reach the required bivalent ion levels calculated as follows:

$$c(Mg^{2+})_{final\ well} = 0.8\ mM\ {Mg^{2+}}_{LCB} + 0.1\ mM\ {Mg^{2+}}_{serum} + \frac{x}{10} mM\ {Mg^{2+}}_{spike\text{-}LCB}$$

For the calcium levels, the 135 nM content from normal LCB is neglected over the much higher concentrations added through serum or the spike-LCB buffer and calculated as follows:

$$c(Ca^{2+})_{final\ well} = 0\ mM\ {Ca^{2+}}_{LCB} + 0.25\ mM\ {Ca^{2+}}_{serum} + \frac{x}{10} mM\ {Ca^{2+}}_{spike\text{-}LCB}$$

Liposomes were prediluted in LCB to a concentration of 100 µM tL. Black 96-well flat bottom microtiter plates were prepared on ice with LCB, spike-LCB wherever necessary and stock solutions of sucrose (1 M sucrose in LCB), EDTA, citrate and OG (300 mM OG in double distilled H_2O) added to the respective wells to reach the desired conditions. Liposomes were added, resulting in a 1/10 dilution in the final well. As the last step, serum was added before incubation at 37 °C for 60 min and fluorescence intensity measurements with a SYNERGY neo2 multi-mode reader from BioTek (Bad Friedrichshall, Germany) (λ_{Ex} = 565 nm and λ_{Em} = 585 nm with bandwidth 5 and gain 150). For each measurement, the plate was read three consecutive times to relativize the influence of the instrument on the signal.

For data evaluation, means and standard deviations were calculated for all samples. Each sample signal intensity after 6 min was subtracted as background, accounting for the background fluorescence signal of intact liposomes. Resulting intensities were normalized to detergent-containing positive controls at the 60 min time point. In all cases, Gaussian error propagation was used to determine the normalized standard deviations. Negative endpoint values between 0 and -10 % after background correction and normalization were set to 0 %.

5.2.4.2 Animal sera studies

Studies on animal sera were performed following the same protocol as the studies on EDTA- and citrate-containing sera, with some adjustments. Apart from the buffer control, active serum and detergent control samples, an inactivated serum sample (negative control) containing 1/10 diluted inactivation buffer (iaCB, 200 mM EDTA and 0.5 µM EGTA, diluted in LCB, pH 7.5 – 8)

was measured. Final inactivated serum wells contained 20 mM EDTA and 0.05 µM EGTA. The serum content was 10 or 25 %vol. in the respective wells, as indicated.

Liposomes were prediluted in LCB to a concentration of 100 µM tL. In case antibodies were used as complement triggers, polyclonal goat anti-biotin antibodies (1.0 mg mL^{-1}) were incubated for 1 hour at RT with the liposome stock solution prior to dilution to 100 µM tL with LCB. Black 96-well flat bottom microtiter plates were prepared on ice with LCB and, sucrose (1 M sucrose in LCB), iaCB and OG (300 mM OG in double distilled H_2O) stock solution additions to the respective wells to reach the desired conditions. Liposomes were added, resulting in a 1/10 dilution in the final well. Measurement conditions and data processing followed the previously described methods for the studies on EDTA- and citrate-containing sera.

5.3 Results and Discussion

5.3.1 EDTA and citrate titration in serum

The investigation on the feasibility of plasma application in the liposome-based complement assay was initiated by studying the effect of the commonly used anticoagulants EDTA and citrate on complement activation. Hence, both EDTA and citrate were titrated in the liposome-based complement assay within a concentration range that covered the typical levels of EDTA and citrate found in standard plasma collection tubes used in clinics. If the collection tubes are filled according to the manufacturer's instructions, EDTA levels of around 1.6 to 1.8 mg/mL should be reached.[40,41] Since most manufacturers do not specify which exact salt of K_2EDTA or K_3EDTA is used in their products, i.e. whether hydrated or not, pure EDTA with a molecular weight of 292.24 g/mol was used for concentration calculations. This overestimates the EDTA concentrations to about 5.5 to 6.2 mM EDTA compared to the real values in the collection tubes. Nevertheless, for investigations on the complement system, EDTA concentrations above 10 mM are advised in literature.[42] In these feasibility studies, serum instead of actual plasma was used to investigate the effects of the anticoagulants on complement activation, eliminating interference with the coagulation system. Hence, the effect of EDTA on diluted serum (10 %vol.) was investigated at concentrations of up to 3.2 mM EDTA, which corresponds to 32 mM EDTA in pure serum and is well above the suggested 10 mM. Citrate concentrations in plasma are about 106-109 mM when filled with blood according to the manufacturer's specifications. Hence, a concentration range up to 64 mM in diluted serum (10 %vol.), which corresponds to 640 mM in pure serum, was investigated. To probe general complement activation, anionic liposomes were utilized with lipopolysaccharides (LPS) as surface modification, which has been demonstrated to trigger both the classical and the alternative pathway.[43] The employed liposomes had an average diameter of 168 ± 4 nm and

a PDI of 0.17 ± 0.02, indicating a narrow size distribution. The negative zeta potential of LPS-containing liposomes of -6.7 ± 0.7 mV was higher than the zeta potential of comparable liposomes without LPS, which was between -16 and -20 mV (**Table S 5-1**). This indicates the successful incorporation of LPS into the lipid bilayer. LPS subsequently shields the anionic, less bulky lipids, resulting in a less negatively charged surface exposed to the surroundings.

For citrate, the theoretical plasma condition in commercially available tubes corresponding to 10 mM citrate in 10 %vol. serum showed a final lysis value of 22 % (**Figure 5-1, a**). This is drastically below the lysis obtained without complement inhibition of 82 %, but above complete inhibition, which was reached at the investigated concentrations of 16 mM citrate and higher. For EDTA, the sample containing 0.55 mM EDTA in 10 %vol. serum, which corresponds to the theoretical plasma condition in commercially available tubes, showed 63 % lysis in comparison to 74 % without inhibitor (**Figure 5-1, b**). Full inhibition was reached at the investigated EDTA concentrations of 1.6 mM and higher. This corresponds to an EDTA concentration of 16 mM in pure serum or plasma, which is in accordance with the EDTA concentration of at least 10 mM suggested in literature.[42]

It should be noted that samples containing 32 mM citrate and higher are prone to elevated background signals (**Figure 5-1, ai**), which indicates liposome destabilization. Such high citrate concentrations should not be used in this assay, but are also practically not relevant, as full inhibition is already reached at 16 mM citrate in dilute serum (10 %vol.), corresponding to 160 mM citrate in pure serum.

Overall, these data suggest that in both cases, citrate and EDTA, the commercially available plasma collection tubes are not sufficient to fully inhibit complement activation. To reduce the risk of early *in vitro* complement activation before complement analysis, it is advisable to handle plasma samples collected in commercial collection tubes with care, i.e. similar to complement-preserved serum samples. Furthermore, either the EDTA or citrate content of the commercial collection tubes should be supplemented, or the collection tubes should not be filled completely to reach higher inhibitor concentrations.

Nevertheless, if samples are collected using these collection tubes, filled completely and handled with care, a qualitative complement activity analysis can still be performed directly, although the complement activity will be lower compared to serum samples that do not contain inhibitors. Based on these data, EDTA plasma could be used to qualitatively determine severe complement activity loss due to overconsumption or deficiencies. However, to obtain more reliable results, replenishing the samples with Mg^{2+} and Ca^{2+} was tested to investigate how

much activity can be recovered from previously inhibited samples, allowing for more accurate complement activity determination.

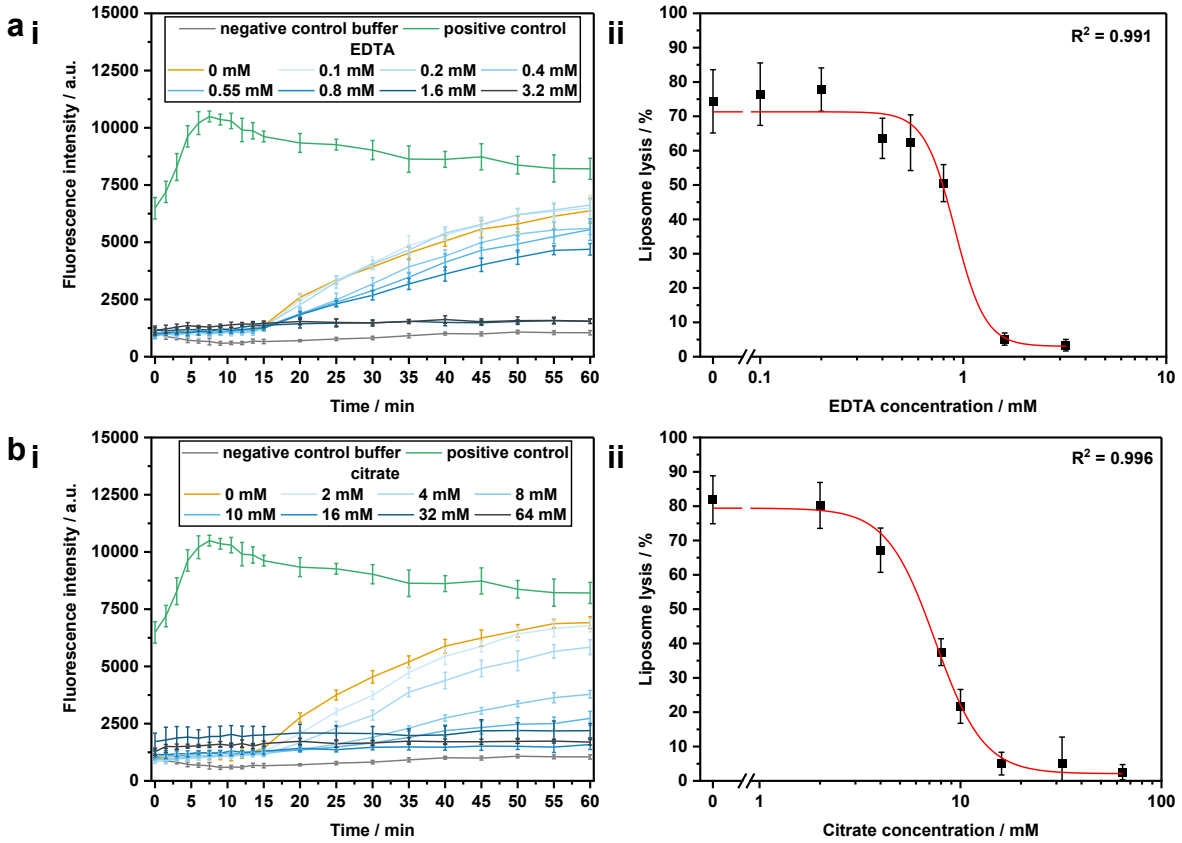

Figure 5-1: EDTA and citrate titration. Complement assays investigating the LPS-Liposome (1 %mol. LPS, 10 µM tL) with varying concentrations of **a**, EDTA or **b**, citrate inactivation. **i** shows the time-resolved fluorescence intensity values, **ii** shows the background-corrected and normalized endpoint values. Complement assays were performed in LCB. Serum content was 10 %vol. per well. λ_{Ex}=565 (5) nm and λ_{Em}=585 (5) nm, 37 °C, gain=150, n=3.

5.3.2 Replenishing EDTA and citrate serum samples with Mg^{2+} and Ca^{2+}

Plasma or serum magnesium levels are usually expected to be around 0.8 to 1.0 mM Mg^{2+} in healthy adults,[44,45] while serum calcium levels are expected to be in the range of 2.2 to 2.7 mM.[46] Here, the concentrations in the assay were calculated assuming Mg^{2+} and Ca^{2+} concentrations of 1 mM and 2.5 mM, respectively. Based on a total volume of 100 µL per well, with each well containing 80 µL of LCB (with 1 mM Mg^{2+} and 135 nM Ca^{2+}), 10 µL of serum (for 10 %vol.) and 10 µL of spike-LCB buffer (for Mg^{2+} and Ca^{2+} level adjustments), the Mg^{2+} levels were calculated as follows:

$$c(Mg^{2+})_{final\ well} = 0.8\,mM\ Mg^{2+}{}_{LCB} + 0.1\,mM\ Mg^{2+}{}_{serum} + \frac{x}{10} mM\ Mg^{2+}{}_{spike\ LCB}$$

Given the much higher amounts of calcium added through serum or spike-LCB, the contribution to the calcium concentration by the amount of calcium in normal LCB (135 nM) is neglected, and the calcium levels are calculated as follows:

$$c(Ca^{2+})_{final\ well} = 0\ mM\ Ca^{2+}{}_{LCB} + 0.25\ mM\ Ca^{2+}{}_{serum} + \frac{x}{10} mM\ Ca^{2+}{}_{spike\ LCB}$$

The EDTA and citrate content was maintained at the levels found in plasma collection tubes, i.e. 0.55 mM EDTA or 10 mM citrate for 10 %vol. serum. Since complete inhibition is not achieved under these conditions, the potentially enhancing and reducing effects of replenished Mg^{2+} and Ca^{2+} levels on complement activity were investigated.

In a first step, Mg^{2+} was titrated from 1.0 to 4.2 mM for EDTA containing serum samples (**Figure 5-2**) and from 1 to 52.2 mM for citrate containing serum samples (**Figure 5-3**). In the case of EDTA, a slight increase in liposome lysis was observed with increasing Mg^{2+} content up to 1.4 mM Mg^{2+} (**Figure 5-2**). At this point, the highest level of liposome lysis was restored compared to the control sample (71 vs. 81 % lysis). Higher Mg^{2+} concentrations again resulted in lower lysis values, down to 58 %. Interestingly, not only was the endpoint lysis value influenced by the Mg^{2+} concentration, but also the lysis kinetics of the liposomes (**Figure 5-2, a**). While Mg^{2+} concentrations up to 1.4 mM primarily affected the endpoint lysis value, with the course of the lysis curve remaining almost the same, higher concentrations, especially 2.6 and 4.2 mM Mg^{2+}, influenced the lysis kinetics. Here, an increasing Mg^{2+} content resulted in a steeper and earlier onset of lysis. This was followed by a flattening of the lysis curve's slope over the examined time, resulting in overall lower lysis values at the end compared to the lysis achieved with 1.4 mM Mg^{2+}. 1.4 mM Mg^{2+} was therefore chosen for the subsequent titration of Ca^{2+} levels of the serum for recalcification.

Similar trends were observed in citrate containing samples with 10 mM citrate. Increasing Mg^{2+} concentrations up to 7.4 or 13.8 mM caused the overall liposome lysis levels to rise (**Figure 5-3**). Both Mg^{2+} concentrations yielded a similar endpoint lysis value (44 %), with 13.8 mM Mg^{2+} also already altering the lysis kinetics with an earlier and steeper onset of the lysis curve (**Figure 5-3, a**). Even higher Mg^{2+} concentrations of 26.6 mM or even 52.2 mM Mg^{2+}, showed this effect more drastically. However, it is questionable whether the obtained liposome lysis under these conditions is complement-related, as the lysis kinetics do not align with those of the typically observed complement-mediated reaction. In literature, it is described that high bivalent ion concentrations (Mg^{2+} or Ca^{2+}) promote anionic liposome destabilization in the form of aggregation or fusion and subsequent leakage of their encapsulant.[47–49] Consequently, too high bivalent ion concentrations at which the lysis curve is characterized by this early and steep onset should be avoided. Therefore, 7.8 mM Mg^{2+} was chosen as condition to investigate additional recalcification of the serum containing 10 mM citrate.

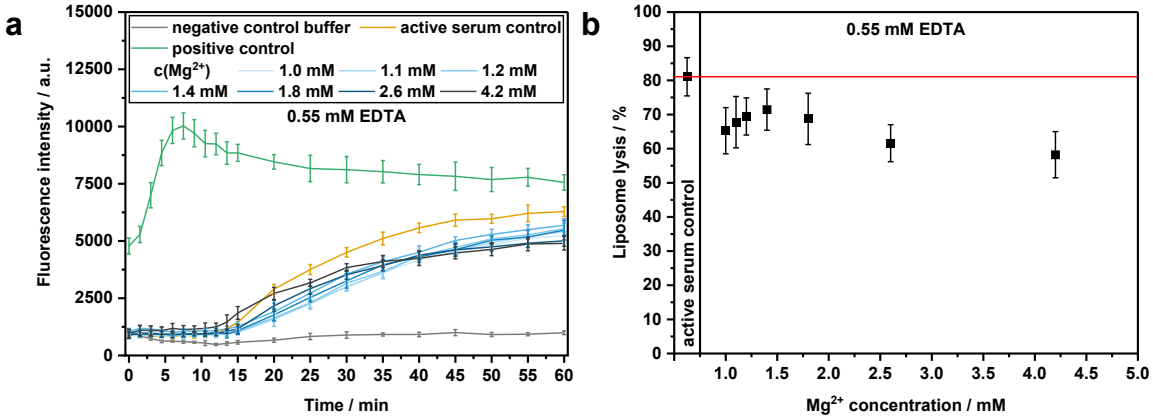

Figure 5-2: Mg^{2+} titration in EDTA serum. Complement assays investigating the LPS-Liposome (1 %mol. LPS, 10 µM tL) with varying concentrations of Mg^{2+} in 0.55 mM EDTA serum. **a** shows the time-resolved fluorescence intensity values, **b** shows the background-corrected and normalized endpoint values. Complement assays were performed in LCB. Serum content was 10 %vol. per well. λ_{Ex}=565 (5) nm and λ_{Em}=585 (5) nm, 37 °C, gain=150, n=3.

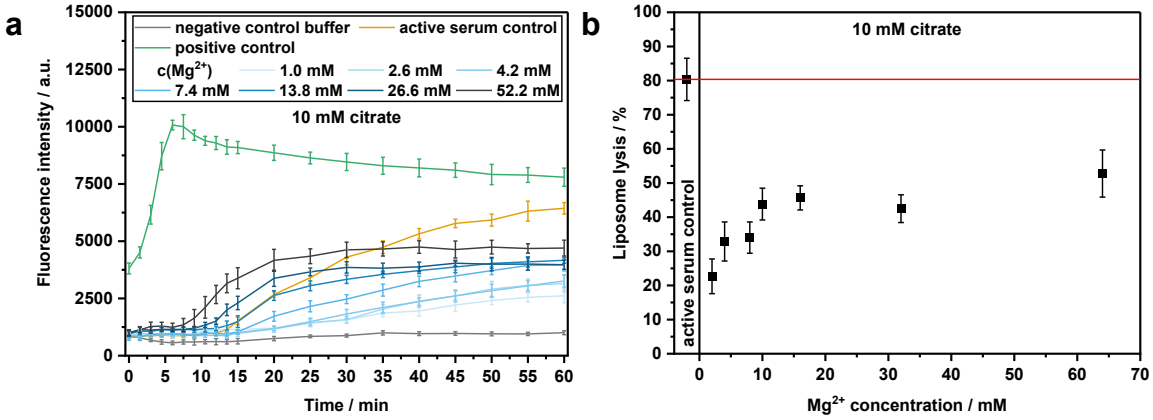

Figure 5-3: Mg^{2+} titration in citrate serum. Complement assays investigating the LPS-Liposome (1 %mol. LPS, 10 µM tL) with varying concentrations of Mg^{2+} in 10 mM citrate serum. **a** shows the time-resolved fluorescence intensity values, **b** shows the background-corrected and normalized endpoint values. Complement assays were performed in LCB. Serum content was 10 %vol. per well. λ_{Ex}=565 (5) nm and λ_{Em}=585 (5) nm, 37 °C, gain=150, n=3.

Recalcification of EDTA serum (0.55 mM EDTA), with increasing calcium content and a constant magnesium content of 1.4 mM Mg^{2+}, again increased liposome lysis until an optimum was reached at 0.65 mM Ca^{2+} (0.4 mM from buffer, 0.25 mM from 10% serum), showing the highest lysis value of 72 % (**Figure 5-4**). As with the previous study, the higher the Ca^{2+} concentration above this optimum, the more pronounced the effect of the early onset of the lysis curve becomes, which should be avoided. An additional, refined titration of the Mg^{2+} content (1.0 - 1.7 mM in 0.1 mM steps) subsequent to the Ca^{2+} optimization did not lead to further improvements, since the maximum endpoint lysis value remained the same between 1.4 and 1.6 mM Mg^{2+} (**Figure S 5-1**). Therefore, to avoid too high bivalent ion concentrations, the ideal conditions in the well for 10 %vol. serum were determined to be 0.65 mM Ca^{2+} and 1.4 mM Mg^{2+}. Under these conditions, about 90 % of the liposome lysis obtained for the control without EDTA addition could be recovered. The well concentrations of 1.4 mM Mg^{2+} and 0.65 mM Ca^{2+} for 10 %vol. serum can be translated into buffer concentrations of 1.44 mM Mg^{2+}

and 0.44 mM Ca^{2+} for a buffer that can be applied in a simplified setup of the liposome-based complement assay, assuming that 90 %vol. of the wells are filled with this buffer containing the liposomes and 10 %vol. with 0.55 mM EDTA serum or potentially plasma. Together with the previously made estimation that 10 %vol. serum or plasma contains 0.1 mM Mg^{2+} and 0.25 mM Ca^{2+}, the optimized Mg^{2+} and Ca^{2+} levels will be reached with this buffer.

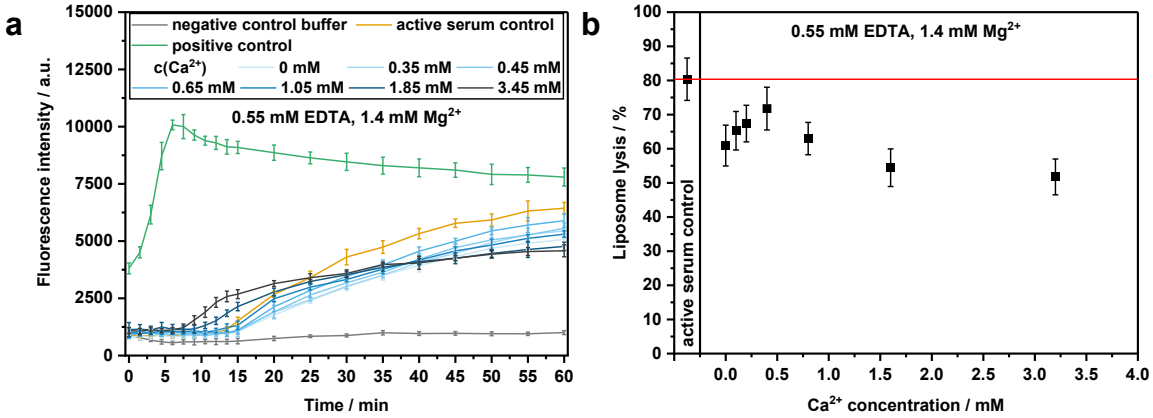

Figure 5-4: Ca^{2+} titration in EDTA serum. Complement assays investigating the LPS-Liposome (1 %mol. LPS, 10 µM tL) with varying concentrations of Ca^{2+} in EDTA serum with previously optimized Mg^{2+} levels (0.55 mM EDTA, 1.4 mM Mg^{2+}). **a** shows the time-resolved fluorescence intensity values, **b** shows the background-corrected and normalized endpoint values. Complement assays were performed in LCB. Serum content was 10 %vol. per well. λ_{Ex}=565 (5) nm and λ_{Em}=585 (5) nm, 37 °C, gain=150, n=3.

Recalcification of citrate serum (10 mM) with increasing calcium content and a constant magnesium content of 7.4 mM Mg^{2+} showed a similar trend of rising liposome lysis with increasing Ca^{2+} content, reaching up to 47 % lysis at 1.85 mM Ca^{2+} in the well (**Figure 5-5**). However, this represents a weak recovery of the original complement activity when compared to the control sample without citrate addition with 65 % lysis. In addition, more refined optimization of the Mg^{2+} content did not result in a further increase in liposome lysis (**Figure S 5-2**). These investigated conditions also showed the early onset of lysis compared to the control sample, which again could indicate that the overall bivalent ion concentrations were too high. Consequently, the reverse approach of optimizing the Ca^{2+} concentration prior to the Mg^{2+} concentration was examined to investigate whether higher complement-induced liposome lysis recovery can be achieved without the early onset of lysis for citrate containing sera. Indeed, this approach already yielded higher lysis values of 55 % after adjusting the Ca^{2+} levels to 2.25 mM in the well (**Figure 5-6**), compared to the previous optimal conditions with 47 % lysis. Subsequent titration of Mg^{2+} did not notably improve the liposome lysis value further (**Figure 5-7**), suggesting that the best conditions were 2.25 mM Ca^{2+} and 4.2 mM Mg^{2+}. Compared to the previously determined concentrations of 1.85 mM Ca^{2+} and 7.4 mM Mg^{2+}, on the one hand, lysis was slightly improved from 47 % to 55 %, while on the other hand the phenomenon of early onset of lysis with reduced endpoint lysis was avoided. However,

compared to EDTA serum, only about 71 % of the control signal could be restored by replenishing the bivalent ions.

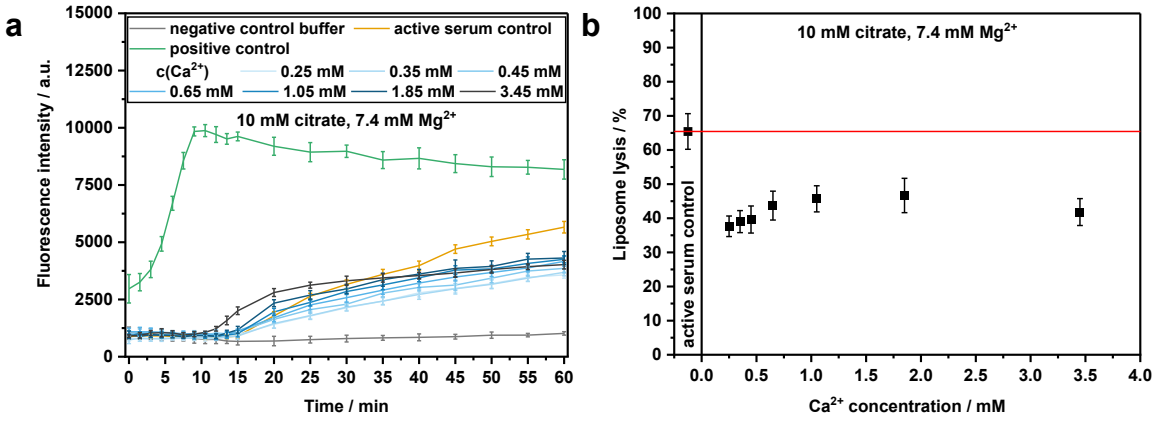

Figure 5-5: Ca^{2+} titration in citrate serum. Complement assays investigating the LPS-Liposome (1 %mol. LPS, 10 µM tL) with varying concentrations of Ca^{2+} in citrate serum with previously optimized Mg^{2+} levels (10 mM citrate, 7.4 mM Mg^{2+}). **a** shows the time-resolved fluorescence intensity values, **b** shows the background-corrected and normalized endpoint values. Complement assays were performed in LCB. Serum content was 10 %vol. per well. λ_{Ex}=565 (5) nm and λ_{Em}=585 (5) nm, 37 °C, gain=150, n=3.

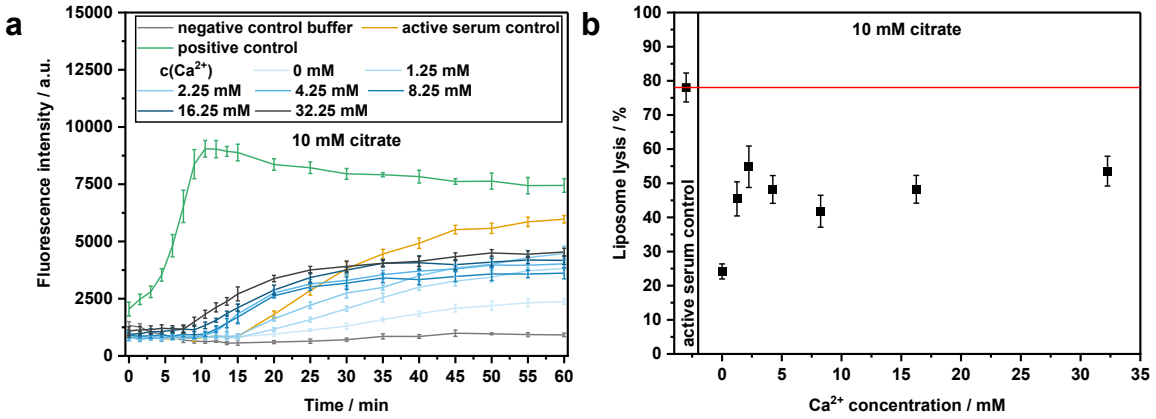

Figure 5-6: Ca^{2+} titration in citrate serum without previous Mg^{2+} optimization. Complement assays investigating the LPS-Liposome (1 %mol. LPS, 10 µM tL) with varying concentrations of Ca^{2+} in citrate serum without previous Mg^{2+} optimization (10 mM citrate, 1 mM Mg^{2+}). **a** shows the time-resolved fluorescence intensity values, **b** shows the background-corrected and normalized endpoint values. Complement assays were performed in LCB. Serum content was 10 %vol. per well. λ_{Ex}=565 (5) nm and λ_{Em}=585 (5) nm, 37 °C, gain=150, n=3.

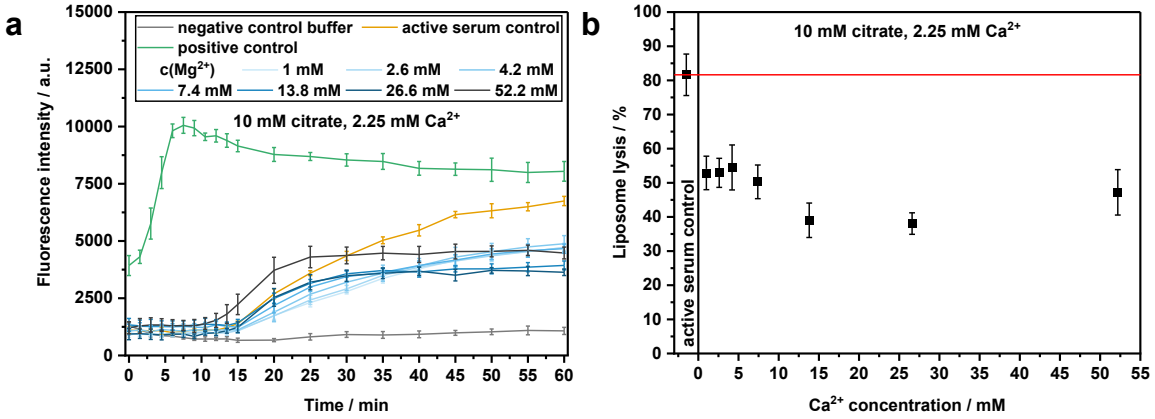

Figure 5-7: Mg^{2+} titration in citrate serum after Ca^{2+} optimization. Complement assays investigating the LPS-Liposome (1 %mol. LPS, 10 µM tL) with varying concentrations of Mg^{2+} in citrate serum with previous Ca^{2+} optimization (10 mM citrate, 2.25 mM Ca^{2+}). **a** shows the time-resolved fluorescence intensity values, **b** shows the background-corrected and normalized endpoint values. Complement assays were performed in LCB. Serum content was 10 %vol. per well. λ_{Ex}=565 (5) nm and λ_{Em}=585 (5) nm, 37 °C, gain=150, n=3.

5.3.3 Applicability of Animal Sera in the Liposome-based Complement Assay

The applicability of mouse, pig and rat complement preserved sera in the liposome-based complement assay was tested with a variety of liposomes, including anionic liposomes with varying cholesterol content as well as with LPS, polyethylene glycol (PEG) and antibody modification. All prepared liposomes were in a size range of 128 to 288 nm, with PDI values between 0.11 and 0.22 and a zeta potential range of 0 to -20 mV, with pegylated liposomes showing significantly higher zeta potential values due to the uncharged PEG-chains shielding the anionic liposome surface (**Table S 5-1**).

Mouse serum was tested with high (42 %mol.) and low (5 %mol.) cholesterol liposomes, as well as 1 %mol. LPS-containing liposomes with 10 and 25 %vol. serum (**Figure 5-8**). In all cases, the liposomes remained intact, even at the highest serum content of 25 %vol.. Only the signal observed for the LPS-Liposomes tested at 25 %vol. serum may indicate minor complement-induced lysis in the time-resolved graph from about 20 to 40 min, finally reaching the same signal intensity as the inactivated serum control (**Figure 5-8**). In literature, it is described that mouse complement activity titers in hemolytic CH50 assays are significantly lower compared to human serum, and hence, mouse complement is difficult to assay.[50,51] Consequently, the absence of complement-induced liposome lysis in this assay can most likely be attributed to low murine complement lysis activity and not to incompatibility with a liposome-based complement assay.

Porcine serum, on the other hand, showed complement-mediated lysis for all investigated liposomes at 10 %vol. serum (high and low cholesterol liposomes as well as 1 %mol. LPS containing liposomes, **Figure 5-9**). Interestingly, low cholesterol liposomes were lysed to a remarkable extent, which was even higher than that of high cholesterol liposomes. This was contrary to the reaction observed for the human complement system on liposomes

encapsulating SRB, where low cholesterol liposomes showed stealth (i.e. complement-stable) behavior and higher cholesterol contents induced significant complement-mediated lysis (**Figure 3-6**).

Refined studies on liposomes to investigate the influence of cholesterol on the liposome lysis in porcine serum were performed with pegylated liposomes with varying cholesterol levels (5, 10, 15, 20, 25, 30, 45 %mol.). These showed a dose-dependent lysis depending on the cholesterol level (**Figure 5-10**). In contrast to the previous results (**Figure 5-9**), complement-induced liposome lysis increased from 5 %mol. cholesterol, at which the liposomes exhibited stealth behavior, to a maximum of 65 % lysis at 20 %mol. cholesterol. Cholesterol contents above 20 %mol. again caused a reduction in lysis down to 38 % lysis for liposomes with 30 %mol. cholesterol. Discrepancies between these data (**Figure 5-10**) and the previous data (**Figure 5-9**) can most likely be attributed to the pegylation of the liposomes, which shields the liposome surface and thereby influences the surface characteristics and accessibility for complement proteins compared to liposomes without pegylation. Nevertheless, the cholesterol content of the liposomal lipid bilayer clearly has a significant impact on how the porcine complement system reacts towards these liposomes. Furthermore, it is evident that the porcine complement system responds distinctly to specific lipid bilayer modifications, which differ from those observed for the human complement system.

For rat serum, three species of laboratory rats (Sprague Dawley, Wistar and Wistar Hannover) were investigated to examine not only the reactivity of rat complement compared to the other animals and humans, but also to observe variations among the species. Apart from the high and low cholesterol liposomes and the 1 %mol. LPS-containing liposomes, low cholesterol pegylated liposomes with and without antibody modification as trigger were also investigated (**Figure 5-11**). For all three rat species, a similar response to the varying liposome characteristics was obtained. Liposomes with a low cholesterol content of 5 %mol. caused significant lysis of 49-56 %, which is contrary to human serum but similar to porcine serum. The high cholesterol content of 42 %mol. caused lysis values of 65-70 % across all rat species, which is slightly higher compared to the low cholesterol liposome versions. It can thus be concluded that, while the cholesterol content has an influence on the activation of the complement system of rats, this influence is less pronounced than that observed for the human complement system. Liposome modification with LPS resulted in lysis values of 70-79 %, depending on the species of rat from which the serum was derived. Since the bare 5 mol% cholesterol liposomes (i.e. without LPS) showed stealth behavior in human serum and already caused liposome lysis values of 49-56 % in rat serum, additional LPS modification of the liposomes increased the lysis by about 46 %. In order to obtain a more precise understanding

of the extent to which LPS induces liposome lysis in rat sera, a liposome composition that exhibits stealth behavior as a control and subsequent LPS modification would be necessary. Similar to the results obtained with porcine serum, including pegylated lipids in the lipid composition causes the liposomes to remain stealth in rat serum. Only upon liposome modification with 0.2 %mol. of an anti-biotin antibody as external complement trigger, which was directed against the biotin-PEG-lipid contained in the lipid composition, liposome lysis values of 51-58 % were obtained across all rat species. The three rat sera from different species varied only slightly in their lysis values by a few percent, but overall showed the same trend. This indicates that variations in complement activity among pooled sera obtained from different rat species may be low. For a more sophisticated answer, higher numbers of rat species would need to be screened. Overall, these data suggest that animal sera can show very different responses towards liposome surface modifications compared to human serum and among each other.

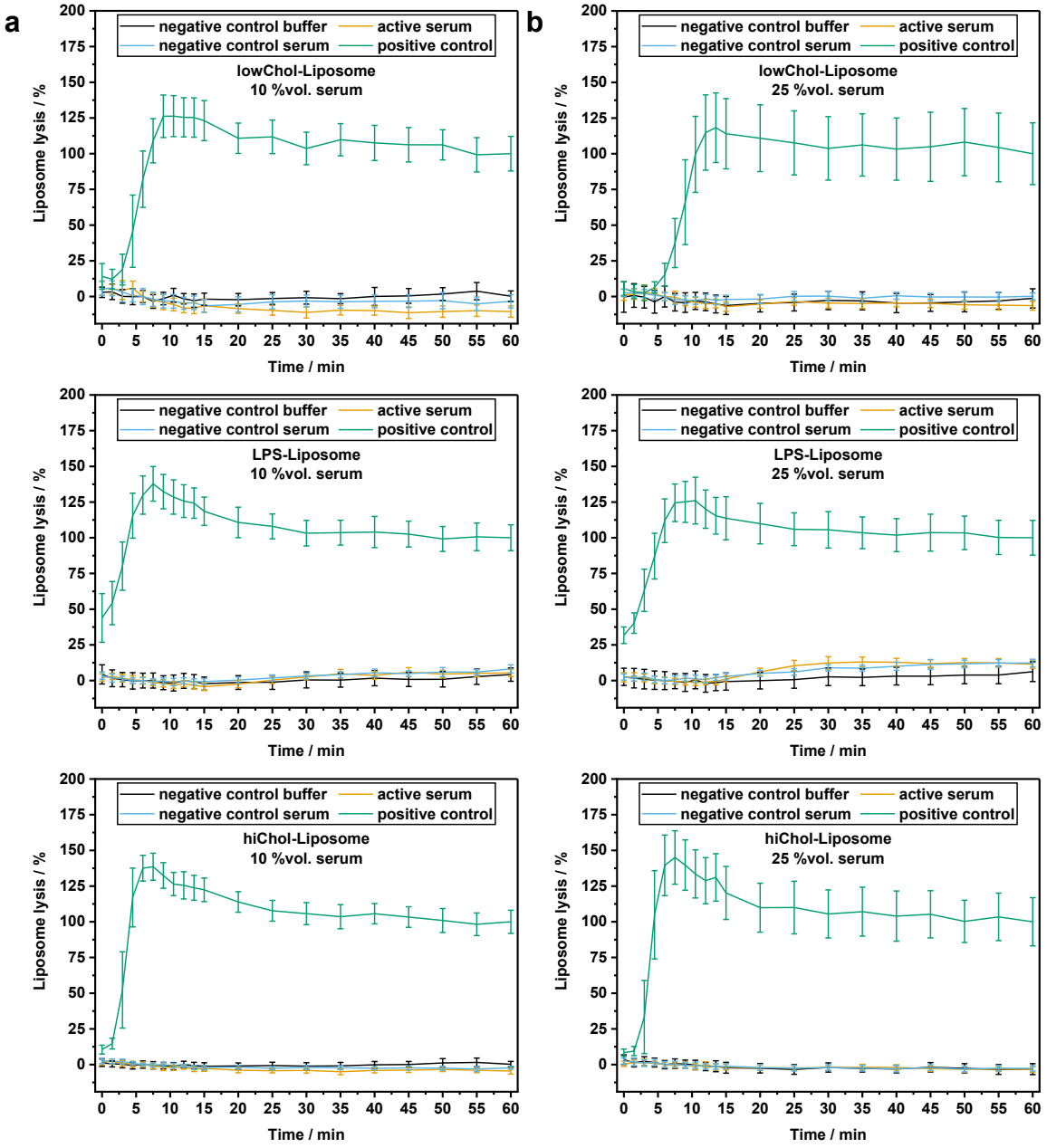

Figure 5-8: Murine serum in the liposome-based complement assay. Time-resolved background-corrected complement assays investigating lowChol- (5 %mol. cholesterol), LPS- (1 %mol. LPS) and hiChol-Liposomes (42 %mol. cholesterol, all 10 µM tL) with **a**, 10 %vol. and **b**, 25 %vol. murine serum. Complement assays were performed in LCB. λ_{Ex}=565 (5) nm and λ_{Em}=585 (5) nm, 37 °C, gain=150, n=3.

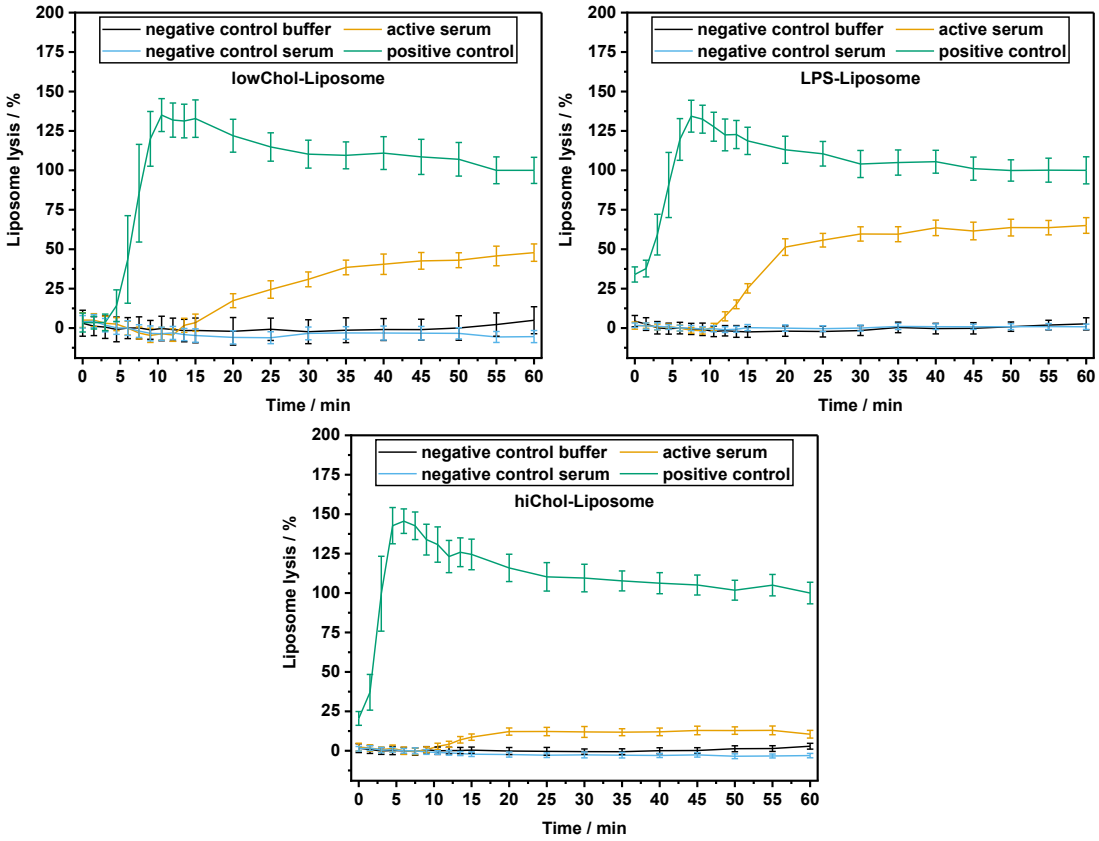

Figure 5-9: Porcine serum in the liposome-based complement assay. Time-resolved background-corrected complement assays investigating lowChol- (5 %mol. cholesterol), LPS- (1 %mol. LPS) and hiChol-Liposomes (42 %mol. cholesterol, all 10 µM tL) with porcine serum. Complement assays were performed in LCB. Serum content was 10 vol.% per well. λ_{Ex}=565 (5) nm and λ_{Em}=585 (5) nm, 37 °C, gain=150, n=3.

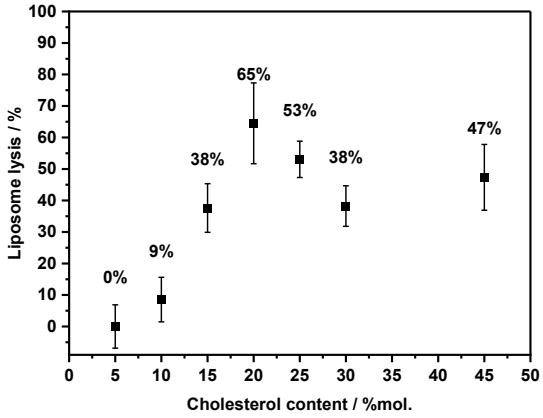

Figure 5-10: Cholesterol content variation with porcine serum in the liposome-based complement assay. Liposome lysis of complement assays investigating pegylated PEG-Liposomes with varying cholesterol content (5-45 %mol. cholesterol, 10 µM tL) with porcine serum. Complement assays were performed in LCB. Serum content was 10 vol.% per well. λ_{Ex}=565 (5) nm and λ_{Em}=585 (5) nm, 37 °C, gain=150, n=3.

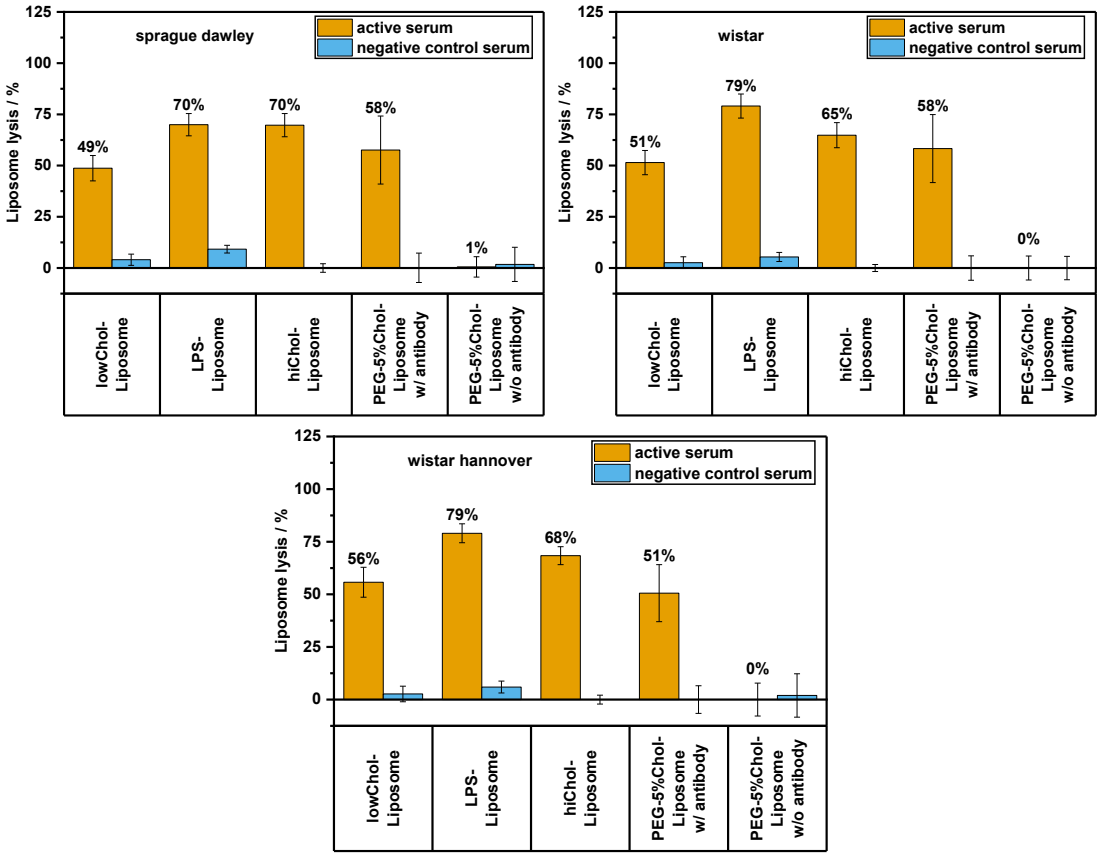

Figure 5-11: Rat serum from varying species in the liposome-based complement assay. Liposome lysis of complement assays investigating investigating lowChol- (5 %mol. cholesterol), LPS- (1 %mol. LPS), hiChol- (42 %mol. cholesterol) and PEG-5%Chol-Liposomes (pegylated, 5 %mol. cholesterol, all 10 µM tL) with and without 0.2 %mol. anti-biotin antibody with rat serum from Sprague Dawley, Wistar and Wistar Hannover rats. Complement assays were performed in LCB. Serum content was 10 vol.% per well. λ_{Ex}=565 (5) nm and λ_{Em}=585 (5) nm, 37 °C, gain=150, n=3.

5.4 Conclusion

Based on the comparison of the liposome lysis recovery in EDTA- and citrate-inhibited sera replenished with Mg^{2+} and Ca^{2+} ions, it can be concluded that EDTA serum is better suited to this liposome-based functional complement assay compared to serum containing citrate. This conclusion is substantiated by the observation that liposome lysis in citrate serum with citrate levels similar to those typically used in the clinic can only be restored to about 71 % of the control level. A higher recovery rate cannot be achieved, as too high bivalent ion concentrations cause liposome instability[47–49] and complement independent fluorophore leakage. While in some applications, such as clotting experiments in clinical settings, citrate is preferred over other anticoagulants in plasma due to its ability to preserve clotting factors, which can be tested after recalcification,[52] the higher stability constants (log K, 37°C, ionic strength of 0.15 M, K^+ salt used as background electrolyte) of EDTA with Ca^{2+} 10.42 and Mg^{2+} 8.92 cause more efficient complexation and overall allow lower bivalent ion concentrations compared to citrate with Ca^{2+} 3.48 and Mg^{2+} 3.44.[53] This makes EDTA the better suited anticoagulant to be used together with this liposome-based assay. Nevertheless, the EDTA

levels used in this study and in fully filled, commercially available EDTA collection tubes only insufficiently block the complement system. To benefit from the enhanced complement preservation under EDTA conditions, collection tubes should not be filled completely to prevent unwanted premature *in vitro* complement activation. It is hypothesized that EDTA-containing, fully inhibited samples could yield similar results when replenished with respective Mg^{2+} and Ca^{2+} levels. The optimal conditions obtained for EDTA-containing serum indicate that the buffer requires an approximately equimolar content of bivalent ions (0.7 mM, Ca^{2+} and Mg^{2+}) in addition to the original buffer concentrations (1 mM Mg^{2+}, 135 nM Ca^{2+}), relative to the EDTA level (0.55 mM) in the sample. However, further investigations with fully inhibited samples would be needed to confirm these assumptions. Overall, the present study suggests that EDTA plasma may be applied in this assay to provide at least qualitative information on complement activity. However, the present study lacks information about coagulation, which should occur in plasma samples after replenishing bivalent ions, in contrast to the currently used serum samples. It is necessary to investigate the extent to which this process occurs in diluted samples and its potential impact on the liposome-based readout to obtain a definitive answer.

From the data obtained for the varying animal sera, it can be concluded that the applied liposome-based assay is generally able to screen the complement response of both human and animal sera. However, sufficiently high complement reactivity is required to cause complement-mediated liposome lysis. Hence, murine serum, which is known to have a weak complement response,[50,51] is not suitable for testing with the applied assay setup. Further optimizations with respect to the serum-to-liposome ratio, i.e. decreasing the liposome content to 1 or 2 µM tL and using buffer additives, which were confirmed to have no inhibitory effects on the complement system, could also enable successful readout in murine sera. In all these studies, sucrose was used as an additive, which has been shown to influence the complement readout (**Figure 4-1a,b**). Substituting sucrose with glycine may therefore improve the readout, especially in cases of weak complement responses. Although animal models have greatly assisted in obtaining a better understanding of the complement system, complement-related diseases and in the development of complement drugs[36,38], the results obtained here emphasize that transferring and the correlating results from animal models to the human complement system must be done carefully due to significant differences in reactivity.[34] Literature suggests that the reactivity of dog complement may be closest to the human complement system upon triggering with nanoparticles.[54] However, this would also need to be confirmed in the liposome-based complement assay.

Overall, this liposome-based complement assay provides a versatile tool with potential for broad applicability to different matrices. Apart from human serum, this study indicates the

applicability of plasma samples, preferably EDTA plasma, and confirms the applicability of animal sera, enabling flexibility in diagnostic situations where sample stocks are limited. In addition, it is anticipated that this will facilitate the investigation of the human and animal complement systems, thereby elucidating their distinct characteristics.

5.5 References

(1) Ricklin, D.; Hajishengallis, G.; Yang, K.; Lambris, J. D. Complement: a key system for immune surveillance and homeostasis. *Nat Immunol* **2010**, *11*, 785–797. DOI: 10.1038/ni.1923.

(2) Carroll, M. V.; Sim, R. B. Complement in health and disease. *Adv Drug Delivery Rev* **2011**, *63*, 965–975. DOI: 10.1016/j.addr.2011.06.005.

(3) Cerenius, L.; Kawabata, S.; Lee, B. L.; Nonaka, M.; Söderhäll, K. Proteolytic cascades and their involvement in invertebrate immunity. *Trends Biochem Sci* **2010**, *35*, 575–583. DOI: 10.1016/j.tibs.2010.04.006.

(4) West, E. E.; Kemper, C. Complosome - the intracellular complement system. *Nat Rev Nephrol* **2023**, *19*, 426–439. DOI: 10.1038/s41581-023-00704-1.

(5) Merle, N. S.; Church, S. E.; Fremeaux-Bacchi, V.; Roumenina, L. T. Complement System Part I - Molecular Mechanisms of Activation and Regulation. *Front Immunol* **2015**, *6*, 262. DOI: 10.3389/fimmu.2015.00262.

(6) Merle, N. S.; Noe, R.; Halbwachs-Mecarelli, L.; Fremeaux-Bacchi, V.; Roumenina, L. T. Complement System Part II: Role in Immunity. *Front Immunol* **2015**, *6*, 257. DOI: 10.3389/fimmu.2015.00257.

(7) Morgan, B. P.; Boyd, C.; Bubeck, D. Molecular cell biology of complement membrane attack. *Semin Cell Dev Biol* **2017**, *72*, 124–132. DOI: 10.1016/j.semcdb.2017.06.009.

(8) Menny, A.; Serna, M.; Boyd, C. M.; Gardner, S.; Joseph, A. P.; Morgan, B. P.; Topf, M.; Brooks, N. J.; Bubeck, D. CryoEM reveals how the complement membrane attack complex ruptures lipid bilayers. *Nat Commun* **2018**, *9*, 5316. DOI: 10.1038/s41467-018-07653-5.

(9) Lombardo, D.; Kiselev, M. A. Methods of Liposomes Preparation: Formation and Control Factors of Versatile Nanocarriers for Biomedical and Nanomedicine Application. *Pharmaceutics* **2022**, *14*. DOI: 10.3390/pharmaceutics14030543.

(10) Lasic, D. D. The mechanism of vesicle formation. *Biochem J* **1988**, *256*, 1–11. DOI: 10.1042/bj2560001.

(11) Dowhan, W. Molecular basis for membrane phospholipid diversity: why are there so many lipids? *Annu Rev Biochem* **1997**, *66*, 199–232. DOI: 10.1146/annurev.biochem.66.1.199.

(12) Pöhnl, M.; Trollmann, M. F. W.; Böckmann, R. A. Nonuniversal impact of cholesterol on membranes mobility, curvature sensing and elasticity. *Nat Commun* **2023**, *14*, 8038. DOI: 10.1038/s41467-023-43892-x.

(13) Doole, F. T.; Kumarage, T.; Ashkar, R.; Brown, M. F. Cholesterol Stiffening of Lipid Membranes. *J Membr Biol* **2022**, *255*, 385–405. DOI: 10.1007/s00232-022-00263-9.

(14) Briuglia, M.-L.; Rotella, C.; McFarlane, A.; Lamprou, D. A. Influence of cholesterol on liposome stability and on in vitro drug release. *Drug Deliv Transl Res* **2015**, *5*, 231–242. DOI: 10.1007/s13346-015-0220-8.

(15) Gulati, M.; Grover, M.; Singh, S.; Singh, M. Lipophilic drug derivatives in liposomes. *Int J Pharm* **1998**, *165*, 129–168. DOI: 10.1016/S0378-5173(98)00006-4.

(16) Nsairat, H.; Khater, D.; Sayed, U.; Odeh, F.; Al Bawab, A.; Alshaer, W. Liposomes: structure, composition, types, and clinical applications. *Heliyon* **2022**, *8*, e09394. DOI: 10.1016/j.heliyon.2022.e09394.

(17) Pande, S. Liposomes for drug delivery: review of vesicular composition, factors affecting drug release and drug loading in liposomes. *Artif Cells Nanomed Biotechnol* **2023**, *51*, 428–440. DOI: 10.1080/21691401.2023.2247036.

(18) Gregoriadis, G.; Ryman, B. E. Liposomes as carriers of enzymes or drugs: a new approach to the treatment of storage diseases. *Biochem J* **1971**, *124*, 58P. DOI: 10.1042/bj1240058p.

(19) Ferreira, M.; Ogren, M.; Dias, J. N. R.; Silva, M.; Gil, S.; Tavares, L.; Aires-da-Silva, F.; Gaspar, M. M.; Aguiar, S. I. Liposomes as Antibiotic Delivery Systems: A Promising Nanotechnological Strategy against Antimicrobial Resistance. *Molecules* **2021**, *26*, 2047. DOI: 10.3390/molecules26072047.

(20) Zylberberg, C.; Gaskill, K.; Pasley, S.; Matosevic, S. Engineering liposomal nanoparticles for targeted gene therapy. *Gene Ther* **2017**, *24*, 441–452. DOI: 10.1038/gt.2017.41.

(21) O'Connell, J. P.; Campbell, R. L.; Fleming, B. M.; Mercolino, T. J.; Johnson, M. D.; McLaurin, D. A. A highly sensitive immunoassay system involving antibody-coated tubes and liposome-entrapped dye. *Clin Chem* **1985**, *31*, 1424–1426.

(22) Kannuck, R. M.; Bellama, J. M.; Durst, R. A. Measurement of liposome-released ferrocyanide by a dual-function polymer modified electrode. *Anal Chem* **1988**, *60*, 142–147. DOI: 10.1021/ac00153a009.

(23) Colletier, J.-P.; Chaize, B.; Winterhalter, M.; Fournier, D. Protein encapsulation in liposomes: efficiency depends on interactions between protein and phospholipid bilayer. *BMC Biotechnol* **2002**, *2*, 9. DOI: 10.1186/1472-6750-2-9.

(24) Edwards, K. A.; Bolduc, O. R.; Baeumner, A. J. Miniaturized bioanalytical systems: enhanced performance through liposomes. *Current Opinion in Chemical Biology* **2012**, *16*, 444–452. DOI: 10.1016/j.cbpa.2012.05.182.

(25) Liu, Q.; Boyd, B. J. Liposomes in biosensors. *Analyst* **2013**, *138*, 391–409. DOI: 10.1039/c2an36140j.

(26) Edwards, K. A.; Baeumner, A. J. Liposomes in analyses. *Talanta* **2006**, *68*, 1421–1431. DOI: 10.1016/j.talanta.2005.08.044.

(27) Masaki, T.; Okada, N.; Yasuda, R.; Okada, H. Assay of complement activity in human serum using large unilamellar liposomes. *J Immunol Methods* **1989**, *123*, 19–24. DOI: 10.1016/0022-1759(89)90025-2.

(28) Hoecherl, K.; Streif, S.; Spitzenberg, C.; Rink, S.; Behrent, A.; Holzhausen, F.; Griesche, C.; Rogoll, C.; Foedlmeier, M.; Gebhard, A.; Kulikowski, K.; Schaefer, N.; Pauly, D.; Baeumner, A. J. A homogeneous immunoassay technology based on liposomes and the complement system enables one-step, no-wash, rapid diagnostics directly in serum. *Anal Bioanal Chem* **2025**, *417*, 3257–3273. DOI: 10.1007/s00216-025-05882-4.

(29) Yamamoto, S.; Kubotsu, K.; Kida, M.; Kondo, K.; Matsuura, S.; Uchiyama, S.; Yonekawa, O.; Kanno, T. Automated homogeneous liposome-based assay system for total complement activity. *Clin Chem* **1995**, *41*, 586–590. DOI: 10.1093/clinchem/41.4.586.

(30) Brandwijk, R. J. M. G. E.; Michels, M. A. H. M.; van Rossum, M.; Nooijer, A. H. de; Nilsson, P. H.; Bruin, W. C. C. de; Toonen, E. J. M. Pitfalls in complement analysis: A systematic literature review of assessing complement activation. *Front Immunol* **2022**, *13*, 1007102. DOI: 10.3389/fimmu.2022.1007102.

(31) Yang, S.; McGookey, M.; Wang, Y.; Cataland, S. R.; Wu, H. M. Effect of blood sampling, processing, and storage on the measurement of complement activation biomarkers. *Am J Clin Pathol* **2015**, *143*, 558–565. DOI: 10.1309/AJCPXPD7ZQXNTIAL.

(32) Mollnes, T. E.; Garred, P.; Bergseth, G. Effect of time, temperature and anticoagulants on in vitro complement activation: consequences for collection and preservation of samples to be examined for complement activation. *Clin Exp Immunol* **1988**, *73*, 484–488.

(33) Andersson, L. I.; Sjöström, D. J.; Brandwijk, R. J. M. G. E.; Toonen, E. J. M.; Mollnes, T. E.; Nilsson, P. H. Complement function and activation in human serum and plasma collected in different blood collection tubes. *J Immunol Methods* **2025**, *538*, 113825. DOI: 10.1016/j.jim.2025.113825.

(34) Moghimi, S. M.; Simberg, D. Critical issues and pitfalls in serum and plasma handling for complement analysis in nanomedicine and bionanotechnology. *Nano Today* **2022**, *44*, 101479. DOI: 10.1016/j.nantod.2022.101479.

(35) Sahu, A.; Pangburn, M. K. Identification of multiple sites of interaction between heparin and the complement system. *Mol Immunol* **1993**, *30*, 679–684. DOI: 10.1016/0161-5890(93)90079-q.

(36) Gibson, B. G.; Cox, T. E.; Marchbank, K. J. Contribution of animal models to the mechanistic understanding of Alternative Pathway and Amplification Loop (AP/AL)-driven Complement-mediated Diseases. *Immunol Rev* **2023**, *313*, 194–216. DOI: 10.1111/imr.13141.

(37) Saez-Calveras, N.; Brewster, A. L.; Stuve, O. The validity of animal models to explore the pathogenic role of the complement system in multiple sclerosis: A review. *Front. Mol. Neurosci.* **2022**, *15*, 1017484. DOI: 10.3389/fnmol.2022.1017484.

(38) Frank, M. M. Animal models for complement deficiencies. *J Clin.Immunol* **1995**, *15*, 113S-121S. DOI: 10.1007/BF01540901.

(39) Kiani, A. K.; Pheby, D.; Henehan, G.; Brown, R.; Sieving, P.; Sykora, P.; Marks, R.; Falsini, B.; Capodicasa, N.; Miertus, S.; Lorusso, L.; Dondossola, D.; Tartaglia, G. M.; Ergoren, M. C.; Dundar, M.; Michelini, S.; Malacarne, D.; Bonetti, G.; Dautaj, A.; Donato, K.; Medori, M. C.; Beccari, T.; Samaja, M.; Connelly, S. T.; Martin, D.; Morresi, A.; Bacu, A.; Herbst, K. L.; Kapustin, M.; Stuppia, L.; Lumer, L.; Farronato, G.; Bertelli, M. Ethical considerations regarding animal experimentation. *J Prev Med Hyg* **2022**, *63*, E255-E266. DOI: 10.15167/2421-4248/jpmh2022.63.2S3.2768.

(40) *Produkt - Sarstedt,* https://www.sarstedt.com/produkte/diagnostik/venenblut/s-monovette/produkt/04.1915.100/ (accessed 2025/06/04).

(41) *BD Vacutainer® EDTA Tubes,* https://www.bd.com/en-us/products-and-solutions/products/product-page.367863#specifications (accessed 2025/06/04).

(42) Frazer-Abel, A.; Kirschfink, M.; Prohászka, Z. Expanding Horizons in Complement Analysis and Quality Control. *Front Immunol* **2021**, *12*, 697313. DOI: 10.3389/fimmu.2021.697313.

(43) Snyderman, R.; Pike, M. C. Interaction of complex polysaccharides with the complement system: effect of calcium depletion on terminal component consumption. *Infect Immun* **1975**, *11*, 273–279. DOI: 10.1128/iai.11.2.273-279.1975.

(44) Lowenstein, F. W.; Stanton, M. F. Serum magnesium levels in the United States, 1971-1974. *J Am Coll Nutr* **1986**, *5*, 399–414. DOI: 10.1080/07315724.1986.10720143.

(45) Sutton, R. Hypomagnesaemia and Magnesium Deficiency. *Journal of the Royal College of Physicians of London* **1968**, *2*, 358–370. DOI: 10.1016/S0035-8819(25)01319-4.

(46) Goldstein, D. A. *Clinical Methods: The History, Physical, and Laboratory Examinations,* 3rd edn.: Boston, 1990.

(47) Saldanha, O.; Schiller, L.; Hauser, K. Calcium-induced compaction and clustering of vesicles tracked with molecular resolution. *Biophys J* **2023**, *122*, 2646–2654. DOI: 10.1016/j.bpj.2023.05.019.

(48) Hincha, D. K. Effects of calcium-induced aggregation on the physical stability of liposomes containing plant glycolipids. *Biochim Biophys Acta* **2003**, *1611*, 180–186. DOI: 10.1016/s0005-2736(03)00053-1.

(49) ZHANG, T.; QIU, Y.; LUO, Q.; CHENG, X.; ZHAO, L.; YAN, X.; PENG, B.; JIANG, H.; YANG, H. Concentration Dependent Effects of Ca^{2+} and Mg^{2+} on the Phosphatidylethanolamine-Phosphatidylglycerol Bilayer. *Acta Phys Chim Sin* **2019**, *35*, 840–849. DOI: 10.3866/PKU.WHXB201811016.

(50) Ong, G. L.; Mattes, M. J. Mouse strains with typical mammalian levels of complement activity. *J Immunol Methods* **1989**, *125*, 147–158. DOI: 10.1016/0022-1759(89)90088-4.

(51) Sassi, F.; Hugo, F.; Muhly, M.; Khaled, A.; Bhakdi, S. A reason for the cytolytic inefficiency of murine serum. *Immunology* **1987**, *62*, 145–147.

(52) Winter, W. E.; Greene, D. N.; Beal, S. G.; Isom, J. A.; Manning, H.; Wilkerson, G.; Harris, N. In Advances in Clinical Chemistry; Makowski, Gregory S., Ed.; Elsevier, 2020; pp. 31–84.

(53) Donald R. Burgess. *NIST SRD 46. Critically Selected Stability Constants of Metal Complexes: Version 8.0 for Windows*; National Institute of Standards and Technology, 2020.

(54) Li, Y.; Wang, G.; Griffin, L.; Banda, N. K.; Saba, L. M.; Groman, E. V.; Scheinman, R.; Moghimi, S. M.; Simberg, D. Complement opsonization of nanoparticles: Differences between humans and preclinical species. *J Control Release* **2021**, *338*, 548–556. DOI: 10.1016/j.jconrel.2021.08.048.

5.6 Supporting information

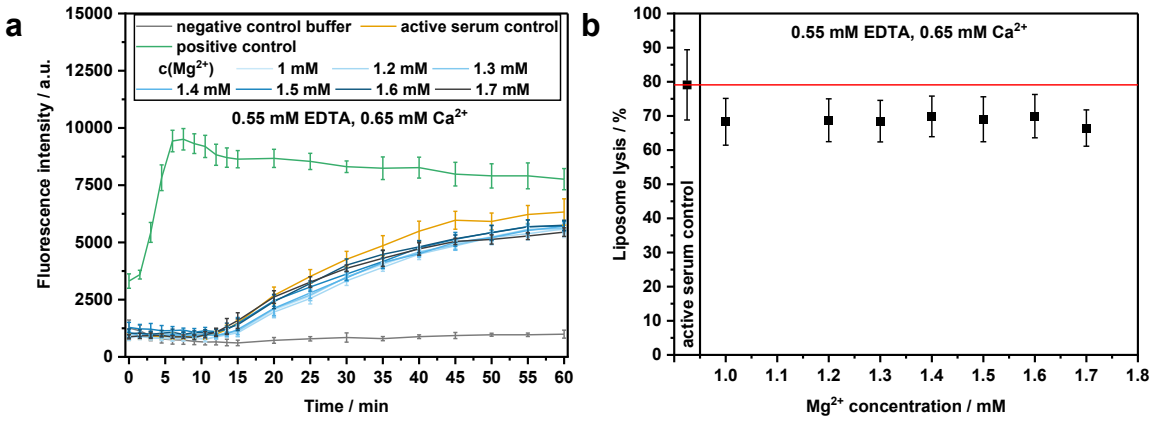

Figure S 5-1: Refined Mg^{2+} titration in EDTA serum. Complement assays investigating the LPS-Liposome (1 %mol. LPS, 10 µM tL) with varying concentrations of Mg^{2+} in EDTA serum with previously optimized Ca^{2+} levels (0.55 mM EDTA, 0.65 mM Ca^{2+}). **a** shows the time-resolved fluorescence intensity values, **b** shows the background-corrected and normalized endpoint values. Complement assays were performed in LCB. Serum content was 10 %vol. per well. λ_{Ex}=565 (5) nm and λ_{Em}=585 (5) nm, 37 °C, gain=150, n=3.

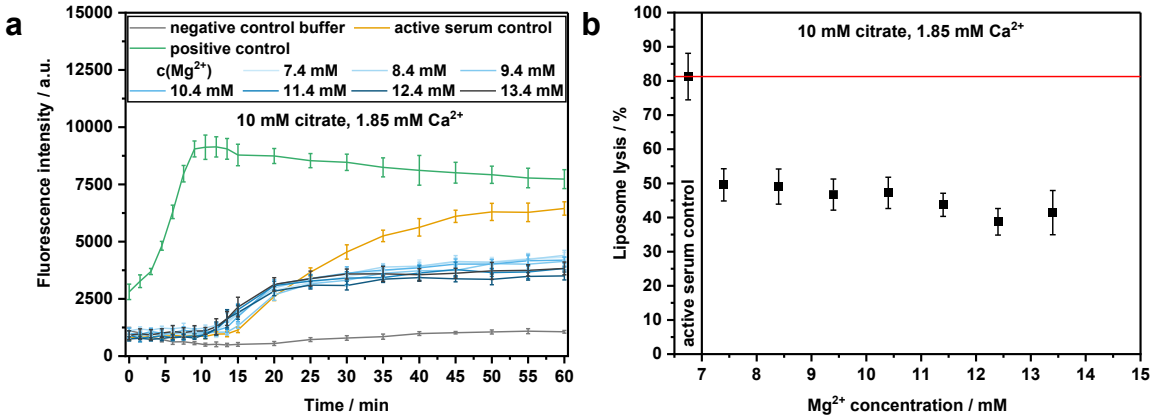

Figure S 5-2: Refined Mg^{2+} titration in citrate serum. Complement assays investigating the LPS-Liposome (1 %mol. LPS, 10 µM tL) with varying concentrations of Mg^{2+} in citrate serum with previously optimized Ca^{2+} levels (10 mM EDTA, 1.85 mM Ca^{2+}). **a** shows the time-resolved fluorescence intensity values, **b** shows the background-corrected and normalized endpoint values. Complement assays were performed in LCB. Serum content was 10 %vol. per well. λ_{Ex}=565 (5) nm and λ_{Em}=585 (5) nm, 37 °C, gain=150, n=3.

Table S 5-1: Liposome characteristics including lipid composition, encapsulant concentrations in 20 mM HEPES (pH 7.5), smallest membrane pore size during extrusion, Hydrodynamic diameter d(H), polydispersity index PDI, zeta-potential and total lipid concentration tL.

Batch	Lipid composition	Encapsulant & membrane pore size	d(H) / nm	PDI	Zeta potential / mV	tL / mM
LPS-Liposome	5 %mol. cholesterol, 74 %mol. DPPC, 18 %mol. DPPG 2 %mol. DPPE-biotin 1 %mol. LPS	10 mM SRB 210 mM NaCl 0.4 µm	168 ± 4	0.17 ± 0.02	-6.7 ± 0.7	13.31 ± 0.05
lowChol-Liposome	5 %mol. cholesterol, 74 %mol. DPPC, 19 %mol. DPPG 2 %mol. DPPE-biotin	10 mM SRB 210 mM NaCl 0.4 µm	164 ± 2	0.22 ± 0.01	-16 ± 1	6.20 ± 0.08
hiChol-Liposome	42 %mol. cholesterol, 36 %mol. DPPC, 20 %mol. DPPG 2 %mol. DPPE-biotin	10 mM SRB 210 mM NaCl 0.4 µm	288 ± 4	0.19 ± 0.04	-20 ± 3	6.44 ± 0.09
PEG-5%Chol-Liposome	5 %mol. cholesterol, 72 %mol. DPPC, 19 %mol. DPPG, 2 %mol. DMPE-PEG2000, 2 %mol. DMPE-PEG2000-biotin	10 mM SRB 210 mM NaCl 0.4 µm	134 ± 2	0.18 ± 0.01	-9 ± 2	5.93 ± 0.06
PEG-10%Chol-Liposome	10 %mol. cholesterol, 67 %mol. DPPC, 19 %mol. DPPG, 2 %mol. DMPE-PEG2000, 2 %mol. DMPE-PEG2000-biotin	10 mM SRB 210 mM NaCl 0.4 µm	127.8 ± 0.4	0.11 ± 0.01	-2.0 ±0.5	13.09 ± 0.06
PEG-15%Chol-Liposome	15 %mol. cholesterol, 62 %mol. DPPC, 19 %mol. DPPG, 2 %mol. DMPE-PEG2000, 2 %mol. DMPE-PEG2000-biotin	10 mM SRB 210 mM NaCl 0.4 µm	138 ± 2	0.18 ± 0.02	-3 ± 1	10.7 ± 0.1
PEG-20%Chol-Liposome	20 %mol. cholesterol, 57 %mol. DPPC, 19 %mol. DPPG, 2 %mol. DMPE-PEG2000, 2 %mol. DMPE-PEG2000-biotin	10 mM SRB 210 mM NaCl 0.4 µm	144 ± 2	0.22 ± 0.01	-1.8 ± 0.6	13.45 ± 0.07
PEG-25%Chol-Liposome	25 %mol. cholesterol, 52 %mol. DPPC, 19 %mol. DPPG, 2 %mol. DMPE-PEG2000, 2 %mol. DMPE-PEG2000-biotin	10 mM SRB 210 mM NaCl 0.4 µm	147.5 ± 0.5	0.21 ± 0.01	-1 ± 1	7.90 ± 0.02
PEG-30%Chol-Liposome	30 %mol. cholesterol, 47 %mol. DPPC, 19 %mol. DPPG, 2 %mol. DMPE-PEG2000, 2 %mol. DMPE-PEG2000-biotin	10 mM SRB 210 mM NaCl 0.4 µm	146 ± 3	0.14 ± 0.01	-2 ± 2	10.9 ± 0.1
PEG-45%Chol-Liposome	45 %mol. cholesterol, 32 %mol. DPPC, 19 %mol. DPPG, 2 %mol. DMPE-PEG2000, 2 %mol.DMPE-PEG2000-biotin	10 mM SRB 210 mM NaCl 0.4 µm	164 ± 3		0 ± 5	9.25 ± 0.07
PEG-5%Chol-Liposome-2	5 %mol. cholesterol, 72 %mol. DPPC, 19 %mol. DPPG, 2 %mol. DMPE-PEG2000, 2 %mol. DMPE-PEG2000-biotin	10 mM SRB 210 mM NaCl 0.4 µm	135 ± 3	0.13 ± 0.02	-3 ± 2	10.40 ± 0.04

6 Conclusion and Future Perspectives

The complement system initially described in the 19th century as heat-labile component which complements the activities of specific antibodies and causes lysis of bacteria[1], is increasingly revealed as fundamental element in pathogen recognition, immune surveillance, and the maintenance of homeostasis.[2,3] Complement dysregulation has been recognized as relevant clinical and diagnostic factor in several diseases.[4] Such diseases range from autoimmune disorders and recurrent infections to more complex conditions such as age-related macular degeneration and atypical hemolytic uremic syndrome.[4] Even in very prominent diseases such as COVID-19 complement plays a decisive role and represents a therapeutic approach.[5,6] It is not only fully involved in acute infections via all activation pathways but also influences the course of the disease in long-COVID patients through chronic dysregulation.[6] However, despite its increasing clinical relevance, complement diagnostics remain challenged by the limitations of current assay methodologies in terms of standardization, reproducibility, and especially complete coverage of all complement pathways in a pathway specific lytic assay. Currently available traditional hemolysis assays are functionally informative but suffer from variability due to their reliance on animal erythrocytes. Furthermore, they are limited to assessing only the classical and alternative complement pathways. ELISA-based approaches, although more standardized and capable of specifically determining the activity of all pathways, lack the capacity to reflect true lytic activity. The growing interest in complement-targeted therapeutics[7] and external quality assurance programs[8] further emphasize the urgent need for standardized, high-throughput, and reliable diagnostic tools.

In order to address these challenges, this thesis aimed to improve the current complement analysis methodologies by developing a liposome-based assay to analyze the pathway specific complement activity. The design goal for the envisioned assay included the capability of reliably analyzing the three complement pathways individually in a lysis-based readout with potential for standardization and multiplexing. Furthermore, its applicability for other species and fundamental studies for the applicability of plasma as complement source apart from serum was investigated.

Liposomes were identified as ideal candidates to substitute erythrocytes in this case, since they provide versatility in encapsulation and surface modification for both diagnostic and research applications.[9,10] In the context of complement analysis, liposome-based assays can offer enhanced stability, reproducibility and the potential for pathway-specific customization. In complement diagnostics, they emerged as a promising alternative to conventional assays. However, current implementations remain limited. Only the classical pathway is routinely assessed commercially with a liposome-based assay.[11] Hence, the development of a unified

liposome platform, which is capable to evaluate all three complement pathways, would represent a significant advancement in this field, enhancing complement analysis in both clinical and research settings.

Systematic investigations on the envisioned multiplexed liposome-based assay to determine the activity of each complement pathway highlighted the critical, yet often understudied, role of encapsulated molecules on the physicochemical and biological behavior of liposomes. Findings with the three fluorophores IR-783, SRB and PTSA underscored the necessity to consider encapsulant-lipid interactions during liposome design, particularly for applications in drug delivery and diagnostics where surface integrity and biological reactivity are essential to be investigated to ensure optimal performance and biocompatibility. Consequently, it is suggested that future liposome-based applications should integrate such investigations as a characterization parameter alongside the established lipid composition, size and surface characteristics. The simple incubation assay established in this work, utilizing ghostisomes and the respective encapsulant followed by dialysis with subsequent liposome analysis, can facilitate the identification of potential encapsulant-lipid interactions with low effort in the future. Nevertheless, the occurrence of the distinct biological responses of the complement system towards liposomes with varying encapsulant restricted the development of a multiplexed complement assay. To realize this, future experiments need to identify encapsulants that result in the same complement response when encapsulated in liposomes. In addition, to avoid the currently necessary Mg^{2+}/EGTA buffers for the specific readout of the alternative pathway a pathway specific trigger would be needed. A simultaneous detection of all pathways in the same sample is currently restricted due to these Ca^{2+} depleted conditions for alternative pathway readouts, since under these the classical and lectin pathway are inhibited. However, a multiplexed detection of the classical and lectin pathway should remain a goal to be pursued in future research.

Nonetheless, successful development of complement pathway specific liposomes was achieved through the high flexibility in liposome preparation and modification. This, in turn, enabled biomimic characteristics, and consequently a platform technology for lysis-based complement functionality assessment. This finding represents a significant breakthrough especially for the lectin pathway, as it solves the long-standing challenge of developing a lysis-based functional assay specific for this pathway, whose activity determination previously was only achievable through secondary means via protein quantification. It is envisioned that this assay can serve as a research instrument, facilitating studies that seek to achieve a more profound comprehension of the lectin complement pathway through mechanistic studies. Moreover, it has the capacity to enhance diagnostics, by facilitating the analysis and monitoring of lectin pathway activity dysfunction in terms of deficiencies or dysregulations, and

consequently lectin pathway associated disease diagnosis. Although the analysis of both other pathways is frequently in the primary focus, the global COVID-19 pandemic has served to underscore the significance of analyzing the lectin pathway activity.[12] Complement activation via the lectin pathway has been demonstrated during SARS-CoV-2 infection with increased activation in severe cases.[13–15] The correlation for the lectin pathway which was demonstrated in the present study between a C3b-deposition ELISA and the liposome-based assay serves to validate the latter. Still, the results can be further enhanced, as the ELISA employed, in contrast to the liposome assay developed, does not take the entire complement cascade into account. Consequently, it is recommended that the liposome-based assay should be compared to an ELISA-based method investigating sC5b-9 deposition in future studies, given that a more suitable erythrocyte assay based on specific lectin pathway lysis is unavailable.

The assay's potential as a versatile tool for complement system analysis was further highlighted by its adaptability to the classical and alternative pathways, yet still exhibits challenges to be faced especially in terms of correlation studies.

For the classical pathway, high-cholesterol liposomes offer a simplified alternative to antibody-triggered systems. Despite this methodological advantage and confirmed pathway specificity examined in this work, no correlation with C3b-deposition ELISAs was observed. This lack of correlation is postulated to be caused by fundamental differences in the mechanisms of complement activation between cholesterol and antibodies as a trigger. Specifically, it is assumed that additional molecules such as C-reactive protein (CRP)[16,17] or other serum components like lipoproteins[18] are involved in complement initiation or modulation via high cholesterol contents in contrast to the direct binding of C1q to antibodies on the liposome surface. CRP is described to exhibit proinflammatory properties upon conformational changes from pentameric CRP (pCRP) to pCRP* or monomeric CRP (mCRP) revealing new epitopes for C1q binding after interaction with phosphocholine containing membranes.[19] Furthermore, elevated liposomal cholesterol levels were described to cause increased CRP-dependent complement consumption and liposome lysis[16], which would agree with the results observed in our studies. These findings indicate that the presence and role of such supposed cofactors need further investigation to understand and improve the assay, its performance and interpretability. Pathway specificity was also confirmed for antibody-triggered liposomes, which are already widely used in both liposome- and erythrocyte-based complement assays. However, antibody-triggered liposomes have not yet been subject to correlation studies within this work. Given their established use, a positive correlation with CH50 or respective ELISAs is anticipated, and future studies should aim to confirm this. Moreover, alternative approaches that simplify the assay preparation, such as the direct immobilization of CRP[17], pentraxin 3[20], antibody Fc fragments[21], C1q-binding peptides[22,23], or other C1q-binding structures, could

serve as an alternative to the high cholesterol content triggered approach and enhance assay efficiency by eliminating incubation steps and improving reproducibility compared to the antibody triggered approach.

The alternative pathway presented additional challenges. Although lipopolysaccharides (LPS) are a common type of trigger in commercial ELISAs, and its application in the liposome-based assay development and specificity studies were successful, the subsequent screening of individual donor sera revealed limited lysis across a significant proportion of these sera. This finding suggests that in this case deposition of early alternative pathway activation products on the liposome surface may be inefficient potentially due to the lack of a specific pattern recognition protein which attracts subsequent complement protein binding. Furthermore, the current anionic liposome surface may not provide suitable binding sites or favorable surface characteristics. To address this, future work should focus on optimizing liposome lipid composition and exploring alternative triggers such as inulin[24], zymosan[25], or liposomes with high amine content[26], either alone or in combination, to enhance the sensitivity and reliability of the alternative pathway readout. However, the direct transfer of triggers and their results described in literature may remain challenging since in most cases no functional lysis but complement consumption, i.e. remaining erythrocyte lysis or increased complement activation products are detected. Furthermore, the impact of particle sizes, such as those of zymosan or higher-order inulin polymorphisms with sizes in the micrometer range, on the stability and reactivity of liposomes in the nanometer range remains to be investigated in the future. Rabbit erythrocytes which are commonly used in AP50 assays for alternative pathway activity determination[27] may also serve as orientation for lipid compositions. Additionally, investigations of serum C3b or C5b levels after incubation with LPS-Liposomes under Mg^{2+}/EGTA conditions should provide information on whether the absence of lysis in the respective sera is rather due to insufficient complement activation or restricted complement deposition on the liposome surface.

Overall, the liposome-based assay developed in this work provides a promising platform for both high-throughput diagnostic applications and detailed mechanistic studies. Especially the assay's capability for time-resolved analysis offers new valuable insights into the kinetics of complement-mediated lysis. Still, there remains potential for optimization, particularly in the previously mentioned complement triggers but also in the use of buffer additives to stabilize background signals and prevent negative lysis values in non-lysing samples caused by the chosen background evaluation. Since 10 or 6-minute data point subtraction as background does not take into account any fluorescence intensity decay over time, non-reactive samples can show lower fluorescence signals after 60-minute incubation compared to the chosen background signal at 10 or 6 minutes. It is expected that additional investigations on buffer

additives, in form of alternative amino acids, proteins or low molecular sugars, can stabilize the background signal over the whole measurement time. Importantly, such additives must be carefully selected to avoid any interference with complement activation.

The plasma feasibility studies demonstrated the advantages of using EDTA as anticoagulant over citrate, in case they are applied with replenished bivalent ions for assessing functional complement activity. EDTA plasma may possess a viable alternative to serum in order to enhance sample flexibility in diagnostic and research settings and help to reduce the risk of artificial pre-analytical complement activation. However, the here performed studies only investigate the reactivation potential of serum samples after anticoagulant addition. This does not fully represent the final conditions in real plasma but can be regarded as solid foundation for future studies. It is recommended to investigate the influence of potential coagulation of diluted plasma upon replenished bivalent ion concentrations in the liposome-based assay in subsequent studies. Comparisons of plasma and serum samples which were drawn simultaneously are finally mandatory to evaluate the real suitability and performance of replenished plasma samples compared to complement preserved serum as established matrix for complement activity determination. Furthermore, the investigation of animal sera revealed significant interspecies variability in complement responses towards varying liposome surfaces. Whilst the present studies underscore the importance of species selection in preclinical studies especially with respect to later translation to humans and suggest that liposome-based assays can serve as effective tools for comparative research, they miss any pathway specific analysis because liposomes which allow a reliable specific readout of each pathway had not yet been achieved. It is therefore recommended that, upon successful completion of the pathway specific liposome development, a comprehensive reinvestigation of various animal species should be conducted to determine their variances in each pathway. In this study, it is suggested to incorporate species that have historically been employed in complement research, such as guinea pigs and rabbits. Additionally, it is recommended to include species for which complement reactivity has been described to be similar to that of humans, such as dogs[28].

In conclusion, this thesis provides a versatile liposome-based platform technology to assess the pathway specific complement activity and functionality via liposome lysis. Further refinement, particularly in correlation studies and surface chemistry optimization, will be essential to fully realize its great potential in diagnostic and research applications. Its future applications range from the quantification of complement activity in serum samples for mechanistic studies or diagnostic patient screenings, pathway-specific evaluation of complement inhibitors and therapeutic agents during development or therapy monitoring to the application as quality control assay of complement-preserved sera, which is critical given the

thermosensitivity of complement proteins and the risk of artificial activation during sample handling. Furthermore, this work also provides the basis for the adaptation of other erythrocyte-based complement assays, for example for the detection of autoimmune antibodies[29] or factor H functionality[30]. Additionally, this work supports the broader applicability of different sample matrices and species in the liposome-based complement assay. It lays the foundation for simpler, more reliable yet flexible approaches for functional complement activity analysis.

6.1 References

(1) Kaufmann, S. H. E. Immunology's foundation: the 100-year anniversary of the Nobel Prize to Paul Ehrlich and Elie Metchnikoff. *Nat Immunol* **2008**, *9*, 705–712. DOI: 10.1038/ni0708-705.

(2) Ricklin, D.; Hajishengallis, G.; Yang, K.; Lambris, J. D. Complement: a key system for immune surveillance and homeostasis. *Nat Immunol* **2010**, *11*, 785–797. DOI: 10.1038/ni.1923.

(3) Carroll, M. V.; Sim, R. B. Complement in health and disease. *Adv Drug Delivery Rev* **2011**, *63*, 965–975. DOI: 10.1016/j.addr.2011.06.005.

(4) Schröder-Braunstein, J.; Kirschfink, M. Complement deficiencies and dysregulation: Pathophysiological consequences, modern analysis, and clinical management. *Mol Immunol* **2019**, *114*, 299–311. DOI: 10.1016/j.molimm.2019.08.002.

(5) Ma, L.; Sahu, S. K.; Cano, M.; Kuppuswamy, V.; Bajwa, J.; McPhatter, J.; Pine, A.; Meizlish, M. L.; Goshua, G.; Chang, C.-H.; Zhang, H.; Price, C.; Bahel, P.; Rinder, H.; Lei, T.; Day, A.; Reynolds, D.; Wu, X.; Schriefer, R.; Rauseo, A. M.; Goss, C. W.; O'Halloran, J. A.; Presti, R. M.; Kim, A. H.; Gelman, A. E.; Dela Cruz, C. S.; Lee, A. I.; Mudd, P. A.; Chun, H. J.; Atkinson, J. P.; Kulkarni, H. S. Increased complement activation is a distinctive feature of severe SARS-CoV-2 infection. *Sci Immunol* **2021**, *6*. DOI: 10.1126/sciimmunol.abh2259.

(6) Zelek, W. M.; Harrison, R. A. Complement and COVID-19: Three years on, what we know, what we don't know, and what we ought to know. *Immunobiology* **2023**, *228*, 152393. DOI: 10.1016/j.imbio.2023.152393.

(7) Ricklin, D. Complement-targeted therapeutics: Are we there yet, or just getting started? *Eur. J. Immunol.* **2024**, *54*, e2350816. DOI: 10.1002/eji.202350816.

(8) Kirschfink, M.; Frazer-Abel, A.; Balogh, E.; Goseberg, S.; Weiss, N.; Prohászka, Z. External quality assurance program for diagnostic complement laboratories: evaluation of the results of the past seven years. *Front Immunol* **2024**, *15*, 1368399. DOI: 10.3389/fimmu.2024.1368399.

(9) Edwards, K. A.; Baeumner, A. J. Liposomes in analyses. *Talanta* **2006**, *68*, 1421–1431. DOI: 10.1016/j.talanta.2005.08.044.

(10) Sforzi, J.; Palagi, L.; Aime, S. Liposome-Based Bioassays. *Biology (Basel)* **2020**, *9*. DOI: 10.3390/biology9080202.

(11) Nandakumar, V.; Braun, K. M. P.; Willrich, M. A. V. Challenges for complement functional assays in the clinical laboratory: From test validation to clinical interpretation. *J Immunol Methods* **2025**, *537*, 113824. DOI: 10.1016/j.jim.2025.113824.

(12) Ali, Y. M.; Ferrari, M.; Lynch, N. J.; Yaseen, S.; Dudler, T.; Gragerov, S.; Demopulos, G.; Heeney, J. L.; Schwaeble, W. J. Lectin Pathway Mediates Complement Activation by SARS-CoV-2 Proteins. *Front Immunol* **2021**, *12*, 714511. DOI: 10.3389/fimmu.2021.714511.

(13) Defendi, F.; Leroy, C.; Epaulard, O.; Clavarino, G.; Vilotitch, A.; Le Marechal, M.; Jacob, M.-C.; Raskovalova, T.; Pernollet, M.; Le Gouellec, A.; Bosson, J.-L.; Poignard, P.; Roustit, M.; Thielens, N.; Dumestre-Pérard, C.; Cesbron, J.-Y. Complement Alternative and Mannose-Binding Lectin Pathway Activation Is Associated With COVID-19 Mortality. *Front Immunol* **2021**, *12*, 742446. DOI: 10.3389/fimmu.2021.742446.

(14) Hurler, L.; Szilágyi, Á.; Mescia, F.; Bergamaschi, L.; Mező, B.; Sinkovits, G.; Réti, M.; Müller, V.; Iványi, Z.; Gál, J.; Gopcsa, L.; Reményi, P.; Szathmáry, B.; Lakatos, B.; Szlávik, J.; Bobek, I.; Prohászka, Z. Z.; Förhécz, Z.; Csuka, D.; Kajdácsi, E.; Cervenak, L.; Kiszel, P.; Masszi, T.; Vályi-Nagy, I.; Würzner, R.; Lyons, P. A.; Toonen, E. J. M.; Prohászka, Z. Complement lectin pathway activation is associated with COVID-19

disease severity, independent of MBL2 genotype subgroups. *Front Immunol* **2023**, *14*, 1162171. DOI: 10.3389/fimmu.2023.1162171.

(15) Niederreiter, J.; Eck, C.; Ries, T.; Hartmann, A.; Märkl, B.; Büttner-Herold, M.; Amann, K.; Daniel, C. Complement Activation via the Lectin and Alternative Pathway in Patients With Severe COVID-19. *Front Immunol* **2022**, *13*, 835156. DOI: 10.3389/fimmu.2022.835156.

(16) Richards, R. L.; Gewurz, H.; Siegel, J.; Alving, C. R. Interactions of C-Reactive Protein and Complement with Liposomes. *The Journal of Immunology* **1979**, *122*, 1185–1189. DOI: 10.4049/jimmunol.122.4.1185.

(17) McGrath, F. D. G.; Brouwer, M. C.; Arlaud, G. J.; Daha, M. R.; Hack, C. E.; Roos, A. Evidence that complement protein C1q interacts with C-reactive protein through its globular head region. *J Immunol* **2006**, *176*, 2950–2957. DOI: 10.4049/jimmunol.176.5.2950.

(18) Moein Moghimi, S.; Hamad, I.; Bünger, R.; Andresen, T. L.; Jørgensen, K.; Hunter, A. C.; Baranji, L.; Rosivall, L.; Szebeni, J. Activation of the human complement system by cholesterol-rich and PEGylated liposomes-modulation of cholesterol-rich liposome-mediated complement activation by elevated serum LDL and HDL levels. *J Liposome Res* **2006**, *16*, 167–174. DOI: 10.1080/08982100600848801.

(19) McFadyen, J. D.; Kiefer, J.; Braig, D.; Loseff-Silver, J.; Potempa, L. A.; Eisenhardt, S. U.; Peter, K. Dissociation of C-Reactive Protein Localizes and Amplifies Inflammation: Evidence for a Direct Biological Role of C-Reactive Protein and Its Conformational Changes. *Front Immunol* **2018**, *9*, 1351. DOI: 10.3389/fimmu.2018.01351.

(20) Nauta, A. J.; Bottazzi, B.; Mantovani, A.; Salvatori, G.; Kishore, U.; Schwaeble, W. J.; Gingras, A. R.; Tzima, S.; Vivanco, F.; Egido, J.; Tijsma, O.; Hack, E. C.; Daha, M. R.; Roos, A. Biochemical and functional characterization of the interaction between pentraxin 3 and C1q. *Eur. J. Immunol.* **2003**, *33*, 465–473. DOI: 10.1002/immu.200310022.

(21) Diebolder, C. A.; Beurskens, F. J.; Jong, R. N. de; Koning, R. I.; Strumane, K.; Lindorfer, M. A.; Voorhorst, M.; Ugurlar, D.; Rosati, S.; Heck, A. J. R.; van de Winkel, J. G. J.; Wilson, I. A.; Koster, A. J.; Taylor, R. P.; Saphire, E. O.; Burton, D. R.; Schuurman, J.; Gros, P.; Parren, P. W. H. I. Complement is activated by IgG hexamers assembled at the cell surface. *Science* **2014**, *343*, 1260–1263. DOI: 10.1126/science.1248943.

(22) Webster, S.; Bonnell, B.; Rogers, J. Charge-based binding of complement component C1q to the Alzheimer amyloid beta-peptide. *Am J Pathol* **1997**, *150*, 1531–1536.

(23) Hamers, S. M. W. R.; Abendstein, L.; Boyle, A. L.; Jongkees, S. A. K.; Sharp, T. H. Selection and characterization of a peptide-based complement modulator targeting C1 of the innate immune system. *RSC Chem Biol* **2024**, *5*, 787–799. DOI: 10.1039/d4cb00081a.

(24) Cooper, P. D.; Petrovsky, N. Delta inulin: a novel, immunologically active, stable packing structure comprising β-D-2 - 1 poly(fructo-furanosyl) α-D-glucose polymers. *Glycobiology* **2011**, *21*, 595–606. DOI: 10.1093/glycob/cwq201.

(25) Fearon, D. T.; Austen, K. F. Activation of the alternative complement pathway due to resistance of zymosan-bound amplification convertase to endogenous regulatory mechanisms. *PNAS* **1977**, *74*, 1683–1687. DOI: 10.1073/pnas.74.4.1683.

(26) Bradley, A. J.; Devine, D. V. The complement system in liposome clearance: Can complement deposition be inhibited? *Adv Drug Delivery Rev* **1998**, *32*, 19–29. DOI: 10.1016/s0169-409x(97)00129-4.

(27) Harboe, M.; Thorgersen, E. B.; Mollnes, T. E. Advances in assay of complement function and activation. *Adv Drug Delivery Rev* **2011**, *63*, 976–987. DOI: 10.1016/j.addr.2011.05.010.

(28) Li, Y.; Wang, G.; Griffin, L.; Banda, N. K.; Saba, L. M.; Groman, E. V.; Scheinman, R.; Moghimi, S. M.; Simberg, D. Complement opsonization of nanoparticles: Differences between humans and preclinical species. *J Control Release* **2021**, *338*, 548–556. DOI: 10.1016/j.jconrel.2021.08.048.

(29) Chabannes, M.; Frémeaux-Bacchi, V.; Chauvet, S. Detection of C3 Nephritic Factor by Hemolytic Assay. *Methods Mol Biol* **2021**, *2227*, 147–158. DOI: 10.1007/978-1-0716-1016-9_15.

(30) Chabannes, M.; Togarsimalemath, S. K.; Dragon-Durey, M.-A. Hemolytic Tests Exploring Factor H Functional Activities. *Methods Mol Biol* **2021**, *2227*, 69–81. DOI: 10.1007/978-1-0716-1016-9_7.

Curriculum Vitae

PERSÖNLICHE DATEN

Name	Clemens Spitzenberg
E-Mail	clemens.spitzenberg@ur.de

BERUFSERFAHRUNG

Fraunhofer IZI-BB seit 01/2025	**Wissenschaftlicher Mitarbeiter** im Bereich chemische Analytik, Sensorentwicklung und Bioprozessierung

AKADEMISCHE AUSBILDUNG

Universität Regensburg	**Promotionsstudium Chemie**
01/2021 – 03/2025	*„Development of a liposome-based complement assay platform for functional complement activity determination”* Institut für Analytische Chemie, Chemo- und Biosensorik (Prof. Dr. Antje J. Bäumner)
Universität Regensburg	**Masterstudium Chemie**
10/2018 – 10/2020	*„Developing functional liposome-based bioanalytical components in nucleic acid and complex protein assays”* Institut für Analytische Chemie, Chemo- und Biosensorik (Prof. Dr. Antje J. Bäumner)
Universität Regensburg	**Bachelorstudium Chemie**
10/2015 – 07/2018	*„Electrochemically reduced graphene oxide decorated electrospun conductive polyaniline nanofibers for electrochemical sensing”* Institut für Analytische Chemie, Chemo- und Biosensorik (Prof. Dr. Antje J. Bäumner)

AUSZEICHNUNGEN

Posterpreis 08/2022	**European Meeting on Complement in Human Disease 2022, Bern** Ausgezeichnet durch das European Complement Network
Studienpreis 06/2019	**Absolventenpreis B.Sc. Chemie** Ausgezeichnet durch die Fachgruppe Analytische Chemie, GDCh

AUSLANDSAUFENTHALTE

Sanquin Research 04+08/2024	**Forschungsaufenthalte** in Amsterdam, Niederlande
Chung-Ang Universität 04/2019	**Forschungsaufenthalt** in Seoul, Südkorea School of Integrative Engineering

Publications and Presentations

Publications

Streif, S.; Neckermann, P.; **Spitzenberg, C.**; Weiss, K.; Hoecherl, K.; Kulikowski, K.; Hahner, S.; Noelting, C.; Einhauser, S.; Peterhoff, D.; Asam, C.; Wagner, R.; Baeumner, A. J. Liposome-based high-throughput and point-of-care assays toward the quick, simple, and sensitive detection of neutralizing antibodies against SARS-CoV-2 in patient sera. *Analytical and bioanalytical chemistry* **2023**, *415*, 1421–1435. DOI: 10.1007/s00216-023-04548-3.

Hoecherl, K.; Streif, S.; **Spitzenberg, C.**; Rink, S.; Behrent, A.; Holzhausen, F.; Griesche, C.; Rogoll, C.; Foedlmeier, M.; Gebhard, A.; Kulikowski, K.; Schaefer, N.; Pauly, D.; Baeumner, A. J. A homogeneous immunoassay technology based on liposomes and the complement system enables one-step, no-wash, rapid diagnostics directly in serum. *Analytical and bioanalytical chemistry* **2025**, *417*, 3257–3273. DOI: 10.1007/s00216-025-05882-4.

Spitzenberg, C.; Bruckschlegel, C.; Holzhausen, F.; Boesl-Bichlmeier, S.; Pasquier, C.; Nuernberger, P.; Bauduin, P.; Baeumner, A. J. Encapsulants Affect Liposome Surface Interactions with Biological Systems. *Small* **2025**, *21* (33), e2505312. DOI: 10.1002/smll.202505312.

Research paper intended for submission in *ACSnano*: **Spitzenberg, C.**; Aichinger, M.; Holzhausen F.; Brouwer M. C.; Poppelaars F.; Pouw R. B.; Pauly D.; Baeumner A. J. Liposomes enable the functional assessment of each complement pathway.

Patent

Patent application by **Spitzenberg C.,** Baeumner A. J., Pauly D., Poppelaars F., **2024**, EU: WO2024099816A1, international: PCT/EP2023/080264, https://worldwide.espacenet.com/patent/search/family/084330560/publication/WO2024099816A1?q=WO2024099816A1, (accessed 2025/06/08)

Presentations

Posterpräsentation	**European Biosensor Symposium**
03/2021	Regensburg, Deutschland (Online)
Posterpräsentation	**Analytica Conference 2022**
06/2022	München, Deutschland
Posterpräsentation	**European Meeting on Complement in Human Disease 2022**
08/2022	Bern, Schweiz
Posterpräsentation	**Analytica Conference 2024**
04/2024	München, Deutschland

Eidesstattliche Erklärung

Ich erkläre hiermit an Eides statt, dass ich die vorliegende Arbeit ohne unzulässige Hilfe Dritter und ohne Benutzung anderer als der angegebenen Hilfsmittel angefertigt habe; die aus anderen Quellen direkt oder indirekt übernommenen Daten und Konzepte sind unter Angabe des Literaturzitats gekennzeichnet.

Weitere Personen waren an der inhaltlich-materiellen Herstellung der vorliegenden Arbeit nicht beteiligt. Insbesondere habe ich hierfür nicht die entgeltliche Hilfe eines Promotionsberaters oder anderer Personen in Anspruch genommen. Niemand hat von mir weder unmittelbar noch mittelbar geldwerte Leistungen für Arbeiten erhalten, die im Zusammenhang mit dem Inhalt der vorgelegten Dissertation stehen.

Die Arbeit wurde bisher weder im In- noch im Ausland in gleicher oder ähnlicher Form einer anderen Prüfungsbehörde vorgelegt.

Regensburg, den _____ Unterschrift: _____

(Clemens Spitzenberg, Author)